



Graduate School Yearbook 2025

Graduate School Yearbook 2025

PhD students solving present and future challenges

I am delighted to present the DTU Chemical Engineering Graduate School Yearbook 2025, showcasing the significant contributions of our PhD students.

Each year, DTU Chemical Engineering welcomes over 100 PhD students from around the globe. They enrich our department with a diverse international atmosphere and are pivotal in driving our ambitious research agenda forward.

This edition of the yearbook offers a glimpse into the wide array of research areas our PhD students are exploring. Some are just beginning their journey, while others are nearing the completion of their theses.

A common thread among all their projects is a strong emphasis on sustainability, aligning with both Danish and UN climate and sustainability goals. Each student has identified the most relevant goals for their research.

We underscore the critical role of technological innovation in fostering sustainable growth. Addressing today's environmental challenges through science and technology is at the heart of our mission at DTU Chemical Engineering.

Our department focuses on developing and applying knowledge, methods, technologies, and sustainable solutions in:

- *Chemical and biochemical process engineering and production*
- *Design of chemical and biochemical products and processes*
- *Energy and environment*

Sustainable growth demands enduring solutions and innovative thinking. We have great confidence in our PhD students, whose work is crucial in shaping future advancements not only in Denmark but globally.

Kim Dam-Johansen

Professor, Head of Department

K

Azade Kafashan <i>Investigation of the Barrier Mechanism in Lignin-Based Epoxy Anticorrosive Coating</i>	72
Leo John Kershaw <i>Development of conducting PDMS compounds for soft robotic applications</i>	74
Elias Kjær-Westermann <i>Synthesis of bio-based polymers for advanced applications</i>	76
Loukas Kollias <i>Modelling of carbon capture processes</i>	78
Amalie Paarup Krebs <i>Catalytic stabilization and upgrading of biomass pyrolysis oil to fuels for heavy transport and aviation</i>	80

L

Mercedes Belda-Ley <i>Advanced sensitivity analysis and comprehensive validation methodology to improve credibility of QRAs studies in chemical process industries</i>	82
Shawn Mike Bruno Lindner <i>Progressing Towards Non-Biocidal Antifouling Coatings</i>	84
Sofia Maria Lindström <i>Recycling of crosslinked elastomer systems</i>	86
Moritz Niklas Link <i>Mechanistic Insights into Short Chain Olefin Oligomerization on Acid Catalysts: The Role of Catalyst Properties, Process Parameters and Feed Composition</i>	88
Ádám Lukács <i>Synthesis of large cyclic polydimethylsiloxane (PDMS) rings for wearable devices</i>	90

M

Oliver Robert Oscar Massaad <i>Digital twin development of high shear granulation processes</i>	92
Anatolii Mishchuk <i>Sustainable biomethanation of pyrolysis gas from residual biomass</i>	94
Behnam Mohammadi <i>Terahertz Spectroscopy for Sustainable Maritime Coatings</i>	96
Claudia Pastor Morell <i>Next generation of deNOx technology for WtE plants</i>	98
Ali Moshkriz <i>Molecular-level understanding of the adhesion mechanisms of waterborne epoxy coatings on steel</i>	100

N

Cristina Nedelcu <i>Cyclic poly(dimethylsiloxane) networks with reactive double bonds enabling post-curing functionalization</i>	102
--	-----

P

Philipp Pably <i>Physiological bioprocess control</i>	104
Konstantinos Papasakellariou <i>Deciphering the anaerobic microbiome for construction of robust microbial consortia for mixed culture fermentations</i>	106
Magnus Nørager Pedersen <i>Modelling and simulation of electrochemical CO₂ and H₂O reduction</i>	108
Ward Peeters <i>In-situ online corrosion and solvent degradation monitoring at Pilot Scale</i>	110
Deborah Pfaff <i>Integrated model for up- and downstream bioprocess intensification</i>	112
Ariadna Pié Porta <i>Oxygen-enzyme in biocatalytic oxidation</i>	114

R

Pavle Ramah <i>Functionalization of PDMS via click chemistry for dielectric elastomers with protein integration</i>	116
---	-----

S

Mohammad Reza Abdollahi Senoukesh <i>Toward oxyfuel cement calcination for efficient CO₂ capture: CFD modeling of a cold-pilot scale calciner</i>	118
Rudini Tua Silitonga <i>Optimising Cell Potential and Current for Enhanced CO₂-to-Methane Conversion in Continuous Microbial Electrosynthesis Reactors</i>	120

T

Mehmet Bengi Taysun <i>Mechanism investigation of corrosion protection and coating degradation</i>	122
Alberto Goicoechea Torres <i>Chemical and Catalytic Conversion of Lignin to Organic Coatings</i>	124
Berivan Tunca <i>Fermentation of carbon monoxide to chemical precursors</i>	126

W

Emilie Overgaard Willer <i>Hydrodynamics effect on gas bubble size distribution in stirred bioreactors</i>	128
Zhang Wenkai <i>Phosphorus Release and Transformation during Biomass Pyrolysis and Char Conversion</i>	130

Z

Zhou Ziyi <i>Molecular equations of state for Electrolyte Solutions</i>	132
---	-----

Effects of particle size distribution on the conversion of kaolinitic clays undergoing flash calcination: A modeling study

(March 2023 – February 2026)



Contribution to the UN Sustainable Development Goals

This project is aligned with the 13th UN SDG for climate action. The knowledge obtained during this PhD Project will give insights towards the design and optimization of clay calcination plants. The use of an increased amount of calcined clay in cementitious materials will reduce the CO₂ emissions from one of the biggest greenhouse gas emitters: the cement industry. This project deals with the development of a particle model of clay calcination that is relevant for the design and operation of clay calciners.



Nicolás

Carro

necac@kt.dtu.dk

Supervisors: Peter Arendt Jensen, Hao Wu

Abstract

In the production of environmentally friendly construction materials, calcined clay cement is a promising alternative. One of the challenges involves obtaining homogeneous calcination of raw material with a broad range of particle sizes. In this work, a particle model is used to study the influence of different particle size distributions on the quality of the calcined product and investigate how it affects the range of viable calciner temperatures where a high yield of metakaolin can be achieved.

Introduction

Currently the cement industry is responsible for 8% of CO₂ emissions, quantity that is projected to increase by 10-15% in the year 2050 [1]. Calcined clays are an adequate alternative for CO₂ reduction on cement production, as cement that includes up to 50% calcined clays obtain similar strength development as Ordinary Portland Cement (OPC), the raw material is widely available, calcined clay production is less energy intensive than clinker needed for OPC and it does not release CO₂ during calcination [2].

Flash calcination is a process that exposes clay to high temperatures at short residence times and subsequently quenches it to prevent calcined clay deactivation by recrystallization. It has gained recent attention for it promises quicker conversion of clays and less energy consumption than the conventional rotary kiln calcination (soak calcination). Clays fed in industrial calciners have a wide distribution of particle sizes and due to agglomeration complete calcination of all particle sizes are difficult. A methodology which can analyze the influence of particle size distribution (PSD) on the quality of the obtained calcined clay for a given set of reactor conditions is desired.

Objectives

A recently developed particle model is used in conjunction with a PSD averaging procedure to obtain the optimum calcination temperatures for a wide range of particle size distributions commonly found in industrial kaolinitic clays.

Modelling strategy

The particle model is a mesh based on the previous work of Teklay [3]. The model uses the Finite Volume Method (FVM) to discretize the conservation equations, that can be written as:

$$\frac{d\rho\phi}{dt} + \text{div}(\rho\mathbf{u}\phi) = \text{div}(\Gamma_\phi(\phi)\nabla\phi) + S_\phi(t, \mathbf{r}, \phi) \quad (2)$$

$$\mathbf{u} = -\frac{K}{\mu}\nabla p \quad (4)$$

$$\frac{d\rho_{s,i}}{dt} = S_s(t, \mathbf{r}, \rho_s) \quad (5)$$

Where for $\phi = \{\mathbf{1}, \mathbf{C}_p \mathbf{T}, \mathbf{y}_{g,i}\}$, ρ is gas density, T is temperature, $y_{g,i}$ is mass fraction of gas i and $\rho_{s,i}$ is the density of solid i . The model is coupled with the appropriate boundary conditions that reflect the conditions inside a flash calciner (gas radiation, heat and mass transfer with the surrounding gas film). The diffusion terms are discretized with central difference, the advection

terms are discretized with the upwind scheme, and the system is solved in time using the Method of Lines with the Backward differentiation method. The PSD average of the metakaolin content $\bar{X}_{MK,out}$ is calculated by definition:

$$\bar{X}_{MK,out}(\mu_r, \sigma_r) = \frac{\int_0^R X_{MK,out}(r) f(r, \mu_r, \sigma_r) dr}{\int_0^R f(r, \mu_r, \sigma_r) dr} \quad (2)$$

Where $f(r, \mu_r, \sigma_r)$ is a lognormal particle size distribution characterized by the logarithms of the average size μ_r and of the dispersion σ_r . The denominator in Equation 2 acts as a normalizing factor for the average.

Results and discussion

A kaolinitic clay of 99% purity is chosen as the material of study. The reactor will be considered isothermal, and the residence time of all particles will be 1 second which is within the common range for industrial calciners [3]. The dispersion $\sigma_r = 0.5$ will be fixed and $\mu_r = [\log 1, \log 300]$, will account for the wide variety of size distributions present in industrial clays. The fine and coarse PSDs used for this study are shown in Figure 1. The discrepancy in magnitude of the peaks between both PSDs is due to the coarser sample (blue line) to be dispersed over a larger particle size range.

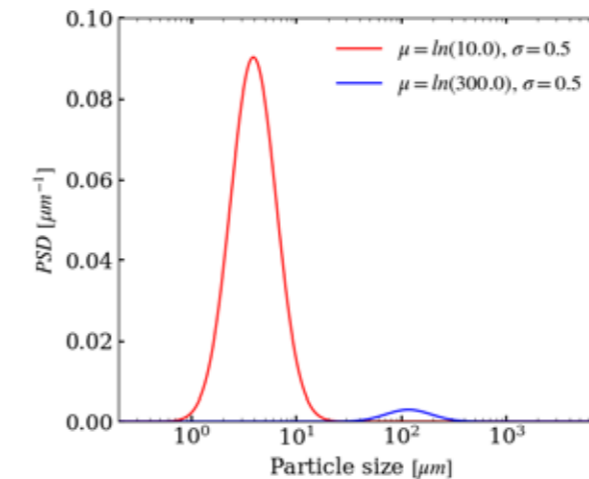


Figure 1: Different lognormal PSDs considered in this study. Red line – fine sample, blue line – coarse sample.

The final average metakaolin mass fraction in the kaolinitic samples with varying PSD is shown in Figure 2. The finest sample considered has an optimum calcination temperature of 900°C and it remains approximately constant up until a mean particle size of 100 μm. For bigger μ_r , the optimum temperature shifts faster to higher temperatures, reaching a value of 950°C for the coarsest PSD evaluated in this work. This is attributed to heat and mass transport limiting the temperature rise at the center of larger particles, therefore reducing dehydroxylation. Nonetheless, the minimum temperature at which we achieve a minimum conversion of 50% increases faster, making the high metakaolin content range delimited by the green lines in Figure 2 narrower for coarser PSDs.

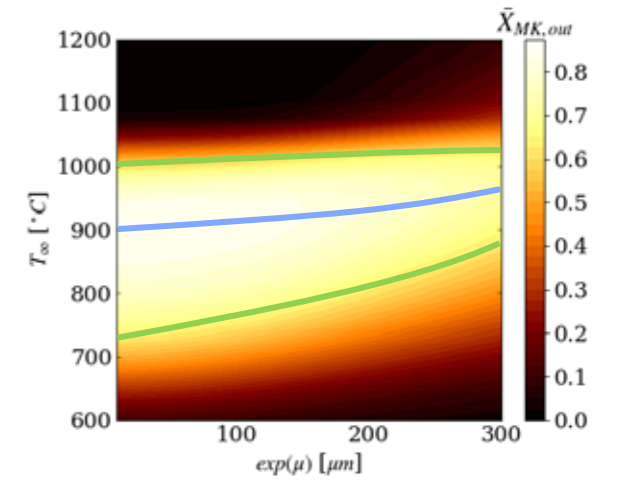


Figure 2: Effects of reactor temperature and the dispersion on $\bar{X}_{MK,out}$ for a kaolinite with $\mu_r = \log 100$ flash calcined for 1s. Lavender line – optimum calciner temperature, green lines – temperature range for high yield of metakaolin (above 80%).

Conclusions

A particle model couple with an averaging procedure was used to study the influence of dispersion and size of a clay collection of particles undergoing calcination on its quality. The procedure shows that there is a significant reduction in the calciner temperature range for high metakaolin yields as the samples get coarser.

References

1. Schneider, M.; Romer, M.; Tschudin, M.; Bolio, H. Sustainable cement production—Present and future. *Cem. Concr. Res.* 2011, 41, 642–650.
2. Scrivener, K., Martirena, F., Bishnoi, S., & Maity, S. (2018). Calcined clay limestone cements (LC3). *Cement and Concrete Research*, 114, 49-56.
3. Teklay, A., Yin, C., Rosendahl, L., & Bøjer, M. (2014). Calcination of kaolinite clay particles for cement production: A modeling study. *Cement and Concrete Research*, 61, 11-19.

Cleanable Cargo Hold Coatings

(April 2023 – March 2026)



Contribution to the UN Sustainable Development Goals

By improving cargo hold coatings for the shipping industry, this project aligns with the United Nations Sustainable Development Goal 7: Affordable and Clean Energy. It promotes sustainability by reducing the need for frequent and energy-intensive cleaning processes and the use of chemicals, and lowering maintenance costs, contributing to more affordable and clean energy solutions in the industry.



Elahe Adibzadeh

elaad@dtu.dk

Supervisors: Søren Kiil, Narayanan Rajagopalan, Stefan Møller Olsen, Zoi Lamprakou.

Abstract

This study evaluates the durability and cleanability of cargo hold coatings using a controlled coal cargo simulation. Two commercial epoxies and a scratch-resistant acrylic panel were exposed to particulate abrasion under pressure and subsequently cleaned with water. Performance was quantified by abrasion mass loss, hardness, elastic modulus, coefficient of friction, and 3D surface profiling, alongside image-based residue ratings. Results show that coatings minimizing surface damage clean more effectively; Epoxy-2 and the acrylic performed best. Overall, balanced bulk and surface properties, not single metrics, govern durable, low-maintenance coatings.

Introduction

Bulk carrier cargo holds operate under severe mechanical and environmental stress. Repeated loading/unloading of abrasive and sometimes corrosive cargoes leads to impact, sliding wear, residue build-up, and challenging cleaning regimes. Epoxy coatings are widely used because they provide corrosion protection and mechanical robustness; however, real performance depends on how well a surface resists damage and releases cargo residues after discharge. Excessive surface damage increases fouling and cleaning time, while aggressive detergent use can undermine long-term durability and environmental goals [1], [2], [3].

This study evaluates representative cargo hold coating solutions with the aim of clarifying which material attributes most strongly govern durability and water-based cleanability in a controlled lab simulation of cargo conditions. In particular, the influence of a balanced combination of bulk wear resistance and surface characteristics on practical performance was assessed.

Experimental

Representative cargo hold coating materials were selected to evaluate the influence of mechanical and surface properties on durability and cleanability.

Two commercial epoxy-based coatings, Epoxy-A and Epoxy-B, were compared with a scratch-resistant acrylic (ACSR) reference panel.

As shown in Fig. 1, a lab-scale cargo simulation was employed to reproduce the combined effects of abrasion, impact, and particulate contamination typical of cargo holds. The test involved exposure of the coated surfaces to coal particles under controlled compression and motion to simulate cargo contact. After exposure, cleaning was performed using water only.

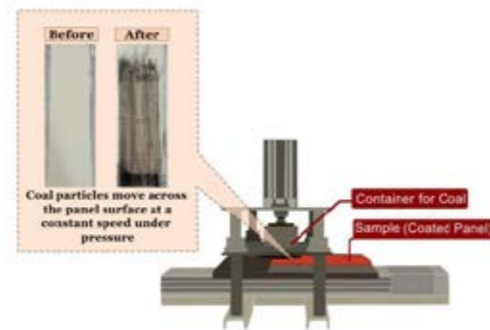


Figure 2: Schematic of the lab setup used to simulate cargo hold conditions.

Performance evaluation included both bulk and surface-level analyses. Mechanical durability was characterized by abrasion mass loss and indentation hardness, while surface damage was

quantified through 3D optical profiling. Elastic modulus and coefficient of friction (COF) were determined to assess deformation behavior and sliding resistance. Cleanability was rated digitally based on residue removal efficiency following the water-cleaning step.

Results

A qualitative comparison of the evaluated coating systems revealed distinct differences in how each material responded to the simulated cargo-hold exposure. All samples experienced visible wear, but the degree of surface damage and ease of cleaning varied noticeably. Epoxy-B demonstrated greater overall durability, maintaining a smoother surface after testing and requiring less effort for water-based residue removal. The scratch-resistant acrylic (ACSR) panel showed comparable performance, suggesting that engineered surface treatments can deliver similar benefits to optimized epoxy systems. In contrast, Epoxy-A exhibited more pronounced surface markings and higher residue retention after the test, indicating lower resistance to combined abrasion and contamination.

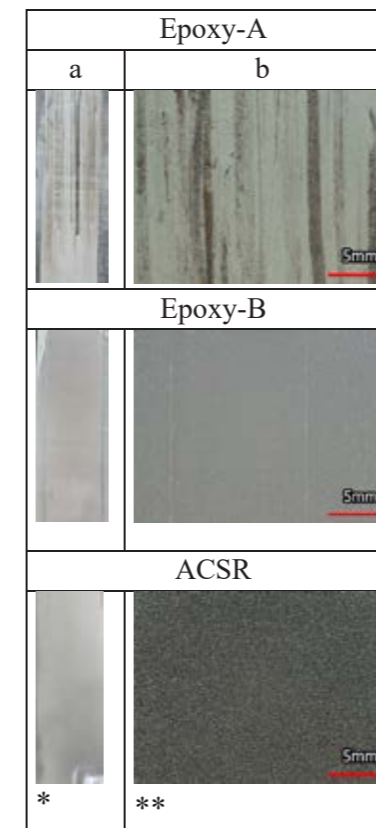


Figure 2: (a) Photographic images of the samples following the coal cargo and cleaning with water. (b) Optical microscopy images (12x magnification) showing scratches and surface damage.

*: A white paper sheet was placed under the transparent ACSR sample to enhance image clarity. **: A black paper sheet was placed under the ACSR

sample; the visible dot points are due to reflections and contrast by the black background.

Representative post-test images are shown in Fig. 2, illustrating the differences in appearance and residue distribution between the coatings. The smoother surface of Epoxy-B remained less stained after water rinsing, whereas Epoxy-A retained visible coal traces. These visual trends were consistent with the general observations made during the simulation.

Microscopic and 3D surface assessments indicated that the extent and morphology of surface damage were the primary factors governing cleanability. Coatings that preserved a uniform and shallow wear profile allowed residues to be removed more easily, while surfaces with deeper grooves or localized fractures tended to trap particulate matter even after repeated cleaning cycles. These results highlight that cleanability depends on the quality of the worn surface rather than on any single bulk property such as hardness or friction coefficient [4], [5], [6].

From a broader perspective, the findings provide insight into how cargo-hold coatings can be designed to minimize maintenance and reduce the need for chemical detergents. By integrating both bulk mechanical integrity and surface damage control, next-generation systems can achieve higher durability, improved water-based cleanability, and lower environmental impact. The present framework offers a practical and non-disclosive way to evaluate coating performance while preserving confidentiality for ongoing research intended for journal publication.

References

1. P. A. Sørensen, S. Kiil, K. Dam-Johansen, and C. E. Weinell. doi: 10.1007/s11998-008-9144-2.
2. Y. Li and C. Ning. doi: <https://doi.org/10.1016/j.bioactmat.2019.04.003>.
3. S. B. Axelsen, O. Knudsen, and R. Johnsen. doi: 10.5006/1.3318281.
4. X. Xu and N. Gupta. doi: 10.1016/j.polymer.2018.10.036.
5. X. Xu and N. Gupta. doi: 10.1016/j.mtla.2018.09.034.
6. B. D. Beake. doi: 10.1016/j.surfcoat.2022.128272.

Benchmark of thermodynamic models for prediction of derivative properties

(January 2024 – January 2026)

9 INDUSTRY, INNOVATION AND INFRASTRUCTURE



Contribution to the UN Sustainable Development Goals

This research analyzes the accuracy of thermodynamic models by evaluating first and second-order properties like vapor pressure, saturation liquid density, isothermal compressibility, isobaric expansivity, heat capacities, speed of sound, and the Joule-Thomson coefficient. These improvements are vital for optimizing industrial processes such as chemical manufacturing and refrigeration, reducing energy consumption and operational costs. By supporting innovation and infrastructure development, the work helps industries design safer and more efficient systems. Accurate models also improve predictions of key variables, ensuring greater safety and resilience in industrial



Javad Amanabadi

javam@dtu.dk

Supervisors:
Xiaodong Liang, Georgios M. Kontogeorgis

Abstract

This study evaluates the performance of PC-SAFT, PCP-SAFT, SAFT-VR Mie, and SAFT-VR Mie-GV models in predicting thermodynamic properties of ketones, ethers, and esters, including vapor pressure, saturation liquid density, isothermal compressibility, expansivity, heat capacities, speed of sound, and the Joule-Thomson coefficient over wide temperature and pressure ranges. SAFT-VR Mie shows consistent and reliable performance for second-order derivative properties. While incorporating the dipolar term aims to enhance accuracy, the extent depends on molecular polarity and the sensitivity to dipole interactions.

Introduction

The development of a universal Equation of State (EOS) model capable of accurately predicting a comprehensive range of properties for a wide variety of compounds and their mixtures across the entire thermodynamic phase space remains one of the key challenges in modern thermodynamics. Despite significant progress, a fully satisfactory solution to this problem has yet to be achieved. As highlighted in our previous study, various equations of state, including cubic and statistical associating fluid theory (SAFT) type models, have been proposed in the literature to describe the thermodynamic behavior of non-polar compounds.

Specific Objectives

While prior studies have extensively evaluated EOS performance for non-polar compounds, polar non-associating compounds (such as ketones, ethers, and esters) have received comparatively less attention. Comprehensive evaluations of models such as PC-SAFT, PCP-SAFT, SAFT-VR Mie, and SAFT-VR Mie-GV for these fluids are scarce, especially for a broad set of thermodynamic properties and over wide ranges of conditions. Furthermore, an SQLite database containing all experimental data is provided for the thermodynamic community.

Results and Discussion

Historically, the primary objective of thermodynamic models has been to provide satisfactory results for phase equilibria and VLE properties, including saturation density and vapor pressure. **Figure 1** presents a comparative AAD% analysis of the two key thermodynamic properties: vapor pressure and saturation liquid density, across various thermodynamic models.

Figure 2 presents the absolute deviation percentage (AAD%) between the thermodynamic derivative properties of ketones, esters, and ethers. From a general standpoint, the SAFT-VR Mie model demonstrates the most consistent and reliable performance among the derivative properties. These observations highlight that while incorporating dipolar terms is beneficial, the magnitude and direction of the improvement depend strongly on the molecular polarity and the sensitivity of the specific

thermodynamic property to dipole interactions.

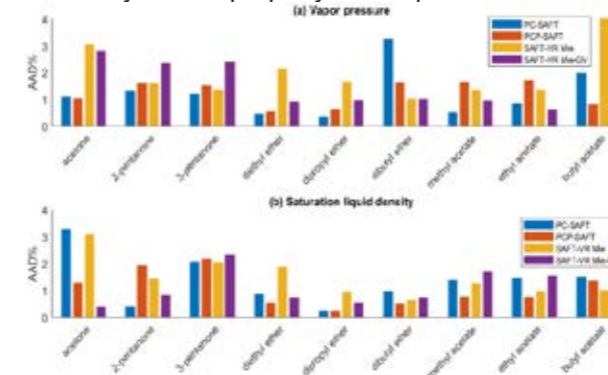


Figure 3. AAD% of (a) vapor pressure and (b) saturation liquid density for the PC-SAFT, PCP-SAFT, SAFT-VR Mie, and SAFT-VR Mie-GV models over temperature ranges of $T_r=0.5-0.99$.

These observations highlight that while incorporating dipolar terms is beneficial, the magnitude and direction of the improvement depend strongly on the molecular polarity and the sensitivity of the specific thermodynamic property to dipole interactions.



Figure 4. Calculated AAD% values of thermodynamic derivative properties for all models using experimental datasets. The empty cell means the lack of data

As shown in **Figure 3**, which presents the difference in residual Helmholtz energy between the polar and non-polar versions of the models, SAFT-VR Mie-GV vs. SAFT-VR Mie (Fig. 3a) and PCP-SAFT vs. PC-SAFT (Fig. 3b), the inclusion of polar terms shows greater sensitivity to temperature variations, particularly at lower temperatures, than to pressure changes. Furthermore, this sensitivity appears to be more pronounced in the SAFT-VR Mie-GV models compared to the PCP-SAFT model. In terms of the second-order temperature derivative ($\partial^2 A^{res}/\partial T^2$), relevant to the calculation of isochoric heat capacity, both the hard-sphere ($\partial^2 A_{hs}^{res}/\partial T^2$) and the dispersion ($\partial^2 A_{disp}^{res}/\partial T^2$) contributions are significant in the SAFT-VR Mie and SAFT-VR Mie-GV models. From a qualitative point of view, the dispersion contribution to ($\partial^2 A^{res}/\partial V \partial T$) derivative exhibits an opposite trend in the PC-SAFT family compared to the SAFT-VR Mie family, which is observed consistently across all examined cases.

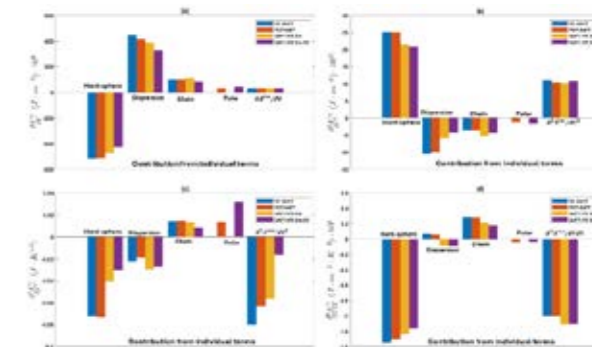


Figure 5. Contribution from individual terms (hard-sphere, dispersion, chain, and polar) to the derivatives of the residual Helmholtz energy ((a) $\partial A^{res}/\partial V$, (b) $A^{res}/\partial V^2$, (c) $\partial^2 A^{res}/\partial T^2$, and (d) $\partial^2 A^{res}/\partial V \partial T$) of acetone at $T_r=P_r=0.6$.

Conclusions

This study provides a comprehensive compilation of experimental thermodynamic data for these compounds, organized in a SQLite database, which could serve as a valuable resource for future evaluations and refinements of thermodynamic models and for the prediction of other thermodynamic properties. This study presents a thorough comparison of various thermodynamic models, namely PC-SAFT, PCP-SAFT, SAFT-VR Mie, and SAFT-VR Mie-GV, for a range of thermodynamic properties.

Acknowledgements

The authors wish to thank the support from the Independent Research Fund Denmark (Case number: 3105-00024B) and the Department of Chemical and Biochemical Engineering, Technical University of Denmark. We would also like to acknowledge the developers of Clapeyron.jl [1] for providing the computational tools used in this work.

References

1. P.J. Walker, H.-W. Yew, A. Riedemann, Clapeyron.jl: an extensible, open-source fluid thermodynamics toolkit, Ind Eng Chem Res 61 (2022) 7130–7153.

List of Publications

1. Amanabadi, J.; Kontogeorgis, G. M.; Liang, X. Fluid Phase Equilib. 2025, 114366.
2. This current work has been submitted and is currently under review in the Industrial & Engineering Chemistry Research journal.

Underwater Evaluation of Antifouling Coatings

(May 2023 – May 2026)



Contribution to the UN Sustainable Development Goals

The goal of coating marine structures and vessels is to protect them from corrosion and marine biofouling. Evaluating and assessing biofouling is still being done subjectively. This project aims to leverage underwater computer vision and machine learning to monitor and evaluate biofouling developments in-situ and provide a standardized evaluation technique towards upholding Goal 14 of the UN SDGs to protect life below water and maintain biodiversity.



Joshua

Anani

josan@kt.dtu.dk

Supervisors: Kim Dam-Johansen & Jochen Dreyer

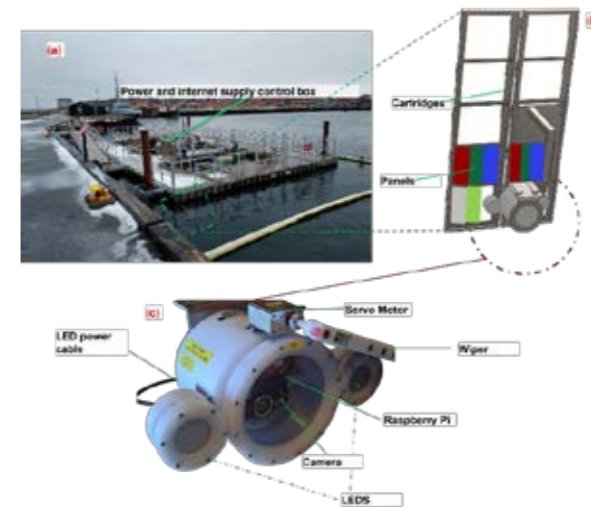


Figure 6: (a) CMTc raft in Hundested, (b) cartridge with panel mounts, and (c) underwater camera setup with LEDs, a fluorescence filter, and a servo motor wiper to prevent fouling accumulation.

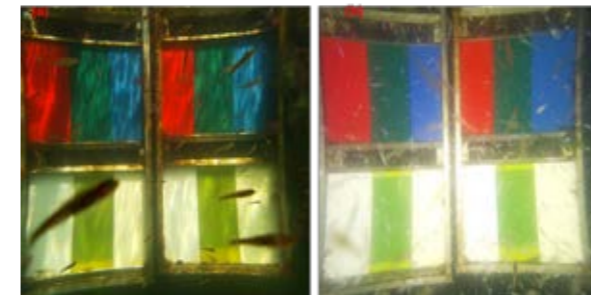


Figure 7: Underwater images challenges at including (a) Uneven illumination and (b) Interference from swimming fish and debris, resolved using median stacking technique.

Capturing clear underwater images is complicated by uneven illumination (a) and interference from swimming fish, debris, and floating materials (b), as illustrated in Figure 2. To overcome these challenges, median stacking techniques were employed to remove transient elements and floating algal tails, resulting in accurate biofouling coverage assessment

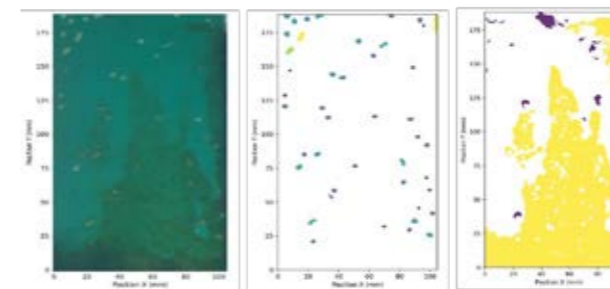


Figure 8: Image processing and machine learning based segmentation of algae, barnacles and their temporal evolution on a coated panel.

In Figure 3, machine learning-based image segmentation is applied to fouled panels, demonstrating automated classification of biofouling organisms including barnacles, algae, and identification of clean panel areas, with quantified percentage coverage for tracking fouling progression over time.

Conclusion

Marine biofouling remains a critical challenge in the marine industry, with classification and quantification methods often subjective and open to interpretation. Long-term underwater camera monitoring and automated data acquisition across varying environmental conditions provide valuable insights into biofouling formation cycles. The resulting datasets enable the development of machine learning models for automated, objective, and highly repeatable classification and evaluation methods, reducing reliance on subjective assessment standards.

Acknowledgements

This project gratefully acknowledges the financial support from the Hempel Foundation.

References

1. Cullinane, K. & Cullinane, S. Atmospheric Emissions from Shipping: The Need for Regulation and Approaches to Compliance. *Transp. Rev.* **33**, 377–401 (2013).
2. Pedersen, M. L., Weinell, C. E., Ulusoy, B. & Dam-Johansen, K. Marine biofouling resistance rating using image analysis. *J. Coat. Technol. Res.* **19**, 1127–1138 (2022).
3. Pedersen, M. L. *et al.* CoAST Maritime Test Centre: an investigation of biofouling propensity. *J. Coat. Technol. Res.* **20**, 857–868 (2023).
4. Santos, J. *et al.* A Tunable Hyperspectral Imager for Detection and Quantification of Marine Biofouling on Coated Surfaces. *Sensors* **22**, 7074 (2022).
5. Culverhouse, P., Williams, R., Reguera, B., Herry, V. & González-Gil, S. Do experts make mistakes? A comparison of human and machine identification of dinoflagellates. *Mar. Ecol. Prog. Ser.* **247**, 17–25 (2003).

Abstract

Developing a standardized method for marine biofouling assessment is critical for formulating new effective and environmentally friendly antifouling coatings, optimizing hull cleaning, and monitoring invasive species. While guidelines for evaluating fouling exist, they are subjective and open to different interpretations. Agreeability among experts is also rare due to the standardized method relying on subjective visual assessment. Computer vision using an underwater camera and Artificial Intelligence can provide an evaluation method devoid of bias and with high repeatability that helps to understand the different cycles of marine biofouling over long periods.

Introduction

Marine biofouling is a major problem in the shipping industry and for offshore structures, accounting for the increase in ship fuel consumption and consequently high CO₂ emissions. It also poses a threat to biodiversity through the transportation of invasive non-indigenous species to new environments through ship hulls and ballast water[1].

Current evaluation of marine biofouling relies on subjective techniques and expert opinions to classify and quantify the degree of fouling. While standards such as the Naval Ships' Technical Manual (NSTM), European Chemical Agency (ECHA) and American Society for Testing and Materials (ASTM-D3623) exists to guide assessment and evaluation of marine biofouling, interpretation of them and agreeability among experts vary. Repeatability of evaluation is therefore affected by the lack of an objective evaluation technique[2]–[5].

This PhD project investigates the use of underwater cameras to monitor the growth and attachment of biofouling organisms and collect data on the attaching organisms over a long period. These datasets are then carefully cleaned and used for training an automated machine learning-based classification model to identify

biofouling species. The long-term goal involves using computer vision from the cameras to make informed decisions on the degree and type of fouling species on the fouled substrates.

Results

Figure 1 shows the waterproof IP camera system deployed at the CoAST Maritime Test Center (CMTc) raft in Hundested, featuring LEDs for various lighting conditions and night-time imaging, a fluorescence filter for detecting certain biofouling organisms, and an automated servo motor wiper to maintain lens clarity. Python scripts and cronjobs enable remote control and automated image capture across different exposures and lighting scenarios, including HDR imaging through merged exposures.

Figure 2 illustrates the challenges of underwater imaging, including uneven illumination (a) and interference from swimming fish, debris, and other transient elements (b). To address these issues, median stacking techniques were employed to filter out moving objects and floating algal tails, ensuring accurate biofouling coverage assessment of the test panels.

Understanding the film formation of waterborne coating systems for high and extreme corrosivity

(April 2023 – March 2026)



Contribution to the UN Sustainable Development Goals

This project aligns with several UN Sustainable Development Goals (SDGs). By reducing the use of volatile organic compounds (VOCs) during coating application and developing sustainable protective coatings, this project mainly contributes to the sustainable production and consumption patterns in industries that rely on protective coatings. Traditional solvent-based coatings often involve VOCs that contribute to air pollution and environmental degradation. In contrast, waterborne (WB) coatings, with their low or zero VOC content, reduce harmful emissions and minimize environmental impact during manufacturing and application.



Abolfazl Arjmandi

aboar@kt.dtu.dk

Supervisors: Huichao (Teresa) Bi, Kim Dam-Johansen, Stefan Urth Nielsen

Abstract

Despite the wide range of environmental benefits of WB coatings, the conventional solvent-based coatings still offer superior performance, especially in higher corrosivity categories (defined in ISO 12944-2). WB systems are much more sensitive towards the coating application conditions compared to their respective solvent-based counterparts. The first goal of the project is to understand film formation/coalescence in WB systems and its sensitivity towards the coating application conditions. Having better film formation under a broader range of environmental factors (e.g., low temperatures and high humidities) and applications conditions (e.g., various types of substrates), and ability to understand key parameters driving coalescence in film formations will ensure the integrity and performance of futuristic WB coatings.

Introduction

The importance of anti-corrosive coatings cannot be overstated, as they play a vital role in safeguarding assets and infrastructure across various industries. Within this context, the emergence of waterborne (WB) coatings stands out for their paramount significance, offering a sustainable alternative to traditional solvent-based (SB) coatings and addressing pressing environmental concerns [1]. WB anti-corrosive coatings are commonly used in various industries to enhance the longevity and durability of metal components, thereby contributing to sustainability by reducing VOC emissions and promoting environmentally friendly practices.

Despite their eco-friendliness, the complexity of their film formation mechanism and the lack of understanding present challenges in enhancing the performance of waterborne coatings for corrosion protection [2]. These coatings are created by dispersing polymers in water, which then form a protective film on a substrate. The process involves stages like water evaporation, particle packing, and polymer interdiffusion, often leading to films with defects and inferior protection against extremely corrosive environments

compared to SB coatings [3]. WB coating systems applied and cured in controlled lab conditions tend to perform on par with solvent-based coating system alternatives. However, necessary application and drying conditions for WB coatings are very narrow and are difficult to replicate in real life industrial conditions, especially in areas with harsh environments.

To address the current challenges in the field, the interplay of factors affecting film formation in application, including coalescing agents, environmental factors, and application conditions are being studied in this project. To achieve this goal, different experimental methods accompanied by computational tools have been developed to simultaneously achieve new understandings and solutions.

Specific objectives

- Effect of substrate properties on the film formation behavior of WB coatings
- Effect of environmental conditions on the film formation behavior.

- Trying new innovative methods to study the film formation behavior in-situ.

Methodology

- Comprehensive literature review to obtain a proper perspective before taking any steps forward.
- Investigating the effects of substrate properties on film formation behavior, as illustrated in Figure 1.
- Investigating the effects of environmental factors on the film formation behavior, by letting the films dry and cure in the climate chamber while monitoring the water-loss (Figure 2).

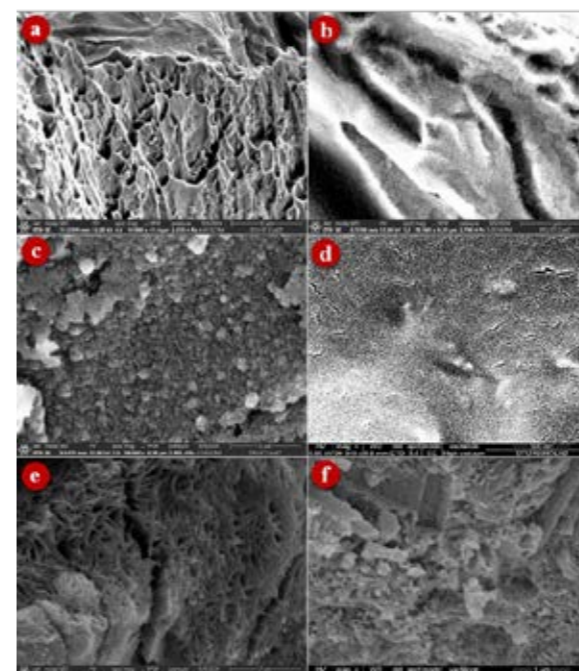


Figure 1. SEM images of the freeze-dried WB coating during formation at the molecular scale: (a) freshly applied film at lower magnification with obvious wholes related to the sublimated water (SB substrate), (b) separated polymer nanoparticles after water sublimation related to the freshly applied film (SB substrate), (c) poorly-ordered polymer nanoparticles after bulk water evaporation (SB substrate), (d) well-ordered polymer nanoparticles after bulk water evaporation (SS substrate), (e) cross-linked structure with large pores related to the poorly-ordered close-packed structure (SB substrate), and (f) highly dense cross-linked structure resulted from the well-ordered close-packed structure (SS substrate) [4].

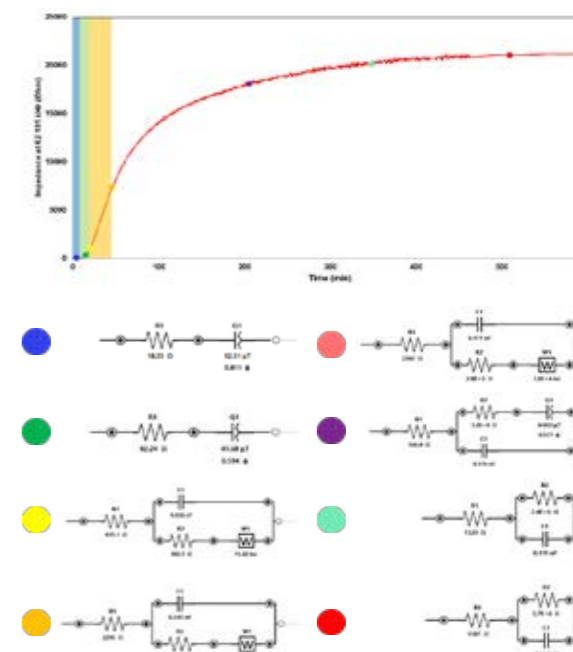


Figure 2. Impedance evolution over the full film formation duration with corresponding equivalent circuit models highlighting key physical and chemical transitions in the WB epoxy-amine coating with color labeling.

Acknowledgement

Financial support from the Hempel Foundation to CoaST (The Hempel Foundation Coatings Science & Technology Centre) is gratefully acknowledged.

References

1. M. Faccini, L. Bautista, L. Soldi, A.M. Escobar, M. Altavilla, M. Calvet, A. Domènech, E. Domínguez, Environmentally Friendly Anticorrosive Polymeric Coatings, *Applied Sciences* 2021, Vol. 11, Page 3446 11 (2021) 3446.
2. P.A. Sørensen, S. Kiil, K. Dam-Johansen, C.E. Weinell, Anticorrosive coatings: A review, *J Coat Technol Res* 6 (2009) 135–176.
3. A. Arjmandi, H. Bi, S.U. Nielsen, K. Dam-Johansen, From Wet to Protective: Film Formation in Waterborne Coatings, *ACS Appl Mater Interfaces* (2024).
4. A. Arjmandi, H. Bi, S.U. Nielsen, K. Dam-Johansen, Unveiling the role of substrate properties in shaping film formation in crosslinked waterborne coatings, *Surfaces and Interfaces* 61 (2025) 106150.

Scale-up, design, and cost estimation of technologies under development

(October 2023 – September 2026)

9 INDUSTRY, INNOVATION AND INFRASTRUCTURE



Contribution to the UN Sustainable Development Goals

MiEI [1] research and training project directly contributes to SDG 9 (Industry, Innovation, and Infrastructure) by developing novel electrosynthesis technology that combines the advantages of electrochemistry, micro-process engineering, and flow chemistry. The project supports sustainable industrialization by enabling reliable, flexible, safe, and environmentally friendly synthetic routes for the chemical industry.



Tuse

Asrav

tusas@kt.dtu.dk

Supervisors:

Gürkan Sin,
Merlin Alvarado-Morales

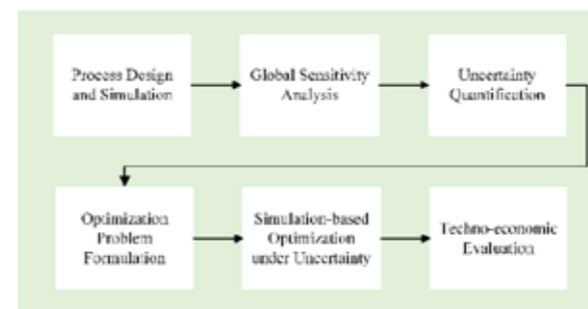


Figure 1: Robust Techno-economic Evaluation Framework

Results and Discussion

A comprehensive, robust TEA framework was successfully developed and validated. The stochastic optimization under uncertainty was benchmarked against a conventional deterministic optimization approach. Through the integration of sensitivity and uncertainty analyses, the framework identifies the most critical parameters influencing process economics. The developed framework enables the simultaneous exploration of process performance and economic feasibility under uncertainty, providing insights into the trade-offs between cost, yield, and process robustness. In the study, the objective function was to minimize the production cost, while yield and reactor residence times were enforced as technical constraints to ensure feasible operation and product quality. This approach reflects industrial practice, where cost efficiency must be achieved without compromising conversion, selectivity, or operability.

The results demonstrate that stochastic, uncertainty-aware optimization provides designs that are more resilient to real-world fluctuations than deterministic approaches. The stochastic approach accounts for fluctuations in process and market parameters, ensuring solutions that maintain both economic viability and technical reliability across a range of real-world scenarios. Having a robust design is important for decision-making in industrial technology adoption.

The next phase focuses on decarbonizing API manufacturing by applying the robust framework to electrochemical carboxylation for ibuprofen synthesis [2]. This work will compare the conventional continuous thermocatalytic route with a novel continuous electrochemical alternative that produces ibuprofen through electrocarboxylation of 1-chloro-(4-isobutylphenyl) ethane. The new study aims to jointly evaluate techno-economic performance and life-cycle impacts under uncertainty using the same simulation-optimization methodology.

Conclusions

The developed and validated framework provides a powerful decision-support tool for transforming novel, high-uncertainty technologies, like microfluidic electrosynthesis, into industrially viable processes. By prioritizing robustness, the research supports

strategic, informed decision-making in the pharmaceutical industry.

Acknowledgements

This work is part of the European Marie Skłodowska-Curie network MiEI. The MiEI project received funding by the European Union under the Grant Agreement no. 101073003. Views and opinions expressed are however those of the author(s) only and do not necessarily reflect those of the European Union. Neither the European Union nor the granting authority can be held responsible for them.

References

1. <https://project-miel.eu/>
2. Asrav, T., Alvarado-Morales, M., Sin, G. (2025). *Simulation-based techno-economic optimization of continuous ibuprofen manufacturing under uncertainty*. [Preprint]. *ChemRxiv*.
3. Mena, S., Sanchez, J., & Guirado, G. (2019). Electrocarboxylation of 1-chloro-(4-isobutylphenyl) ethane with a silver cathode in ionic liquids: An environmentally benign and efficient way to synthesize ibuprofen. *RSC Advances*, 9(26), 15115–15123.

List of Publications

1. Asrav, T., Alvarado-Morales, M., Sin, G. (2024). Optimization with Uncertainty for Pharmaceutical Process Design -Ibuprofen Synthesis as case study. *Computer Aided Process Engineering* 53, 1501-1506.
2. Asrav, T., Alvarado-Morales, M., Sin, G. (2025). Conceptual Modular Design for Continuous Pharmaceutical Processes: A Case Study on Ibuprofen. *35th European Symposium on Computer Aided Process Engineering 2025: Book of Short Papers* (pp. 119-120). Article 1426 EUROSIS.
3. Asrav, T., Alvarado-Morales, M., Sin, G. (2025). *Simulation-based techno-economic optimization of continuous ibuprofen manufacturing under uncertainty*. [Manuscript under review]

Abstract

Evaluating the economic viability of novel processes requires a robust techno-economic assessment (TEA) that accounts for inherent uncertainties. This study presents a comprehensive computational framework that integrates rigorous process simulation with simulation-based optimization under uncertainty. The framework combines conceptual process design, global sensitivity analysis, stochastic optimization, and rigorous economic evaluation in a unified workflow. The stochastic approach provides more conservative, robust optimal solutions compared to conventional deterministic methods, ensuring designs that better reflect real-world process variability and mitigate financial risk, which supports for reliable industrial scale-up of emerging technologies.

Introduction

The pharmaceutical industry is increasingly shifting from traditional batch manufacturing to continuous manufacturing, driven by the potential for significant improvements such as enhanced productivity, better quality control, and decreased costs. While continuous manufacturing adoption in the pharmaceutical industry is growing, the challenge remains in integrating novel, resource-efficient chemistry.

One highly innovative technology is microfluidic electrosynthesis, which is central to the MiEI project's mission of developing sustainable routes for fine chemicals and pharmaceuticals. Electrochemistry is an emerging technology that offers a greener alternative to traditional processes, often eliminating the need for hazardous reagents. However, its industrial application for the synthesis of active pharmaceutical ingredients (APIs) is currently limited, with a lack of data on its economic viability on an industrial scale.

To address this, our research focuses on developing and validating a sophisticated computational framework capable of generating robust design solutions that remain economically competitive and technically feasible despite the inherent

uncertainties. This methodology is essential for reducing risk during the scale-up and industrial adoption of novel electrochemical technologies.

Specific Objectives

The main objectives of this work are to establish and demonstrate early-stage design and economic evaluation capabilities for continuous flow processes. The developed robust techno-economic assessment (TEA) framework integrates a Stochastic Kriging (SK) optimization methodology with the AVEVA® process simulator, creating a unified workflow for process modeling, uncertainty analysis, and economic optimization. A Global Sensitivity Analysis (GSA) approach is systematically employed to identify and quantify the most influential technical and economic parameters affecting cost and process performance.

The framework was validated using the continuous manufacturing of ibuprofen through a thermocatalytic route, serving as a case study to demonstrate its robustness and applicability to real industrial challenges [2].

Transparent Antifouling Coating

(August 2024 – July 2027)

9 INDUSTRY, INNOVATION AND INFRASTRUCTURE



Contribution to the UN Sustainable Development Goals

This project supports **UN Sustainable Development Goal 9: Industry, Innovation, and Infrastructure** by developing innovative transparent antifouling coatings tailored for underwater optical devices, such as solar-powered autonomous underwater vehicles (AUVs), sensors, and cameras. Biofouling on these devices not only obstacles their operational efficiency but also reduces energy generation in underwater photovoltaic systems, increasing maintenance costs and lowering sustainability. The project combines antifouling efficiency with optical clarity, reducing energy loss and maintenance. By enhancing the performance durability and transparency of underwater devices, the project champions innovative approaches to sustainable solutions.

Abstract

The development of transparent antifouling coatings aims to address the persistent challenge of biofouling on underwater equipment, where optical clarity is a critical requirement. This research focuses on optimizing self-polishing coating and incorporating functional nanoparticles to achieve efficient antifouling performance while maintaining transparency for at least three months. The outcomes of this study provide promising insights for applications in solar-powered underwater vehicles and optical devices such as cameras and sensors, where long-term transparency and durability are essential.

Introduction

The colonization of submerged surfaces by marine organisms including algae, bacteria, and barnacles known as biofouling, represents a critical obstacle for both environmental sustainability and the reliable operation of marine technologies [1]. The attachment of these organisms to ship hulls and underwater equipment increases drag, fuel consumption, maintenance costs, and greenhouse gas emissions. For optical-based underwater devices, including sensors, cameras, and solar panels, biofouling poses an additional problem: the obstruction of light transmission, which reduces power generation efficiency and image quality. This issue is particularly critical for long-term deployments of Unmanned Underwater Vehicles (UUVs) and solar-powered Autonomous Underwater Vehicles (AUVs), which rely on clear optical surfaces to maintain performance [2].

Antifouling coatings have been extensively applied to prevent the attachment and growth of marine organisms by providing a protective barrier on submerged surfaces. Among the various antifouling approaches, self-polishing coatings have emerged as one of the most effective solutions to combat marine biofouling, primarily due to their controlled surface erosion when exposed to seawater [3]. These coatings are engineered to gradually wear away, continuously exposing fresh material while enabling the steady

release of active compounds such as antimicrobial pigments or nanoparticles. This leaching mechanism maintains a smooth surface that minimizes the adhesion of fouling organisms, while the ongoing release of biocidal components sustains antifouling activity over extended periods. Organic booster biocides are often incorporated to broaden the spectrum of protection against diverse marine species, further enhancing coating efficiency.

However, most conventional antifouling coatings have been designed with durability in mind rather than optical clarity, which restricts their applicability in systems where transparency is essential. This research aims to address this limitation by developing transparent, self-sustaining antifouling coatings that maintain both optical performance and long-term protection. The proposed system employs a self-polishing coating combined with seawater-soluble nanoparticles possessing strong antifouling activity. This formulation enables continuous surface renewal and stable light transmission throughout extended immersion. Consequently, coatings reduce maintenance demands and eliminate the need for frequent mechanical cleaning, providing a sustainable and cost-effective solution for marine applications that require both transparency and durability.



Zeynep

Aydin

zeynay@dtu.dk

Supervisors: Søren Kiil
Narayanan Rajagopalan

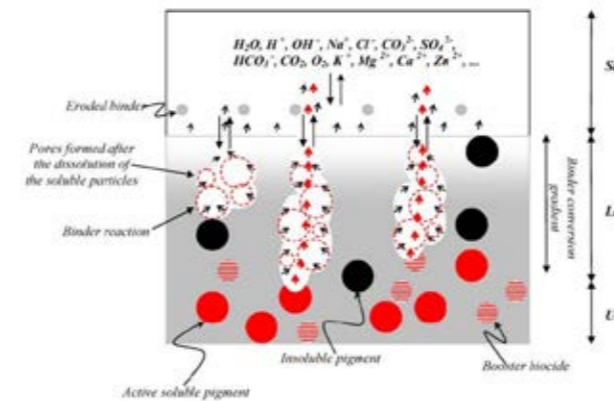


Figure 1. Schematic illustration of the behavior of a biocide-based antifouling system exposed to sea water [1].

The potential applications of these advanced coatings are particularly relevant for underwater optical devices, such as AUVs, cameras, and sensors. By combining high antifouling efficiency with optical transparency, these coatings are expected to significantly improve the operational reliability, energy efficiency, and lifespan of marine technologies used in challenging underwater environments.

further contributed to improved microstructural uniformity and enhanced antifouling resistance without compromising light transmission.

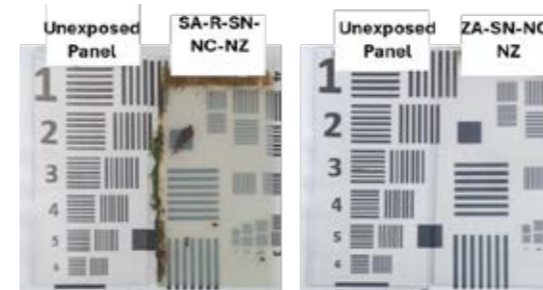


Figure 2. Visual comparison of two different self-polishing transparent antifouling coatings after 8 weeks of seawater exposure. The coatings display clear differences in antifouling performance, water-whitening resistance, and light transmittance, highlighting the importance of formulation optimization.

Conclusions

This study demonstrates the feasibility of developing transparent self-renewing antifouling coatings that maintain both biofouling resistance and optical stability during prolonged exposure. The integration of optimized coating formulation with functional nanoparticles enhances transparency, mechanical strength, and long-term resistance to marine degradation. The self-polishing mechanism enables continuous surface renewal, effectively minimizing fouling and reducing maintenance needs. Overall, the findings highlight a promising approach for creating durable, transparent coating systems

Specific Objectives

Preliminary investigations into transparent antifouling coatings have demonstrated promising antifouling capabilities; however, prolonged exposure to seawater has resulted in the formation of surface haze, thereby reducing optical transparency [4]. The central objective of this research is to elucidate the mechanisms responsible for this haziness and to develop coating formulations that can maintain high transparency for at least three months under static seawater conditions. This involves a detailed understanding of formulation behavior and the incorporation of seawater-soluble nanoparticles, specifically nano-Cu₂O and nano-ZnO, which are known to enhance both antifouling efficacy and optical performance. By strategically combining these components, the study aims to achieve coatings that offer long-lasting protection and superior transparency.

Results and Discussion

Preliminary findings indicate that the optimization of coating composition significantly influences both the durability and optical clarity of the coatings. The incorporation of functional additives

tailored for underwater optical applications such as sensors, cameras, and solar-powered devices.

Acknowledgements

The authors would like to acknowledge the Office of Naval Research (ONR), US Navy, USA for financial support (Project TBAC II, Award Number: N000142412349) and the Hempel Foundation for funding to CoaST (The Hempel Foundation Coatings Science and Technology Centre).

References

1. D. M. Yebra, S. Kiil, and K. Dam-Johansen, Prog. Org. Coatings 50 (2) (2004) 75–104.
2. G. Wang, Y. Yang, and S. Wang, Applied Energy 728 (2020) 115752.
3. D. M. Yebra, S. Kiil, K. Dam-Johansen, and C. Weinell, Prog. Org. Coatings 53 (4) (2005) 256–275.
4. N. Rajagopalan and S. Kiil, Prog. Org. Coatings 196 (2024) 108756.

Sustainable Blowing Agent Systems for Intumescent Coatings: From Lab to Application

(September 2025 – August 2028)

9 INDUSTRY, INNOVATION AND INFRASTRUCTURE



Contribution to the UN Sustainable Development Goals

The project develops safer high-performance fire-protective coatings for steel structures. By keeping steel cooler for longer during fires, they lower the risk of building and infrastructure collapse. These coatings lower the toxicity exposure of workers during application and produce less toxic smoke during a fire. Overall, this improves the resilience and sustainability of infrastructure while driving innovation in fire protection.



Apostolos Batsinis

apoba@dtu.dk

Supervisors: Kim Dam-Johansen, Emil Lidman Olsson

Abstract

At 500 °C steel has lost 40 to 45% of its load bearing capacity, which is why intumescent coatings are often used to protect it against fire. Conventional intumescent coatings typically use ammonium polyphosphate as acid source, pentaerythritol as carbon source, and melamine as blowing agent. However, these chemicals release toxic chemicals such as CO, NH₃, and HCN. Furthermore, melamine has been classified as possibly carcinogenic. Although many studies have investigated various aspects of intumescent formulations, including replacement of melamine, systematic comparisons that clarify the blowing agent mechanism are rare. This project will identify a viable substitute for melamine, clarify its mechanism, quantitatively benchmark it against melamine. Furthermore, the structure and reactivity will be characterized to enable targeted modification, and integrate the optimized material into intumescent coating formulations.

Introduction

In every country, the construction sector is critical, as it provides the infrastructure that ultimately influences the economy. In this sector, a variety of materials are used, such as steel, concrete, wood, plastic, and composites. Steel is the most popular choice among these, as evidenced by the fact that 50% of the total global steel production is used in the construction industry [1]. For all types of public and private buildings, a well thought out strategy for fire prevention and protection is needed and must be implemented [2], [3]. There are various ways to achieve this. These methods are typically divided into active fire protection, such as alarms and detection systems, and passive fire protection, such as cement coatings and intumescent coatings [4]. Regardless of the method applied, the main aim is to keep the steel substrate cool for a sufficiently long time. Because when steel reaches 500 °C, it has lost 40 to 45%

of its load bearing capacity, which leads to an increased risk of building collapse [1].

Nowadays, it is common to use steel as part of the design of buildings, which is why it is important for the shape and appearance of the steel structures to be visible. To achieve this, the applied fire protection method needs to be very thin, leading to a growing interest in the use of intumescent coatings [5]. These coatings are specially designed products that rely on three key chemicals: an acid source, a carbon source, and a blowing agent, and these must be aligned in both their ratios and their behavior under fire [5]. When a fire breaks out and the coatings start to heat up, a series of reactions takes place. First, the whole matrix starts to soften, then the protective char is created, and in the last step gases are released, which leads to the expansion of the char [1]. This creates an insulative barrier separating the steel substrate from the fire [1].

The current state of the art systems are based on formulations with a high content of organic

chemicals. In both literature and industry, ammonium polyphosphate, pentaerythritol, and melamine or similar derivatives of these compounds are often used. However, the main drawback of organic intumescent systems has always been their release of toxic gases such as CO, NH₃, and HCN during a fire [6]. Furthermore, due to the classification of melamine as possibly carcinogenic, there is a need to find a viable alternative [7].

Many studies focusing on adjusting the formulation of intumescent coatings have been published [5,8]. Although published work has partly focused on a transition from melamine to other blowing agents, no studies perform systematic comparisons to explain the working mechanism of the new blowing agent. This project aims to identify a viable substitute for melamine, clarify its mechanism of action, quantitatively benchmark its performance against the established standard, and characterize its chemical structure and reactivity.

Experimental

The experimental work will focus on evaluating alternative blowing agents for intumescent coatings. This will be done by preparing formulations with and without a reference blowing agent, while holding all other compounds and processing parameters constant. This approach enables a direct comparison of how the blowing agent choice influences activation temperature, gas release, char yield, and the insulating performance of the expanded layer.

Various techniques will be employed to link molecular-level behavior to fire protection performance. Thermogravimetric analysis will be used to determine thermal stability, mass-loss steps, and decomposition onset, defining the activation window and gas-generation profile. Scanning electron microscopy will be used to examine the morphology of the expanded char, including cell size, wall thickness, and crack distribution, which are closely related to thermal insulation and mechanical integrity. With X-ray diffraction, crystalline phases before and after heating will be identified, clarifying whether inorganic phase evolution takes place. Nuclear magnetic resonance spectroscopy will be used to probe the chemical structure of the organic components and possible interactions between the blowing agent, acid source, and carbon source that may influence intumescent efficiency and char cohesion.

Hot-stage digital microscopy provides real-time visualization of softening, foaming onset, bubble growth, and collapse as a function of temperature,

thereby connecting decomposition events to expansion kinetics and final microstructure. Finally, furnace tests on coated steel panels supply an application-oriented measure of performance by quantifying expansion, char stability, and the ability to reduce heat transfer to the substrate under controlled high-temperature exposure.

Together, these methods are used to (i) map the decomposition pathway and gas evolution of each candidate, (ii) relate microstructural features of the char to its insulating function, and (iii) quantify protection effectiveness relative to the reference.

References

1. M. Yasir, et al., Surf. Eng. 36 (4) (2020) 334–363.
2. A. Sciarretta, F. Sousa, M.L. Dimova, S. Athanasopoulou, The status and needs for implementation of fire safety engineering approach in Europe, 2003
3. J. Abrahams, P. Stollard, Fire from first principles: A design guide to building fire safety, 2003
4. R.G. Puri, A.S. Khanna, J. Coat. Technol. Res. 14 (1) (2017) 1–20.
5. A. Lucherini, C. Maluk, J. Constr. Steel Res. 162 (2019) 105712.
6. A. Fu, et al., Prog. Org. Coat. 190 (2024) 108354.
7. Health and Environment Alliance (HEAL), (2024). https://www.env-health.org/wp-content/uploads/2024/05/HEAL_contribution_PC_AnnexXIV_incl_Melamine_final.pdf
8. T. Mariappan, J. Fire Sci. 34 (2) (2016) 120–163.

Corrosion mitigation of steel monopiles for the offshore wind industry by coatings

(December 2022 – November 2025)

12 RESPONSIBLE CONSUMPTION AND PRODUCTION



Contribution to the UN Sustainable Development Goals

The development of an effective and feasible corrosion mitigation method for the offshore wind turbines will lead to an increase in their life expectancy. As a result, the required materials for production, installation and corrosion protection for the offshore wind turbines will be reduced, combined with a simultaneous decrease in the use of fossil fuels for their production, installation, and transportation, contributing to a more sustainable consumption and production and reducing CO₂ emissions.



Charalampos Belesakos

charbel@dtu.dk

Supervisors: Huichao (Teresa) Bi, Kim Dam-Johansen, Claus Erik Weinell

Abstract

Offshore steel monopiles are highly vulnerable to corrosion, that can compromise their structural integrity and reduce their service-life. As offshore wind deployment accelerates, there is a growing need for more efficient corrosion protection strategies improving protection against the aggressive marine conditions. A combined approach utilizing coatings and cathodic protection offers strong potential for improved durability. This study will explore the influence of environmental parameters on internal monopile corrosion and assess the performance of coatings and cathodic protection systems through both lab and real-field tests, aiming on developing an effective mitigation method, extending the monopile's service-life.

Introduction

The rapid expansion of offshore wind energy is driving the installation of monopile foundations, large steel cylinders, favored for their simple design, cost-efficiency, and suitability in waters up to 30 m [1]. Yet, despite being designed for a 25-year lifetime, monopiles face severe durability challenges in the offshore environment, where corrosion is accelerated by high salinity, dissolved oxygen, wet-dry cycles, and changes in pH and temperature [2]. The monopile installation and maintenance represent a major share of windfarm costs, requiring effective corrosion mitigation for extending service life and reducing lifetime costs [1]. Current protection strategies combine corrosion allowance, coatings, and cathodic protection using Sacrificial Anodes (SACP) or Impressed Current systems (ICCP) [3]. Internal monopile corrosion remains a major concern: stagnant seawater, oxygen and seawater ingress, and limited ventilation sustain corrosion despite early assumptions of oxygen-depleted conditions [4–6]. These environments may become anaerobic, promoting microbial-induced corrosion

(MIC), and both localized and uniform corrosion [4–6].

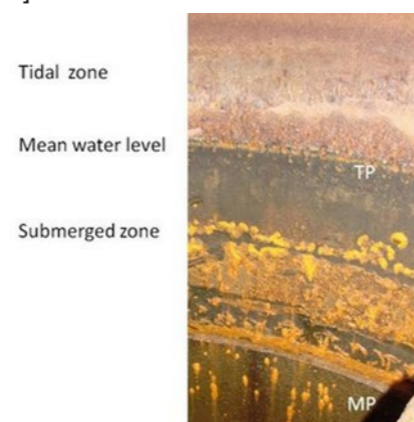


Figure 9: Observed internal corrosion during field inspection [4].

To ensure long-term stability, ICCP systems must be carefully designed, often in combination with coatings [7,8]. Although internal protection with coatings is considered optional, increasing evidence highlights its importance for long-term structural integrity [9].

Specific Objectives

The aim of this study is to identify the key environmental factors of internal monopile corrosion and develop an effective long-term mitigation strategy. The work focuses on the corrosion process under varying conditions, and on improving corrosion protection by both organic coatings and ICCP. The study utilizes coatings science to advance protective solutions by combining multiple technologies with an emphasis on holistic and emerging strategies in offshore corrosion mitigation. Coating and ICCP systems will be assessed for performance and limitations through lab and field-testing. The correlation between lab-scale and field data will support a robust protection strategy that enhances the long-term durability of offshore wind monopiles.

Results

The corrosion mitigation strategy will be evaluated on steel panels exposed both in the lab and in real-field conditions at the CoaST Maritime Test Center (CMTC), in Hundested harbor. Custom test setups simulating internal monopile conditions will allow direct comparison of lab and field performance. Post-exposure analyses will assess coating behavior, while the ICCP will be continuously monitored in both environments. The lab and field setups are shown in Figure 2.



Figure 10: Lab (left) and field (right) experimental setups.

The combined mitigation strategy showed that ICCP performance depended strongly on the applied conditions. Future work will further clarify coating protection mechanisms and ICCP efficiency through targeted testing and post-exposure characterization. **Conclusions**

Offshore wind monopiles operate in highly aggressive marine environments that accelerate corrosion, lower lifespan and raise maintenance costs. Effective mitigation is therefore essential to maintain structural integrity and limit lifetime costs. Combining organic coatings with ICCP shows strong potential, but their performance under internal monopile conditions is not yet fully understood. This study develops and evaluates a corrosion protection strategy based on coatings and cathodic protection, demonstrating effective performance. By investigating the monopile internal corrosion and environmental impacts, this

work aims to optimize corrosion mitigation and support long-term monopile durability.

Acknowledgements

Financial support from the Hempel Foundation to CoaST (The Hempel Foundation Coatings Science and Technology Centre) is greatly acknowledged.

References

1. P. Iwicki, J. Przewłócki, Short review and 3-d fem analysis of basic types of foundation for offshore wind turbines, *Pol. Marit. Res.* 27 (2020) 31–39. <https://doi.org/10.2478/pomr-2020-0044>.
2. T. Kirchgeorg, I. Weinberg, M. Hörnig, R. Baier, M.J. Schmid, B. Brockmeyer, Emissions from corrosion protection systems of offshore wind farms: Evaluation of the potential impact on the marine environment, *Mar. Pollut. Bull.* 136 (2018) 257–268. <https://doi.org/10.1016/j.marpolbul.2018.08.058>.
3. C. Erdogan, G. Swain, Conceptual sacrificial anode cathodic protection design for offshore wind monopiles, *Ocean Eng.* 235 (2021) 109339. <https://doi.org/10.1016/j.oceaneng.-2021.109339>.
4. L.R. Hilbert, A.R. Black, F. Andersen, T. Mathiesen, Inspection and monitoring of corrosion inside monopile foundations for offshore wind turbines, in: *European Corrosion Congress 2011, EUROCORR, European Federation of Corrosion, Stockholm, 2011*: pp. 2187–2201.
5. I.A. Chaves, R. Petersen, R.E. Melchers, R. Jeffrey, Corrosion of the interior steel surfaces of offshore monopiles, *Ships and Offshore Structures.* (2022). pp. 1–9
6. W. Khodabux, P. Causon, F. Brennan, Profiling corrosion rates for offshore wind turbines with depth in the North Sea, *Energies* 13 (10) (2020)2518.
7. A. Delwiche, P. Lydon, I. Tavares, Concerns over utilizing Aluminium alloy anodes in sealed environments, in: *CORROSION 2017 Conference and Expo, NACE International, New Orleans, LA, USA, 2017*: pp. 1–14. <https://doi.org/10.5006/C2017-08956>.
8. Q.T. Tran, G. Benoit, O. Le Guennec, C. Leballeur, Optimization of the corrosion protection for offshore windfarm monopile foundation-Engineering design lessons learnt, *NACE International Corrosion Conference & Expo*, (2019).
9. H. Osvoll, G.Ø. Lauvstad, T. Mathiesen, CP design and retrofit for offshore wind turbine monopile foundations, in: *EUROCORR 2015, European Federation of Corrosion, Graz, Austria, 2015*.

Microplastics from fouling control coatings

(February 2023 – January 2026)

14 LIFE BELOW WATER



Contribution to the UN Sustainable Development Goals

Plastic pollution in the world's oceans has been a known and growing problem for marine wildlife. Particularly, microplastics have received a lot of concern from both society and the scientific community. Amongst other sources, fouling control coatings on ships have been found to generate microplastics. How these microplastics are formed and how much of the coating gets released as microplastics is currently not fully understood. By gaining more knowledge on these microplastics, the groundwork will be laid for future solutions to reduce or mitigate their release into the environment.



Matthias

Bork

merbo@kt.dtu.dk

Supervisors: Kim Dam-Johansen, Søren Kiil

Abstract

Microplastics are a persistent and ubiquitous contaminant in the marine environment. There are various sources of microplastics, amongst which are fouling control coatings. These coatings are used to combat biofouling on the hull of a ship or other submerged structures by employing biocides and self-polishing polymer matrices. While these matrices are expected to polish away over a coating's lifetime, how much of this is released as microplastics is not fully understood. This project aims to provide a perspective on release rates and gain a better understanding of the release mechanisms and properties of microplastics from fouling control coatings. This is done by performing controlled laboratory experiments, simulating ship hulls under different conditions to analyze different types of ship coatings and the microplastics they release.

Introduction

Submerged artificial structures experience the attachment of a wide variety of organisms to their surfaces. This is called biofouling and causes a variety of problems, for ships this is primarily the increase of drag and accelerated deterioration of the ship hull. To compensate for the increased drag resistance, a ship needs to use more fossil fuel to maintain the same speed, resulting in more harmful emissions. Modern ships make use of fouling control coatings on the hull to combat biofouling [1].

Fouling control coatings can be classified based on the mechanism used to combat biofouling. The main categories are antifouling coatings, employing biocides to deter organisms, and foul release coatings, using surface hydrophobicity to prevent the attachment of organisms. Antifouling coatings contain biocides (often Cu- or Zn-based) [2]. The release of these biocides is controlled through the porous leached layer which forms when the coating is in contact with seawater. This leached layer polishes away during sailing to maintain biocide release. Self-polishing coatings use acrylic copolymeric binders which are initially water insoluble, however through

hydrolysis of hydrophobic functional groups they become hydrophilic and eventually water soluble [3].

It has thus far been assumed that self-polishing binders dissolve and pose little further harm to non-target organisms, aside from the emitted biocides. However, in recent oceanic microplastic surveys, microplastics have been identified which likely originate from these antifouling coatings, seemingly challenging this assumption [4].

Microplastics are microscopic insoluble solid anthropogenic polymer particles and are a ubiquitous contaminant in nearly every natural environment. In the marine environment they pose a great threat due to their potential toxicity to marine life and continual poorly reversible accumulation [5]. While microplastic surveys have been ongoing since their rise in popularity 20 years ago, only recently have paint particles been found to make up a significant part of the total microplastic count [6].

As with many other types of microplastics found in the marine environment, the exact mechanisms of the formation of these microplastics are unknown. Through controlled laboratory experiments and specialized analysis techniques, a more

comprehensive understanding of the generation and nature of fouling control coating microplastics can be found.

Specific Objectives

The specific objectives of this project are:

1. Develop a robust testing methodology for microplastic release from fouling control coatings.
2. Quantify microplastic release from fouling control coatings and compare different coatings.
3. Understand and compare the properties and release mechanisms of fouling control microplastics during sailing and during cleaning.

Results and Discussion

Coatings were exposed using a rotor setup, simulating the surface of a sailing ship. The water was then filtered to collect released microplastics. The filters were analyzed using an automated scanning electron microscope (SEM) and energy dispersive x-ray spectroscopy (EDX) procedure. Figure 1 shows an example of how the analysis of one image with this method.

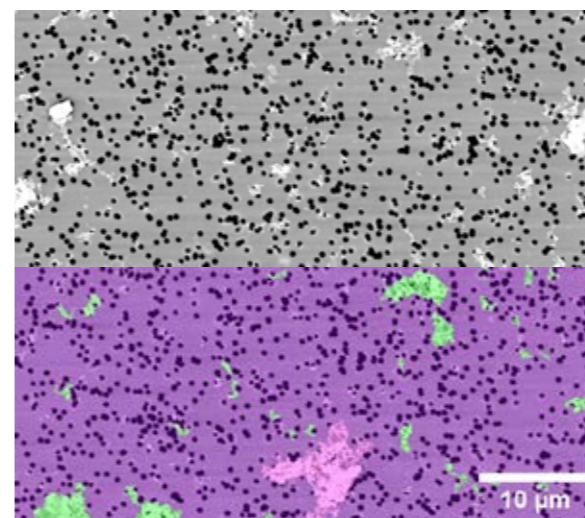


Figure 11: SEM image of released particles. Top half shows the original image and the bottom half shows where particles were detected.

From this it was found that a significant portion of the polished coating gets released as microplastic. The particles have a mean size of around 1-3 μm and follow a logarithmic distribution (Figure 2). They are predominantly made up of polymeric materials. However, they can also contain a Cu and Zn from the biocides in the coating. They are likely released from the porous leached layer. This layer at the surface of the coating is mechanically weaker than the bulk of the coating and can therefore easily fragment under stress from eg. sailing or cleaning.

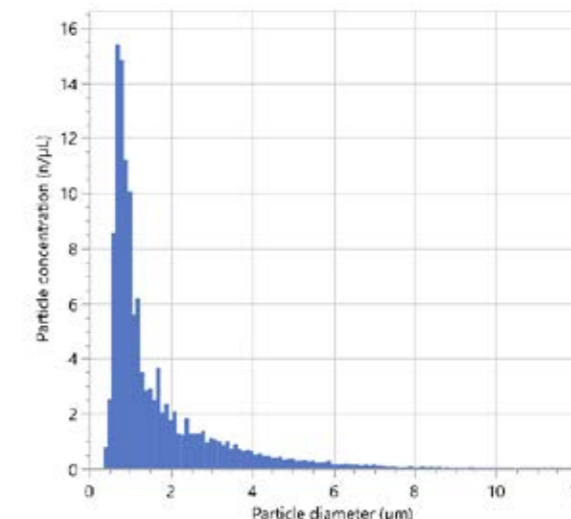


Figure 2: Example of a particle size distribution of particles released from an antifouling coating.

Conclusions

Antifouling coatings release microplastics while a ship is sailing. These particles come from the leached layer and can contain biocides. This is an issue for the sustainability of these coatings, as global release might be significant, compared to other microplastic sources.

Acknowledgements

Financial support from the Hempel Foundation to CoaST (The Hempel Foundation Coatings Science and Technology Centre).

References

1. D.M. Yebra, S. Kiil, K. Dam-Johansen, Prog. Org. Coat. 50 (2) (2004) 75-104
2. Amara, W. Miled, R.B. Slama, N. Ladhari, Environ. Toxicol. Pharmacol. 57 (2018) 115-130
3. Q. Xie, J. Pan, C. Ma, G. Zhang, Soft Matter 15 (6) (2019) 1087-1107
4. C. Dibke, M. Fischer, B.M. Scholz-Böttcher, Environ. Sci. Technol. 55 (4) (2021) 2285-2295
5. M. MacLeod, H.P.H. Arp, M.B. Tekman, A. Jahnke, Science 373 (2021) 61-65
6. Turner, Water Res. X 12 (2021) 100110

List of publications

M.Bork, S. Kiil, P.F. Gostin, K.Dam-Johansen, Environmental pollution 386 (2025) 127251

Unveiling the water-energy nexus for water utilities wastewater reuse for district heating applications

(March 2023 – February 2026)



Contribution to the UN Sustainable Development Goals

Wastewater treatment plants (WWTP) significantly impact energy, climate, and water, making these facilities a major contributor to environmental challenges and climate change. This project aims to transform WWTPs into resource recovery facilities by converting wastewater into an energy resource and contribute to Denmark's goal of achieving carbon neutrality by 2050, assessing the potential to reuse wastewater for energy purposes.



Francisca Braga

franbra@dtu.dk

Supervisors: Krist V.Gernaey, Søren Erbs Poulsen (VIA University College), Kurt Poulsen (Skanderborg Forsyning), Xavier Flores-Alsina and Carina Gargalo

Abstract

Wastewater treatment plants (WWTPs) are significant contributors to global energy use and greenhouse gas emissions, largely due to aging infrastructure and inefficient operations. This project develops a decision support tool that integrates multiple assessment methods like economic analysis, life cycle assessment, and mathematical modelling to evaluate the trade-offs between centralized and decentralized WWTP configurations. Using a real-world case study, the tool supports strategic planning by considering technical, environmental, and economic dimensions. It also explores opportunities for integrating wastewater heat recovery (WWHR), helping identify where thermal energy can be effectively utilized to enhance system sustainability and resilience.

Introduction

Aging infrastructure in wastewater treatment plants (WWTPs) poses a growing challenge for the water sector. Around 27% of active WWTPs in Europe are either overloaded or outdated [1]. Additionally, WWTPs account for approximately 3% of global energy demand [2], making them significant contributors to greenhouse gas emissions and climate change. Efficient management of these facilities is therefore essential for sustainable development.

Wastewater from households, industries, and businesses contains untapped thermal energy—generated through heating, cooling, and chemical processes. Recovering this energy can reduce overall consumption and mitigate emissions. Advanced wastewater heat recovery (WWHR) technologies, such as heat exchangers and heat pumps, enable the capture and reuse of this thermal energy. These systems offer energy savings and emissions reductions across residential, commercial, industrial, and district heating applications. By integrating

WWHR into both new and existing WWTPs, we can shift the perception of wastewater from waste to a valuable energy resource, supporting a more sustainable future.

Objectives of the project

The primary objective of this collaborative project between Skanderborg Forsyning, DTU, and VIA University College is to develop a framework using various decision support tools, such as economic analysis, life cycle assessment (LCA), and mathematical models, to evaluate infrastructure scenarios in a real case study involving the consolidation of five WWTPs into two WWTPs. The project also explores how wastewater heat recovery can be effectively implemented within this context.

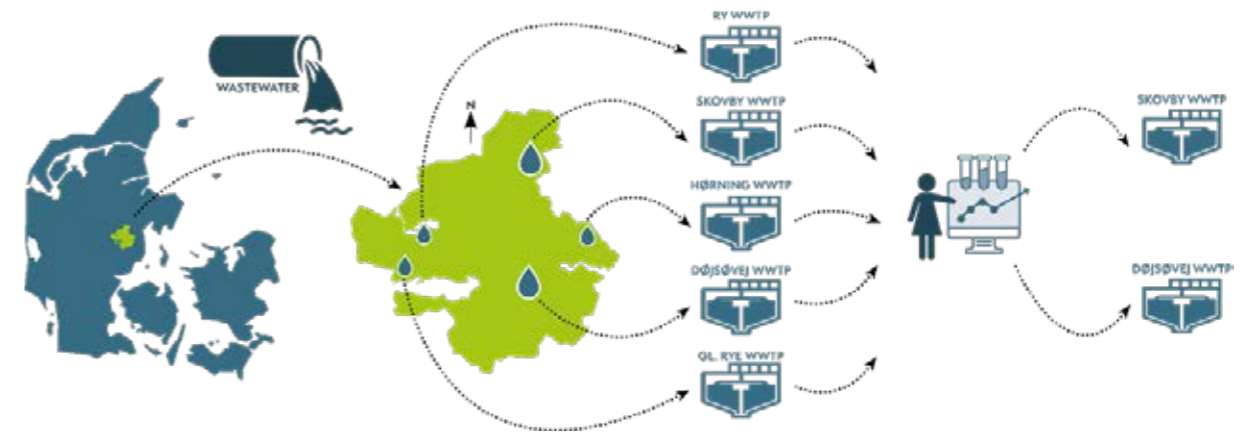


Figure 12: Conceptual framework of the project

Data collection and model development

Mathematical models (influent generator, WWTP, and catchment) have been developed to capture the characteristics and dynamics of the WWTPs and assess the capacity of Skovby and Døjsøvej WWTPs to receive the extra flow from the other plants [3,4].

The influent generator model presented has been used to capture the variation of the inlet water and how this can affect the heat recovery locations in the catchment or within the WWTP.

The WWTP performance model was utilised to analyse the behaviour and performance of the WWTP. This model can also predict the quality of the effluent and evaluate the economic benefits and operating costs of the WWTPs.

The techno-economic analysis evaluates the costs of a centralised scenario, where flows from three smaller WWTPs are redirected to Skovby and Døjsøvej WWTPs. This includes OPEX, pipeline construction, maintenance, staffing, CAPEX, and renovation costs over 40 years.

The life cycle assessment (LCA) identifies the environmental trade-offs between centralisation and decentralisation and assesses the impact of integrating heat recovery on overall environmental performance.

In addition to optimisation, the developed tools serve a wider purpose in addressing decisive questions. These include exploring the effects of centralisation on system performance, assessing the impact of temperature reduction on the nitrification process, determining reactor capacity adjustments, and evaluating infrastructure resilience under uncertain climate scenarios. The scenario analysis helps in understanding the potential challenges and opportunities associated with the implementation of WWHR systems in different contexts.

Conclusions

The findings from this project highlight several important insights for the future planning and optimization of wastewater treatment systems:

- Centralised systems are economically more viable compared to decentralised alternatives.
- Decentralised systems, however, tend to have lower environmental impacts.
- The framework supports utilities in comparing centralised and decentralised WWTP options, particularly in the context of ageing or overburdened infrastructure. However, the tool must be adapted to local conditions to ensure relevance and effectiveness.

Acknowledgments

The author gratefully acknowledges the financial support from Innovation Fund Denmark under Grant Number 2108-00003B.

References

1. European Environmental Agency European Environmental Agency. Waterbase - UWWTD: Urban Wastewater Treatment Directive – reported data 2024
2. Nakkasunchi, S., Hewitt, N.J., Zoppi, C. and Brandoni, C., Journal of Cleaner Production 279 (2021).
3. Gernaey, K.V. et al, Dynamic influent pollutant disturbance scenario generation using a phenomenological modelling approach. Environmental Modelling & Software. 26 1255-1267 (2011).
4. Solís B. et al, A plant-wide model describing GHG emissions and nutrient recovery options for water resource recovery facilities. Water research. 215 118223 (2022)

Digital quality by design with model-based design of experiments

(January 2024 – January 2027)



Contribution to the UN Sustainable Development Goals

This project contributes to UN Sustainable Development Goal 12: Responsible Consumption and Production.

By implementing a model-based design of experiments (MBD_{oE}) approach, the project aims to make bioprocess development more efficient. MBD_{oE} enables the design of informative experiments that minimize redundancy, thus reducing the consumption of materials, time, and energy associated with traditional experimental design. The resulting workflow promotes a more sustainable and knowledge-driven approach to developing and optimizing biological processes.



**Ana Helena
Valdeira Caetano**

ahvca@dtu.kt

Supervisors: Krist V. Gernaey and Julian Kager

Abstract

This project demonstrates the application of model-based design of experiments (MBD_{oE}) to dynamically optimize glucose feed profiles in a *Saccharomyces cerevisiae* fed-batch process. An *in silico* study is performed to study the Crabtree effect, which is the metabolic shift from respiration to fermentation. The aim is to utilize an MBD_{oE} approach to improve the identifiability of key kinetic parameters while reducing the number of experiments required for model calibration, when using only off-gas data. This framework should pave the way for real-time adaptive MBD_{oE} and result in a reduction of the required number of experiments to obtain the desired model accuracy.

Introduction

Model-based design of experiments (MBD_{oE}) is becoming a key concept within the Quality by Design (QbD) and Process Analytical Technology (PAT) frameworks, as it offers an automated and knowledge-driven approach, in contrast to traditional experimental design [1]. While the first stage of this project demonstrated the implementation of MBD_{oE} for oxygen transfer characterization (namely the determination of the volumetric mass transfer coefficient, k_{La}) in a stirred-tank reactor, the current work extends the MBD_{oE} methodology to a dynamic biological system – a *Saccharomyces cerevisiae* fed-batch process.

In this system, yeast cells undergo the Crabtree effect, which is the metabolic shift from respiration to fermentation at high sugar uptake rates. This phenomenon dictates the distribution of carbon fluxes and overall process productivity, hence capturing it is crucial for accurate model calibration and process understanding. Because this metabolic behavior is nonlinear and time-dependent, it requires dynamic experiments to excite different key states and parameters.

By combining mechanistic modeling, sensitivity analysis, and design optimization, MBD_{oE} allows experiments to be planned iteratively, thus ensuring that each new run contributes with maximal information towards identifying the process kinetics [2]. This digital workflow aims to demonstrate how MBD_{oE} can improve parameter identifiability and reduce experimental redundancy for complex biological systems.

Specific Objectives

The main objective of this phase of the project is to apply MBD_{oE} to the design of dynamic glucose feed trajectories in *S. cerevisiae* fed-batch processes, thereby maximizing the information content of each experiment. A mechanistic model describing *S. cerevisiae* growth and ethanol formation, based on the formulation of Sonnleitner and Käppli (1986) [3], serves as the benchmark. The model includes ten kinetic parameters.

The study aims to compare optimized feed trajectories, which are generated by the MBD_{oE} algorithm and evaluate improvements in information gain, parameter accuracy, and robustness. Furthermore, this framework seeks to

demonstrate that reliable model calibration can be achieved using only online off-gas measurements (O_2 , CO_2 and ethanol). Ultimately, the goal is to build a foundation for a real-time adaptive MBD_{oE} strategy capable of updating experimental inputs during ongoing fermentations.

Results and Discussion

A mechanistic model representing yeast metabolism, including both oxidative and reductive pathways, is employed to simulate fed-batch fermentations. The glucose feed rate serves as the manipulated variable, while the off-gas composition (O_2 , CO_2 and ethanol) represents the measurable outputs.

Each simulated run corresponds to a full lab-scale fed-batch fermentation with a unique combination of feed trajectories. After each feed trajectory, the model parameters are re-estimated from the synthetic data, and local sensitivities of the output with respect to the parameters were calculated. These sensitivities form the basis for constructing the Fisher Information Matrix (FIM), which quantifies the expected information content of an experiment.

The overall MBD_{oE} workflow is illustrated in Figure 13, where experimental data and model calibration are iteratively coupled with model analysis and experimental redesign. Following each iteration, model confidence is assessed through identifiability, sensitivity, and uncertainty analysis. If the confidence is insufficient, the next experiment is automatically redesigned to maximize information gain based on the FIM. This loop continues until the model achieves the desired level of precision and robustness.

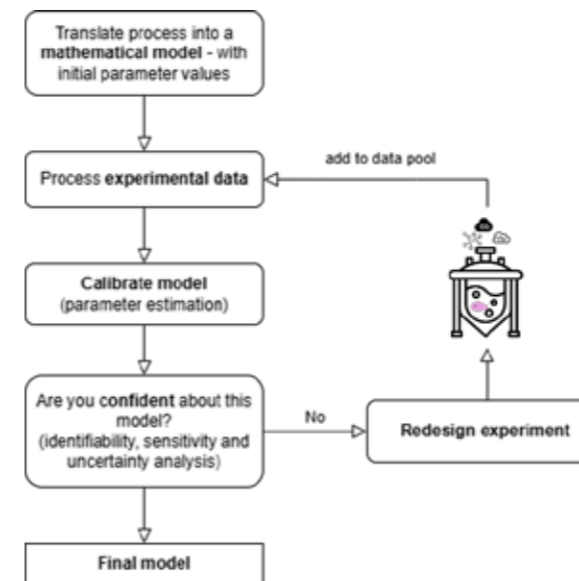


Figure 13: Overview of the MBD_{oE} *in silico* workflow applied in this study.

The MBD_{oE} algorithm was successfully implemented to redesign feed ramps according to a selected optimality criterion. The resulting feed

profiles produce distinct responses in the off-gas signals and allow a systematic investigation of how feed dynamics affect parameters' sensitivity and identifiability. At this stage, the *in silico* results primarily confirm the feasibility of applying this MBD_{oE} framework to the Crabtree effect, demonstrating that the framework can generate realistic and dynamically rich feed profiles, and that the model remains numerically stable during repeated parameter re-estimation. Further simulations are being conducted to quantify the achieved information gain and compare optimized feed profiles with a baseline, a non-optimized feed profile, in terms of parameter precision and robustness.

Conclusions

The present work establishes the feasibility of using model-based design of experiments to explore dynamic feed strategies in *S. cerevisiae* fermentations. The developed *in silico* framework successfully integrates model simulation, sensitivity analysis, and experimental design optimization in a single workflow, enabling the systematic testing of dynamic feed trajectories under realistic process conditions.

While full quantitative validation is still in progress, preliminary results indicate that the MBD_{oE} approach can be applied to complex biological models characterized by nonlinear dynamics and limited observability. The next steps will involve comparing optimized and baseline feed profiles to assess improvements in information and parameter precision, followed by *in vivo* and real-time validation using automated fed-batch experiments.

Acknowledgements

The authors acknowledge the financial support provided by the Novo Nordisk Foundation Start Package grant for Bioprocess Control and Digitalization (NNF220C0081250) and the collaboration with the CAPE-Lab at the University of Padua for computational modeling and simulation studies.

References

1. T. Barz, J. Kager, C. Herwig, P. Neubauer, M.N.C. Bournazou, F. Galvanin, Simulation and Optimization in Process Engineering: The Benefit of Mathematical Methods in Applications of the Chemical Industry (2022) 273–319.
2. G. Franceschini, S. Macchietto, Chem Eng Sci 63 (2008) 4846–4872.
3. B. Sonnleitner, O. Käppli, Biotechnol Bioeng 28 (1986) 927–937.

Continuous hydrogenation of pharmaceutical intermediates

(June 2023 – June 2026)

9 INDUSTRY, INNOVATION AND INFRASTRUCTURE



Contribution to the UN Sustainable Development Goals

Hydrogenation is a fundamental process in the pharmaceutical industry, essential for synthesizing numerous active ingredients and intermediates. Conventional batch reactors often suffer from mass transfer limitations in triphasic systems, whereas continuous technologies such as jet loop reactors enhance gas–liquid–solid mass transfer and overall process efficiency. By enhancing energy and raw material utilization while increasing process flexibility, jet loop reactors support process intensification and sustainable pharmaceutical manufacturing, aligning with the UN Sustainable Development Goals through innovation and resource efficiency.



Pelin Caglayan

hpeca@kt.dtu.dk

Supervisors: Martin Høj, Anker Degn Jensen, Kim Dam-Johansen, Tommy Skovby

Abstract

Batch reactors remain the standard reactor technology for hydrogenating pharmaceutical intermediates, yet growing emphasis on sustainable energy use and operational adaptability drives the exploration of continuous processes. Among these, jet loop reactors (JLRs) stand out for their ability to enhance mass and heat transfer while significantly shortening operation times. This study aims to develop and optimize a JLR system for the efficient hydrogenation of different pharmaceutical intermediates at Lundbeck A/S.

Introduction

Heterogeneous catalysis plays a key role in the processing of pharmaceutical intermediates, where complex structures make catalyst design, reaction conditions, and reactor configuration critical for high conversion and selectivity. Batch reactors are widely used due to their ease of operation and maintenance, but they face limitations in scalability, flexibility, and long reaction times. Continuous reactors offer greater flexibility, shorter reaction times, adjustable conditions, and more consistent product quality, making them attractive alternatives. Consequently, research on continuous reactor technologies in the pharmaceutical industry has been increasing in recent years.

Continuous reactor types for hydrogenation include trickle bed reactors, tubular reactors (plug flow reactors), and slurry-type reactors, such as JLRs for hydrogenation. [1] Jet loop reactors (JLRs) are continuous reactors designed to enhance mass and heat transfer through a circulating loop combined with a jet ejector. In a JLR, the reaction mixture is continuously circulated by a pump, while the mixing facilitated within the jet ejector due to the entrained gas further improves mass transfer. The simplified version of the JLR system utilized in this project is illustrated in Figure 1.

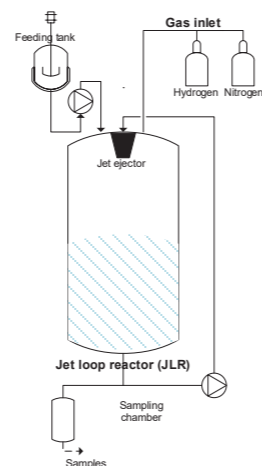


Figure 14. General PID diagram of JLR setup.

Acetophenone (AP), a simple aromatic ketone, was selected as the model compound, and a kinetic study with batch hydrogenation was conducted using both a small-scale autoclave and in a jet loop reactor (JLR). The experimental data were well described by a Langmuir–Hinshelwood model incorporating competitive and dissociative adsorption mechanisms. The kinetic parameters obtained from these studies were subsequently applied to predict

concentration profiles under continuous operation in the JLR.

Experimental

Batch experiments were conducted in a 300 mL autoclave and an 11 L JLR. Acetophenone (AP) was chosen as a model compound with 5 wt.% Pd/C as the catalyst and ethanol as the solvent. With the Pd catalyst, the target is the carbonyl group; hence, the reaction has two steps: the first step is the hydrogenation of AP to 1-phenylethanol (EP), and the second step is EP hydrodeoxygenation to ethylbenzene (EB). The reaction run time was 3 h for batch reactions, and samples were taken throughout the run. The products were quantified with GC-FID.

Results and Discussion

The results for batch experiments in the JLR are given in Figure 2. The catalyst loading, H₂ pressure, and temperature were fixed for all four experiments. The only variance was the initial AP concentration. The rate of hydrogenation was faster at lower initial AP concentration, whereas at initial AP concentrations of 0.5 and 1 M, the amount of EB produced was much lower compared to low AP concentration experiments due to high inhibition from competitive adsorption between organic molecules and H₂.

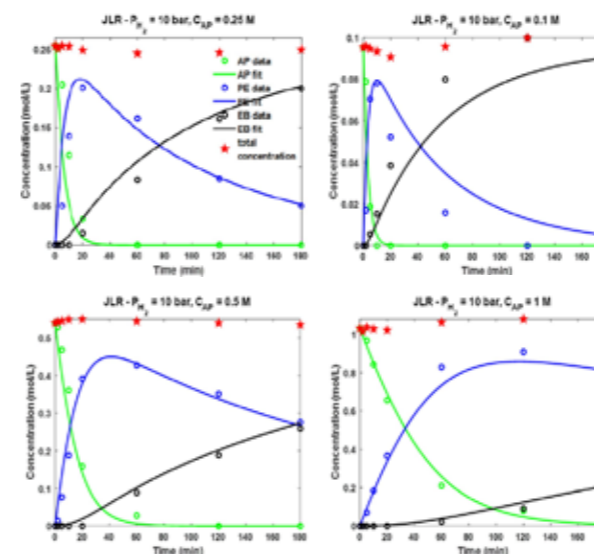


Figure 15. GC-FID results of batch AP hydrogenation experiments in JLR with four different (0.1, 0.25, 0.5, and 1 M) initial AP concentrations.

Using the Langmuir–Hinshelwood kinetic model fitted to batch experiments in the JLR, a continuous run was performed with a feed and discharge rate of 30 mL/min. The concentration plots of AP, PE, and EB are given in Figure 3. The concentration profile

presented represents the entire operation period of the JLR, and the initial variations correspond to the reactor startup behavior. The steady CSTR operation can be seen after 150 min run time.

It should be noted that discharge in the continuous JLR mode was performed in a pulse-like manner; however, due to a low discharge volume and high frequency, the discharge was approximated as a constant flow, similar to a CSTR.

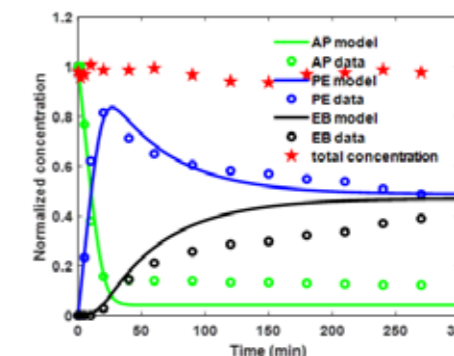


Figure 16. Normalized concentrations of AP, PE, and EB for the continuous JLR experiment with 30 mL/min feeding rate. The following conditions were used for all experiments: 1 g/L catalyst loading of 5 wt.% Pd/C, liquid volume of 3 L, 60 °C, and H₂ pressure of 10 bar(g). Dots represent the experimental data quantified by GC-FID, and lines represent the fit predicted by the Langmuir–Hinshelwood model. GC-FID quantified mass balance is shown with stars.

Conclusions

Kinetic parameters for the Langmuir–Hinshelwood model were derived from batch hydrogenation experiments in JLR for the model compound. Kinetic model predicted fits were compatible with the experimental data obtained in JLR with continuous operation at 30 mL/min feeding and discharge rate. The ongoing work is focused on varying the feeding/discharge rate to observe the changes in concentrations. Additionally, more experiments will be tested in batch-to-continuous type operation for different feeding/discharge rates.

Acknowledgements

The authors thank Lundbeck A/S for funding this project.

References

1. Masson, E.; Maciejewski, E. M.; Wheelhouse, K. M. P.; Edwards, L. J. Fixed Bed Continuous Hydrogenations in Trickle Flow Mode: A Pharmaceutical Industry Perspective. *Org Process Res Dev* 2022, 26 (8), 2190–2223.

Mathematical Modeling of Zinc-Rich Coatings

(September 2025 – September 2028)



Contribution to the UN Sustainable Development Goals

Thanks to modeling we can better optimize parameters of coatings and its application, including the type and amounts of components used. Furthermore, we can better select the active ingredients and their amount in the coating using less of it and possibly opting for more renewable sources.



Ludovico Italo Casati

litca@dtu.dk

Supervisors:

Kim Dam-Johansen
Claus Erik Weinell
Søren Kiil

Abstract

Corrosion is a thermodynamically favorable process that affects metals, and thus metallic structures need to be protected. Steel can be protected from corrosion through barrier coatings, chemical inhibitors or galvanically active system. While barrier and inhibitor approaches are well established, this research focuses on galvanically active organic coatings, which offer sacrificial protection. The underlying mechanisms of how these coatings interact with steel are not yet fully understood, and our work aims to close this knowledge gap.

Introduction

Corrosion is a thermodynamically favorable process that affects metals and alloys. It is the natural propensity of the metal to return to its ore state. Corrosion is an electrochemical process and as such it can be described by electrochemistry theory at the local level in idealized setting [1], but in order to address the full system in real case scenarios, transport phenomena need to be considered.

Few attempts in modeling and simulating the evolution of corrosion of metals, by means of classical diffusion reaction equations which are not protected by coatings exist. K. B. Deshpande et al. [2] and W. Sun et al. [3] leverage Lagrange-Eulerian methods to solve coupled diffusion, reaction and Maxwell equations for the evolution of galvanic corrosion of connected metals in aqueous solution. The complexity arises in the fact that phenomenological description of corrosion requires the possibility to incorporate the creation and destruction of new phases, and the creation and movement of boundaries.

In order to protect metal structures in corrosive environments, coatings are applied [4],[5]. The marine environment is particularly aggressive due to its high salinity, humidity, and mechanical

stresses, making corrosion protection especially challenging. If the structure one aims to protect is

submerged, cathodic protection by imposed current may also be applied in conjunction to coatings. Although many commercial products offer reliable solutions, the research in this field remains vibrant and driven by increasing environmental concerns and the demand for durable, economical, and eco-friendly alternatives [5]. Anti-corrosion coatings typically rely on one or more protection mechanisms: barrier effect, inhibitive effect, and galvanic effect [6]. Each mechanism depends on the type of pigments present in the coating system and environmental exposure conditions. The barrier effect aims to block the ingress of corrosive species such as water, oxygen, and chloride ions [6]. This can be achieved by incorporating impermeable fillers such as glass fibers into the polymer matrix, which create a tortuous path for ion diffusion [6]. Zinc rich coatings, on the other hand, provide cathodic protection to the substrate, thus they use galvanic effect. Furthermore, the zinc reacts instead of the iron in the steel, and the reaction products are also thought to provide barrier properties [8].

Once a type of coating system is selected, then different samples are created by choosing the parameter space to vary. Thickness, size distribution of pigment type, pigment volume

concentration, curing time, presence of other layers, support preparation, hydrophobicity, and adhesion durability are among the important parameters for coating effectiveness [6]. Pigment volume concentration in particular is a critical parameter due to the fact that at high value the coating loses its mechanical properties but at a low value the anti-corrosion properties fade out [7].

Specific Objectives

This research aims at uncovering the fundamental mechanisms of corrosion when an organic zinc rich coating system is applied to a metal substrate.

Diffusion coefficients of aggressive species in the coating depend on the nature and characteristics of the coating itself, curing condition and also addition of barrier pigments and filler to the binder matrix.

Reactions in the coating encompass anodic reaction of the substrate, in the case of absence of sacrificial anodes, and cathodic reaction at the substrate of oxygen gas, or free protons into hydrogen gas. Kinetics of reactions depend upon the addition of anticorrosive pigments that can reduce or inhibit the oxidation of iron. Classical kinetic reaction rates modeling and electrochemical reaction rate modeling will be considered in order to achieve full knowledge of the mechanism given the specific case. Depending on the environment, different species at different concentrations can be present, and the former can affect not only the overall rate but also the mechanism of corrosion.

References

1. C. Hamann, A. Hamnett, W. Vielstich, *Electrochemistry*, Wiley, 2007.
2. K. B. Deshpande, Validated numerical modelling of galvanic corrosion for couples: Magnesium alloy (ae44)–mild steel and ae44–aluminium alloy (aa6063) in brine solution, *Corrosion Science* 52 (10) (2010) 3514–3522.
3. W. Sun, G. Liu, L. Wang, et al., An arbitrary lagrangian–eulerian model for studying the influences of corrosion product deposition on bimetallic corrosion, *Journal of Solid State Electrochemistry* 17 (2013) 829–840
4. G. Bierwagen, The physical chemistry of organic coatings revisited—viewing coatings as a materials scientist, *Journal of Coatings Technology Research* 5 (2008) 133–155.
5. W. Pei, X. Pei, Z. Xie, J. Wang, Research progress of marine anti-corrosion and wear-resistant coating, *Tribology International* 198 (2024) 109864

6. P. A. Sørensen, S. Kiil, K. Dam-Johansen, et al., Anticorrosive coatings: a review, *Journal of Coatings Technology and Research* 6 (2009) 135–176.
7. C. Hare, J. Kurnas, Reduced pvc and the design of metal primers, *Journal of Coatings Technology* 72 (2012) 21–27
8. Z. Li, C. Qi, H. Bi, M. Fedel, K. Dam-Johansen, Biochar nanoparticles in zinc epoxy coatings: Dual-function as conductive filler and inhibitor carrier for enhanced anticorrosive performance, *Progress in Organic Coatings*, (2025), 206

Silicone-protein hybrid materials

(October 2024 – October 2025)

12 RESPONSIBLE CONSUMPTION AND PRODUCTION



Contribution to the UN Sustainable Development Goals

By integrating biodegradable proteins into PDMS networks, we enable selective degradation of the protein phase while modifying the overall material composition and behavior. This approach promotes more efficient resource use and opens pathways for partial material recovery, reducing reliance on incineration. Through tailored design strategies, the project contributes to sustainable production practices and encourages circular material innovation in sectors like biomedical devices and soft electronics.



Virginia

Celestre

virgce@kt.dtu.dk

Supervisors:

Anne Ladegaard Skov, Anders Egede Daugaard

Abstract

Polydimethylsiloxane (PDMS) is a versatile elastomer known for its flexibility, biocompatibility, thermal stability, and ease of processing, widely used in biomedical devices, microfluidics, soft robotics, and flexible electronics. However, conventional PDMS networks are electrically insulating, limiting their use in electronic applications. This research introduces hybrid silicone–protein elastomers, where biodegradable proteins are used as crosslinkers, enabling chemical and physical interactions with PDMS chains. By tuning PDMS architecture and protein composition, we achieve customizable mechanical and electrical performance for advanced soft electronic and bio-integrated systems. Additionally, the protein phase offers selective degradability, contributing to more sustainable material design.

Introduction

Polydimethylsiloxane (PDMS) networks are highly versatile elastomers widely used in biomedical devices, microfluidics, soft robotics, and flexible electronics due to its exceptional flexibility, biocompatibility, thermal stability, and ease of molding[1]. However, PDMS networks formed through permanent chemical crosslinking are inherently electrically insulating[2] and lack recyclability, limiting their functionality and sustainability in specific applications.

To address these limitations, our research focuses on engineering hybrid silicone–protein elastomers (see Figure 1) that will enable a wider range of applications than traditional PDMS systems. By introducing biodegradable proteins as dynamic crosslinking agents, we enable chemical and physical interactions between PDMS chains and protein structures. This approach not only preserves the mechanical integrity of PDMS but also introduces electrical properties, such as charge mobility, ionic responsiveness, and conductivity, that are typically absent in conventional PDMS systems unless conductive fillers like graphene or nanoparticles are added[3].

The functionality and architecture of the PDMS, including its molecular weight, end-group chemistry, and branching, plays a crucial role in tuning the mechanical behavior of the network. Shorter PDMS chains yield stiffer materials with higher crosslink density, while longer chains enhance flexibility and elongation[4]. Branched PDMS molecules, due to their multi-functional end groups and compact structure, can promote the formation of highly crosslinked yet soft networks, offering a balance between elasticity and mechanical integrity. Meanwhile, the amino acid composition and sequence of the protein component can be leveraged to introduce charge mobility, enabling electrical conductivity, ionic responsiveness, or bioactivity within the network[5].

Once permanently crosslinked, PDMS networks are difficult to recycle, leaving incineration or landfill as the primary disposal options, both of which pose significant environmental concerns[6]. As global awareness of sustainability grows, so does the demand for greener alternatives to conventional materials like PDMS. The hybrid silicone–protein systems developed in this project will offer the potential for selective degradability of the protein phase under mild conditions and

recovery of the PDMS matrix. These advancements support circular material design and represent a promising step toward more sustainable use of silicone-based materials.

Specific Objectives

1. Development of hybrid silicone-protein elastomers with tunable mechanical and electrical properties through selective protein conjugation using mild and scalable synthetic methods.
2. Engineer reversible crosslinked networks by integrating biodegradable proteins as physical crosslinking points, allowing for enhanced permittivity, charge stabilization, and recyclability of the PDMS matrix.
3. Systematic synthesis, characterization, and application testing will contribute to sustainable material design for sensors, actuators, and flexible electronics.

Experimental setup

PDMS chains are first functionalized with chemical groups specifically designed to interact with selected amino acids in the target protein. After functionalization, the PDMS is reacted with the protein under mild conditions that preserve the protein's native structure and biological activity.

Once the proteins are introduced into the functionalized PDMS matrix, the mixture is poured into a mold and cured to form a solid film. These silicone-protein hybrid materials can then be subjected to various characterization techniques.

The PDMS and its functionalization are typically analysed using ¹H-NMR and FT-IR spectroscopy. After curing, the solid films are characterized using FT-IR, Differential Scanning Calorimetry (DSC), and other methods to evaluate material properties such as mechanical flexibility and electrical conductivity, depending on the intended application.

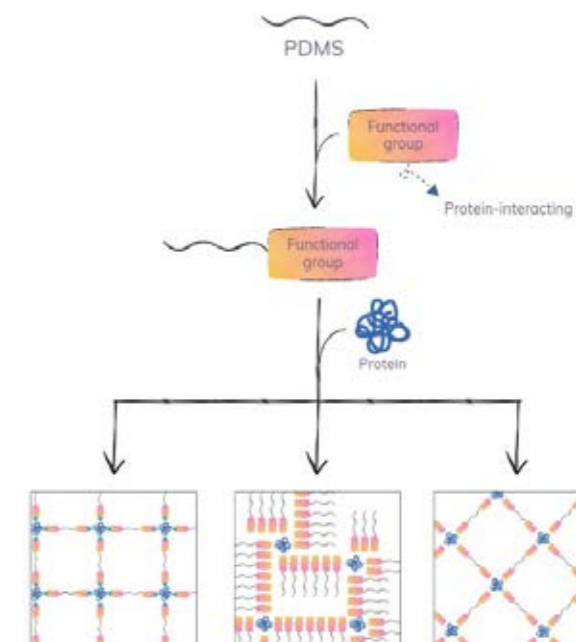


Figure 17: schematic overview of the PhD project described

References

1. Miranda, A. Pereira, J. Silva, J. *Funct. Biomater.* 13 (1) (2021) 2
2. Cordoba, M. Renteria, L. Torres, *Molecules* 30 (10) (2025) 2107
3. S. Li, Y. Wang, H. Zhang, *Adv. Sci.* 10 (34) (2023) 2304506
4. Volkov, in: E. Drioli, L. Giorno (Eds.), *Encyclopedia of Membranes*, Springer, Berlin, Heidelberg (2013)
5. N. Niccolai, E. Morandi, A. Bernini, *Int. J. Mol. Sci.* 25 (2024) 13375
6. S. Lindström, P. Svensson, A.E. Daugaard, A.L. Skov, *Nordic Polymer Days 2024*, Helsinki, Finland (2024)

Dynamic Silicone Elastomers from Natural Phenols

(August 2023 – August 2026)



Contribution to the UN Sustainable Development Goals

This project aligns with UN Sustainable Development Goal 12 by introducing an environmentally friendly approach to silicone elastomers. It aims to lower the significant energy consumption associated with conventional silicone production and mitigate the environmental footprint of silicone waste. By encouraging responsible consumption, improving resource efficiency, and advancing sustainable manufacturing practices, this work contributes to a more sustainable and circular future.



Cagla Cinalioglu

cagci@kt.dtu.dk

Supervisors:

Anne Ladegaard Skov
Cody Brian Gale
Frederikke B. Madsen

Abstract

This work aims to improve recyclability and establish a more sustainable approach to silicone material development by leveraging supramolecular interactions to enable reprocessing. Silicone elastomers were formed by mixing polyphenols with silicone polymers containing functional groups capable of partaking in hydrogen or ionic bonding. Using this approach, a systematic library of elastomers was synthesized with a series of model phenolic compounds to elucidate structure-property relationships. Overall, this research marks a step forward in advancing the sustainability of silicone elastomers and reducing industrial waste by furthering understanding of dynamic silicone networks.

Introduction

Silicones, like many polymers, are attracting increasing attention due to their limited recyclability and inefficient waste management, which contribute to rising environmental concerns [1]. The environmental impact of silicones is also problematic due to their production process.

Silicone production is energy-intensive and results in significant greenhouse gas production [2]. Therefore, landfilling or incineration of these materials represents a serious sustainability issue. Utilizing non-covalent bonding, such as hydrogen bonds, π - π interactions, ionic linkages, or dynamic interactions, within the structure of thermoplastic elastomers makes these materials thermally reprocessable, enabling reuse, repurposing, and ultimately recycling [3].

This project seeks to understand and utilize the dynamic bonding between the hydroxyl group of phenolics and the amine group of aminopropyl-terminated polydimethylsiloxane (PDMS). The contribution of both ionic interactions and hydrogen bonding (H-bonding) leads to the formation of a dynamic polymer network. The possible bonding motifs are shown in Figure 1 for the phenol pyrogallol.

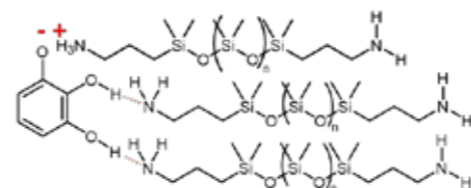


Figure 1. Possible bonding motifs in silicone elastomers formed from mixing the phenol, pyrogallol, and aminopropyl-terminated PDMS.

Specific Objectives

The objectives of this project are:

1. To investigate the influence of phenolic type, PDMS chain length, and OH: NH₂ molar ratio on the resulting network architecture, mechanical, and thermal performance.
2. To identify the separate effects of ionic and H-bonding interactions on the network formation.

Results and Discussion

Phenol-containing silicone elastomers were synthesized via a three-step process. First, catechol (CAT), resorcinol (RES), or hydroquinone (HQ) were dissolved in ethyl acetate. Next, aminopropyl-terminated PDMS ($M_n = 5000$ g/mol) was added to the phenol solution in varying ratios to adjust the phenol-to-amine molar ratio, followed by curing of the pre-elastomer mixture at 60 °C for 4 days. Long curing times

were required to fully remove the solvent and achieve a crosslinked network. Using this procedure, three elastomers with varying OH:NH₂ ratios were prepared with CAT, RES, and HQ.

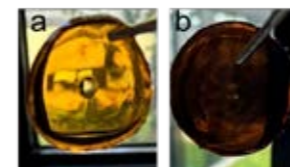


Figure 2. Representative images of elastomers formed from CAT a) 1:3 OH:NH₂ ratio b) 3:1 OH:NH₂ ratio.

The impact of OH:NH₂ molar ratio on the mechanical properties of the formed elastomers made from RES was investigated via tensile testing and is shown in Figure 3.

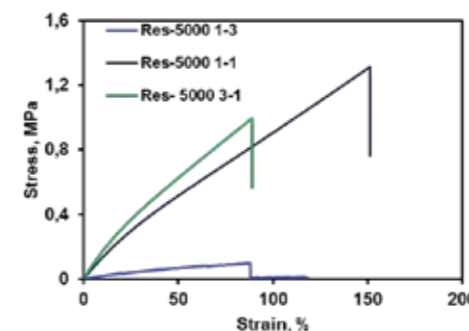


Figure 3. Stress vs strain curves of RES-containing elastomers at the three different OH: NH₂ ratios

The mechanical properties depended on the OH:NH₂ ratio. As this ratio increases from 1:3 to 3:1 the Young's modulus increases because of both an increase in H-bonding between the phenol and amines and π - π interactions between the phenols. However, the sample with a OH: NH₂ ratio of 1:1 shows the highest elongation at break, likely because the phenols and amines are stoichiometrically balanced and H-bonding interactions are maximized. The same trend in Young's modulus and elongation at break was observed in CAT and HQ samples.

Broadband dielectric spectroscopy (BDS) was employed to investigate the dynamic nature of the bonds and calculate the activation energy (E_a) of the elastomers, which represents the energy threshold that must be overcome for the dynamic bonds, such as hydrogen bonds, to rearrange [4]. The dielectric loss modulus was measured at different temperatures and frequencies. Spectra were fitted using the Havriliak-Negami equation to extract relaxation times and calculate the E_a of elastomers (Figure 4).

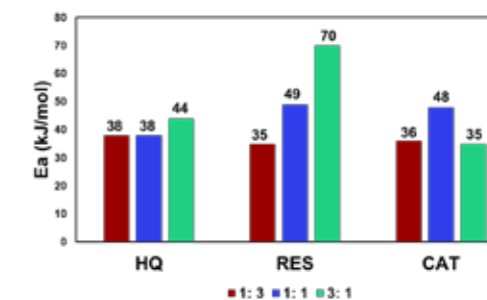


Figure 4. Activation energies of elastomers crosslinked with HQ, RES, and CAT at different OH: NH₂ ratios.

RES and HQ elastomers showed the highest E_a at a 3:1 OH:NH₂ ratio, with the RES-containing elastomer having an E_a value of 70 kJ/mol compared to 44 kJ/mol for HQ. The CAT elastomer had the highest E_a of 48 kJ/mol at a 1:1 OH:NH₂ ratio. The differences in E_a may arise from variations in both stoichiometry and the types of hydrogen bonding present within the networks, as amine-phenol, phenol-phenol, and amine-amine interactions are all possible. The positioning of the hydroxyl groups in RES, CAT, and HQ likely determines the predominant type of hydrogen bonding, thereby accounting for the observed differences among the three systems.

Conclusion

In conclusion, silicone elastomers with tunable mechanical properties can be made via a simple process from phenols and aminopropyl-terminated PDMS. Furthermore, preliminary dielectric spectroscopy analysis suggests that the networks are crosslinked by thermally activated dynamic hydrogen bonds, which may provide a pathway for reprocessing these materials.

Acknowledgements

This project is funded by the Independent Research Fund Denmark.

References

1. A.T. Wolf, A. Stammer, *Polymers* 16 (2024) 2220.
2. Global Silicones Council, *Si-Chemistry Carbon Balance: Greenhouse Gas Emissions and Reductions*, Executive Summary, Brussels, 2019.
3. K. Tamim, C.B. Gale, K.E.C. Silverthorne, G. Lu, C.H. Iao, M.A. Brook, *ACS Sustainable Chem. Eng.* 11 (2023) 7062–7071.
4. N.J. Bongiardina, K.F. Long, M. Podgórski, C.N. Bowman, *Macromolecules* 54 (2021) 8341.

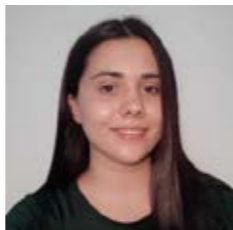
Protein Integration into Silicone Elastomers: Towards New Functional Materials

(March 2023 - February 2026)



Contribution to the UN Sustainable Development Goals

Responsible Consumption and Production by exploring biodegradable and tunable silicone-gelatin composites. By integrating natural polymers like gelatin into synthetic elastomers, we aim to reduce reliance on non-degradable materials and enable sustainable design strategies for soft robotics, sensors, and printing technologies.



Florina-Elena Comanici

flocom@dtu.dk

Supervisors: Anne Ladegaard Skov, Frederikke Brath Madsen

Abstract

This study investigates the integration of gelatin, a hydrophilic protein fragment, into hydrophobic silicone to create novel elastomeric composites. By varying the temperature during mixing, two distinct material types were obtained: emulsion-based and emulgel-based elastomers. The composites exhibit different microstructures and mechanical properties. The emulgel-based materials demonstrate shape memory capabilities driven by hydration of the gelatin within the silicone matrix. The work highlights the potential of protein-silicone elastomers in sustainable material design and functional applications.

Introduction

Silicone elastomers are widely used in a wide range of applications due to their elasticity, stretchability, and excellent chemical stability. These properties make them ideal candidates for applications ranging from biomedical devices to soft robotics [1]. Proteins, on the other hand, possess numerous chemical functionalities and structural diversity. For example, proteins can form secondary structures such as alpha helices and beta sheets, which influence their mechanical and chemical behavior. Gelatin, a protein fragment derived from collagen, is a particularly attractive protein due to its ability to form hydrogels in aqueous environments. Gelatin hydrogels exhibit temperature-sensitive viscosity, transitioning from solid-like to liquid-like behavior around 35°C due to the breaking of hydrogen bonds. This property makes gelatin suitable for extrusion-based processing [2].

One major challenge in the fabrication of gelatin-PDMS composites is the difference in polarity between the two components, namely, gelatin's hydrophilic nature with the hydrophobic silicone matrix. Silverthorne et al. [3] fabricated silicone-gelatin composites by crosslinking the two phases using formaldehyde at the oil-water interface.

Within the elastomer matrix, gelatin can act as a degradable linker, enabling the formation of biodegradable silicone elastomers [3]. The current study explores how the physical state of gelatin during mixing, either as a hydrogel or a liquid, affects the structure and properties of the resulting composite. By leveraging gelatin's solid-to-liquid transition, we aim to create materials with tunable properties, which can be used in novel applications [4].

Specific objectives

- Develop silicone-gelatin composites.
- Investigate the effect of gelatin's physical state during mixing.
- Explore shape memory behavior.

Results and discussion

The initial phase of the study investigated the effect of gelatin hydrogel temperature during the preparation step. This step is crucial, as gelatin hydrogel undergoes a solid-to-liquid phase transition upon heating. Mixing solid gelatin hydrogel with silicone at room temperature yields a liquid emulsion (Fig 1 A). Microscopy revealed discrete gelatin droplets within a continuous silicone phase. Mixing warm, liquid gelatin with silicone produced a semi-solid emulgel (Fig. 1 B).

A continuous 3D gelatin network was formed within the silicone matrix.

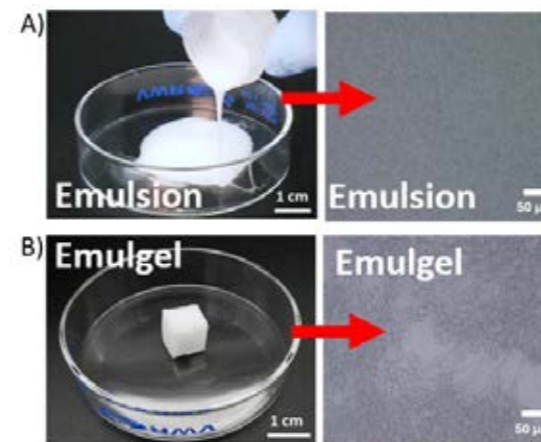


Figure 1: A) The emulsion mixture formed upon mixing gelatin hydrogel with PDMS. B) The emulgel mixture formed upon mixing the liquid gelatin solution with PDMS.

To fabricate the elastomers, the mixtures were crosslinked using glutaraldehyde. During the reaction, the amine groups of PDMS and gelatin react with the aldehyde groups to form imine bonds [5], [6].

Figure 2 shows the mechanical properties of the obtained elastomers. The emulsion-based elastomers are soft and stretchable, with gelatin acting as a reinforcing filler. Emulgel-based elastomers are much stiffer, with a Young's modulus reaching up to 8 MPa. Here, the gelatin network dominates mechanical behavior, limiting stretchability after drying.

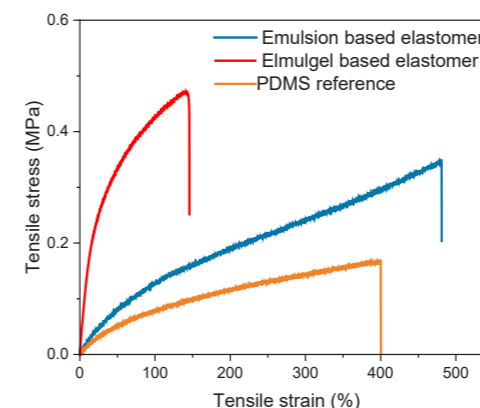


Figure 18: Stress-strain curves obtained from emulsion-based composites and emulgel-based composites and a PDMS elastomer without gelatin.

The shape memory behavior of the emulgels was further investigated. As seen in Fig. 3, the gelatin network swells in water, disrupting intermolecular forces and softening the material. Upon drying, the gelatin becomes rigid again. Meanwhile, the silicone component ensures elasticity and shape recovery. The combination of gelatin's malleability

and silicone's resilience gives rise to a composite with shape memory capabilities, responsive to hydration, temperature, and mechanical stress.

In the hydrated form, the composite becomes malleable and can be temporarily deformed and reshaped in different geometries, for instance, by stretching, twisting, coiling, or folding. While drying, the composite loses its malleability and is locked in its new temporary shape. Recovery is then triggered by rehydration, a process that occurs over a time scale of minutes.

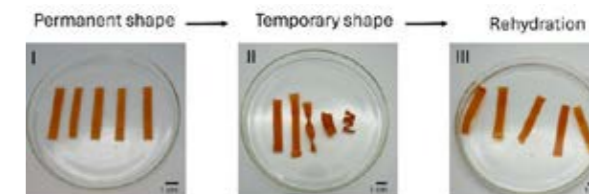


Figure 3: Photographs showing the emulgel-based elastomer hydration and its recovery process: I Hydrated elastomer sample in its permanent state; II elastomer deformed from left to right, control, stretched, twisted, coiled, and folded sample; III samples recovered after 30 min from adding water (40 °C).

Conclusion

Two distinct types of elastomers were fabricated by changing the temperature upon mixing. The temperature of the hydrogel upon mixing influences the microstructure of the materials, which in turn affects the mechanical properties. The advantages of incorporating proteins, namely gelatin in PDMS, were highlighted in novel applications, such as shape memory elastomers.

References

1. P. Mazurek, S. Vudayagiri, A.L. Skov, Chem. Soc. Rev. 48 (6) (2019) 1448-1464.
2. U. Abid, Y.Q. Gill, M.S. Irfan, R. Umer, F. Saeed, Int. J. Biol. Macromol. 181 (2021) 1-29.
3. K.E.C. Silverthorne, E.M. Donahue-Boyle, A. Pricu, A.Y. Li, M.A. Brook, Green Chem. 26 (10) (2024) 6200-6208.
4. F.-E. Comanici, F.A.L.S. Bahrt Madsen, Advanced Materials Technologies, (2025), 2500170.
5. I. Migneault, C. Dartiguenave, M.J. Bertrand, K.C. Waldron, Biotechniques 37 (5) (2004) 790-802.
6. R. Bui, M.A. Brook, Adv. Funct. Mater. 30 (23) (2020) 2000737.

Catalytic Upgrading in a Continuous Slurry Reactor of Biomass Pyrolysis Oil to Fuels for Heavy Transport and Aviation

(January 2024 – December 2026)

7 AFFORDABLE AND CLEAN ENERGY



Contribution to the UN Sustainable Development Goals

With the eminent energy shift that the world needs to perform in order to achieve the UN sustainable development goals regarding greenhouse gas emissions, major efforts are necessary to find new processes that can provide energy sources that are not only clean, but also affordable and reliable. This project belongs to this field, as it aims to study and optimize a pilot-scale unit in continuous operation for the production of liquid fuel from biomass, which can be used in heavy transport and aviation.



Rui

Pedro da Cruz

rpdac@dtu.dk

Supervisors: Anker Degn Jensen, Martin Høj, Alexander Søgaard, Magnus Zingler Stummann

Abstract

Biomass derived pyrolysis oil has the potential to replace fossil fuel sources. However, due to its negative properties, catalytic upgrading is necessary. In this work, a slurry reactor is studied as an alternative to the traditional fixed bed reactors. Initial experiments with a guaiacol (10 wt%) in octanol mixture showed that the catalyst did not deactivate after 90 hours of processing. However, when furfural (12.5 wt%) and octanoic acid (2.5 wt%) were added, keeping the same amount of guaiacol, the catalyst deactivated and the conversion of guaiacol was inhibited. Addition of thiophene (50 wt-ppm sulfur) to the feed, led to a quick and irreversible deactivation of the catalyst, due to sulfur poisoning.

Introduction

Fossil fuels are known to be limited and impact the environment; therefore, new alternatives need to be found. Biomass-derived fuels are an alternative for aviation and heavy transport, where electric and hydrogen mobility are difficult to execute.

Fast pyrolysis converts solid biomass into liquid bio-oil, solid char and non-condensable gases. Bio-oil is characterized by high water and oxygen contents, resulting in corrosiveness and acidity. Moreover, the heating value is low and limits its immediate applicability as a fuel [1]. Upgrading the oil by catalytic hydrogenation with a selective catalyst leads to improved properties, close to the ones of fossil fuels. During this catalytic process, oxygen is removed through hydrodeoxygenation (HDO), and the carbon and hydrogen contents are increased which leads to an increase in the heating value [2].

Fixed bed reactors are the usual benchmark in this process. However, they often lead to plugging and coking of the catalyst. A slurry set-up can be an alternative, since it allows the catalyst to be well dispersed and mixed with the oil. Moreover, the

catalyst contacts with partly converted and only low concentrations of fresh reactive bio-oil [3].

Ni based catalysts are promising for bio-oil upgrading as they promote a fast hydrogenation of aldehydes, ketones and aromatics, even at mild temperatures [4]. However, their sulfur resistance has been debated, and Ni leaching can also become a problem in long running times [5].

Specific Objectives

The main goal of this project is to optimize the operation in the continuous slurry reactor.

Initially, a metallic Ni catalyst was tested at mild temperatures, with model compounds. Following this, a newly developed catalyst basket was also tested. Future testing will include more studies on the catalyst basket, using a sulfided NiMo catalyst. Higher temperatures will be targeted, and more catalysts will be used per experiment.

Finally, real bio-oil feeds will be tested on the optimum design.

Results and Discussion

A mixture containing guaiacol (10 wt%) in octanol was processed at different temperatures steps, with 24 hours spent in each step. The steady state average conversion of the reactants is shown in Figure 1. The first observation is that octanol is not extensively converted in this temperature range. Regarding guaiacol, high conversions, above 90 %, are reached at temperatures above 150 °C. From the two different steps at 120 °C, it is possible to conclude that the catalyst did not deactivate, even after 90 hours of processing, as the conversion of both guaiacol and octanol is the same in both steps.

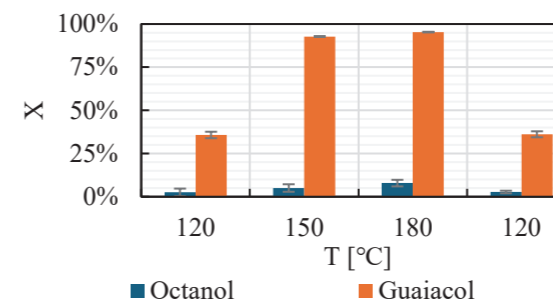


Figure 19: Steady state conversion of octanol and guaiacol at different temperatures; 100 bar H₂, 1 g catalyst, 200 min residence time, 600 H₂/oil feed.

The same mixture, with the addition of thiophene, was processed at 120 °C. This addition was such that 50 wt-ppm of sulfur would be present in the feed. Figure 2 shows that the conversions of guaiacol and octanol decrease to 0%, after the addition of sulfur to the feed. Moreover, once sulfur was removed from the feed, the conversion of neither reactant improved. Thus, it can be concluded that the catalyst deactivated rapidly and irreversibly due to the presence of sulfur in the feed due to conversion of metallic Ni to NiS.

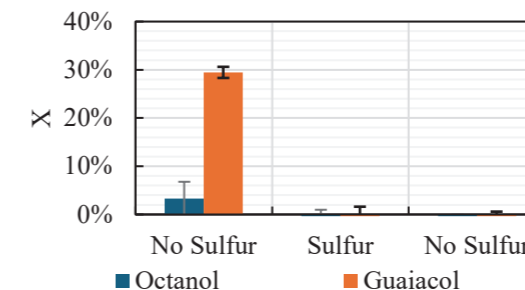


Figure 20: Steady state conversion of guaiacol and octanol before, during and after addition of sulfur; 100 bar H₂, 1 g catalyst, 200 min residence time, 600 H₂/oil feed, 50 wt-ppm of sulfur as thiophene.

An experiment similar to the one from Figure 1 was performed. In this case, the feed also contained furfural (12.5 wt%) and octanoic acid (10 wt%), while keeping the same concentration of

guaiacol (10 wt%). The results are shown in Figure 3. The conversions of furfural are quite high, reaching close to 99 %. However, the conversion of guaiacol is much lower than the ones shown in Figure 1, which suggests that its conversion is inhibited by the presence of furfural. Furthermore, the conversions on the second step at 120 °C are much lower than on the first step, showing that the catalyst is deactivating, due to metal leaching.

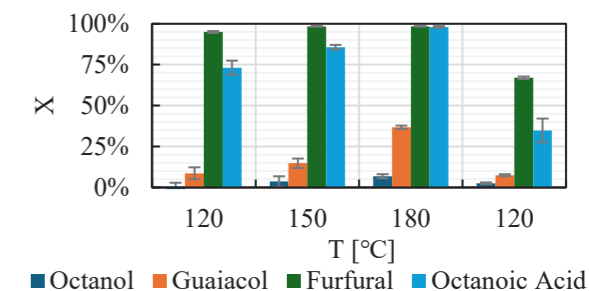


Figure 21: Steady state conversion of octanol, guaiacol, furfural and octanoic acid at different temperatures; 100 bar H₂, 1 g catalyst, 200 min residence time, 600 H₂/oil feed.

Conclusions

The slurry set-up was successful at converting two model compound mixtures, and continuous operation for over 100 hours was achieved. Catalyst deactivation was not observed when only Guaiacol and Octanol were fed. However, a fast and irreversible poisoning of the catalyst after a short period of time exposed to sulfur was observed. The addition of furfural and octanoic acid to the feed led to severe Ni leaching over long running times. These results suggest that the catalyst used is not suitable to process real bio-oil in a continuous slurry reactor.

Acknowledgements

The authors acknowledge Innovation Fund Denmark for funding this research through the project "HyProFuel" (case no.: 0224-00029A). Further acknowledged is Topsoe A/S for the close cooperation on this PhD project.

References

1. H. Wang et al., ACS Catal 3 (2013) 1047–1070.
2. T.M.H. Dabros et al., Prog Energy Combust Sci 68 (2018) 268–309.
3. N. Bergvall et al., Energy and Fuels 35 (2021) 2303–2312.
4. P.M. Mortensen et al., ACS Catal 3 (2013) 1774–1785.
5. P.M. Mortensen et al., Catal Sci Technol 4 (2014) 3672–3686.

Converting plastic waste to synthesis gas: The effect of main operating parameters

(March 2023 – February 2026)



Contribution to the UN Sustainable Development Goals

This research could significantly contribute to the achievement of more sustainable consumption and production patterns, aligning with the SDG 12. The overall objective of the project is to develop a carbon-neutral technology for converting plastic waste to methanol. The technology is designed to accept the plastic waste which cannot currently be recycled. Its implementation will reduce the amount of plastic waste sent to landfills and incineration plants, and lead to a decline in traditional carbon-based methanol production.



Andrea De Silvestri

andsilv@kt.dtu.dk

Supervisors: Peter Arendt Jensen, Anker Degn Jensen, Jan Kamyno Rasmussen

Abstract

The project explores the conversion of plastic waste into sustainable methanol through fluidized-bed gasification, partial oxidation (POX) and methanol synthesis using the gas. Systematic experiments on polyethylene revealed how temperature, oxygen, and steam conditions affect syngas yield, composition, and contaminant formation. Higher temperatures and moderate steam improved carbon conversion, while oxygen enrichment enhanced tar removal. The results form the experimental basis for the design and commissioning of a new POX reactor, supporting future plastic-to-methanol technologies.

Introduction

The thermochemical conversion of end-of-life plastics into syngas suitable for methanol synthesis represents a promising route to produce recycled carbon fuels (RCF) [1] and reduce reliance on fossil feedstocks. Bubbling fluidized bed (BFB) gasifiers are attractive for this application due to their fuel flexibility, high heat transfer rates, and scalability [2]. However, while biomass gasification has been extensively characterised [3], systematic parametric studies on plastic feedstocks gasification remain limited, especially in relation to downstream integration with partial oxidation (POX) reactors for tar abatement [4].

Recent pilot- and lab-scale studies have examined the effects of oxygen enrichment and steam addition on mixed plastic waste gasification, showing that operating conditions strongly influence syngas composition, heating value, and contaminant formation [5,6]. However, quantitative datasets for single-polymer feedstocks under controlled BFB conditions, coupled with detailed tar speciation, remain scarce. This study addresses this gap by experimentally evaluating the influence of key operational parameters on syngas yield and

composition, heating value, and carbon conversion efficiency (CCE) during polyethylene gasification. The results also provide input for the design of a POX reactor aimed at upgrading raw syngas for methanol production.

Materials and methods

Experiments were performed in a 1.4 m tall BFB gasifier shown on Figure 1 and made of heat-resistant steel 2520. The system comprises a gas supply with mass flow controllers, a twin-screw feeder with a water-cooled inlet, a steam generator, and a multi-stage tar sampling line consisting of a heated filter, condenser, twist filter, glass-wool filter, and Peltier cooler.

The feedstock was commercial polyethylene (PE), and the main operating parameters were varied systematically. The temperature was set between 750 and 850 °C, the equivalence ratio (ER) was adjusted from 0.20 to 0.30, and the steam-to-carbon ratio (S/C) ranged between 0.25 and 0.75. Oxygen content in the oxidising stream was increased up to 72 %vol, while the PE feed rate varied from 75 to 360 g/h. Gas composition was measured using GC-FID/TCD. Tars were analysed by GC-MS and thermogravimetric

analysis (TGA). The performance indicators included nitrogen-free gas yield ($\text{Nm}^3/\text{kg}_{\text{daf}}$), lower heating value (LHV), CCE, and gas quality ratios (H_2/CO and CO_2/CO).

Results and discussion

Raising the temperature from 750 to 850 °C increased the H_2 concentration to 34.2 vol.% and CO to 26.3 vol.%. The gas yield rose from 0.9 to 1.74 $\text{Nm}^3/\text{kg}_{\text{daf}}$, while CCE improved from 75.2 to 92.7 %, in agreement with trends reported for biomass and waste-derived feedstocks [3,5]. Tar speciation shifted towards lighter aromatics, and the PAHs decreased by about 40 %.

Variations in ER produced a non-monotonic trend for H_2 and CO, with a minimum at ER = 0.25 (24 and 20 vol.% respectively), while CO_2 increased almost linearly from 20 to 29 vol.% when raising ER from 0.2 to 0.3. Higher ER also promoted the formation of PAHs, consistent with previous findings [6]. Increasing the S/C ratio up to 0.5 resulted in the highest H_2 production (36 vol.%) and gas yield (1.77 $\text{Nm}^3/\text{kg}_{\text{daf}}$), accompanied by an almost linear reduction in soot formation from 1.3 to 0.2 $\text{g}/\text{kg}_{\text{daf}}$, a trend also observed in mixed-plastic and biomass studies [3,6]. Further increases in steam content provided only marginal benefits.

Oxygen enrichment produced more complex effects: at moderate levels (around 30 % O_2), tar and char yield decreased down to 12.9 and 6.2 $\text{g}/\text{kg}_{\text{daf}}$ respectively; whereas at high enrichment (around 72 % O_2) the concentrations of CH_4 and C_2H_4 rose (from 10.2 to 11.6 vol.%, and 12.8 to 14.1 vol.% respectively) alongside an increase in soot production [6].

The observed trends confirm that operating conditions significantly affect both syngas quality and contaminant profiles. The comprehensive tar characterization performed here provides input data for simulations of tar oxidation, supporting the sizing and operational window definition of the POX reactor under development.

Conclusions

This work provides a comprehensive parametric evaluation of polyethylene gasification in a bubbling fluidized bed reactor under conditions relevant to plastic-to-methanol conversion. Operating conditions that maximise syngas yield and quality while controlling tar and soot formation have been identified. The tar yield and speciation data are directly applicable to the engineering design of downstream POX reactors. Future work will focus on validating the POX reactor under real syngas conditions and extending the study to mixed plastic waste streams for pilot-scale integration.

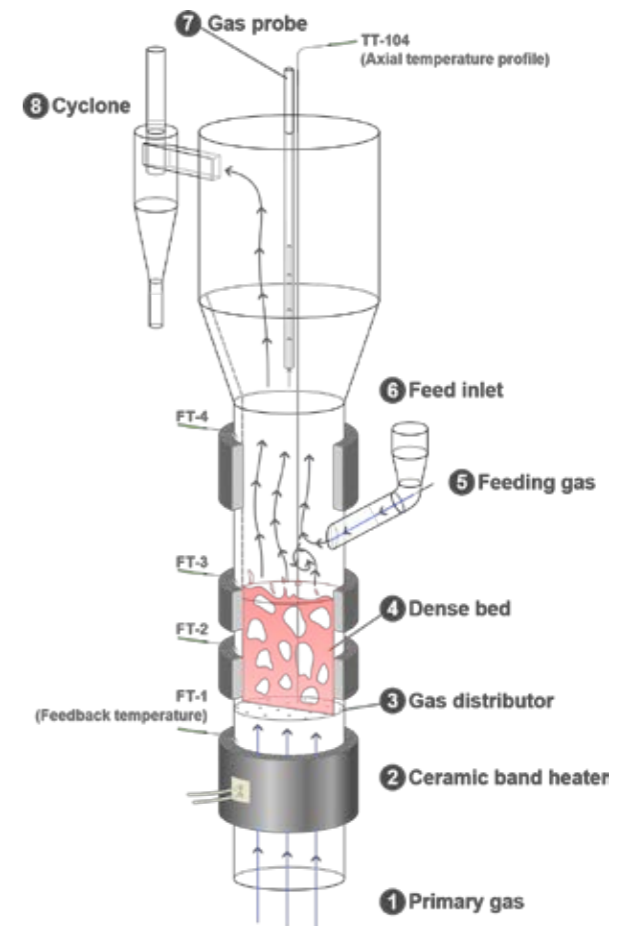


Figure 22: Schematic of the laboratory-scale bubbling fluidized bed.

References

- Parrillo, F., et al. (2024). Mixed Plastic Waste Gasification in a Large Pilot-Scale Fluidized Bed Reactor Operated with Oxygen-Enriched Air and Steam. *Energy & Fuels* 38, 10514–10527.
- Basu, P. (2018). *Biomass Gasification, Pyrolysis and Torrefaction*. Academic Press.
- Campoy, M., et al. (2008). Air–steam gasification of biomass in a fluidised bed: Process optimisation by enriched air. *Fuel* 87, 1644–1653.
- Milne, T.A., et al. (1998). Review of biomass gasification tar. NREL/TP-570-25357.
- Mastellone, M.L., et al. (2012). Fluidized bed pyrolysis of plastic waste. *Waste Management* 32, 733–742.
- Arena, U., Di Gregorio, F. (2014). Gasification of plastic waste: Optimisation of operating conditions. *Waste Management* 34, 2228–2236.

Acknowledgement

Funding from EUDP to this project is gratefully appreciated.

Advanced configurations for carbon capture and flue gas cleaning

(January 2024 – December 2026)

13 CLIMATE ACTION



Decarbonizing the hard-to-abate industries for good this time

Efficient carbon dioxide removal technologies are urgently needed to mitigate human-induced climate change sooner than it is too late. Carbon dioxide is emitted in large quantities from hard-to-abate industries such as energy production and cement manufacturing. Amine-based carbon capture is the most mature technology available for this purpose. This PhD project aims to advance the technology to TRL 7+ by improving its cost-effectiveness, reliability, and even social acceptance. To achieve this, advanced heat configurations are tested at pilot-scale using real cement flue gas, supported by new reliability methods and an accurate process simulation model.



Can Demir

cande@kt.dtu.dk

Supervisors:

Philip Loldrup Fosbøl,
Jens Abildskov

Abstract

Carbon dioxide is emitted in large quantities from hard-to-abate sectors and must be effectively captured for storage and utilization (CCUS) to mitigate human-induced climate change. Amine-based capture is the most mature and efficient technology for carbon dioxide removal on a large scale. The CESAR1 solvent, which is 27 wt% aminomethyl propanol (AMP) mixed with 13 wt% piperazine (PZ) in water, is considered the new benchmark amine blend for large-scale carbon dioxide removal from high CO₂-content industrial flue gas streams. This PhD project investigates advanced heat-integration configurations for CO₂ capture, including absorber intercooling, altered stripper pressure, cold-rich stream, and lean vapor compression. The resulting steady-state pilot data are highly reliable to support accurate thermodynamic modeling for process optimization and intensification.

Introduction

Since the Industrial Revolution, greenhouse gas emissions (GHGe) have caused global temperatures to rise by at least 1 °C above pre-industrial levels. Among these gases, CO₂ has drawn particular concern because it remains in the atmosphere for up to 1,000 years, contributing significantly to global warming^{1,2}. The Paris Agreement, signed by 194 member states of the United Nations, aims to limit global warming to well below 2 °C, with an ambitious goal of limiting the increase by 1.5 °C, through effective greenhouse gas emission reduction strategies³. Achieving these targets requires substantial emission reduction policies complemented with effective CO₂ removal programs from major industrial CO₂ emission sources, including hard-to-abate sectors like power generation and large-scale industry, which continue to drive GHGe.

Amine-based CO₂ capture

Many countries continuously adapt new CCUS strategies to decarbonize the industries that are difficult to abate. Amine solutions have been proposed by Robert Roger Bottoms in 1930 to absorb CO₂ from high CO₂ content gas streams such as natural gas, and desorb as a high purity CO₂ gas at higher temperatures around 120 °C⁴. Shown in Fig. 1, the well understood amine scrubbing process is still relevant today.

Flue gas from hard-to-abate industries is fed to the bottom of the packed absorber, where it contacts the lean amine solvent containing available nitrogen sites that react with acidic gases. The exothermic absorption

of acidic gas CO₂ into amines releases heat, which increases the reaction rate but simultaneously reduces the driving force for the chemical equilibrium. Introducing intercooling sections within the absorber is an advanced heat-integration strategy that leverages the temperature dependence of both the reaction rate and equilibrium constant, thereby reducing the required column height and lowering the cost of the packing materials in capital expenditure (CAPEX)⁵. Following a temperature bulge, endothermic water evaporation offsets the liquid-phase temperature rise caused by the exothermic CO₂ absorption, leading to a temperature decrease toward the absorber bottom. The rich solvent typically leaves the column at a slightly higher temperature than the lean solvent.

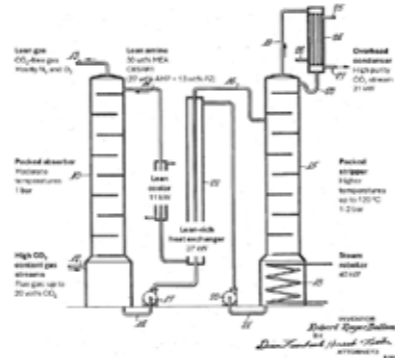


Fig. 1: Acid gas separation with amines, proposed by Robert Roger Bottoms in 1930⁴.

The exothermic absorption of CO₂ into amines releases heat, which increases the reaction rate but simultaneously reduces the driving force for the chemical equilibrium. Introducing intercooling sections within the absorber is an advanced heat-integration strategy that leverages the temperature dependence of both the reaction rate and equilibrium constant, thereby reducing the required column height and lowering the cost of the packing materials in capital expenditure (CAPEX)⁵. Following a temperature bulge, endothermic water evaporation offsets the liquid-phase temperature rise caused by the exothermic CO₂ absorption, leading to a temperature decrease toward the absorber bottom. The rich solvent typically leaves the column at a slightly higher temperature than the lean solvent.

The heat from the hot regenerated lean amine solvent is exchanged with the warm rich solvent leaving the absorber, following the primary design philosophy of reducing the reboiler duty. However, the heat exchanger can be partially bypassed for a fraction of the rich solvent feed to optimize the performance of both the reboiler and condenser to minimize the overall cost of capture⁵. This configuration enables a wider selection of heat sources from available heat sinks at different temperature levels, enhancing the scalability of amine-based capture technologies.

Scaling up the technology towards TRL 7+

Scaling up amine-based CO₂ capture technologies largely depends on the willingness of member states to pay for the amount of CO₂ captured at each point in the value chain. However, there are several constraints, including the risk of equipment failure due to amine corrosion and precipitation, oxidative and thermal solvent degradation that reduces the solvent cyclic capacity and overall performance, potential environmental hazards from nitrous amine emissions, and public acceptance challenges related to capture plant design and operation.

The EU-funded CESAR project investigated various amine solvents at the pilot-scale and benchmarked the CESAR1 blend (27 wt% AMP mixed with 13 wt% PZ in water) for post-combustion capture. The results show that the combination of lean vapor compression (LVC) and intercooled absorber could reduce the specific reboiler duty (SRD) down to 2.6 GJ/tCO₂ captured compared to 2.9 GJ/tCO₂ for MEA under the same advanced process configurations applied in Esbjerg pilot plant with capacity of capturing one ton of CO₂ per hour from the flue gas of a coal-burning power station⁶. The recent long-term testing of the modified CESAR blend (26 wt% AMP and 6 wt% PZ) from cement flue gas at the Danish cement production plant Aalborg Portland further revealed that SRD can be decreased down to 2.03 GJ/tCO₂ with a lot of opportunities for advanced heat integration configurations^{5,7}.

Furthermore, solvent management becomes critical when scaling up amine-based capture technologies. Amines undergo thermal degradation at high temperatures and oxidative degradation in the presence of oxygen in the flue gas. The solvent is typically regenerated at a higher pressure of 1.8-2.0 bara and a temperature of 100-120 °C at the stripper to optimize the specific reboiler duty (SRD) and compression work. However, our results have shown that the amine degradation rate triples even at 2 bara compared to atmospheric pressure⁸. Moreover, PZ enhances the

CO₂ absorption rate of the blend at increasing absorber temperatures, but causes precipitation when used at higher concentrations, especially at lower temperatures and lower CO₂ contents, as shown with our extended-UNIQUAC model predictions below.

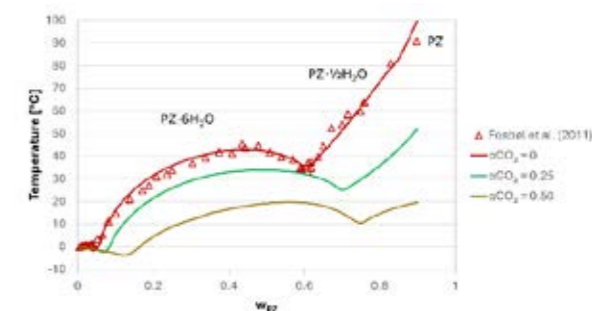


Fig. 2. Solid-liquid equilibrium (SLE) of the PZ-CO₂-H₂O system predicted by extended-UNIQUAC and supported by measurements from Fosbøl et al⁹.

Conclusions

Efficient scale-up of amine-based CO₂ capture technologies will play a key role in decarbonizing hard-to-abate industries in the coming decades. Benchmarking new amine blends at the pilot scale, supported by accurate process models, is essential for optimizing and intensifying capture processes to inform policy decisions. PZ precipitation remains a major operational risk, particularly as most European capture projects will be located north of Brussels to supply CO₂ for storage in the North Sea. In this context, advanced heat-integration configurations combined with accurate process models offer unique opportunities for chemical engineers to innovate in climate technology.

References

- Intergovernmental Panel on Climate Change (IPCC). *Climate Change 2021: The Physical Science Basis. Contribution of Working Group I to the Sixth Assessment Report of the Intergovernmental Panel on Climate Change*. (Cambridge University Press, Cambridge, UK, 2023). doi:10.1017/9781009157896.
- Solomon, S., Plattner, G.-K., Knutti, R. & Friedlingstein, P. Irreversible climate change due to carbon dioxide emissions. *Proceedings of the National Academy of Sciences* 106, 1704–1709 (2009).
- United Nations Framework Convention on Climate Change (UNFCCC). *The Paris Agreement*. (2015).
- Robert Roger Bottoms. *Process for separating acid gases*. (1930).
- Appelquist Løge, I. et al. Pilot-scale CO₂ capture in a cement plant with CESAR1: Leveraging absorber intercooling and cold-feed heat-integration to lower the SRD. *Chemical Engineering Journal* 524, 169153 (2025).
- Knudsen, J. N., Andersen, J., Jensen, J. N. & Biede, O. Results from test campaigns at the 1 t/h CO₂ post-combustion capture pilot-plant in Esbjerg under the EU FP7 CESAR project. in *1st Post Combustion Capture Conference (PCCC1)* (2011).
- Løge, I. A. et al. Pilot-scale CO₂ capture in a cement plant with CESAR1: Comparative analysis of specific reboiler duty across advanced process configurations. *Chemical Engineering Journal* 159429 (2025) doi:10.1016/j.cej.2025.159429.
- Løge, I. A. et al. Pilot-scale CO₂ capture in a cement plant with CESAR1: Higher stripper pressure reduces energy demand and compression work but increases solvent degradation. *Chemical Engineering Journal* 518, 163900 (2025).
- Fosbøl, P. L., Neerup, R., Arshad, M. W., Tecle, Z. & Thomsen, K. Aqueous Solubility of Piperazine and 2-Amino-2-methyl-1-propanol plus Their Mixtures Using an Improved Freezing-Point Depression Method. *J Chem Eng Data* 56, 5088–5093 (2011).

Chemical resistance and solvent absorption characteristics of coatings for sustainable fuels

(May 2024 – April 2027)



Contribution to the UN Sustainable Development Goals

Industries adopting sustainable fuels like methanol will require advanced solutions to safeguard their metal infrastructure from the corrosive effects of this energy source. Development of methanol-resistant epoxy coatings will lead to more durable fuel storage facilities and will thereby enable wider adoption of sustainable fuels, resulting in reduced environmental impact and advancement towards sustainable industrial practices. To achieve that, understanding how solvent absorption causes chemical and structural changes is crucial.



Maria Echarri-Giacchi

maecgi@dtu.dk

Supervisors:
Søren Kiil
Narayanan Rajagopalan
Omar Brun

Abstract

The global transition toward sustainable fuels demands materials that can tolerate new chemical environments. Many renewable fuels, such as methanol, hydrogen, ammonia, and free-fatty-acid-based blends, are corrosive to metals and can degrade conventional protective coatings. This project aims to understand how such fuels interact with epoxy systems and design novel, chemically resistant coatings capable of protecting metallic structures in harsh service conditions.

Introduction

Global efforts to mitigate greenhouse gas emissions have accelerated the search for cleaner energy carriers and the implementation of stricter environmental policies. Maritime transportation, responsible for around 2.6 % of global CO₂ emissions, has become a central focus of decarbonization strategies. The International Maritime Organization (IMO) has set an ambitious target to reduce greenhouse gas emissions from shipping by at least 50 % by 2050 compared with 2008 levels [1].

Reaching the IMO ambitious goal requires the introduction of sustainable fuels such as methanol, ammonia, hydrogen and bio-based free fatty acids. These emerging fuels offer cleaner combustion profiles and significant potential for carbon reduction. Among them, methanol (CH₃OH) has attracted considerable interest in the maritime sector due to its favorable hydrogen-to-carbon ratio and its ability to burn cleanly without producing NO_x and SO_x gases. Additionally, methanol can be carbon-neutral when produced from biomass. In Denmark, the industrial sector is integrating sustainable fuel technologies as part of its transition strategy. Some companies, such as Maersk, have already adopted methanol-fueled

ships, reflecting the growing industrial shift toward cleaner shipping practices (Figure 1) [2].



Figure 1: The first methanol-powered ship [2].

Despite its promising potential, methanol's polar nature and electrically conductive properties can induce galvanic corrosion on metallic surfaces, creating risks for steel fuel storage tanks [3]. Such corrosion poses safety and economic challenges, resulting in substantial costs associated with maintenance, repair, and replacement. To mitigate these effects, high-performance protective coatings are essential. These coatings act as barriers that prevent corrosive agents from

interacting with the underlying metal substrate, significantly extending the service life of industrial tanks.

Epoxy-based coatings are among the most efficient solutions for aggressive environments due to their exceptional adhesion, mechanical strength, and overall chemical resistance [4]. In particular, bisphenol-based epoxy-amine systems and epoxy novolacs exhibit strong resistance to many chemicals, making them effective barriers in harsh environments [5]. However, epoxy coatings are susceptible to degradation in certain chemical environments, especially in the presence of acids and polar solvents such as methanol [6].

When an epoxy coating is exposed to methanol, degradation is inevitable and can proceed through two primary pathways: physical degradation and chemical degradation. Physical degradation involves the diffusion of the penetrant through a coating, resulting in swelling, loss of flexural strength, blistering, and delamination [7]. In contrast, chemical degradation involves the reaction of the aggressive chemical with the coating network [8]. The interplay between these processes is complex and often synergistic, as initial physical changes can facilitate subsequent chemical deterioration.

While the degradation of epoxy coatings in contact with water and electrolytes has been extensively studied, the effects of organic solvents, such as methanol, remain significantly underexplored. Methanol is known to cause severe physical and chemical disruptions in epoxy networks, including rapid plasticization, swelling, and reduction of mechanical performance [9]. Despite clear experimental evidence of its aggressive behavior, a fundamental understanding of how methanol interacts with epoxy systems is still lacking. This gap presents a major limitation in current coating science, as many conventional formulations fail prematurely under methanol exposure. Advancing knowledge in this area is crucial for overcoming existing material limitations and enabling the development of coatings with the resilience necessary for methanol-rich environments.

Specific Objectives

The objectives of this project are to gain a comprehensive understanding of the interactions between methanol and epoxy coatings, particularly how methanol exposure influences the chemical structure and performance of coatings. Another key objective is to develop an analytical method capable of monitoring and characterizing the chemical changes that the epoxy network undergoes after contact with methanol. Finally, the project aims to investigate the effects of various sustainable fuels, such as ammonia and fuels derived from free fatty acids, on the chemical stability, durability, and overall performance of epoxy coatings.

Acknowledgements

This project is funded by the Hempel Foundation for Coating Science & Technology and carried out in collaboration with Hempel A/S Denmark and Hempel SAU Spain.

References

1. C. M. Noor, M. M. Noor, R. Mamat. Renewable and sustainable energy reviews 94 (2018) 127-142.
2. A Maritime Energy Transition. MAN Energy Solutions.
3. X. Rao, C. Yuan, Z. Guo, Y. Xu, and C. Sheng. Renewable Energy (2025) 123562.
4. F. L. Jin, X. Li, S. J. Park. Industrial and Engineering Chemistry 29 (2015) 1-11.
5. K. Frank, J. Wiggins. Journal of Applied Polymer Science, 130 (1) (2013) 264-276.
6. V.B. Møller, K. Dam-Johansen, S.M. Frankær, S. Kiil. Journal of Coatings Technology and Research (2017) 14(2) 279-306.
7. Ultrimax. Paint Cracking, Bubbling, Blistering, and Orange Peel: 42 Paint Problems Solved (No. 1-10). Accessed October 21, 2025.
8. L. Baij, J. Hermans, B. Ormsby, P. Noble, P. Iedema, K. Keune. Heritage Science (2020) 8(1).
9. S. Zheng, P. A. Lucas. Coating World 29 (2020) 35-45.

Investigation of the anomalous behavior of water using a new hypothesis

(August 2025 – August 2028)

6 CLEAN WATER AND SANITATION



Contribution to the UN Sustainable Development Goals

A deeper understanding molecular-level behavior of water is crucial for the design of more efficient and sustainable industrial processes that utilize water or aqueous solutions. Since water exhibits unusual behavior and has many anomalous physical properties that are not entirely understood, this research aims to produce advanced thermodynamic models to represent the anomalous properties of water and aqueous solutions. By providing more accurate property predictions, this work might contribute to the conservation of water resources through improved tools for process design.



Alican Ertas

alier@dtu.dk

Supervisors: Georgios M. Kontogeorgis, Xiaodong Liang, Nefeli Novak

Abstract

Water is the most important substance on Earth, especially for living things. Although many experimental studies have revealed hundreds of its properties, its molecular-level behavior remains incompletely understood. Its unique molecular structure leads to numerous anomalous properties, many of which exhibit local extrema, not observed in other liquids. The two-state theory has become a useful tool in describing this unusual behavior, contrary to other traditional approaches. Therefore, this study combines the theory with the SAFT-VR Mie model to accurately predict the properties of water and aqueous solutions.

Introduction

Water is one of the most extensively studied substances, and numerous theoretical models have been developed to represent its thermophysical properties. Yet, the accurate prediction of water and aqueous solutions behavior remains challenging, and it plays a critical role in the design of more efficient industrial processes with less water consumption. Although many Statistical Associating Fluid Theory (SAFT)-type models are found to accurately represent the phase behavior of compounds with hydrogen bonding, they are unable to provide high accuracy in the property predictions for pure water [1]. The main reason for this inaccuracy lies in water's unique structure that provides water with anomalous properties exhibiting local extrema, unlike most liquids. The conventional models fail to capture this unusual behavior, and this limits the predictive accuracy for pure water and aqueous mixtures. A powerful explanation for these anomalies is the two-state (TS) theory, which suggests that pure liquid water actually consists of a mixture of high-density (HDL) and low-density liquids (LDL) [2]. Although the theory is still debated in the scientific community, the theoretical models based on this theory

demonstrated an ability to represent the water's unusual behavior, and hence most of the anomalous properties. For instance, Novak et al. successfully combined the theory with the Perturbed Chain (PC)-SAFT equation of state, and they showed that the new PC-SAFT-TS and PC-SAFT-TS-CAF models could accurately represent several anomalous properties of pure water, as well as the minimum hydrocarbon solubilities in water [3,4]. This success supports the TS theory and shows that integrating it into different SAFT-type models is worth further investigation.

Specific Objectives

Although the previous models with PC-SAFT were found to be useful to describe the liquid water's behavior, the authors observed that there were still some deviations from the experimental data for the properties, especially for the derivative ones, such as the speed of sound and heat capacities [3,4]. To improve upon this model, using the SAFT-variable range (VR) Mie model might result in lower deviations because it employs the more general Mie potential instead of the Lennard-Jones potential, and some researchers have found that it represents the

derivative properties of fluids more accurately compared to traditional SAFT-type EOSs [5]. Therefore, it is worth investigating whether successful overall representations of the anomalous properties of both pure water and solutions can be obtained using the TS theory within the SAFT-VR Mie model, and that will be the first objective of the study. Moreover, following a successful validation for pure water, this new approach also offers an opportunity to predict the phase behavior of aqueous mixtures, especially electrolyte solutions. Therefore, the second objective will be to capture the properties related to the ion-water interactions, such as the temperature dependency of activity coefficients of water-salts and individual ion activity coefficients, as well as the ion effects on the water structure. Overall, throughout the project, the aim is to strengthen the theoretical foundation of the debated theory. Success in these objectives might provide a more reliable predictive tool for the thermodynamics of aqueous systems.

Results and Discussion

The initial phase of the project focused on building the theoretical and computational background. A comprehensive literature survey has been conducted regarding both the two-state theory and SAFT variants. Significant progress has been made in understanding the computational algorithm of SAFT-type models, particularly regarding the calculation of Helmholtz free energy contributions and the derivation of thermodynamic properties. Meanwhile, as a verification step, algorithms for PC-SAFT-TS-CAF have been implemented to successfully reproduce literature data for pure water properties, as shown in the figure with experimental data from the literature [6].

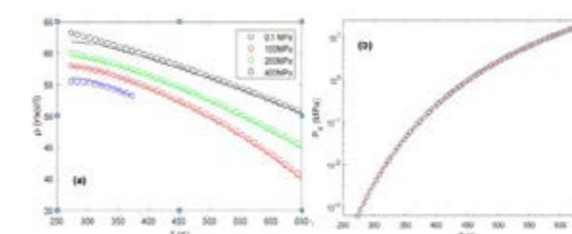


Figure 23: Prediction results from PC-SAFT-TS-CAF model [4] and experimental data [6] for pure-water (a) density and (b) saturation pressure. The solid lines represent the prediction results, while the points represent the experimental data.

The successful reproduction work done so far shows the general feasibility of combining the TS theory with a SAFT framework. This result supports the integration of the theory with SAFT-VR Mie and helps identify the possible challenges to be faced through this process.

Future Work

The next step in this research will be the integration of the new model, SAFT-VR Mie-TS. After obtaining the pure-water property prediction

results following parameter optimizations, the accuracy of the model will be evaluated, and its parameters will be refined to improve its performance. Following successful validation for pure water, the model will be extended to electrolyte solutions. There, not only the representation of anomalous properties of water-salts but also the properties related to ion-water interactions, such as the temperature dependency of activity coefficients and individual ion activity coefficients, will be investigated.

Conclusions

This study plans to investigate the prediction capability of the TS theory-based, SAFT-type models on the anomalous properties of water and electrolyte solutions. It began by establishing a foundation in both theoretical understanding and computational methods for the advanced thermodynamic models. The work completed so far includes a literature review and reproduction of results from existing models, leading to setting a path for the construction of a novel SAFT-VR Mie-TS model. A successful implementation of this model is expected to provide insights into the molecular behavior of water and yield a practical tool to simulate aqueous systems.

Acknowledgements

The authors would like to acknowledge the Independent Research Fund Denmark | Natural Sciences for the support of this project.

References

1. E. Tsochantaris, X. Liang, G.M. Kontogeorgis, *Journal of Chemical & Engineering Data* 65 (2020) 5718–5734.
2. W.C. Röntgen, *Annalen Der Physik* 281 (1892) 91–97.
3. N. Novak, X. Liang, G.M. Kontogeorgis, *The Journal of Chemical Physics* 160 (2024).
4. N. Novak, X. Liang, G.M. Kontogeorgis, *Fluid Phase Equilibria* 598 (2025) 114475.
5. S. Dufal, T. Lafitte, A. Galindo, G. Jackson, A.J. Haslam, *AIChE Journal* 61 (2015) 2891–2912.
6. E.W. Lemmon, I.H. Bell, M.L. Huber, M.O. McLinden, NIST Chemistry Webbook: NIST Standard Reference Database Number 69, NIST, 2000.

CFD modeling of kaolinite flash calcination in a lab-scale drop tube reactor

(September 2022 – December 2025)



Contribution to the UN Sustainable Development Goals

The cement industry is one of the largest industrial sources of CO₂ emissions, mainly from the calcination of limestone during clinker production. Partially replacing clinker with calcined clay offers a practical route to lower these emissions, since clay calcination releases much less CO₂. This research contributes to that effort by improving understanding of the clay calcination process through advanced modeling, helping to identify efficient operating conditions and guide the design of more sustainable cement technologies, thereby supporting UN Sustainable Development Goal 13 (Climate Action).



Roohangiz Shivaee Gariz

roshga@kt.dtu.dk

Supervisors: Peter Arendt Jensen, Hao Wu, Carsten Bang Mikkelsen, and Jens Abildskov

Abstract

Calcined clay is a promising supplementary cementitious material that can significantly reduce CO₂ emissions from cement production. This study investigates flash calcination of kaolinite clay in a lab-scale drop tube reactor using computational fluid dynamics (CFD) modeling. The predicted gas temperature profile agrees well with the experimental data, and the model reproduces the observed increase in kaolinite conversion with reactor wall temperature. The results provide valuable insight to support the scale-up of clay calciners for industrial applications.

Introduction

This work models an electrically heated flash calcination process to activate kaolinite clay. A sensitivity analysis is performed to evaluate the effect of the main process and design parameters on the process. Cement production accounts for about 8 % of global CO₂ emissions [1], mainly from limestone calcination [2]. Replacing part of the clinker with calcined clay can substantially lower emissions [3]. While calcined clay has been widely studied experimentally, modeling of the process remains limited.

Specific Objectives

The objectives of this work are to:

- Develop a computational fluid dynamics (CFD) model of a lab-scale drop tube reactor for flash calcination of kaolinite clay.
- Validate the model against experimental measurements of temperature and calcination degree.
- Apply the model to understand gas–solid flow, heat transfer, and reaction behavior during clay calcination and to support future scale-up of the process.

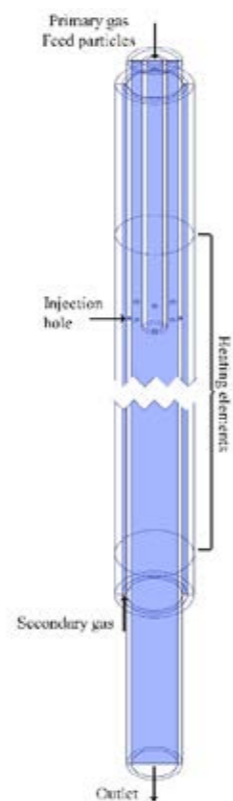


Figure 24: Schematic of the drop tube reactor

Method

The reactor, shown in Figure 1, consists of three concentric tubes with electrical heating elements surrounding the main section. Primary gas carrying clay particles enters from the top, while secondary gas enters from the bottom, is heated within the annular space by surrounding electrical elements, and then passes through holes in the inner tube into the main flow.

The CFD simulations were performed in ANSYS Fluent using the Euler–Lagrange approach. The model accounts for gas–solid heat transfer, reaction heat effects, and radiation.

Result and Discussion

The reactor was first simulated without particle injection to assess its thermal behavior. Figure 2 shows that at a wall temperature of 950 °C, the simulated gas temperature profile agrees well with the experimental data from Koutsouradi et al. [4].

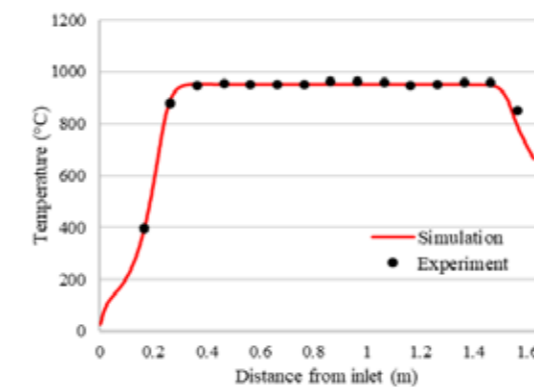


Figure 2: Comparison of simulated and measured centerline gas temperatures along the reactor for wall temperatures of 950 °C

Figure 3 shows the calculated cross-sectional average gas and particle temperatures along the reactor at a wall temperature of 950 °C. The gas cools gradually as heat is transferred to the incoming particles and consumed by moisture evaporation and the endothermic reaction.

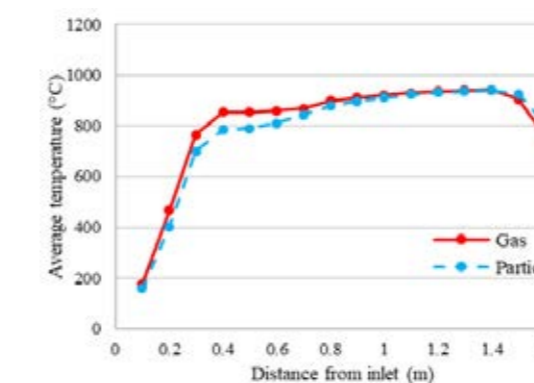


Figure 3: Comparison of simulated average gas and particle temperatures along the reactor for wall temperatures of 950 °C

Figure 4 compares predicted and measured conversions versus wall temperature. The CFD model reproduces the overall increasing trend, though some deviations are observed.

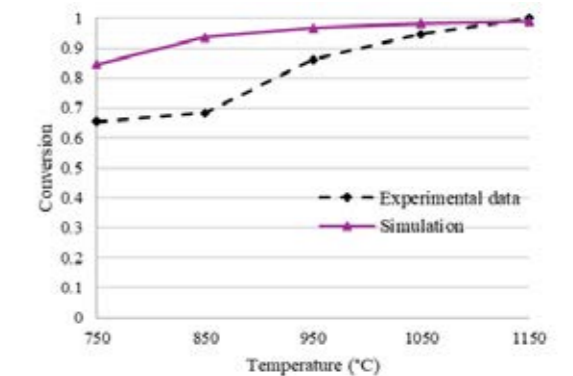


Figure 4: Comparison of simulated and experimental kaolinite conversion as a function of wall temperature

Conclusions

The simulated gas temperature profile in the non-reactive case showed good agreement with the experimental data, confirming that the model accurately represents heat transfer in the reactor. When particles were injected, the gas temperature decreased due to heat absorption by the particles, moisture evaporation, and the endothermic dehydroxylation reaction. The CFD model reproduced the experimental trend of increasing kaolinite conversion with temperature, although some deviations were observed. These differences may be attributed to particle agglomeration, the applied kinetic model, and variations in the feed flow rate.

Acknowledgments

This work is supported by the ECoClay project: Electric Calcination of Clay, funded by EUDP, in collaboration with Danish Technological Institute, FLSmidth, Chemney lab, Cementos Argos, VICAT, RONDO, and the Technical University of Denmark.

References

1. R. M. Andrew, Earth System Science Data 10(1) (2018) 195-217.
2. M. Pisciotta, H. Pilorgé, J. Davids, P. Psarras, Clean Eng. Technol. 15 (2023) 100667.
3. T. Hanein, K. C. Thienel, F. Zunino, A. Marsh, M. Maier, B. Wang, F. Martirena-Hernández, Materials and Structures 55(1) (2022) 1-29.
4. Koutsouradi, W. R. L. da Silva, A. J. Damø, P. A. Jensen, Appl. Clay Sci. 265 (2025) 107649.

Biopolymer-based fiber composites from waste materials

(November 2024 – October 2027)

12 RESPONSIBLE CONSUMPTION AND PRODUCTION



Contribution to the UN Sustainable Development Goals

The Architecture Engineering and Construction (AEC) sectors are significantly contributing to the GHG emissions. In Europe the focus was mostly on improving the energy efficiency of buildings, ignoring the effect of raw materials. Therefore, this project aims to use alternative biobased materials for construction applications to minimize the contribution of the AEC sector to the climate change. The materials come from renewable or waste sources with a focus on plant-based biopolymers and fast-growing fibers like hemp fibers.



Eleftheria

Gitsouli

elegi@dtu.dk

Supervisor: Anders Egede Daugaard

Abstract

Biopolymers have several advantages as they are natural and nontoxic. They can be processed in various methods like solvent casting and 3D printing or thermoprocessing methods like extrusion and compression molding. In this project, biopolymers are being used in combination with waste fibers either in composite or coating applications. An investigation of the properties of the composites can help in finding the ideal application for each product. In particular, this study investigated the extrusion of three plant-based proteins to result in products with advanced mechanical properties.

Introduction

The Architecture, Engineering, and Construction sectors (AEC) are contributing to a great extent to global climate change, according to the Global Status Report for Buildings and Construction [1]. In 2022, the global GHG emissions attributed to the construction industry were around 37%, of which 7-9% were due to manufacturing of the building materials, including steel, cement, and glass [1]. In Europe, in order to minimize these emissions, the focus is mostly on energy efficient buildings, ignoring the environmental problems caused by the material usage.

To address this challenge, the present project investigates biopolymer-based fiber composites as sustainable alternatives for construction materials. Biopolymers have attracted considerable research attention in the last 15 years due to their renewability, biodegradability, thermoformability, and excellent film-forming abilities. These properties make them appealing for industrial applications, including potential use as substitute to conventional construction elements. Some preliminary studies show the use of materials like starch in cladding applications, to protect buildings from heat radiation and weather conditions [2]. However, broader applications of

biopolymer systems in the construction industry remain underexplored.

In this project, plant-based proteins (such as soy protein isolate, pea protein, and wheat gluten) are investigated as primary binder systems for the development of fiber-reinforced composites. Plant-based proteins were selected as they have different functional groups due to the diverse amino acids, enabling multiple modification routes to enhance their properties. To enhance product sustainability, waste fibers have been investigated as fillers for reinforcement of plant-based proteins. Biopolymers can also be utilized as coatings of yarns made from fast-growing fibers. The use of biopolymer coatings can help in higher stress resistance, facilitating the knitting process, which can benefit both textile and architectural composite manufacturing. Biopolymer based fiber composites can offer significant potential in the construction industry, as they can contribute to the AEC sector by increasing the CO₂ storage in buildings.

So far, biopolymers have been typically processed via solvent casting due to their water solubility. This method has several drawbacks, including

high water consumption, the production of thin films, and limited industrial scalability [3]. To overcome these limitations, extrusion was explored as an alternative thermoprocessing technique. The high shear and high temperatures lead to the formation of a melt with the denaturation of the protein resulting in different types of crosslinking and alternation of the overall structure of the protein [4].

Objectives

- Characterization of several plant-based proteins.
- Preparation of biopolymer composites with waste fillers.
- Investigation of different processing methods including solvent casting, extrusion or 3D printing.

Here a comparative example illustrates the effects of processing plasticized plant-based proteins by extrusion produce films with advanced mechanical properties and compares it with solvent casting to elucidate the differences in the produced films. This study aims to expand the applicability of biopolymer-based composites in the construction sector, facilitating the transition toward circular, low-carbon building practices.

Results and Discussion

The extrusion of the proteins was successfully achieved with minor adjustments to the processing conditions. The mechanical properties presented in *Figure 1* show the differences between the extruded and the solvent casted films. The extruded films exhibited higher thickness, and they were more resistant to manual deformation. The tensile strength of the extruded protein undergoes an increase of approximately 350%. Additionally, the flexibility of the film is increasing, proving that extrusion is a promising method for improving the properties of the proteins.

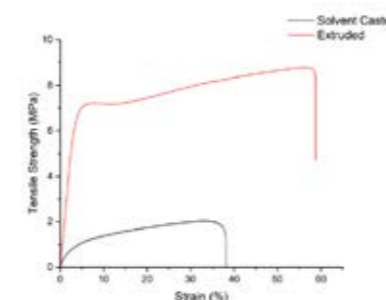


Figure 25: Comparison of mechanical properties of solvent casted and extruded soy protein isolate.

Additionally, extrusion of the three proteins (soy protein isolate, pea protein, and wheat gluten) indicate that proteins cannot be processed under similar conditions. The main differences were associated with the temperature and speed of

extrusion and the amount and type of plasticizers used (water and glycerol). Plasticizers play a critical role in enabling biopolymer processing, as through hydrogen bonding they allow extrusion at elevated temperatures without inducing thermal degradation. Pea protein and soy protein needed lower extrusion speeds to produce smooth and homogenous films. Soy protein demanded the highest amounts of water to be processed, while the solubility of pea protein enables processing with reduced water content. Wheat gluten exhibits distinct behavior in the presence of water, causing the formation of a dough-like consistency with high amounts of water; as a result, it is extruded with low to no water. Figure 2 presents the different extruded films.



Figure 2: Extruded films of soy protein isolate, pea protein and wheat gluten.

Conclusions

The results indicate that extrusion is a promising method for obtaining biopolymer films with increased mechanical properties. Even though soy protein isolate, pea protein and wheat gluten are all plant-based proteins, their processing conditions differ significantly. It is expected that this difference correlates to the different amino acids present in the proteins but also the inter- and intramolecular interactions that arise from folding of the proteins can influence processing. Understanding these differences can facilitate the selection and optimization of each protein for the most suitable application.

References

1. E. A. I. Glob. Alliance Build. Constr. (GlobalABC), 2023.
2. T. Nazrun, M.K. Hassan, M.D. Hossain, B. Ahmed, M.R. Hasnat, S. Saha, Sustainability (Switzerland) 16 (1) (2024) 27
3. M. Matet, M.C. Heuzey, E. Pollet, A. Ajji, L. Avérous, Carbohydr. Polym. 95 (2013) 241–251.
4. T. Garrido, M. Peñalba, K. De La Caba, P. Guerrero, Compos. Part B: Eng. 86 (2016) 197–202.

Microbially assisted syngas biomethanation to renewable natural gas standards

(January 2023 – December 2025)

7 AFFORDABLE AND CLEAN ENERGY



Contribution to the UN Sustainable Development Goals

Methane produced from renewable sources such as dry waste biomass from agriculture or forestry is an attractive alternative to fossil natural gas. Waste feedstocks are cost-effective, the process is scalable, and its implementation can be decentralized. It can also be used as a Power-to-X application, where excess electricity during peak production from renewable sources is used to produce hydrogen. This hydrogen can then be used to achieve higher methane purity while storing the energy in a stable and flexible energy carrier for which transport and use infrastructures are already in place.



Estelle Goonesekera

esgo@kt.dtu.dk

Supervisors: Antonio Grimalt-Alemany, Irini Angelidaki

Abstract

Syngas biomethanation is a biotechnological approach to valorizing syngas that depends on the interrelated metabolic reactions of a mixed microbial community. This study shows that not all microbial interactions are beneficial for the conversion of syngas to methane. Specifically, key microbes cannot synthesize all the necessary amino acids and depend on external sources, which in turn can lead to competition between them. This knowledge is key to optimizing syngas biomethanation productivity.

Introduction

Syngas (or synthesis gas) is one of the products of pyrolysis and gasification, thermochemical processes that treat dry, woody biomass. This gas is mainly composed of hydrogen (H₂), carbon monoxide (CO), carbon dioxide (CO₂), and methane (CH₄) and requires downstream processing to convert it into a recoverable, storable product, such as methane (CH₄).

The biological transformation of syngas to CH₄ can be carried out by a mixed microbial community through interconnected biochemical reactions [1]. A large part of the community is made up of four main trophic groups (see Figure 1) who consume the main components of syngas. They often have syntrophic relationships, where the product of one is the substrate of another.

However, interactions based on substrates (H₂, CO₂, acetate) may not be the only ones present in the community. Other compounds – like amino acids or vitamins – may also be shared or competed for. Furthermore, the microbial community contains a large number of less abundant microbes not directly involved in syngas transformation. These may, and surely do, play key roles in providing the amino acids and vitamins that the main players are not capable of synthesizing themselves [2].

Specific objectives

The genomes of the microbial community were reconstructed from experimental samples. The

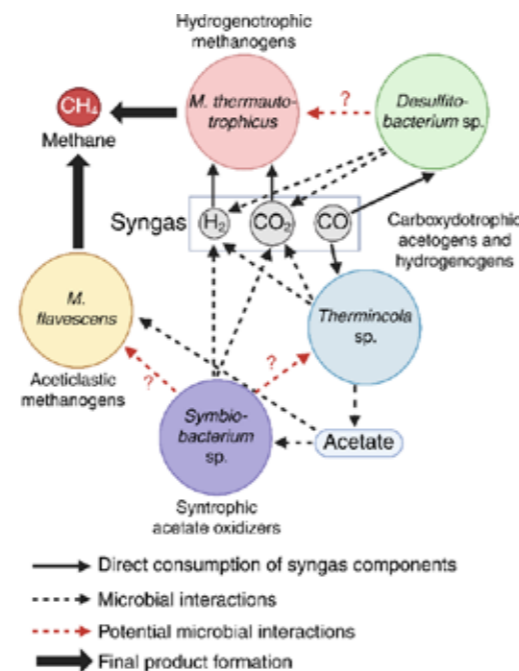


Figure 26: Main trophic groups and their most abundant representatives of the syngas biomethanation community and the interactions between them.

information encoded in the assembled genomes was used to assess their metabolic potential and get a broader view of potential metabolic interactions. Specifically, the presence of amino

acid synthesis pathways was studied, focusing on the main players in Figure 1.

Table 1: Presence and absence of amino acid synthesis pathways of the most abundant and functionally significant reconstructed genomes in the community. Presence is marked with a ●, and absence is marked with a ○.

Amino acid	<i>M. thermotrophicus</i>	<i>M. flavescens</i>	<i>Desulfitobacterium</i> sp.	<i>Thermincola</i> sp.	<i>Symbiobacterium</i> sp.
Glycine	○	○	○	○	○
Alanine	○	○	○	○	○
Valine	●	●	●	●	○
Leucine	○	○	○	○	○
Isoleucine	●	●	●	●	○
Aspartic acid	○	○	○	○	○
Glutamic acid	○	○	○	○	●
Asparagine	○	○	○	○	○
Glutamine	○	○	○	○	○
Proline	○	●	●	●	●
Phenylalanine	○	○	○	○	○
Tryptophan	○	●	●	●	●
Tyrosine	○	○	○	○	○
Lysine	●	●	●	●	●
Arginine	●	●	○	●	●
Histidine	●	●	●	●	●
Cysteine	○	●	●	●	●
Methionine	○	○	●	○	●
Serine	○	○	○	○	○
Threonine	●	●	●	●	●

Results and Discussion

Table 1 shows the amino acid synthesis pathways found in the genomes of the main microbes involved in syngas biomethanation. First, it is clear that none of these microbes can synthesize all the amino acids they need to produce proteins, making them dependent on a source in the environment. Absent this external source, these microbes would depend on the ability of others in the community to produce the amino acids they lack, leading to a community network with more interdependence than originally anticipated.

For example, *M. thermotrophicus* and *Desulfitobacterium* sp. are syntrophs when it comes to substrate: *Desulfitobacterium* takes up CO and produces the H₂ and CO₂. *M. thermotrophicus* needs to make CH₄. They could also be syntrophs for methionine, which *Desulfitobacterium* can produce but *M. thermotrophicus* cannot. The same could happen in the inverse direction with arginine. However, neither can produce glycine, and they would thus likely compete for the glycine produced by other members of the community (not shown in Table 1). It is thus clear from these results that microbial interactions are more complex than at first glance, and that amino acid exchange is an integral part of the interaction network.

Process optimization in such systems often assumes a purely syntrophic relationship between key microorganisms, like *M. thermotrophicus* and *Desulfitobacterium* sp. However, an incomplete picture of the total set of interactions between them can lead to discounting possible competition for limited resources, like amino acids they cannot synthesize themselves. Optimization also seldomly focuses on the minority keystone species that play such crucial roles as synthesizing those amino acids, potentially leading to dissatisfactory results.

Conclusion

Detailed understanding of microbial interactions is key for the advanced optimization of processes that rely on multiple microbial groups. Despite syntrophy being common, potential competition also needs to be accounted for, as does the role of minority keystone species.

Acknowledgements

This work was financially supported by the Technical University of Denmark (DTU), and the EU Horizon projects SEMPRES-BIO (101084297) and CRONUS (101084405).

List of publications

This work has yet to be published.

References

1. A. Grimalt-Alemany, M. Łężyk, D. M. Kennes-Veiga, I. V. Skiadas, and H. N. Gavala, *Waste Biomass Valori.*, 11 (2) (2020) 465–481.
2. S. Banerjee, C. A. Kirkby, D. Schmutter, A. Bissett, J. A. Kirkegaard, and A. E. Richardson, *Soil Biol. Biochem.*, 97 (2016) 188–198.

Tackling biofouling through coatings coupled with underwater cleaning

(March 2024 – February 2027)



Contribution to the UN Sustainable Development Goals

Marine biofouling poses serious environmental and economic challenges. Although effective, fouling control coatings cannot completely prevent biofouling, highlighting the importance of underwater cleaning. The aim of this project is to develop and optimize underwater cleaning methods to minimize the need for harmful substances, while reducing the overall impact of biofouling. By enhancing cleaning efficiency and coating durability, the project contributes to more sustainable marine operations and long-term environmental protection.



Pascal Alexander Guth

pasgu@kt.dtu.dk

Supervisors:
Kim Dam-Johansen,
Huichao Bi

Abstract

Despite advancements in coating technologies and maintenance strategies, marine biofouling, which refers to the accumulation of organisms on submerged surfaces, continues to pose major challenges. This study focuses on optimizing the ultrasonic cleaning process, with emphasis on adjusting the ultrasonic parameters and system configurations to enhance cleaning efficiency, while minimizing damages to the coating and environmental release. The performance of the ultrasonic cleaning process and its environmental impact were evaluated using samples exposed to real biofouling conditions.

Introduction

Marine biofouling, the accumulation of unwanted marine organisms such as algae and barnacles on submerged structures, poses substantial operational and environmental challenges [1]. Biofouling reduces the performance of marine structures, especially moving ones like ships. Increased surface roughness and added weight leads to higher hydrodynamic drag, resulting in greater fuel consumption, greenhouse gas emissions, and maintenance and operational costs [2]. Additionally, vessels operating in various geographical regions may unintentionally spread invasive species, which poses significant risks to native ecosystems and marine biodiversity [3].

Fouling control coatings are the primary method of mitigating the adverse effects of marine biofouling. Conventional antifouling coatings contain biocides that prevent marine organisms from settling and growing [4]. However, the increasing awareness of the ecological risks of biocide accumulation and persistence in marine environments has led to the development of biocide-free alternatives in recent years [5]. While fouling control coatings in general reduce the overall growth on the surface, they do not entirely prevent it. The formation of e.g. biofilms can still occur during exposure periods.

Cleaning technologies have been developed to overcome the limitations of current fouling control coatings and maintain clean surfaces [6]. These methods, which include e.g. the use of rotary brushes, high-pressure water jets, and ultrasonic cleaning, primarily rely on mechanically removing fouling from affected surfaces [7]. Although cleaning operations can be performed during dry-docking or anchorage, underwater cleaning is more cost-effective [8]. However, excessive cleaning can result in coating degradation and environmental contamination [9]. Therefore, it is essential to have a comprehensive understanding of fouling processes, coating behavior, and cleaning parameters to optimize cleaning strategies and ensure the long-term durability and environmental compatibility of marine coatings with the cleaning methods.

Specific Objectives

The objectives of this research project are:

- Optimizing underwater ultrasonic cleaning: coating-cleaning compatibility
- Implementing laboratory scale underwater cleaning simulation devices for fouling control coatings
- Comparison effectiveness for multiple underwater cleaning strategies

Methodology

A laboratory-scale cleaning device that simulates proactive underwater ultrasonic cleaning was developed to quantify the key parameters that influence cleaning performance. These parameters include frequency, power intensity, exposure duration, sonotrode-to-sample distance, and amplitude. Figure 1 shows the experimental setup.

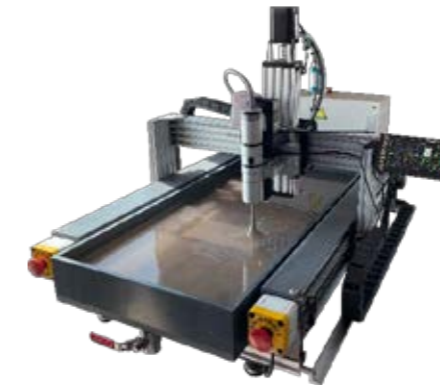


Figure 27: Automated underwater cleaning system (AUCS) with attached ultrasonic transducer for laboratory scale simulation of proactive under-water ultrasonic cleaning

This system allows for interchangeable transducer configurations, enabling controlled and repeatable cleaning trials. In this study, different transducers were used to examine the impact of variations in ultrasonic sonotrode design and other operating parameters on cleaning efficiency. Figure 2 shows the transducer geometries and their corresponding operating amplitudes used in the experiments.

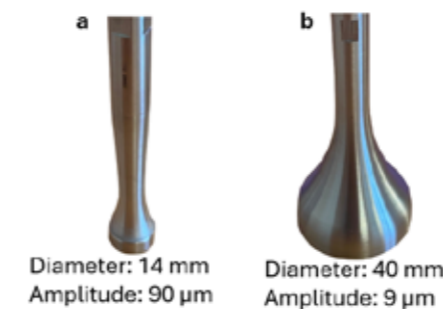


Figure 2: Different ultrasonic transducers with varying geometry, size and amplitude

To simulate cleaning on realistically fouled surfaces coated with different fouling control systems, tests were conducted on panels that had been naturally exposed in the Baltic Sea. Additionally, cleaning experiments were performed on panels that had been artificially exposed to evaluate the impact of ultrasonic cleaning on surface properties and coating integrity.

This dual approach allows to assess the effectiveness of cleaning actual fouling and the potential effects of cleaning on the durability and performance of different coating types.

Progress and future work

The developed laboratory-scale cleaning device enables controlled testing under reproducible conditions and allows systematic adjustment of key operational parameters. Through experiments, the main factors influencing cleaning performance and coating response can be identified. Additionally, the study provided valuable insights into the impact of ultrasonic cleaning on coating integrity and its environmental implications.

Future work will extend these findings by conducting comparative studies with other underwater cleaning methods. This comparison will establish a comprehensive understanding of the advantages, limitations, and environmental performance of different cleaning technologies. This will contribute to the development and optimization of sustainable maintenance strategies for fouling control coatings.

Acknowledgement

Grateful acknowledgment is given to the Hempel Foundation for their financial support.

References

1. D. M. Yebra, S. Kiil, and K. Dam-Johansen, *Progress in Organic Coatings* 50 (2) (2004) 75-104
2. H. Qiu, K. Feng, A. Gapeeva, K. Meurisch, S. Kaps, X. Li, L. Yu, Y. K. Mishra, R. Adelung, M. Baum, *Progress in Polymer Science* 127 (2022) 101516
3. D. M. Coutts, K. M. Moore, C. I. Hewitt, *Marine Pollution Bulletin* 46 (11) 1510-1513
4. J. D. Adkins, A. E. Mera, M.A. Roe-Short, G. T. Pawlikowski, R. F. Brady, Jr, *Progress in Organic Coatings* 29 (1-4) (1996) 1-5
5. L. Li, H. Hong, J. Cao, Y. Yang, *Coatings* 13 (11) (2023) 1893
6. F. Weber, N. Esmaeili, *Biofouling* 39 (6) (2023) 661-681
7. C. Song, W. Cui, *Journal of Marine Science and Application* 19 (3) (2020) 415-429
8. D. R. Oliveira, M. Lagerström, L. Granhag, S. Werner, A. I. Larsson, E. Ytreberg, *Journal of Cleaner Production* 356 (2022) 131882
9. S. Lin, H. Bi, C. E. Weinell, K. Dam-Johansen, *Applied Ocean Research* 144 (2024) 103860

First-Principles prediction of phase inversion temperature for nonionic microemulsion systems

(January 2024 – January 2027)



Contribution to the UN Sustainable Development Goals

This research developed a new method for predicting (micro)emulsion phase diagrams from first principles, based on density functional theory (DFT) and COSMO-RS theory. The proposed method will be used to understand and predict fundamental multi-phase behavior of surfactant-oil-water systems including dynamic emulsion behavior such as stability over time. Our method will provide a valuable tool for chemical and biochemical product formulators, in industry and academia.



Fei

Han

feiha@dtu.dk

Supervisors:

Georgios M. Kontogeorgis
Xiaodong Liang
Martin P. Andersson

Abstract

This study employs Density Functional Theory (DFT) in combination with COSMO-RS to predict microemulsion phase behavior in water–oil–surfactant systems directly from molecular structure. Interfacial tension (IFT) and surfactant partition coefficients ($\log P$) were computed to identify phase transition conditions. COSMO-RS accurately reproduces IFT in binary systems and captures solubility trends consistent with experimental observations. In ternary mixtures, the joint analysis of minimum IFT and $\log P$ successfully predicts the temperature window of the Winsor III region. Deviations observed for long-chain surfactants underscore the importance of conformer selection when modeling flexible molecules.

Introduction

Microemulsions have important applications in numerous fields, ranging from drug delivery to enhanced oil recovery. Their functionality depends on Winsor phase behavior, particularly the Winsor III region characterized by ultralow interfacial tension. This phase behavior can be intuitively represented by a "fish-shaped" phase diagram. However, computational methods for predicting phase diagrams typically rely on empirical parameters or are computationally expensive. This study aims to develop an efficient, first-principles DFT/COSMO-RS-based method that requires no empirical parameters, enabling rapid prediction of phase behavior in ternary microemulsion systems and providing a new tool for formulation design.

Specific Objectives

Our goal is to develop a new method for predicting (micro)emulsion phase diagrams from first principle, based on density functional theory (DFT) and COSMO-RS theory. The proposed method will be used to understand and predict fundamental multi-phase behavior of surfactant-oil-water systems including dynamic emulsion behavior such as stability over time. Our method

will provide a valuable tool for chemical and biochemical product formulators, in industry and academia.

Results and Discussion

We first performed calculations for binary systems. As test cases, the water/hexane and water/octane systems have been evaluated. The results, shown in **Figure 1**, demonstrate that the calculated IFT values are in close agreement with experimental data [1], with deviations of less than 5 mN/m. In particular, the temperature dependence is reasonable. These results confirm that our method provides reliable accuracy in predicting IFT for biphasic (oil–water) systems.

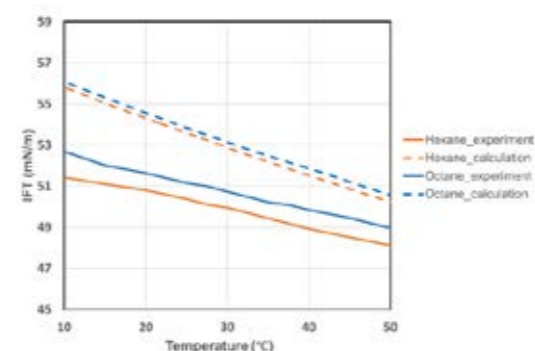


Figure 1. Comparison of calculated (dashed) and experimental (solid) interfacial tension (IFT, $\text{mN}\cdot\text{m}^{-1}$) for water–hexane (orange) and water–octane (blue) as a function of temperature ($^{\circ}\text{C}$).

After validating the method for binary systems, it was extended to ternary water–oil–surfactant mixtures by computing IFT and $\log(P)$ as a function of temperature and surfactant weight fraction. As shown in **Figure 2**, for each composition, the minimum IFT point was extracted and fitted to obtain the min-IFT curve, which corresponds to the most favorable conditions for Winsor III formation. The $\log(P)=0$ contour was plotted in parallel and was found to closely coincide with the min-IFT line, indicating balanced surfactant. Both indicators successfully capture the location and temperature trend of the Winsor III region.

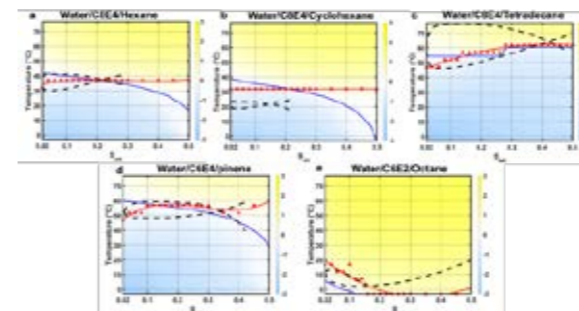


Figure 2. Overlay diagram of the min-IFT curve (red), $\log(P)$ curve (blue), and experimental phase boundary (black) [2-5] for various water/surfactant/oil systems, plotted as a function of temperature and surfactant weight fraction (S_{wt}).

COSMOconf generates the ten lowest-energy conformers for COSMO-RS input, which is sufficient for short-chain surfactants but inadequate for long, flexible molecules such as C12E5 and C12E6, where interfacial or aqueous-phase conformations are not sampled. The resulting conformers mainly resemble oil-phase geometries, leading to inaccurate IFT predictions. A comparison between COSMOconf-generated and manually constructed conformers confirms that conformer selection has a major impact on COSMO-RS results (**Figure 3**). These findings show that accurate modeling of long-chain surfactants requires improved conformational sampling beyond lowest-energy structures.

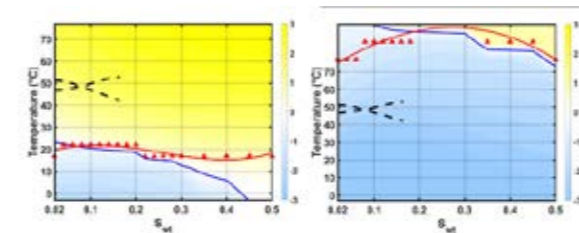


Figure 3. Overlay diagram of the min-IFT curve (red), $\log(P)$ curve (blue), and experimental phase boundary (black) [6] for Water/C12E6/n-Octane, a) C12E6 conformer generated by COSMOconf; b) C12E6 conformer generated manually.

Conclusions

This study demonstrates that a first-principles DFT/COSMO-RS approach can successfully predict the characteristic "fish" phase diagrams of ternary microemulsion systems. Without requiring empirical parameters, the method accurately identifies key phase boundaries by computing interfacial tension and partition coefficients. The results show that the model correctly captures the temperature dependence and shifts of the Winsor III region across different oils and surfactants, particularly for short, linear nonionic surfactants. The framework is both computationally efficient and predictive, offering a reliable theoretical tool for rapid screening and formulation design of microemulsions.

Acknowledgements

The authors wish to thank the financial support from the Independent Research Fund Denmark (Case No. 10.46540/3105-00126B) and the Department of Chemical and Biochemical Engineering, Technical University of Denmark.

References

1. S. Zeppieri, J. Rodríguez, A.L. López de Ramos, J. Chem. Eng. Data 46 (5) (2001) 1086–1088.
2. J.-M. Aubry, J.F. Ontiveros, J.-L. Salager, V. Nardello-Rataj, Adv. Colloid Interface Sci. 276 (2020) 102099.
3. H. Matsuda, Y. Nakazato, R. Tsuchiya, Y. Inoue, K. Kurihara, T. Tsuji, K. Tochigi, K. Ochi, Fluid Phase Equilib. 559 (2022) 113492.
4. F. Bouton, M. Durand, V. Nardello-Rataj, A.P. Borosy, C. Quillet, J.-M. Aubry, Langmuir 26 (11) (2010) 7962–7970.
5. T. Sottmann, R. Strey, Fundam. Interface Colloid Sci. 5 (2005) 5.1–5.96.

List of Publications

This work is preparing to be submitted recently.

Sustainable Epoxy Coatings: Leveraging Aquatic Plant Extracts for Corrosion Resistance

(March 2024 – February 2027)



Contribution to the UN Sustainable Development Goals

Focusing on the development of sustainable epoxy coatings incorporating aquatic plant extracts contributes to UN SDG 12 (Responsible Consumption and Production) by promoting the use of renewable and environmentally friendly materials in corrosion protection. By replacing conventional toxic inhibitors with natural plant-based alternatives, this project aims to minimize chemical waste, lower environmental impact, and enhance the lifespan of steel coatings. Through improving durability and reducing maintenance needs, the research supports more responsible resource use and advances the sustainability of industrial coating practices.



Abolfazi

Hasanzadeh

abhas@dtu.dk

Supervisors: Huichao (Teresa) Bi, Kim Dam-Johansen

Abstract

This study explores the use of extracts from fast-growing aquatic plants as sustainable corrosion inhibitors in epoxy coatings. These plants, often seen as environmental challenges, contain bioactive compounds that can form protective films on metal surfaces. The extracts were obtained through solvent extraction and characterized to confirm the presence of active functional groups. When incorporated into epoxy coatings, they improved corrosion resistance and barrier properties, demonstrating their potential as green, renewable alternatives to conventional inhibitors. The results highlight a sustainable approach to developing eco-friendly protective coatings while contributing to responsible resource use and environmental protection.

Introduction

Corrosion of steel structures is a significant challenge in marine and industrial environments, resulting in substantial economic losses and environmental impacts worldwide. Protective coating remains one of the most effective strategies to combat corrosion; however, traditional coating systems often depend on synthetic inhibitors and toxic compounds that raise environmental and safety concerns. In recent years, the shift toward sustainable and eco-friendly materials has driven research on coatings that not only perform effectively but also minimize ecological harm [1].

Aquatic plants, particularly fast-growing species, represent a unique opportunity within this context. These plants proliferate rapidly, often clogging waterways, depleting oxygen levels, and disrupting aquatic ecosystems — posing serious environmental management problems. Yet, their abundant biomass and rich phytochemical composition make them valuable renewable resources. Many of these plants contain bioactive molecules such as polyphenols, flavonoids, tannins, and alkaloids that can adsorb onto metal

surfaces and inhibit corrosion processes [2], [3], [4].

This project explores the potential of converting these problematic aquatic plants into functional corrosion inhibitors that can be incorporated into sustainable epoxy coatings. By transforming an ecological burden into a technological advantage, the research contributes to the development of green coating systems that enhance durability, reduce maintenance needs, and align with the principles of the circular economy and environmental responsibility.

To achieve this goal, a comprehensive experimental approach was employed. The extracts were thoroughly characterized to determine their chemical composition and physical properties, while various electrochemical and surface analyses were performed to evaluate their corrosion inhibition performance and coating behavior. These investigations confirmed the strong protective performance of the coatings and demonstrated the potential of bio-based epoxy systems as sustainable alternatives to conventional formulations.

Materials and Methods

Fresh aquatic plants were collected from a natural freshwater source and cultured in tap water under controlled laboratory conditions with a balanced light–dark cycle. Nutrient supplements were periodically added to maintain optimal growth. After a period of cultivation, the biomass was harvested, thoroughly rinsed with deionized water to remove impurities, and air-dried under ambient laboratory conditions. The dried material was then ground into a fine powder using a laboratory mill and stored in the dark until further use. Under these conditions, a consistent amount of dry biomass was obtained after each cultivation cycle. The dried biomass was subsequently subjected to solvent extraction, as illustrated in Figure 1. In this process, the powdered material was immersed in an ethanol–water solution under gentle stirring, followed by vacuum filtration. The resulting filtrate was concentrated by rotary evaporation to remove the solvent. The obtained extract was then dried, weighed, and stored in light-protected containers until use.



Figure 1. Schematic representation of the extraction process of bioactive compounds from aquatic plant biomass.

Results

Characterization of the extract revealed the presence of various active organic compounds containing functional groups known to interact with metal surfaces and inhibit corrosion. These findings confirmed that the obtained extract possesses chemical constituents suitable for use as a natural corrosion inhibitor. The results of the corrosion tests demonstrated that incorporating the extract into epoxy coatings significantly enhanced their protective performance. Improved barrier properties, higher corrosion resistance, and enhanced surface stability were observed,

confirming the effectiveness of the bio-based formulation in protecting steel substrates.

Conclusion

The research demonstrated that bioactive extracts obtained from aquatic plants can effectively function as natural corrosion inhibitors in epoxy coating systems. Characterization confirmed the presence of functional compounds capable of interacting with metal surfaces, while corrosion tests verified that their incorporation improved the protective performance and durability of the coatings. The findings provide a practical example of how renewable biomass can be transformed into high-value materials, offering both environmental and technological benefits. Overall, this work contributes to the advancement of green coating technologies and supports global efforts toward sustainable and resource-efficient industrial development.

Acknowledgements

Financial support from the Hempel Foundation Coating Science and Technology Centre at CoaST is gratefully acknowledged.

References

1. J. R. Adsetts, N. Ebrahimi, J. Zhang, F. Jalaei, and J. J. Noël, "Steel Bridge-Coating Systems and Their Environmental Impacts: Current Practices and Future Trends," *Coatings*, vol. 13, no. 5, p. 850, Apr. 2023, doi: 10.3390/coatings13050850.
2. R. K. Sharma *et al.*, "Antioxidant activities and phenolic contents of the aqueous extracts of some Indian medicinal plants," 2009. [Online]. Available: <http://www.academicjournals.org/jmpr>
3. T. Sarkar *et al.*, "Underutilized green leafy vegetables: frontier in fortified food development and nutrition," *Crit Rev Food Sci Nutr*, vol. 63, no. 33, pp. 11679–11733, Dec. 2023, doi: 10.1080/10408398.2022.2095555.
4. Y. Karamalakova, E. Georgieva, V. Ivanov, K. Parlapanska, and G. Nikolova, "ANTIOXIDANTLY-MODULATIVE, CHEMOPREVENTIVE AND ANTI-SARS-COVID 19 ACTION OF MEDICINAL PLANTS," *Trakia Journal of Sciences*, vol. 20, no. 4, pp. 267–282, 2022, doi: 10.15547/tjs.2022.04.001.

Self-stratifying fouling control coatings

(November 2022 – November 2025)



Contribution to the UN Sustainable Development Goals

Multilayer coating systems are commonly used in industry but require large quantities of raw materials and involve complex, time-consuming and labor-intensive application procedures. This challenge is particularly pronounced in the shipping industry. Self-stratifying coatings could overcome these limitations by spontaneously forming two functional layers in a single application, potentially reducing material consumption and markedly improving operational efficiency.



Luis Heller

luihel@kt.dtu.dk

Supervisors: Søren Kiil, Kim Dam-Johansen

Abstract

Coating systems applied to commercial ships typically consist of multiple layers to provide the required protective and fouling control properties. However, when applying such systems during new-built and dry-docking, valuable time is lost in which the ship cannot operate. Self-stratifying coatings, coatings forming automatically two functional layers upon application, could offer substantial ecological and economic benefits to the shipping industry. This unique property has the potential to make the coating application process more efficient in terms of time and material usage, while also enhancing long-term protective performance. The present research focuses on the development and formulation of self-stratifying coatings, investigating their underlying mechanisms and employing novel characterization techniques.

Introduction

Seagoing ships face various environmental impacts, including harsh corrosive conditions and the growth of marine organisms on the ship hull. The latter is also known as marine biofouling. The most common method to protect ships from these impacts is the application of functional organic coatings [1]. State-of-the-art coating systems typically consist of at least three layers: an anticorrosive primer, an adhesion-promoting tiecoat, and a topcoat which mitigates marine biofouling [2].

Commercial merchant ships must undergo frequent dry-docking, usually every five years, for hull cleaning, repairs, or complete coating system replacement [2]. During these periods, the ship is out of water, resulting in lost operational time in addition to dry-docking related costs [3]. The coating process often dictates the overall duration of dry-docking, as each layer requires a specific drying time before the next can be applied. Unfavorable weather or logistical issues can further delay the process. Therefore, reducing the time needed for coating application is of significant ecological interest.

A well-designed self-stratifying coating spontaneously forms multiple, usually two layers as

soon as the coating is applied to the substrate (ship hull) [4]. This distinctive characteristic offers considerable advantages compared to conventional multilayer coating systems. For instance, the time required for the application process could be reduced as no additional drying or overcoating interval is required. Additionally, it has been proposed that gradient-shaped interfaces are formed between the stratified layers, potentially making the coating less susceptible to interlayer adhesion failures [5].

The comparison between a conventional multilayer coating system and the approach of self-stratifying coatings for ship hull coatings is schematically illustrated in Figure 1.

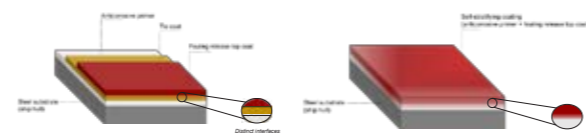


Figure 28: Schematic illustration of a conventional three-layer coating system (left) and a self-stratified coating (right) for ship hulls.

Specific objectives

This research focuses on the development of self-stratifying coatings and establishing a fundamental understanding of their underlying mechanisms, including how these depend on coating formulation (e.g., binder types and effect of pigments) and external parameters (e.g., substrate type). It also involves identifying suitable characterization methods to monitor self-stratification both in real-time and in the final solid state.

Results and discussion

A reactive binder combination of epoxy and silicone was selectively chosen for the development of self-stratifying coatings intended for ship hull applications. Epoxy is commonly used in anticorrosive primers, while silicone compounds are the primary components of current fouling release coatings [3]. Therefore, in this system, epoxy is intended to form the anticorrosive primer (bottom layer) adhering to the substrate and silicone the top layer during self-stratification. Figure 2 presents an exemplary cross-sectional SEM image of a developed self-stratifying coating based on this binder combination in its cured state.

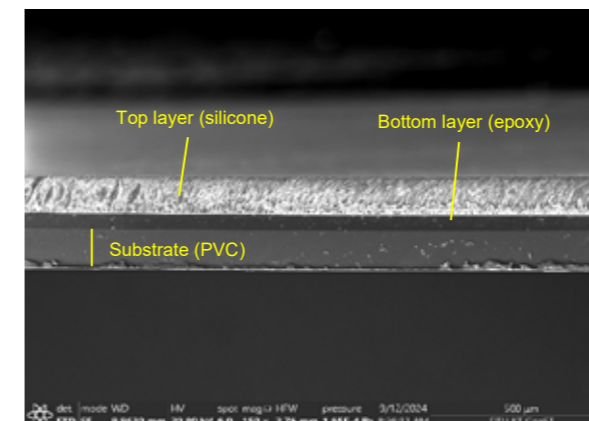


Figure 2: Cross-sectional image of a developed epoxy/silicone self-stratifying coating applied on PVC.

In contrast, a change in coating morphology was observed when the same coating composition was applied to a substrate with a different surface energy (see Figure 3). This behavior has been attributed to altered surface tension relations, and a systematic model describing these interactions and the resulting formation mechanisms has been developed [6]. Additionally, the role of pigments during self-stratification and their final positioning within the coating has been elucidated [7].

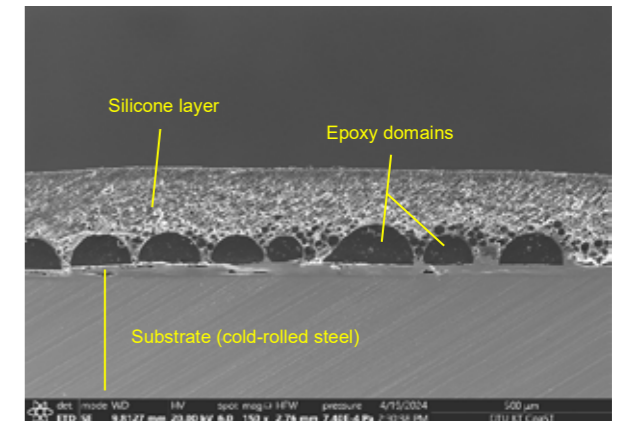


Figure 3: Cross-sectional SEM image of the same coating composition applied to cold-rolled steel.

Conclusions

The technology of self-stratifying coatings can offer a more sustainable alternative to conventional multilayer coating systems. The potential key advantages lie in time and cost savings during the coating application process. Experiments have shown the feasibility of the successful production of self-stratifying coatings that form layers in the desired order. Additionally, an approach has been developed to define the conditions required for successful stratification, taking into account the underlying formation mechanisms.

Acknowledgements

Financial support from the Hempel Foundation to CoaST (The Hempel Foundation Coatings Science and Technology Centre) is gratefully acknowledged.

References

1. D.M. Yebra, S. Kiil, K. Dam-Johansen, *Progress in Organic Coatings* 50 (2004) 75-104.
2. M. Lejars, A. Margailan, C. Bressy, *Chemical Reviews* 112 (8) (2012) 4347-4390.
3. Apostolidis, *Journal of Ship Production and Design* 28 (3) (2012) 134-143.
4. Beaugendre, S. Degoutin, S. Bellayer, C. Pierlot, S. Duquesne, M. Casetta, M. Jimenez, *Progress in Organic Coatings* 110 (2017).
5. V.V. Verkholtantsev, *Progress in Organic Coatings* 13 (1985) 71-96.
6. L. Heller, S. Kiil, K. Dam-Johansen, *Surfaces and Interfaces* 72 (2025) 107116.
7. L. Heller, S. Kiil, A.C.C. Esteves, K. Dam-Johansen, *Progress in Organic Coatings* 210 (2026) 109713.

Fire Safety in Biochar Handling and Storage

(January 2025 – December 2027)



Contribution to the UN Sustainable Development Goals

Biochar production supports a circular economy by converting organic waste, such as agricultural residues, into carbon-sequestering soil amendments and other value-added products. However, widespread adoption of biochar requires safe handling and storage. This project develops a safety framework that identifies and mitigates fire and explosion risks to ensure biochar can be transported and stored safely.



Angel Hurtado

ahugo@kt.dtu.dk

Supervisors: Hao Wu, Wolfgang Norbert Stelte, Peter Arendt Jensen, Flemming Jappe Frandsen

Abstract

Biochar is globally recognized for its potential in soil improvement and climate change mitigation through carbon sequestration. The expansion of biochar production necessitates a critical investigation into associated fire safety hazards. This PhD project addresses the risks of self-heating, self-ignition, and dust explosions during biochar handling and storage. Initial investigations, utilizing Simultaneous Thermal Analysis (STA) and off-gassing experiments, have shed light on the mechanisms governing self-heating induced by low-temperature oxidation. Preliminary results demonstrate that the biochar's reactivity is strongly dictated by the pyrolysis temperature and subsequent aging time. The low-temperature oxidation appears to be kinetically controlled, with no significant correlation observed with particle size or specific surface area. These findings are foundational for developing safety protocols and effective detection and mitigation strategies, which are essential for the responsible and large-scale implementation of biochar technology.

Introduction

Biochar, a carbon-rich material produced through the pyrolysis of biomass, has gained prominence globally, and especially in Denmark, as a sustainable solution for soil enhancement, carbon sequestration, and organic waste valorization [1]. However, with increased production and a broader range of feedstocks, it also brings potential fire safety challenges. Literature and past incidents in biomass and coal storage emphasize the importance of understanding these phenomena to design safe handling protocols and appropriate regulatory frameworks [2].

This PhD project addresses the safe handling and storage of biochar products from a fire safety perspective. In particular, the risks associated with biochar self-heating, self-ignition, and dust explosions during production, storage, and application.

Specific Objectives

1. Identify key properties of biochar that influence self-heating, ignition, and explosibility, with a focus on the role of biomass feedstock properties and biochar production conditions.

2. Gain insights into the interplay of environmental factors, e.g. moisture and oxygen availability, during biochar storage, transport, and handling, and understand their impact on self-heating.
3. Conduct experimental investigations to advance the fundamental understandings on self-heating, self-ignition, and dust explosions of biochar.
4. Design and implement a custom experimental setup to study fire safety, self-ignition, self-heating, and dust explosions in biochar at a lab scale.
5. Explore detection and mitigation strategies based on experimental findings to minimize the risks of biochar self-heating, self-ignition, and dust explosions.

Materials and Methods

The initial phase of the project involved the selection and characterization of biomass feedstocks for biochar production. Three representative feedstocks were chosen: pine wood (PW), wheat straw (WS), and biogas residue fiber (BRF). These feedstocks represent a variety of material types relevant to large-scale biochar production.

Their proximate, ultimate, and ash compositions were characterized. Subsequently, different biochar samples were produced in a muffle furnace. To date, all samples have been generated using a consistent heating rate (5°C/min) but at three distinct final temperatures: 350, 500, and 700 °C.

In addition to the properties analyzed in the raw biomass, biochar's specific surface area and thermal conductivity were measured.

Unlike high-temperature char combustion, char oxidation at low temperatures is an inherently slow process, making its evaluation challenging [2]. Consequently, a dual-methodology approach was adopted for low-temperature reactivity assessment.

Firstly, Simultaneous Thermal Analysis (STA) was performed. This widely used technique measures the simultaneous mass change and heat flow of a sample. However, the slow reaction rate of biochar oxidation at low temperatures limits the operating temperature range that can yield significant mass change and/or heat release.

Secondly, off-gassing experiments in a tubular reactor were conducted to measure the evolution of CO₂, CO and the consumption of O₂ during biochar oxidation between 100 and 200 °C (Figure 1). The production of CO₂ and CO during oxidative self-heating is closely correlated with the heat evolved, making off-gassing a sensitive proxy for low-temperature reactivity.

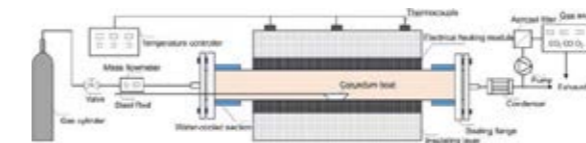


Figure 29: Tubular oven set-up for off-gassing experiments [3]

Results and Discussion

In contrast to other carbonaceous materials, biochar's properties are heavily influenced by the specific pyrolysis conditions used during its production. These conditions directly determine its initial reactivity. Furthermore, it is critical to control the initial exposure of freshly produced char to oxygen, as its reactivity decreases significantly over time as it undergoes atmospheric oxidation (aging).

The STA experiments were highly effective in elucidating the impact of intrinsic and extrinsic properties on char oxidative self-heating at temperatures above 200 °C. As shown in Figure 2, a key finding from the STA experiments was the significant liberation of heat and mass increase that occurs rapidly during the initial exposure to oxygen after pyrolysis. Following this initial

exposure, biochar oxidation proceeds at a slow rate below 200 °C. The observed initial mass increase is plausibly the exothermic chemisorption of oxygen onto surface functional groups. Higher pyrolysis temperatures produce more condensed, less oxygenated biochar with fewer active sites, so they take up less O₂, release less heat on initial exposure and show greater oxidation stability

The off-gassing experiments corroborated the trends observed in the STA tests. Biochar produced at higher pyrolysis temperatures exhibit lower reactivity upon oxidation, resulting in the production of less heat and the release of less CO₂. Additionally, increased aging time systematically resulted in the lowest heat release and carbon oxides evolution during the self-heating tests.

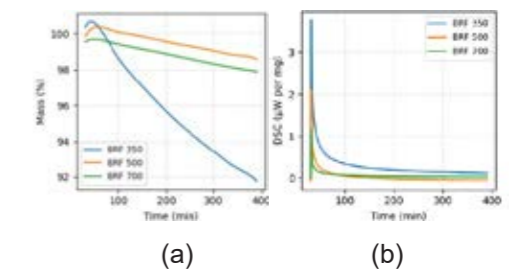


Figure 2: TG (a) and DSC (b) results of oxidation of BRF biochar produced from different temperatures (350 °C, 500 °C and 700 °C) at 200 °C and 80% O₂

No significant correlation was observed between the specific surface area or the particle size. This finding suggests that the low-temperature oxidation process is kinetically controlled rather than diffusion-limited.

Conclusions

This study identified the key factors driving oxidative self-heating in biochar. It shows that pyrolysis temperature and ageing largely determine the material's reactivity. Future research will focus on: deriving kinetic models to describe low temperature char oxidation, construction of set-up to test the observed trends and validating detection and mitigation strategies under realistic storage conditions.

References

1. Thomsen, T. Introduction to Production and Use of Biochar 2022 Working towards a More Circular and Bio-Based Danish Economy; 2022.
2. Sheng, C.; Yao, C. *Energy Fuels* 2022, 36 (2), 731–7
3. Zhang, W.; Lidman Olsson, E. O.; Enemark-Rasmussen, K.; Glarborg, P.; Dam-Johansen, K.; Li, S.; Khazraie, T.; Kinnunen, H.; Roppo, J.; Wu, H. *Fuel* 2025, 398, 135554.

Understanding Pyrolysis Bio-Oil Hydrotreating

(April 2025 – March 2028)



Contribution to the UN Sustainable Development Goals

The shipping and aviation sectors are currently heavily dependent on non-renewable fossil fuels and therefore have large climate impacts. Upgraded bio-oils produced from renewable biomass feedstocks using catalytic fast pyrolysis and subsequent hydrotreating could phase out fossil fuels used in these industries. By aiming to increase the understanding and robustness of the complex hydrotreating process, this project may potentially decrease the current dependence on fossil fuels in shipping and aviation and reduce climate change.



Ole Hauge Jensen

ohaje@kt.dtu.dk

Supervisors:
Anker D. Jensen
Martin Høj
Klas Andersson

Abstract

Hydrotreating of catalytic fast pyrolysis (CFP) bio-oils is a promising pathway to produce renewable fuels for hard-to-abate sectors like shipping and aviation. Yet, the complex composition of these oils and their nitrogen-containing impurities challenges catalyst stability and hydrogen efficiency. This project aims to improve the understanding and robustness of the complex hydrotreating process through batch and flow hydrotreating experiments and kinetic modeling using both real and model CFP bio-oils.

Introduction

In 2019, transportation accounted for 23% of global energy-related greenhouse gas emissions, with shipping and aviation contributing roughly one fifth of this amount. These sectors are especially difficult to decarbonize due to their reliance on dense liquid fuels [1].

Fast pyrolysis of biomass and subsequent upgrading of the resulting bio-oil offers a promising route toward renewable transportation fuels, particularly when using low-value residues such as forestry waste or sewage sludge. However, the high oxygen and water content of pyrolysis oils leads to poor stability, high acidity, and low heating value, necessitating upgrading [2]. Catalytic fast pyrolysis (CFP), where vapors are treated with a catalyst before condensation, can improve the oil quality by converting reactive oxygenates, though at the cost of a reduced yield. Further upgrading is typically done by catalytic hydrotreating, where high-pressure hydrogen removes oxygen and stabilizes the oil [3]. Figure 1 summarizes this proposed pathway of producing transportation fuels.

Sulfided NiMo catalysts are especially attractive for this hydrotreating process due to their cost-effectiveness and high hydrodeoxygenation activity [2]. Yet, mild hydrotreating of advanced bio-oils on these catalysts and its inhibition by impurities remain poorly understood. This project aims to improve the understanding of these

phenomena through controlled hydrotreating experiments and kinetic modeling based on both model mixtures and real CFP bio-oils.

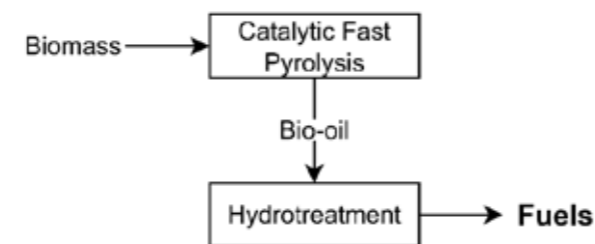


Figure 30: Schematic diagram of the proposed process for making transportation fuels from biomass through catalytic fast pyrolysis and hydrotreatment.

Specific objectives

The overall objectives of this project are:

- 1) To improve the understanding of the hydrotreating process through well-defined hydrotreating experiments in batch and trickle bed setups using real CFP bio-oils and/or model compound mixtures resembling CFP bio-oils.
- 2) To investigate the effect of common impurities in CFP bio-oils on catalyst activity and coke formation with an emphasis on nitrogen-containing compounds.

- 3) To construct and fit a kinetic model that can describe the hydrotreating process with real CFP bio-oils.

Methods

The main body of work in this project will involve hydrotreating experiments in batch and trickle bed reactors. Real bio-oils are difficult to work with in flow setups due to their tendency to polymerize upon heating. In addition, the real oils are difficult to analyze in detail due to the large number of distinct chemical species present in the oil.

Consequently, experiments involving real CFP bio-oils will mainly be conducted in a Parr 4575 batch reactor, and the analysis of the raw and hydrotreated oils will mainly focus on bulk properties such as elemental composition and acid content.

In contrast, model compound mixtures meant to resemble real bio-oils are easier to analyze in detail using e.g. GC-MS/FID and are easier to work with in flow reactors. Consequently, these mixtures will likely be used whenever working in a newly established flow setup and when a detailed mechanistic understanding is required. Figure 2 sketches the methodological framework applied in this

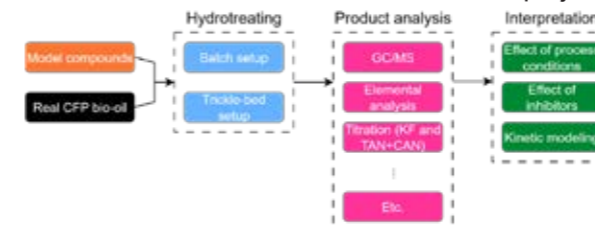


Figure 31: Sketch of the methodological approach applied in this project.

Results and Discussion In order to understand the batch hydrotreating behavior of CFP bio-oil, a series of hydrotreating experiments at different temperatures have been done on a wood-derived CFP oil provided by Valmet. These experiments were done with sulfided NiMo catalyst in a catalyst-to-oil ratio of 1:10, a hydrotreating period of 2h and an initial H₂ pressure of 90 bar. Figure 3 shows the oxygen content of the hydrotreated oil and the hydrogen consumption calculated from these experiments.

As it may be seen, hydrotreating the oil at 350°C results in a near full deoxygenation of the bio-oil but has a high H₂ consumption.

These initial experiments will provide a baseline for future hydrotreating experiments using bio-oil spiked with known amounts of nitrogen-containing compounds to study the inhibiting effect of these compounds on the hydrotreating process and the resulting oil-quality.

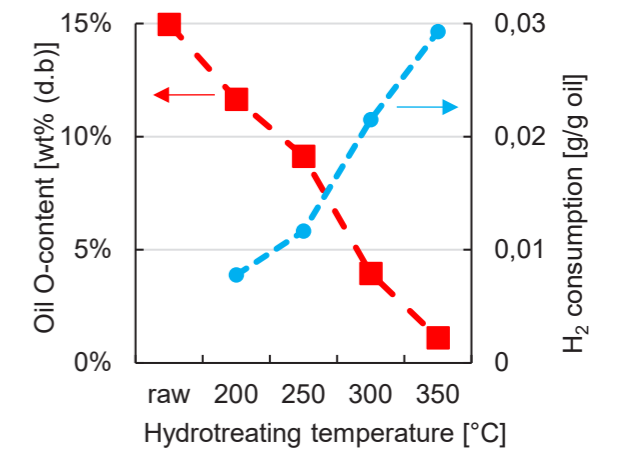


Figure 32: The O-content of the hydrotreated CFP bio-oil and H₂ consumption of the initial series of batch hydrotreating experiments.

Conclusions

Early results confirm that the hydrotreating process can effectively remove oxygen from CFP bio-oils under relatively mild conditions but also highlight the trade-off between deoxygenation and hydrogen consumption. These findings provide a benchmark for upcoming studies focused on the influence of nitrogen compounds and their impact on catalyst behavior and oil quality. In future work, more detailed mechanistic experiments will be conducted using model compounds in a trickle bed reactor setup. The broader goal is to translate the insights from these experiments into predictive kinetic models and more resilient upgrading strategies, advancing the transition toward renewable fuels for marine and aviation applications.

Acknowledgements

This project is carried out in collaboration with Topsoe A/S who also provide catalyst materials, oil analyses and guidance. The CFP oil used in the study has been provided by Valmet. The project is funded by EUDP.

References

1. IPCC, *Climate Change 2022 – Mitigation of Climate Change*, Full Report, 2022.
2. P. M. Mortensen, J. D. Grunwaldt, P. A. Jensen, K. G. Knudsen, and A. D. Jensen, *Appl. Catal. A: Gen.*, 407 (1–2) (2011) 1–19.
3. K. Iisa, R. J. French, K. A. Orton, A. Dutta, and J. A. Schaidle, *Fuel*, 207 (2017) 413–422.

List of publications

No publications have been made at this time of the project period.

Investigation of the Barrier Mechanism in Lignin-Based Epoxy Anticorrosive Coating

(July 2024 – July 2027)

12 RESPONSIBLE CONSUMPTION AND PRODUCTION



Contribution to the UN Sustainable Development Goals

Large steel structures like ships, wind turbine towers, and oil rigs depend on anticorrosive coatings, which are typically fossil-based. This project promotes a more sustainable alternative by using lignin, a renewable byproduct, as a bio-based pigment in epoxy coatings. Replacing fossil-derived materials with lignin helps reduce carbon emissions, industrial waste, and supports more responsible resource use in line with SDG 12.



Azade Kafashan

azkaf@kt.dtu.dk

Supervisors:
Kim Dam-Johansen
Narayanan Rajagopalan

Abstract

This study explores the effect of lignin molecular weight on water uptake in epoxy-based anticorrosive coatings. Two lignin types, high-Mw sieved kraft lignin (KL-sieved) and low-Mw ethyl acetate-extracted lignin (KL-EtOAc), were compared with conventional iron oxide pigment (FeOOH). Gravimetric and electrochemical impedance spectroscopy (EIS) revealed that KL-EtOAc coatings had the lowest water uptake and most stable electrochemical behavior, demonstrating superior dispersion and barrier performance. In terms of water uptake, KL-EtOAc outperformed both KL-sieved and FeOOH, highlighting its potential as a high-performing bio-based pigment.

Introduction

Epoxy coatings protect steel structures in marine, energy, and infrastructure sectors, but commonly rely on fossil-based pigments like iron oxides, raising environmental concerns. Lignin, a bio-based byproduct of the pulp industry, offers a sustainable alternative due to its aromatic structure and functional groups that promote interaction with epoxy matrices.

The performance of lignin in coatings is influenced by its molecular weight and uniformity, which affects dispersion and water resistance. This study compares KL-sieved (high Mw) and KL-EtOAc (low Mw) lignin pigments with FeOOH to assess how molecular characteristics influence water transport and barrier behavior using gravimetric and EIS methods.

Specific Objectives

- To assess the impact of lignin molecular weight on water uptake and diffusion behavior in epoxy coatings.
- To compare KL-sieved, KL-EtOAc, and FeOOH pigments in terms of barrier performance.

Experimental

Epoxy coatings were formulated using KL-sieved, KL-EtOAc, or FeOOH pigments dispersed in a bisphenol-A epoxy resin with MXDA as curing agent. KL-EtOAc was prepared via ethyl acetate solvent fractionation, and KL-sieved was obtained through mechanical sieving. Coatings were applied to steel panels and free films using a PET foil pressing technique and cured under ambient conditions. Water uptake was analyzed using gravimetric sorption and EIS in 3.5 wt% NaCl solution. Molecular weights were determined by SEC-MALS.

Result And Discussion

Molar Mass Determination Size exclusion chromatography (Fig. 3) confirmed that KL-EtOAc had a significantly lower weight-average molecular weight ($M_w = 2.12$ kDa, dispersity $\bar{D} = 1.33$) compared to KL-sieved ($M_w = 15.97$ kDa, $\bar{D} = 4.07$). The lower M_w and narrower distribution of KL-EtOAc improved miscibility and reduced structural heterogeneity, contributing to decreased water uptake and enhanced coating uniformity.

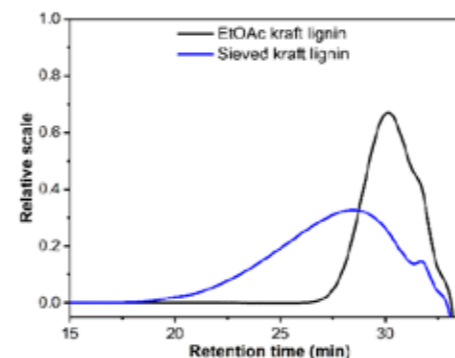


Figure 1. SEC-MALS chromatography of lignin

Gravimetric Water Uptake Analysis
Water uptake behavior was evaluated by tracking mass gain in epoxy coatings during immersion. As shown in Fig. 2, KL-sieved-EP exhibited the highest uptake (3.93%), likely due to limited dispersion and stronger water affinity through polar surface groups. KL-EtOAc-EP showed significantly lower uptake (2.21%), reflecting better dispersion and reduced polarity due to its lower molecular weight. FeOOH-EP, the reference system, showed similar uptake (2.18%) to KL-EtOAc-EP but is likely influenced by microvoids at pigment-matrix interfaces [1].

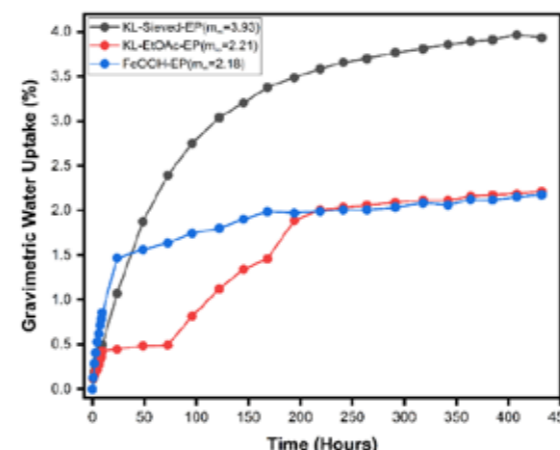


Figure 2. Gravimetric water uptake (%) as a function of immersion time for KL-sieved-EP, KL-EtOAc-EP, and FeOOH-EP coatings. The curves represent average values.

Equilibrium water uptake by EIS

Electrochemical behavior during immersion is shown in Fig. 11. KL-EtOAc-EP maintained high impedance magnitude and a stable phase angle near 90° throughout 672 hours, indicating minimal water ingress and excellent barrier integrity. In contrast, KL-sieved-EP and FeOOH-EP showed a marked decrease in impedance and a phase angle drop at low frequencies, especially after prolonged exposure. These changes reflect the

formation of conductive pathways and loss of capacitive behavior, suggesting early-stage degradation and reduced corrosion resistance [2].

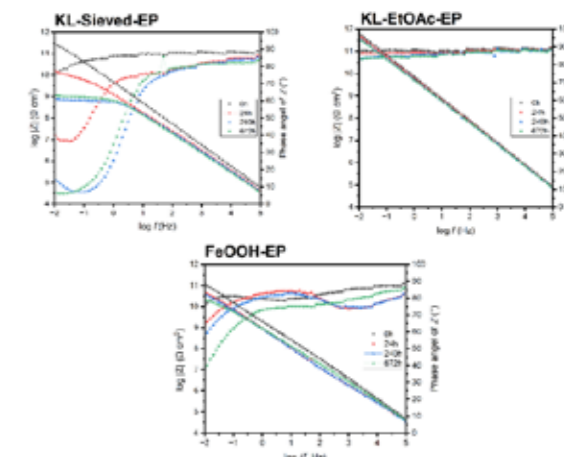


Figure 3. Bode plots of (a) KL-sieved-EP, (b) KL-EtOAc-EP, and (c) FeOOH-EP coatings showing impedance magnitude ($|Z|$) and phase angle over a frequency range (10^{-2} – 10^5 Hz) at different immersion times (0 h, 24 h, 240 h, and 672 h) in 3.5 wt% NaCl solution.

Conclusion

Gravimetric and EIS analyses confirmed that lignin molecular weight strongly influences water uptake and barrier performance in epoxy coatings. The low-Mw lignin coating (KL-EtOAc-EP) exhibited the lowest water uptake, slowest diffusion, and most stable electrochemical behavior, indicating superior barrier integrity. In contrast, the high-Mw lignin (KL-sieved-EP) absorbed more water and degraded faster, while the FeOOH reference showed moderate uptake but higher diffusion rates. Overall, solvent-fractionated low-Mw lignin provided the most effective moisture resistance and corrosion protection among the tested systems.

Acknowledgment

We are grateful to the Hempel Foundation for its financial support to CoaST (The Hempel Foundation Coating Science and Technology Center).

References

- N.A. Bratasyuk, A. V. Latyshev, V. V. Zuev, Water in epoxy coatings: Basic principles of interaction with polymer matrix and the influence on coating life cycle, *Coatings* 14 (2023) 54.
- A.S. Castela, A.M. Simões, Water sorption in freestanding PVC films by capacitance measurements, *Prog Org Coat* 46 (2003) 130–134.

Development of conducting PDMS compounds for soft robotic applications

(August 2023 – August 2026)



Contribution to the UN Sustainable Development Goals

Developing soft artificial muscles represents a significant stride in enhancing human health and well-being. These innovative, bio-inspired actuators emulate the mechanisms of biological muscles and have garnered attention for their potential to revolutionize several facets of healthcare and overall quality of life. They solve issues across various healthcare applications, spanning assistive devices, rehabilitation, human-robot interaction, wearable technology, and soft robotics.



Leo Kershaw

leokers@dtu.dk

Supervisors:
Anne Ladegaard Skov

Abstract

This project focuses on developing novel highly soft electrodes for artificial muscles. Previous research has sacrificed the compliant mechanical properties in favor of strong conductive pathways. Here, I will present the concept of utilizing novel silicone-based materials, which demonstrate extremely low values of Young's moduli and high strains, to produce soft conducting electrodes.

Introduction

Soft artificial muscles, in general

In the fabrication of wearable actuators, soft robotic systems can solve many challenges that traditional hard robotics fail to address. New technologies are paving the way for soft actuators that are compliant with the human body[1].

The ideal wearable actuators must provide muscle-like force when on, yet be mechanically transparent when off. This apparent contradiction, from infinitely soft when off, to generating useful mechanical work when needed, presents a significant challenge for soft actuators. New materials, device architectures, and ways of integrating wearables on the body are required.

Soft electrodes

The evolving landscape of modern wearable devices necessitates the development of flexible, soft, and stretchable electronic components that can seamlessly conform to complex shapes, accommodate mechanical deformations, and interface with biological tissues. Achieving these objectives hinges on the design and synthesis of materials that exhibit high electrical conductivity while maintaining mechanical compliance.

Various methodologies have been explored to balance electrical conductivity with mechanical

compliance. Conducting polymers, such as poly(3,4-ethylenedioxythiophene) poly(styrenesulfonate) (PEDOT:PSS), exhibit notable promise owing to their flexibility and tunable electrical properties. Doping of nanoparticles, including carbon derivatives, ionic liquids and metal nanoparticles, offers exceptional conductivity and mechanical resilience. Emerging 2D materials like transition metal dichalcogenides (TMDs) further diversify the soft electrode landscape due to their remarkable electronic properties. Moreover, biocompatible hydrogels and elastomers, such as polydimethylsiloxane (PDMS) and polyurethane, provide soft electrodes with the requisite compliance for seamless integration with biological tissues.

Nanoparticle doping stands out as a pivotal approach due to its potential to synergistically harness the polymer matrix's mechanical properties and the nanomaterial dopant's electrical properties, leading to a significant enhancement in electrical conductivity while preserving the mechanical compliance intrinsic to soft electrodes.

Nanoparticle Doped Polymers

Thus far, most nanoparticle filled polymer composites have utilized commercial polymer products and doped them with nanoparticles with

the desired properties. This approach ignores the possibility of tailoring polymer properties through carefully selecting the matrix. Commercial polymers are often designed with a limited inherent softness for practical applications and thus restrict the intrinsic softness of the resulting composites. My work will focus on custom polymer design to enhance desirable properties upon nanoparticle doping.

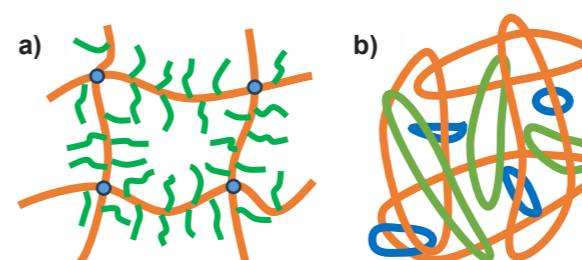
Specific Objectives

- 1) Synthesis of a highly soft electrode capable of good conductivity at large strains.
- 2) Facile fabrication of novel electrodes in a variety of different architectures.

Results and Discussion

Novel Networks

Two novel networks have been developed at the Danish Polymer Center (DPC) capable of extremely large strains before breakage and impressive softness (Fig. 1).



Network type	Maximum strain (%)	Young's modulus (KPa)	Reference
Concatenated rings	2400	600	[2]
Bottle Brush	500	12	[3]
Sylgard 184	120	2050	[4]

Figure 1: a) The structure of the bottle brush networks. b) The structure of the concatenated ring networks. c) A comparison of mechanical properties between the DPC networks and a commercial network.

The bottle brush (Fig. 1a) and concatenated ring networks (Fig. 1b) exhibit extraordinary softness and extensibility compared to the commercial PDMS network (Sylgard 184) (Fig. 1c). The addition of conductive nanoparticles often introduces stiffness to such networks, resulting in a trade-off in the softness of the materials and the conductivity. The inherent softness of these materials becomes a paramount advantage as increased quantities of nanoparticles can be

added without surpassing the mechanical threshold needed for practical compliant electrodes.

Additionally, the bottle brush networks have the potential to greatly improve soft electrode design due to the capacity to exert precise control over the network's structural configuration. This fine-tuned control offers many opportunities for property modification, including the facilitation of nanoparticle dispersion through both nanoparticle binding and the effective modulation of free space within the network.

The synthesis of concatenated ring networks occurs in the absence of traditional crosslinking agents. This unconventional approach leverages a unique form of physical crosslinking, creating potential percolation pathways within the network, thus fundamentally reshaping its conduction capabilities.

Conclusions

In conclusion, bottle brush and concatenated ring networks can provide a new era for soft electrode materials. These networks, characterized by exceptional softness and extensibility, surpass conventional alternatives. They enable the introduction of conductive nanoparticles without sacrificing softness, expanding the horizons for tailored soft electrodes. The structural precision of bottle brush networks and unconventional crosslinking in concatenated ring networks promise transformative advancements in conduction capabilities.

Acknowledgements

This project is funded by the Novo Nordisk Foundation.

References

1. M. Li, A. Pal, A. Aghakhani, A. Pena-Francesch, and M. Sitti, 'Soft actuators for real-world applications', *Nat Rev Mater*, vol. 7, no. 3, Art. no. 3, Mar. 2022, doi: 10.1038/s41578-021-00389-7.
2. P. Hu, J. Madsen, Q. Huang, and A. L. Skov, 'Elastomers without Covalent Cross-Linking: Concatenated Rings Giving Rise to Elasticity', *ACS Macro Lett.*, vol. 9, no. 10, pp. 1458–1463, Oct. 2020, doi: 10.1021/acsmacrolett.0c00635.
3. P. Hu, J. Madsen, and A. L. Skov, 'One reaction to make highly stretchable or extremely soft silicone elastomers from easily available materials', *Nat Commun*, vol. 13, no. 1, Art. no. 1, Jan. 2022, doi: 10.1038/s41467-022-28015-2.
4. R. Moučka, M. Sedláčik, J. Osička, and V. Pata, 'Mechanical properties of bulk Sylgard 184 and its extension with silicone oil', *Sci Rep*, vol. 11, no. 1, Art. no. 1, Sep. 2021, doi: 10.1038/s41598-021-98694-2.

Synthesis of bio-based polymers for advanced applications

(May 2025 – April 2028)

13 CLIMATE ACTION



Contribution to the UN Sustainable Development Goals

The majority of the world's plastic is currently coming from fossil fuel. These fossil fuels are a major source of pollution of the environment. Reducing the reliance on plastic is a very difficult task, that cannot happen overnight. In the meantime, we need solutions that provide a renewable feedstock, reducing pollution from fossil fuel, and permanent plastic waste. Synthesizing plastics from renewable feedstock gives a bio-based material that is better for the climate in production, and hopefully also in end of life.



Elias Kjær-Westermann

elikj@dtu.dk

Supervisors: Anders Egede Daugaard, Jeppe Madsen

Abstract

A major challenge the world is facing today is the sourcing of feedstock for materials. Currently, the vast majority is sourced from fossil fuel. There are multiple possible alternatives to fossil fuel, but none of them have large scale commercial success. Zosteric acid from fermentation is outlined as a possible alternative. Zosteric acid can be both be used as a pesticide in agricultural applications, and as a platform molecule for bio-based plastics. The approach pursued here is to prepare monomers from zosteric acid using an impurity-tolerant method, in water, thus eliminating the need for expensive purifications, and toxic solvents. The final goal is to fully understand and optimize the entire process from zosteric acid to polymer properties.

Introduction

Since the 1970s the use, and the need for, plastic has grown faster than any other material [1]. Single-use plastic accounts for over one third of all plastic and is based 98% on fossil fuels. Furthermore, pesticide use has doubled since the 1990s [2], damaging both the climate and water supplies. This is not a sustainable trend.

There are multiple different ways this trend can be halted, but no single solution is sufficient by itself. The consumption of single use plastics needs to be reduced, but it cannot be entirely avoided. Therefore, there is a clear need for greener alternatives, not based on fossil fuels. The proposed solutions will need to satisfy some difficult conditions. On one hand, there is economics. There needs to be an economic incentive to use the new solutions. On the other hand, there is the environment. Paul Anastas and J.C. Warner have set up guidelines for what makes chemistry green [3], see Figure 1. In this project, zosteric acid is proposed as part of the solution to these problems.

Zosteric acid is a material made from fermentation of sugars [4]. It acts as a pesticide in itself [5] and can be used as a platform for further synthesis.

Figure 1: the 12 principles of green chemistry.

Using zosteric acid as a raw material for polymers fully satisfies principles 3, 4, 5, 7, and 12. It is an inherently more sustainable chemical than the fossil fuel-based alternatives currently in use, and it has a renewable feedstock. The only main downside is atom economy.

However, using zosteric acid as a pesticide does not compromise atom economy. It thus fulfills principles 2, 3, 4, 5, 6, 7, 10, 11, and 12. The entire molecule is being used, it does not require toxic solvents in production. Pesticides increase the food output of farms and are therefore by definition designed for energy. Zosteric acid being bio-based means that degradation is also easier in a natural environment. Furthermore, because it is designed for farming pollution prevention is a crucial element in the entire project. In agriculture it is interesting as a preventative measure. The onset of problems can be prevented by a coating of zosteric acid, instead of treating problems after they arise.

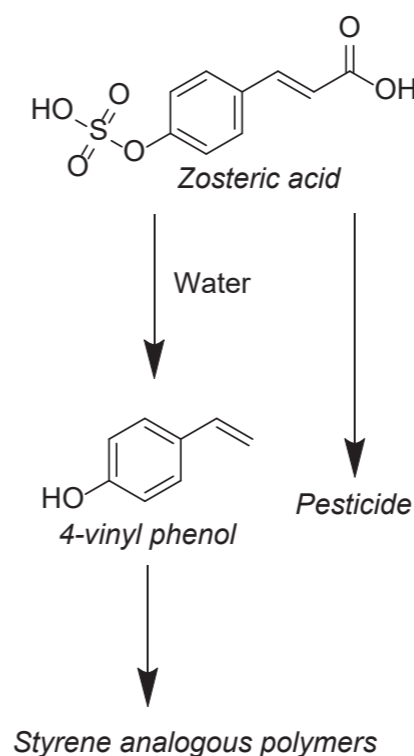
Specific objectives

The goal of the current study is to explore the most prominent uses of zosteric acid.

- Demonstrate that it is possible to change the solubility of zosteric acid, increasing the affinity for plant surfaces, targeting residence time.
- Illustrate how zosteric acid can be used as a platform molecule for various types of polymers.

Results and Discussion

The synthesis of 4-vinylphenol from zosteric acid has been done in water, without the use of metal catalysts, and from fully bio-renewable ingredients, see Scheme 1. This can be done on zosteric acid from fermentation, even in impure samples. The resulting phenol, see Figure 2, can then be polymerized.



Scheme 1: Use of zosteric acid to make polymers

Zosteric acid has also been tested as a natural alternative to pesticides, with no

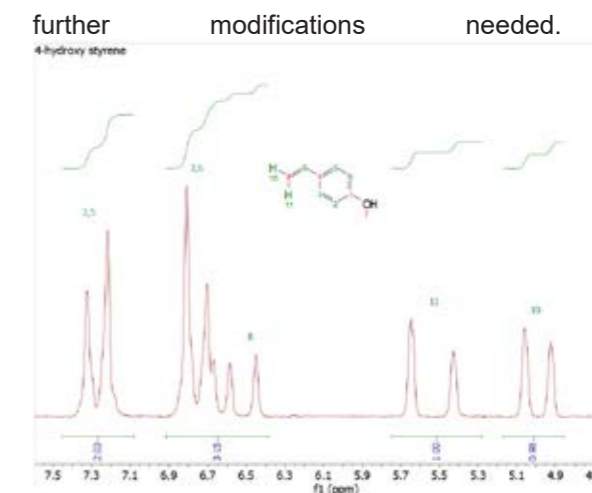


Figure 2: Assigned ¹H-NMR spectrum of the platform chemical 4-vinylphenol

Conclusions

A method to create polymers from zosteric acid has been proposed. This method works with only mild chemicals as catalyst, and appears to allow a considerable concentration of organic byproducts while still giving the desired product.

Acknowledgements

This work is financially sponsored by Innovation Fund Denmark, in collaboration with Cysbio ApS.

References

1. FROM POLLUTION TO SOLUTION A GLOBAL ASSESSMENT OF MARINE LITTER AND PLASTIC POLLUTION, 2021. <https://www.unep.org/>.
2. FAO, Pesticides use and trade, 1990–2022, Rome, 2024. <https://doi.org/10.4060/cd1486en>.
3. P.T. Anastas, J.C. Warner, Green Chemistry: Theory and Practice, Oxford University Press, 2000.
4. C.B. Jendresen, A.T. Nielsen, Production of zosteric acid and other sulfated phenolic biochemicals in microbial cell factories, Nat Commun 10 (2019). <https://doi.org/10.1038/s41467-019-12022-x>.
5. F. Villa, B. Pitts, P.S. Stewart, B. Giussani, S. Roncoroni, D. Albanese, C. Giordano, M. Tunesi, F. Cappitelli, Efficacy of Zosteric Acid Sodium Salt on the Yeast Biofilm Model Candida albicans, Microb Ecol 62 (2011) 584–598. <https://doi.org/10.1007/s00248-011-9876-x>.

Modelling of carbon capture processes

(June 2025 – May 2028)



Contribution to the UN Sustainable Development Goals

This PhD develops tools for uncertainty analysis in carbon capture simulations, supporting cleaner and more affordable energy systems. By improving confidence in capture performance, the work helps reduce risks and costs for low-carbon power generation. Accurate models enable efficient design and operation, minimizing energy use and emissions. These methods guide smarter decisions in integrating carbon capture with renewable and flexible power sources.

The project contributes to UN Goal 7: Affordable and Clean Energy.



Loukas

Kollias

louko@dtu.dk

Supervisors: Nicolas von Solms, Xiaodong Liang, Phillip Loldrup Fosbøl

Abstract

This work focuses on model validation and uncertainty analysis for carbon capture processes using the CapSim simulator developed at DTU-CERE. The objective is to assess the model's ability to reproduce CO₂ absorption in amine-based solvents under various pilot plant conditions and to quantify the uncertainties influencing model predictions. Simulations were compared against steady-state experimental data from three different pilots published in Tobiesen [1], Gløshaugen [2] and Esbjerg-CASTOR Pilot Plant[3]. The model demonstrates good agreement with experimental rich loadings (average absolute relative deviation <10%), confirming its suitability for further uncertainty propagation and sensitivity analysis. Future work will extend this validation to uncertainty-aware optimization and robust process design.

Introduction

Carbon Capture and Storage (CCS) plays a vital role in achieving net-zero emission targets. Within the Center for Energy Resources Engineering (CERE), this PhD project focuses on "Optimizing carbon capture simulation through advanced modeling tools: CapSim." The overarching goal is to incorporate uncertainty quantification (UQ) and sensitivity analysis (SA) into process simulation to improve model robustness and reliability.

The CapSim model [4] integrates kinetic, thermodynamic, and transport submodels describing the absorption of CO₂ into aqueous amine solutions. Validation of this model against pilot datasets is essential before performing large-scale uncertainty propagation studies.

Motivation & Scope

The first stage of this project aims to evaluate the DTU-CERE CapSim model using publicly available pilot datasets. Three independent pilot plants—Tobiesen (NTNU Trondheim), Flø (NTNU Gløshaugen), and CASTOR (Esbjerg) -were selected for model validation because they span a wide operational range, from laboratory to industrial scales.

For each pilot, rich and lean loadings, temperature profiles, and key hydrodynamic parameters were compared with experimental data. The objective is

to assess model consistency, quantify deviations, and identify potential uncertainty sources in thermodynamics, kinetics, and transport properties.

Results and Discussion

Figure 1 presents a parity plot comparing experimental and simulated rich loadings for the three pilots. The CapSim model demonstrates strong predictive performance, with an overall average absolute relative deviation (AARD) of approximately 6%.

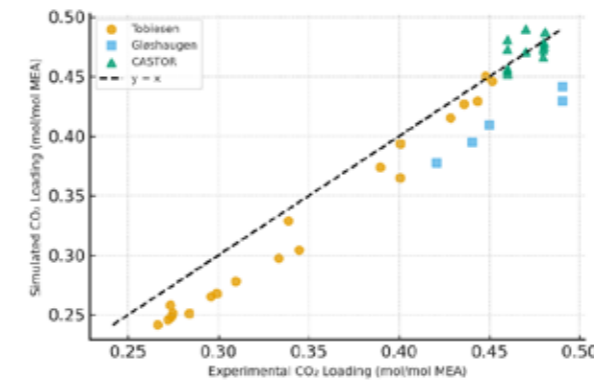


Figure 33 Parity plot of experimental versus simulated CO₂ rich loadings for Tobiesen, Gløshaugen, and CASTOR datasets.

The Tobiesen pilot, characterized by moderate gas and liquid flow rates, exhibits the best agreement, with an AARD of 6.9%. Temperature profiles from selected runs capture the location and intensity of the exothermic temperature bulge, indicating that the model correctly predicts heat release and reaction behavior. Indicatory temperature profile including experimental points is included in Figure 2.

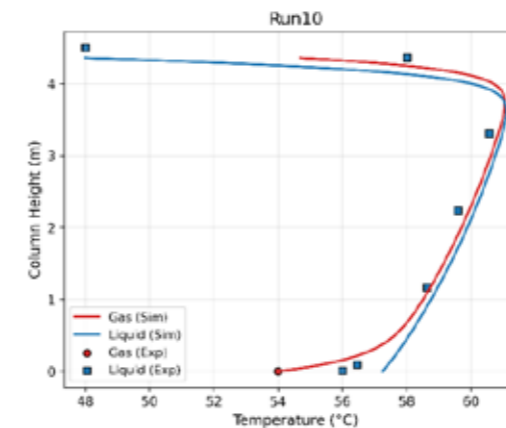


Figure 34 Temperature profile for the steady state Run 10 in Tobiesen pilot dataset.

For the Gløshaugen pilot, the deviation is slightly higher ($\approx 10\%$). In this pilot rich loading is underestimated.

The CASTOR industrial-scale pilot confirms that the model scales well with process size, showing deviations below 2% for both loading and temperature data. Temperature profiles for this pilot are also quite successfully simulated. In Figure 3 comparison is done with temperature profile 1A published in Neveux[3].

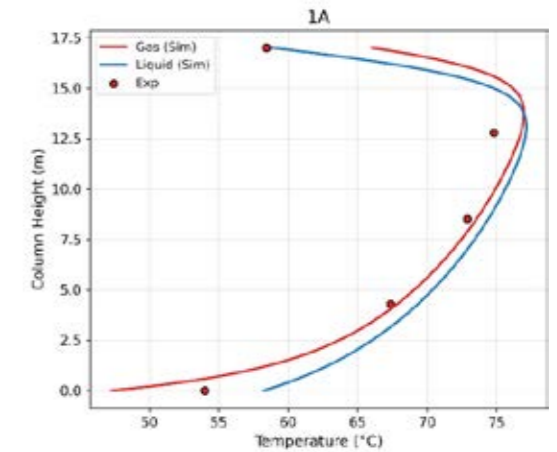


Figure 35 Temperature profile for run 1A in Esberg-CASTOR pilot

Conclusions

The CapSim process simulator has been successfully validated against three benchmark pilot datasets, covering a wide range of flow rates and operating conditions. Rich loading, temperature, and CO₂ concentration profiles show good agreement with experimental data, confirming the model's predictive capability. Some discrepancies not shown in this article indicate a mass transfer model refinement which is a subsequent work to be performed.

Outlook

Future work will focus on: (1) quantifying parameter uncertainty in thermodynamic, hydrodynamic and mass transfer submodels and (2) integrating confidence intervals into process optimization for robust absorber design and operation. These steps will advance uncertainty-aware process modeling for carbon capture applications.

References

1. F.A. Tobiesen, H.F. Svendsen, O. Juliussen, *AIChE Journal* 53 (2007) 846–865.
2. N. Enaasen Flø, H. Knuutila, H.M. Kvamsdal, M. Hillestad, *International Journal of Greenhouse Gas Control* 41 (2015) 127–141.
3. T. Neveux, Y. Le Moullec, J.-P. Corriou, E. Favre, *Ind Eng Chem Res* 52 (2013) 4266–4279.
4. J. Gabrielsen, *CO2 Capture from Coal Fired Power Plants*, 2007.

Catalytic stabilization and upgrading of biomass pyrolysis oil to fuels for heavy transport and aviation

(August 2022 – December 2025)

7 AFFORDABLE AND CLEAN ENERGY



Contribution to the UN Sustainable Development Goals

Access to affordable, reliable, and clean energy is only possible if greener alternatives to fossil fuels are found. Biomass derived fuels are a promising alternative due to their high volumetric energy density, and fast pyrolysis of biomass is interesting since it produces a high yield of crude bio-oil. However, this oil contains a high concentration of oxygen-rich compounds, that need to be hydrotreated before the biofuel can be used instead of conventional fossil fuels.



Amalie Paarup

Krebs

apakr@kt.dtu.dk

Supervisors: Anker Degn Jense, Martin Høj, Magnus Zingler Stummann (Topsoe)

Abstract

Biomass-derived fuel is a promising alternative to conventional fossil fuels. Conversion of biomass by fast pyrolysis produces a high yield of crude bio-oil. This product is however highly unstable, corrosive, and has a poor heating value due to a high oxygen content. This oxygen can be removed by catalytic hydrotreatment, but the process is difficult and challenges like catalyst deactivation and reactor plugging still need to be overcome.

Introduction

Fossil fuels are major contributors to the world's current high carbon dioxide emissions, and therefore greener alternatives are needed. In terms of heavy transport and aviation, it is necessary to find sustainable fuel of high volumetric energy density [1]. Liquid hydrocarbons have a high volumetric energy density and are therefore well suited as fuel for these purposes [1]. Biomass-derived liquid hydrocarbons can be produced from fast pyrolysis of biomass, which provides a high oil yield (up to 80 wt.%) [1]. Unfortunately, the resulting crude bio-oil from the fast pyrolysis has high amounts of oxygen-rich compounds, resulting in a lower heating value, high acidity, immiscibility with conventional petroleum oils, and poor stability, both thermal and chemical [1]. Thus, it is necessary to remove the oxygen from the oil.

Catalytic hydrodeoxygenation (HDO) is a process to remove oxygen in the presence of excess H_2 gas at elevated temperatures [2]. Attempts have previously been made to perform this HDO in a single step, which resulted in significant catalyst deactivation and plugging of the reactor [3]. As a result, it was suggested to perform the HDO of the crude bio-oil in a two-

step process: first catalytic stabilization of the oil is carried out at lower temperatures (< 200 °C) followed by the actual HDO step at elevated temperatures. The purpose of dividing the process into these two steps is prevention of polymerization of the bio-oil, which happens if it is heated to a higher temperature in its unstabilized form [4]. During the stabilization the unstable components in the bio-oil will be hydrogenated to more stable compounds, e.g., aldehydes and ketones will be converted to alcohols [5, 6].

Specific Objectives

The objective of this project is to develop a fixed bed reactor-based process and catalyst for stabilization and subsequent hydrodeoxygenation of the pyrolysis oil. A literature study furthered the understanding of the process. The following catalyst screening experiments lead to the identification of the most promising catalyst(s) and the most reactive species in the pyrolysis oil. Additionally, the project included participation in setting up and performing experiments on a high pressure two-stage trickle bed reactor setup for the two-step process.

As the project is part of the Innovation Fund Denmark (IFD) project, HyProFuel, collaboration with the project partners is also an important part of the PhD project.

Results and Discussion

Two different catalysts, a reduced Ni/Al_2O_3 and a sulfided $NiMo/Al_2O_3$, were tested in a series of experiments in a 500 mL batch reactor at 120, 180, and 220 °C, and 90 bar H_2 for 2 h. 50 g of a wood-derived pyrolysis oil (PO) was used as reactant with a 5-15 wt% catalyst/oil ratio (see [7] for more details).

Both the carbonyl number and the micro carbon residue (MCR) are good measures of the degree of stabilization of the PO. A low carbonyl number is desired since the carbonyls are known to polymerize under heating, and the MCR provides an indication of the oil's tendency to coke. In Figure 1, the MCR is plotted against the carbonyl number for both the treated and the fresh oils. It should be noted that the MCR for all the treated oils are higher than that of the fresh PO, however it makes more sense to compare to the blank experiment (42.8 wt.%, db), since the heating of the oil itself will cause polymerization.

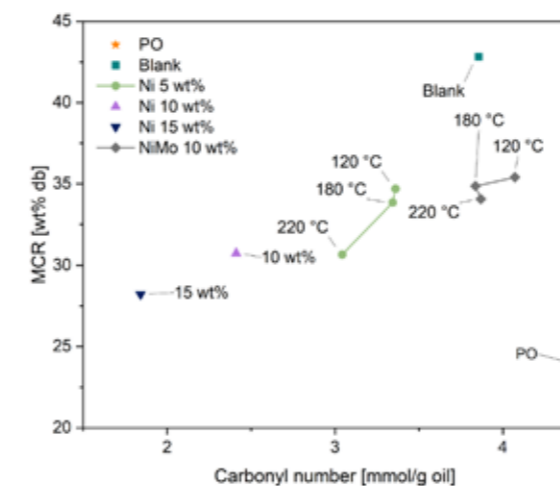


Figure 36: MCR for the organic phase plotted vs the average carbonyl number for both phases of the different products and the fresh PO (orange star). All experiments were performed at 90 bar initial pressure of H_2 , with a hold time of 2 h and a reaction temperature of 180 °C, unless specified otherwise [7].

Ni/Al_2O_3 was the best at reducing both the carbonyl number and the MCR compared to the sulfided $NiMo/Al_2O_3$. Increasing the catalyst/oil ratio significantly furthered the stabilization activity.

Unfortunately, Ni leaching was observed from the catalyst in all experiments with the Ni/Al_2O_3 catalyst, as can be seen in Figure 2. The leaching was observed to be particularly severe at 120 °C and 5 wt% catalyst/oil ratio, while increasing both the temperature and the catalyst to oil ratio helped mitigate the issue.

The lower leaching at higher catalyst/oil ratios signify that the oil (and gas) phase most likely has a saturation level. Unfortunately, this cannot be transferred to continuous operations, as fresh oil will continuously be introduced to the catalyst.

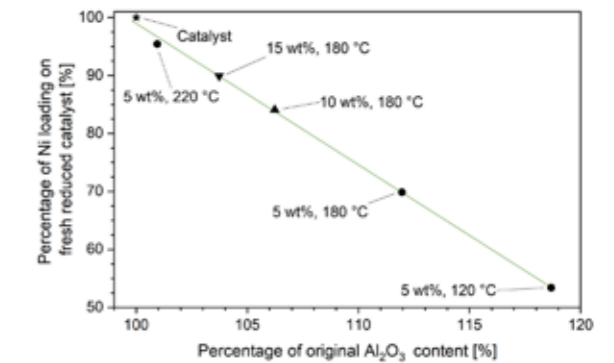


Figure 37: Ni contents of the spent catalysts compared to the fresh Ni/Al_2O_3 catalyst (measured by XRF). The Ni and Al_2O_3 contents of the original content in the fresh catalyst (located in the top left corner). All experiments were performed at 90 bar initial pressure of H_2 with a hold time of 2 h [7].

Conclusions

It can be concluded that the Ni/Al_2O_3 catalyst showed the best activity toward stabilization of woody pyrolysis oil, especially at higher temperatures and catalyst/oil ratios. However, Ni leaching was observed from the Ni/Al_2O_3 catalyst, which is a concern, especially for continuous operations. While it may be possible to mitigate the leaching by increasing the temperature, this may not be a feasible path for stabilization.

Acknowledgements

This project has been funded by Innovation Fund Denmark (project # 0224-00029A), and the Department of Chemical Engineering, DTU.

References

1. T. M. Dabros et al., *Progress in Energy and Combustion Science* 68 (2018) 268-309.
2. W. Yin et al., *Catal. Sci. Technol.* 6 (2016) 5899-5915.
3. F. Lin et al., *ACS Catal.* 12 (2022) 13555-13599.
4. D. Han et al., *Catalysts* 10 (402) (2020)
5. W. Yin et al., *Fuel Processing Technology* 2019 (2021) 106846.
6. D. C. Elliott, *Energy & Fuels* 21 (3) (2007) 1792-1815.
7. A. P. Krebs et al., *Energy & Fuels* 39 (32) (2025) 15300-15309

Advanced sensitivity analysis and comprehensive validation methodology to improve credibility of QRAs studies in chemical process industries

(June 2024 – May 2027)



Contribution to the UN Sustainable Development Goals

Technology and industry have evolved significantly in the last centuries, delivering to society substantial improvements in products and services. However, the rapid changes associated with this strong evolution have also provided new and unforeseen hazards associated with industrial activities. By enhancing the quality and consistency of risk estimates obtained through Quantitative Risk Assessment (QRA), we are also facilitating safer and more sustainable industrialization. Thus, this project has the potential to support innovation by assisting in decision-making with a safety perspective.



Mercedes Belda-Ley

mbele@kt.dtu.dk

Supervisors: Gürkan Sin, Merlin Alvarado-Morales, Jens Abildskov

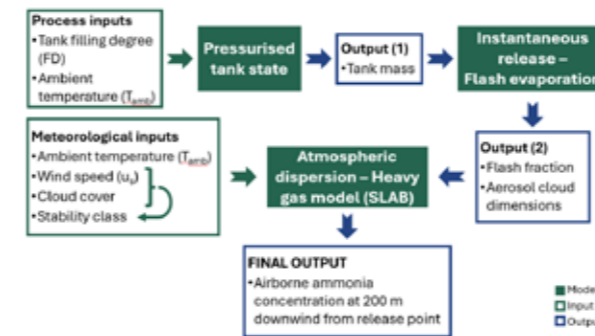


Figure 1: Ammonia case study MC simulations sequence.

The main objectives in this particular work include:

1. The execution an UA on the case study to analyse output variability.
2. The computation of several sensitivity indices to explain output uncertainty.
3. The determination and comparison of most influential inputs considering different sensitivity indices.

Methodology

Uncertain inputs included in the analysis are the ambient temperature (T_{amb} , °C), the tank filling degree (FD, %), the wind speed (u_s , m/s) and the cloud cover. The uncertainty of the inputs related to atmospheric conditions is fitted day-time conditions according to weather data in Denmark for 2024. All the Pasquill-Gifford stability classes for day-time conditions are included in the analysis by deducting the corresponding stability class based on the sampled cloud cover and wind speed [3].

UA is executed using $N = 1,000$ MC simulations and Latin Hypercube Sampling, LHS, to perform the analysis. Multiple linear regression is applied to the obtained MC samples to obtain Standardized Regression Coefficients (SRCs) as well as an approximation of the first order sensitivity index through the binning method. Subsequently, the first- and total-order sensitivity indices, also known as Sobol indices, based on the Jansen approximation [4] by generating more sets of output samples.

Results and Discussion

The obtained output distribution is characterised by a sample mean of 10.364 g/m^3 and a sample standard deviation of 3.493 g/m^3 , with a Monte Carlo error of 1.006 %, suggesting that the number of MC samples, N , is sufficient for the analysis.

A key aspect is that the SRCs are valid with $R^2 = 0.87$, despite the generated sample output comprising different stability classes, which are often treated as separate scenario.

Furthermore, as shown in figure 2, the sensitivity indices show agreement that the ambient temperature is the input having the smallest impact on the output uncertainty. This makes T_{amb} an adequate candidate to do factor fixing in the context of SA in dispersion modelling in QRA. On the other hand, the remaining inputs analysed consistently prove to be influential inputs that demand careful treatment in QRA to ensure reliable risk estimates.

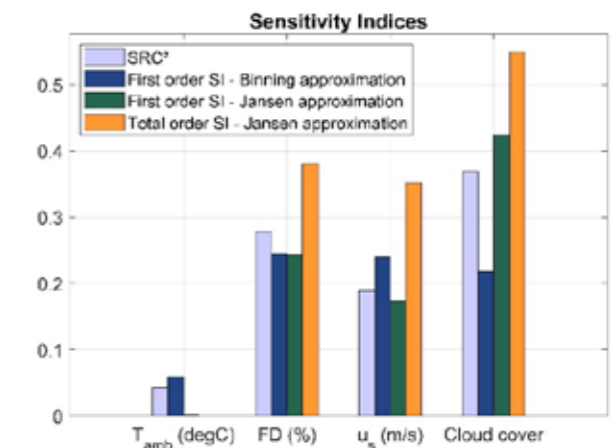


Figure 2: Comparison of different sensitivity indices for the studied inputs.

Conclusions

This project focuses on enhancing the reliability of QRA studies and their risk estimates through the rigorous study of uncertainties and determination of most critical inputs. The successful application and comparison of different sensitivity indices in this work, help identify most and least influential inputs, i.e., assumptions in dispersion modelling in QRA.

Acknowledgement

This work is funded by the EU Horizon 2022 call HORIZON-MSCA-2022-DN-01, project number 101119358 as part of the Marie Skłodowska-Curie Actions.

References

1. M. Abrahamsson, Uncertainty in Quantitative Risk Analysis - Characterisation and Methods of Treatment, Fire Safety Engineering and Systems Safety, Lund University, 2002.
2. N. Pandya, N. Gabas, E. Mardsen, Journal of Loss Prevention in the Process Industries 25 (1) (2012) 20-32.
3. D.A. Crowl, J.F. Louvar, Chemical process safety: fundamentals with applications, Prentice Hall, p. 185. M.J.W. Jansen, Analysis of variance designs for model output 117 (1-2) (1999) 35-43.

Abstract

Quantitative Risk Assessment (QRA) is a widely used process safety technique which characterizes the risks associated with engineering projects and activities. Due to its comprehensive nature and inherent uncertainties, the risk estimates obtained can vary considerably. This variability raises concerns about the dependability of the QRA outputs, which are used to assist decision-making, land use planning and emergency planning. The aim of this research is to advance the rigor and reliability of QRA studies to support risk management and decision-making based on more dependable and uncertainty-aware risk estimates thereby supporting safer and more sustainable industrialization. Specifically, a probabilistic approach based on Monte Carlo (MC) methods is used to perform uncertainty and sensitivity analysis on QRA case studies. By achieving this, the research provides better understanding of QRA results uncertainties, leading to more informed and robust judgment in process safety and risk management.

Introduction

QRA is a comprehensive methodology for quantifying risks associated to engineering and chemical facilities. This extensive endeavour involves several steps and assumptions leading to diverse sources of uncertainty: epistemic or stochastic; [1] quantitative or qualitative, etc. The obtained risk estimates can thus exhibit in a high variability, and its validity and reliability continue to be a pressing concern. The Monte Carlo (MC) methods offer a valid framework to propagate uncertainties within complex problems, and applying these methods to perform Uncertainty Analysis (UA) and Sensitivity Analysis (SA) delivers a better understanding of uncertainties associated with QRA models.

There have already been several attempts on quantifying and analysing these uncertainties using the Monte Carlo methods for similar uncertain settings [e.g. 1, 2], however these often compute sensitivity indices discretizing scenarios for different stability classes. As a result, a limited

picture of the uncertainty related to atmospheric conditions is achieved. This work addresses

Specific objectives

The present work is based on a case study for an instantaneous release of ammonia from a pressurised tank focusing on the discharge and dispersion models. Figure 1 showcases the configuration of the MC simulations in the case study, including the models, inputs and outputs considered. The models describe the behaviour of liquid ammonia from the steady-state thermodynamic properties of the pressurised tank, the adiabatic phase change for rapid depressurization, and finally the conservation equations for heavier-than-air atmospheric dispersion. These models are then deployed to calculate as final and objective output the airborne concentration of ammonia at a certain distance of interest, 200 m downwind in this case.

Progressing Towards Non-Biocidal Antifouling Coatings

(February 2024 – February 2027)

14 LIFE BELOW WATER



Contribution to the UN Sustainable Development Goals

The reduction of biocides in marine antifouling coatings directly supports SDG 14. Biocides in traditional coatings leach into the ocean, causing toxic effects on marine life, disrupting ecosystems, and reducing biodiversity. By developing biocide reduction alternatives, the release of harmful chemicals is minimized, promoting healthier marine ecosystems and preserving the quality of ocean waters. This approach aligns with SDG 14's objectives to prevent marine pollution and sustainably manage and protect marine and coastal ecosystem.



Shawn Lindner

shlin@kt.dtu.dk

Supervisors: Kim Dam-Johansen, Markus Schackmann, Narayanan Rajagopalan

Abstract

Hydrogel-based antifouling coatings offer a biocide-reduction strategy by preventing marine organism adhesion through the formation of a hydration layer. However, the mechanisms of hydrogel formation remain poorly understood, visualized, and quantified. Optical Coherence Tomography (OCT) provides a non-destructive approach to simultaneously quantify the hydrogel structure and coating surface with micron-scale resolution. This technique enables in situ visualization of hydrogel formation, swelling dynamics, and interfacial changes under marine-relevant conditions. Quantitative parameters such as layer thickness, surface roughness, and structural homogeneity can be extracted from OCT data, allowing direct correlation of coating morphology with antifouling performance. Ultimately, this approach supports the development of longer lasting and more durable hydrogel coatings, further reducing the need for biocides in marine applications.

Introduction

Marine biofouling poses significant economic and environmental challenges, not only by causing structural damage to marine infrastructure, but also by increasing ship drag [1]. To address these issues, fouling control coatings are essential. Biocidal antifouling coatings have been the industry standard for decades due to their proven efficacy and ease of use. These coatings typically feature an ablative self-polishing mechanism, where a hydrolysable binder gradually dissolves in seawater, continuously releasing biocides like cuprous oxide (Cu_2O) along with other organic biocides that enhance its effect [2]

Hydrogels are a promising way to minimize biocides in antifouling applications because they mimic the wet, soft surfaces of marine organisms to naturally resist fouling. Hydrogels can hold large amounts of water and swell significantly. However, current methods for crosslinking hydrogels, UV [3], chemical reactions between reactive groups [4], or thermal cycling [5], are impractical for large-scale hull applications due to the complexity of application and curing, high cost, toxicity factors and the necessity of a tie-coat. Butschle et al. [6] introduced a hydrogel that is built in-situ on top of the AFC without external curing, allowing a

50 wt% reduction of Cu_2O content without compromising antifouling efficacy in static environments. Dry polysaccharide-based hydrogel particles (Xanthan Gum) which are renewable, biodegradable and inexpensive, are used. The gel formation occurs when the coated surface approaches sea water due to the self-gelling properties of the particles (see Figure 1).

Specific Objectives

The objective is to visualize and quantify the hydrogel system despite its thin, transparent and fast-drying nature. However, a time-resolved quantification of those systems is necessary to assess their dynamic structure and to mature the technology. Optical Coherence Tomography (OCT) is a valuable candidate to quantify hydrogel systems since it can enable continuous, non-destructive visualization of wet, optically scattering materials in air or underwater. Using near-infrared light, OCT provides high-resolution cross-sectional images of semi-transparent materials and has been applied previously to systems such as biofilms [7]. This technique allows real-time, micrometer-scale quantification of both the hydrogel and coating surface in parallel.

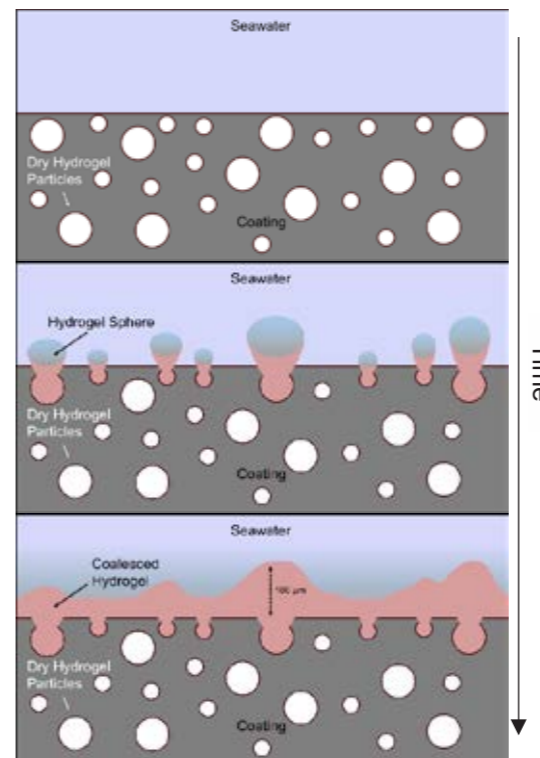


Figure 38: Hydrogel Formation Scheme in Xanthan Gum-based hydrogel antifouling coatings

Methodology

For OCT imaging, an 880 nm system (Ganymede Series, Thorlabs) acquired 10 mm B-scans with $3.5 \mu\text{m}/\text{pixel}$ resolution at 50 Hz, averaging 5 A- and B-scans to reduce noise. Measurements were performed on dry and immersed samples under $\sim 2 \text{ cm}$ of artificial sea water. Triple B-scan-based quantification enabled rapid imaging with simple analysis and minimal contrast-related errors. An ImageJ workflow separated the hydrogel and coating surface via grayscale thresholding, and extracted XZ-coordinates were analyzed using an in-house Python script to calculate surface roughness, gel thickness, coverage, and volume over time, correcting for coating waviness and filling overhangs (see Figure 2).

Results, Discussion & Conclusions

OCT accomplishes real-time monitoring of hydrogel formation, providing key insights into the development and optimization of hydrogel-based coating systems. Through quantitative analysis of hydrogel thickness, volume, surface coverage, and coating roughness, OCT reveals dynamic structural changes during swelling and formation. Complementary rheological analysis further enhances the understanding by characterizing the hydrogel's mechanical properties as applied in our previous study [6]. Together, these methods deliver a comprehensive and robust characterization approach, facilitating the design of more effective, durable, and biocide-reduced hydrogel antifouling coatings and offering applicability to other hydrogel systems.

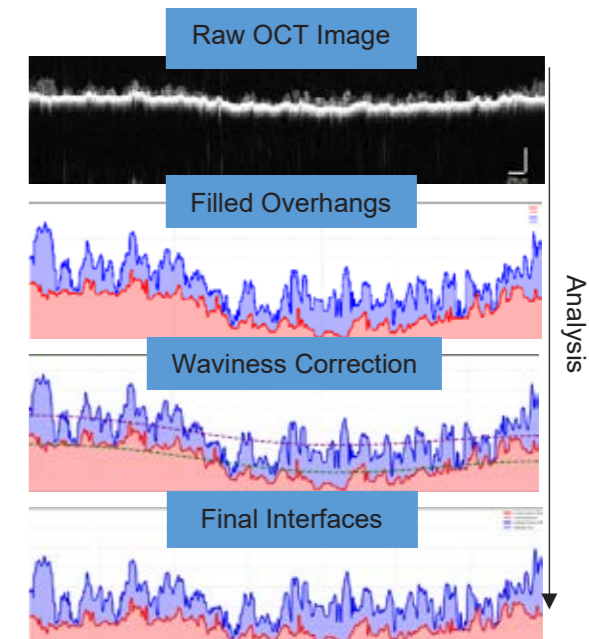


Figure 39: OCT analysis from raw OCT image (top) to final interfaces that are quantifiable (bottom) with hydrogel in blue and coating in red

Acknowledgments

Financial support from the Hempel Foundation to CoaST (The Hempel Foundation Coatings Science and Technology Center)

References

1. M. P. Schultz, Biofouling, vol. 23, no. 5, pp. 331–341, (2007)
2. C. A. Paz-Villarraga, Í. B. Castro, and G. Fillmann, Environ Sci Pollut Res, vol. 29, no. 20, pp. 30090–30101 (2022)
3. M. He, H. Jiang, R. Wang, Y. Xie, W. Zhao, and C. Zhao, Journal of Colloid and Interface Science, vol. 484, pp. 60–69 (2016)
4. W. Yu et al., ACS Appl. Bio Mater., vol. 4, no. 3, pp. 2385–2397 (2021)
5. K. Nishinari and R. Takahashi, Current Opinion in Colloid & Interface Science, vol. 8, no. 4–5, pp. 396–400 (2003)
6. M. Butschle, S. Lindner, M. Schackmann, and K. Dam-Johansen, Progress in Organic Coatings, vol. 188, p. 108197 (2024)
7. C. Xi, D. L. Marks, S. Schlachter, W. Luo, and S. A. B. M.d, JBO, vol. 11, no. 3, p. 034001 (2006)

List of publications:

M. Butschle, S. Lindner, M. Schackmann, and K. Dam-Johansen, *Progress in Organic Coatings*, vol. 188, p. 108197 (2024)

Recycling of crosslinked elastomer systems

(May 2023 – April 2027)



Contribution to the UN Sustainable Development Goals

Elastomers are used in various applications and environments, from heavy mining industries to medical devices inside human bodies. Some examples are seals and gaskets, tires, conveyor belts, implants and catheters, footwear, and roofing membranes. It is crucial for the industry to find efficient ways to recycle these elastomers to be able to close the loop between consumption and production. However, as of today, no such recycling processes for elastomers exist. This project investigates solutions to this problem.



Sofia Lindström

soflind@dtu.dk

Supervisors:

Anne Ladegaard Skov
Anders Egede Daugaard

Abstract

The producers of crosslinked elastomers are facing a significant challenge in finding efficient recycling processes for their products. This project presents a recyclable silicone elastomer with crosslinks constituted by silyl ethers. A simple recycling process, which involves hydrolysis of the crosslinks, is proven to reclaim polymers with high chemical similarity to the starting polymers.

Introduction

There are two distinct categories of polymeric materials – thermoplastics and thermosets. Thermoplastic materials consist of polymers held together by intermolecular forces such as hydrogen bonding and van der Waals forces. These intermolecular forces are generally weak enough to allow the material to melt and flow at temperatures above its specific melting temperature, enabling recycling of the material into new products via thermomechanical processes. Thermosets, on the other hand, have irreversible bonds, called crosslinks, between the polymer chains, which enhance the mechanical, chemical, and thermal stability of the material. Indeed, having crosslinks increases the material's stability so much that it can no longer melt and flow, thus complicating the recycling of these. [1] [2]

Rubbers and elastomers are crosslinked through different mechanisms, depending on the chemical nature of the polymers and the desired end properties. The presence of crosslinks between the polymer chains greatly improves the elasticity of the material. The interlocking of the polymers through crosslinks creates a three-dimensional network which together with the presence of long chain molecules (polymers) with freely rotating links and weak intermolecular forces between these molecules, enable the polymer network to be elongated elastically. [3]

Silicone elastomers are commonly regarded as having high chemical and thermal stability, being biocompatible, and having unique elastic properties. The combination of these properties makes them suitable for a variety of applications, amongst them biomedical devices and construction machinery. The crosslinking of silicones can be introduced via different chemical reactions. The most common methods are addition curing through hydrosilylation, condensation curing, and radical curing using classical radical initiators such as peroxides. As already mentioned, having crosslinks makes recycling a complex task and silicones are no exception. There are, however, ongoing research efforts which try to solve this issue. The suggested reaction pathways often lead back to either monomers or cyclic polysiloxanes, which then require a preceding repolymerization step before the reintroduction of the polymers into the material loop. [4] [5]

Specific objectives

The objective of this project was to develop a selective recycling process where only the crosslinks are broken, meaning a de-crosslinking process. With this idea in mind, a silicone elastomer with hydrolysable crosslinks constituted by silyl ethers was developed and proven to be recyclable.

Experimental methods

A silicone elastomer was produced by speedmixing a carbinol end-functionalized silicone polymer (Silmer OHT Di-400) with 5 PHR

polysilazane (Durazane 1800/IOTA 9108), 50 ppm benzotriazole as a catalyst, 140 PHR solvent (Dowsil OS-20), and 20 PHR hydrophobic silica filler (HDK H2000). After mixing to homogeneity, the mixture was transferred into Teflon molds which were thereafter left at room temperature for 48 hours. The films were then transferred onto Teflon films and kept in an oven at 80°C for 24 hours. 0.4-0.6 g of circular samples of 8 mm in diameter were punched out from the fully cured film and then put into glass vials containing a solution of 0.055 M acetic acid (AcOH) in tetrahydrofuran (THF). The vials were put under magnetic stirring at 200 rpm and kept at 40°C. The solutions from the vials were precipitated into methanol (MeOH) after 2, 6, 12, and 24 hours. Size exclusion chromatography (SEC) was conducted on the 24 hours sample, as well as on the starting polymer (Silmer OHT Di-400).

24 hours at 40 °C	95 000	2.1
Silmer OHT Di-400	36 000	1.5

The molar mass of the recycled polymer after 24 hours, 95 000 g mol⁻¹, is higher compared to the starting polymer, 36 000 g mol⁻¹. A higher molar mass after the hydrolysis tells that not all crosslinks have been hydrolyzed, which can be explained by permanent, non-hydrolysable, crosslinks being present in the material. It is likely that other crosslinks, in addition to silyl ethers, are formed as well during the curing with the polysilazane. Nevertheless, the elastomer can be recycled, and the polymers can be reclaimed, showing the potential for applying the de-crosslinking approach to other material development projects with recyclability as a goal.

Conclusion

A novel approach curing of carbinol end-functionalized silicone utilizing polysilazane successfully yielded a silyl ether crosslinked silicone elastomer. Small-scale experiments demonstrated that combining a high-swelling solvent (THF) and a low concentration of acetic acid could open the polymer network to allow hydrolysis of the sensitive crosslinks via the acid.

Acknowledgements

This project is funded by Roxtec International AB.

References

- J.E. Marks, Applied Plastics Engineering Handbook, Elsevier, Oxford, U.K., 2017, p. 109-125.
- L. Imbernon, S. Norvez, European Polymer Journal 82 (1) (2016) 347-376
- Treloar, L. R. G, The Physics of Rubber Elasticity, Oxford University Press, New York, U.S.A., 2005.
- Mazurek, P., Vudayagiri, S., Skov, A. L., Chemical Society Reviews 48 (6) (2019) 1448-1464.
- Wolf, A. T., Stammer, A., Polymers 16 (2024) 2220

List of publications

S. Lindström, R. Sønderbæk-Jørgensen, A. L. Skov, A. E. Daugaard, Journal of Polymer Science 64 (14) (2025) 2891–2902.

Results and discussion

Polysilazane-cured silicone elastomer discs were placed in vials containing a solution of 0.055 M AcOH in THF and maintained at 40°C for different times. The resulting mixtures were precipitated into MeOH to reclaim the polymers. Figure 1 shows the initial samples (1-A), and the precipitated samples after 2 hours (1-B), 6 hours (1-C), 12 hours (1-D), and 24 hours (1-E).

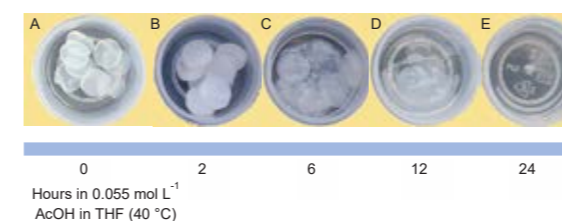


Figure 40: Photos of samples during degradation at 40 °C in 0.055 mol L⁻¹ AcOH in THF: **(A)** Before immersion **(B)** 2 hours **(C)** 6 hours **(D)** 12 hours

The samples get visible surface defects already after 2 hours (Figure 1-B), and, as time goes on, start to dissolve after 6 hours (Figure 1-C). After 12 hours (Figure 1-D), the samples still form somewhat cohesive samples, but they become fully dissolved after 24 hours (Figure 1-E). This experiment shows how the material initially just swells in the solvent, and how this swelling is followed by acid hydrolysis of the crosslinks as the polymers start to dissolve in the solvent. The precipitated samples after 24 hours were tested using SEC to evaluate how the hydrolysis affects the molar mass of the polymers. Table 1 presents the results from the SEC analysis.

Table 2: The molar masses of the reclaimed polymers and the starting polymer.

Sample	M _w [g mol ⁻¹]	M _w /M _n
--------	---------------------------------------	--------------------------------

Mechanistic Insights into Short Chain Olefin Oligomerization on Acid Catalysts: The Role of Catalyst Properties, Process Parameters and Feed Composition

(March 2023 – February 2026)



Contribution to the UN Sustainable Development Goals

To mitigate climate change and ensure universal access to affordable and reliable energy, the development of viable alternatives to fossil fuels is crucial. This is particularly important for heavy-duty transport sectors such as aviation, which rely on fuels with high energy density. One promising route for producing sustainable aviation fuel (SAF) is the methanol-to-jet (MTJ) process. A detailed understanding of the oligomerization mechanism, as a key step in the process, is essential for the rational optimization of catalyst design and operating conditions.



Moritz Niklas Link

mnil@kt.dtu.dk

Supervisors: Anker Degn Jensen, Martin Høj, Martin Dan Palis Sørensen & Pablo Beato (Topsoe)

Abstract

Methanol-to-Jet is a promising route for producing sustainable aviation fuel. The central step of oligomerization has been studied in this project, with the focus on gas-phase propene oligomerization. Microporous and mesoporous acid catalysts were investigated, displaying 1st order reaction kinetics in all cases. It was found that the catalyst activity increases with the acid site density, especially linear for the microporous zeolites. However, structural properties such as pore size and mesopore surface area appear to be of central importance as well, resulting in higher activities for the amorphous silica-alumina (ASA) compared to a n-H-ZSM-5 at similar acidity. A synthesized hierarchical silica alumina (HSA) appears to combine both benefits yielding the highest activity at given process conditions.

Introduction

The production of sustainable aviation fuels (SAF) is expected to play a central role in decarbonizing the aviation sector [1]. The Methanol-to-Jet (MtJ) process represents a viable and attractive pathway for SAF production, offering advantages such as flexible feedstock utilization and high selectivity toward branched hydrocarbons within the targeted jet-fuel range [2,3]. The latter benefit arises primarily from the acid-catalyzed oligomerization of light olefins. However, this process and its underlying reaction mechanisms are highly complex, involving multiple competing pathways such as isomerization, β -scission, and hydrogen transfer [4]. Further limitations within the reaction framework are given by diffusional constraints, governing the catalyst activity, selectivity and deactivation mechanism [5].

Understanding the individual influences of catalyst properties, process conditions and feed composition on the reaction mechanism is therefore essential in optimizing the overall efficiency of the process.

Specific Objectives

In this project, acid catalysts with varying acidity and structural properties were investigated at varying process conditions, in order to facilitate kinetic and mechanistic insights of the gas-phase oligomerization of short chain olefins, with regard to activity, selectivity and deactivation behavior.

Methods and Materials

The catalysts investigated in this study were microporous nano-H-ZSM-5 with varying Si/Al ratios, mesoporous amorphous silica-alumina (ASA), Al-MCM-41 and a hierarchical silica-alumina (HSA). Physicochemical properties of the catalysts have been characterized by N₂-physisorption, XRD and NH₃-TPD; an overview of the main properties is presented in Figure 1. Experiments were conducted in a pressurized flow set-up at pressures of 15-35 bar, 200 °C and varying space velocities (WHSV = 10 – 45 h⁻¹). The evaluation of the process is based on GC

peak areas, correlated through the carbon response factor.

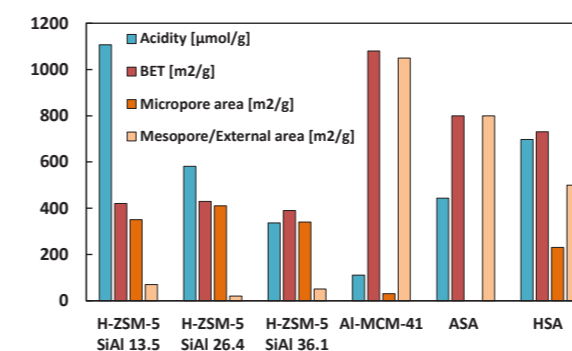


Figure 41. An overview of the physicochemical properties of studied catalysts.

Results and Discussion

Through variations in space velocity and partial pressure of propene at constant temperature, a set of conversion (X) at varying space times (τ) can be obtained. Following first order kinetics, the PFR model as stated in Eq.1 should then be able to describe the system sufficiently.

$$\ln\left(\frac{1}{1-X}\right) = k\tau \quad \text{Eq.1}$$

Figure 2 demonstrates this for all catalysts, displaying linear correlations between the left-hand side of the equation and the space time. Evaluating the slope of each linear correlation allows for the determination of the 1st order rate constant.

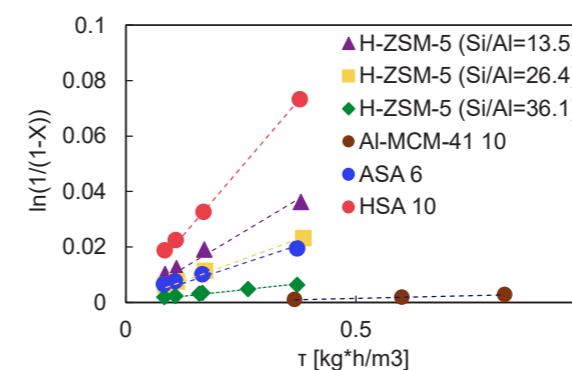


Figure 42. 1st order kinetic rate fit for microporous and mesoporous catalysts.

As can be seen for the n-H-ZSM-5 samples, the slope of the linear correlation, the rate constant, is increasing with increasing acidity i.e. decreasing Si/Al ratio. This is also true when comparing the mesoporous catalysts among each other. However, when comparing the two types of catalysts against each other, the ASA shows a similar activity to the n-H-ZSM-5 with Si/Al ratio of 26.4, despite having a lower acidity. Even more

so, the HSA with medium-high acidity, displays the steepest slope i.e. the highest activity at given conditions.

From these results, it becomes evident that not just the individual acid or structural properties determine the catalysts activity, but rather a complex interplay.

Progress and Future Work

For this project, targeting the production of hydrocarbons in the jet-fuel range of C₈ – C₁₆, the study of catalyst properties and process parameters on the product selectivity is of crucial importance and is being investigated in detail.

In addition, the effect of feed composition is examined by replacing propene with larger olefins such as pentene and hexene to evaluate their impact on activity and product selectivity, particularly considering the structural limitations present in microporous materials.

Ongoing work also focuses on the co-oligomerization of mixed feedstocks to simulate industrially relevant compositions representative of the preceding Methanol-to-Olefins process.

Finally, future efforts will be dedicated to developing a simplified kinetic model that integrates the mechanistic insights obtained in this study into a unified description of oligomerization over microporous and mesoporous acid catalysts.

Acknowledgements

This Project received funding from The Innovation Fund Denmark – 1150-00001B.

References

1. M. Kousoulidou, L. Lonza, Transp Res D Transp Environ (46) (2016) 166 – 181.
2. P. Schmidt, V. Batteiger, A. Roth, W. Weindorf, T. Raksha, Chemie-Ingenieur-Technik (90) (2018) 127 – 140.
3. Yarulina et al., Catal Sci Technol (6) (2016) 2663 – 2678.
4. F. Dubray, V. Paunović, M. Ranocchiaro, J. A. van Bokhoven, Journal of Industrial and Engineering Chemistry (114) (2022) 409 – 417.
5. E. Bickel; R. Gounder, JACS Au (2) (2022) 2585-2595.

Synthesis of large cyclic polydimethylsiloxane (PDMS) rings for wearable devices

(January 2025 – December 2027)

3 GOOD HEALTH AND WELL-BEING



Contribution to the UN Sustainable Development Goals

My project targets the development of soft, stretchable silicone materials made from interlocked ring molecules. Due to their increased softness, these materials could be used in prosthetics and wearable health-monitoring technology. This softness can lead to a higher sense of comfort when wearing such devices, helping with patient compliance and general well-being. Softer materials also better conform to the body, improving sensor accuracy and making devices more accessible to children and the elderly.



Ádám Lukács

adamlu@kt.dtu.dk

Supervisors: Anne Ladegaard Skov, Cody Brian Gale, Frederikke Bahrt Madsen

Abstract

Concatenated ring network elastomers have been shown to exhibit excellent softness and stretchability. However, they are difficult to synthesize and characterize and most methods afford little control over network properties. This study aims to construct said networks piece-by-piece, to achieve more control over the network components and overall properties. The current challenge is the synthesis and the purification of rings of sufficient size that allow for threading by linears for subsequent network formation.

Introduction

Cyclic polymers by their nature possess no end-groups leading to a difference in properties when compared to their linear counterparts, such as lower viscosity, smaller hydrodynamic volume and better resistance to degradation [1].

There are three common strategies for cyclic polymer synthesis as shown in Figure 1: Unimolecular ring closure, bimolecular ring closure and ring expansion. The first two strategies require high dilutions and lead to products with controlled molecular weights and narrow product distributions. The ring expansion strategy does not require high dilutions, can achieve very high molar masses, but the product distribution tends to be broader [2].

Analysis of cyclic polymers can be somewhat challenging and there is no universally accepted method for proving a polymer's cyclic nature. For this reason, usually several methods are used simultaneously to characterize the polymers' topology that complement each other. The most popular method is end-group analysis via different spectroscopic methods, like nuclear magnetic resonance spectroscopy (NMR), or Fourier-transform infra-red spectroscopy (FT-IR). However, due to the relatively low concentration of end-groups compared to the main chain, especially in higher molecular weight polymers,

these methods can be unreliable. Alternatively, size exclusion chromatography (SEC) can be used to detect single rings because the decreased hydrodynamic volume of ring polymers compared to their linear counterparts can be used as the basis of separation, and an indicator of ring formation. Single ring polymers also diffuse more quickly in solution than linears, which can be measured using diffusion ordered NMR spectroscopy (DOSY). This method is especially useful as it combines end-group analysis with diffusion data allowing us to differentiate between ring polymers and chain-extended linear byproducts.

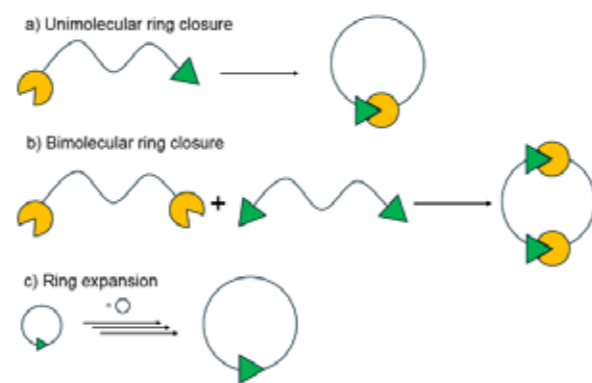


Figure 1: Synthetic strategies for cyclic polymers

Concatenated silicone networks consisting of interlocked rings have been shown to possess greater softness compared to traditional chemically cross-linked silicone elastomers. This is thought to originate from the fact that these networks are linked through physical cross-links that are able to slide freely, giving rise to this unique property [3],[4]. Currently concatenated silicone elastomers are synthesized using a one-pot strategy where linear starting materials are mixed and form ring networks spontaneously via reactive end-groups [3],[4].

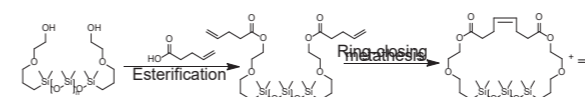
Specific Objectives

- 1) Synthesis of single large-sized PDMS rings
- 2) Development of a method for the preparation of concatenated ring networks
- 3) Fine-tuning network properties towards increased softness through variation of quality and quantity of individual components

Results and Discussion

Synthesis and analysis of large single PDMS rings

Cyclic polydimethylsiloxane of various sizes has been synthesized using literature methods [5] in two steps via alkene metathesis from commercially available silicone materials as shown in Scheme 1.



Scheme 1: Ring synthesis in two steps from commercial silicone via alkene metathesis.

The reaction products have been analyzed via size exclusion chromatography and diffusion ordered NMR spectroscopy. SEC analysis (shown in Figure 2) shows that the retention volume of the product is higher than the starting material, indicating a lower hydrodynamic volume, and therefore ring formation. However, the appearance of a shoulder peak points towards the formation of chain-extended linear byproducts.

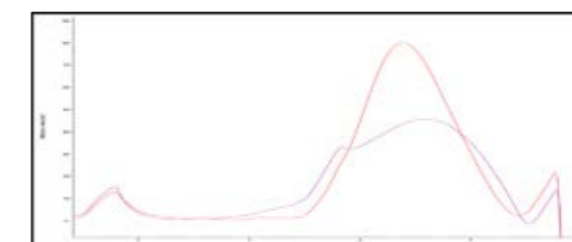


Figure 2: SEC results comparing starting material (red) and reaction product (purple).

DOSY analysis of polymer end-groups in the alkene region (shown in Figure 3) reveals a new signal corresponding to internal alkenes formed during alkene metathesis, that are present in two distinct species. One only possessing the new internal alkene group with a higher diffusion constant, indicating ring formation, and one where end-groups are present alongside, indicating chain-extended byproduct formation.

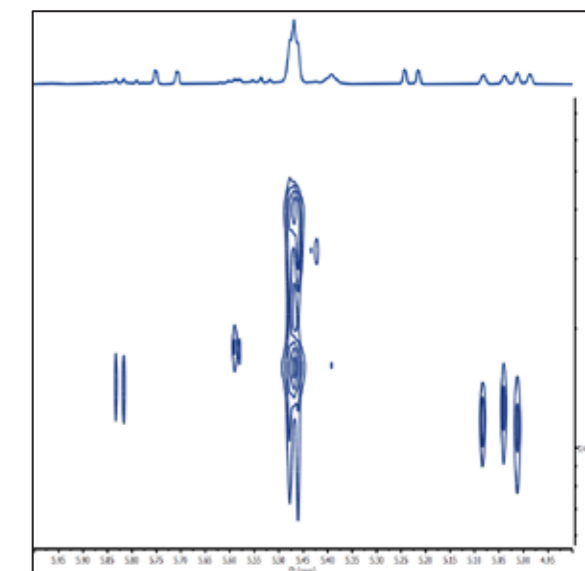


Figure 3: DOSY results of alkene region. Assignment of signals: Internal alkenes: 5,35-5,65 ppm; Terminal alkenes: 4,95-5,10 ppm and 5,80-5,85 ppm

Conclusions

Cyclic silicones of various sizes have been synthesized and analyzed via SEC and DOSY techniques. Analysis revealed the formation of ring polymers as well as chain-extended linear side products. Further work to purify the reaction products is ongoing.

References

1. F. M. Haque, S. M. Grayson, Nat Chem, 12 (5) (2020) 433–444
2. R. T. Gao, L. Xu, S. Y. Li, N. Liu, Z. Chen, Z. Q. Wu, Chemistry – A European Journal 29 (41) (2023) e202300916
3. P. Hu, J. Madsen, Q. Huang, A. L. Skov, ACS Macro Lett, 9 (10) (2020) 1458–1463
4. [4] Goff, J., Sulaiman, S., Arkles, B. and Lewicki, J.P, Adv. Mater 28 (2016) 2393–2398
5. M. Ebe, A. Soga, K. Fujiwara, B. J. Ree, H. Marubayashi, K. Hagita, A. Imasaki, M. Baba, T. Yamamoto, K. Tajima, T. Deguchi, H. Jinnai, T. Isono, T. Satoh, Angewandte Chemie International Edition 62 (35) (2023) e202304493

Digital twin development of high shear granulation processes

(December 2024 – December 2027)

9 INDUSTRY, INNOVATION AND INFRASTRUCTURE



Contribution to the UN Sustainable Development Goals

This project is part of a greater movement seen in recent years to create digital representations of real physical manufacturing processes. The virtual simulation of these processes enables faster and cheaper testing of various product formulations and operating conditions. This speeds up development, optimization, and scaleup of these processes, while reducing waste, enabled through virtual testing and the increased understanding obtained by insights derived from the simulation of these processes.



Oliver Massaad

oroma@dtu.dk

Supervisors: Ulrich Krühne, Pär Tufvesson

Abstract

High Shear Wet Granulation is a process used in the production of a variety of products from pharmaceuticals to fertilizers. Despite its industrial significance, predicting the properties of its products remains challenging. To address this, modeling can be done, where in powder processes the Discrete Element Method (DEM) is commonly used. But the application and usability of such models is hindered by their computational complexity. The objective of this work is to approximate DEM by developing a Machine Learning (ML) based surrogate model to enable near real-time simulation of these processes.

Introduction

In High Shear Wet Granulation (HSWG) powders are processed with a liquid binder to agglomerate larger homogenous granules. Mechanical mixing homogenizes the material distribution across the powder bed, while also promoting binder dispersion. Binder forms liquid bridges between the powder particles to form granules.

At the microscopic level, various phenomena are seen in HSWG, classified as nucleation, growth, and breakage processes, illustrated in Figure 1. Nucleation occurs when the liquid contacts the powder. Growth involves particle coalescence, powder layering, and granule densification ("squeezing" liquid and air out of the granule). Breakage occurs by fragmentation or attrition.

The characteristics of the granule depend on the dominance of each of those processes. These microscopic phenomena are difficult to observe, and thus hard to quantify, which poses a challenge to predicting product outcomes of HSWG.

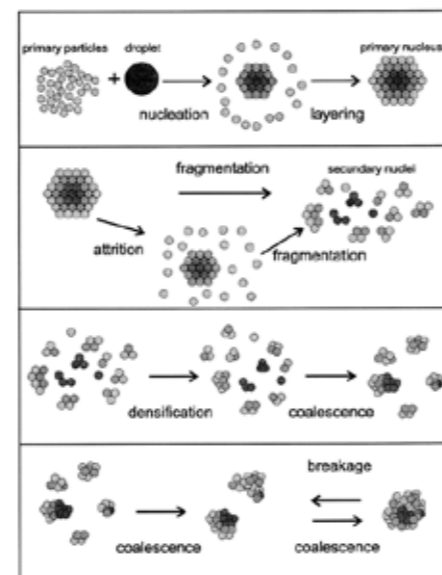


Figure 1: HSWG mechanisms [1].

Objectives

The aim of this project is to develop a (near) real-time model of HSWG to predict the evolution of granule characteristics during processing and understand the driving mechanisms. A graph-based Machine Learning (ML) Surrogate Model (SM) will be used to approximate powder flow behavior at low computational cost. The SM will be

trained with data generated by Discrete Element Method (DEM) simulations. The SM will also relay flow characteristics information to a Population Balance Model (PBM) to estimate the evolution of granule properties. Each method is expanded in the following sections.

Discrete Element Method (DEM)

In DEM solid particles are represented as elements in a domain with specific mass, position, and linear and angular motions. As particles move over time, they may collide. During contact events, particles may overlap, giving rise to interaction forces dependent on material properties [2].

Accuracy is contingent on the complexity of the contact models, material parameters, and the fidelity of the particle shape and size distribution. But the primary factor limiting the use of DEM is the computational toll associated with applying it at scale. As models for realistic powder systems could easily have billions of particles, making their computation infeasible by current standards.

Development of faster algorithms, parallelized codes, and coarse-grained models (lumping particles into parcels to decrease their count) have emerged to address these limitations. Yet have not sufficed to reduce simulation times to near real-time [3]. This project follows an alternative approach, by using DEM simulations to train SMs to approximate powder flow dynamics.

Surrogate Modelling (SM)

A common approach is to encode particles as nodes in a graph, connected by edges that satisfy a proximity criterion, as shown in Figure 2. These SMs learn local interactions to predict particle accelerations used in numerical time integration. The permutation-invariant/equivariant nature of graphs with respect to data ordering, emphasizes learning of relational structures, making these models more generalizable [4]. This approach has already proven effective in simpler systems [5].

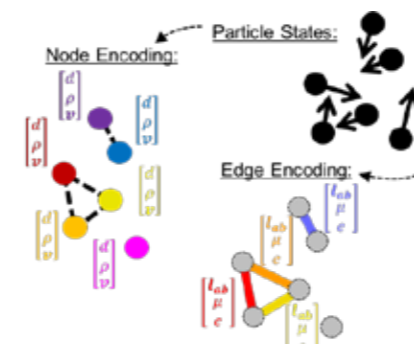


Figure 2: Particle state graph embedding.

Population Balance Modelling (PBM)

The time scale of HSWG far exceeds what is computationally feasible with DEM, so PBM is

used to estimate the evolution of granule characteristics. PBM, a mesoscale approach, links microscopic phenomena to macroscopic property distributions ($n(x, t)$) by solving a number-flux balance driven by source terms (R), as shown in Equation 1 below.

$$\frac{\partial n(x, t)}{\partial t} + \nabla_x [\dot{X}(x, t) n(x, t)] = R_{nucleation} + R_{growth} + R_{breakage}$$

Where the impact of the source terms is weighted by the extent to which each of the governing microscopic phenomena dominate granulation.

The DEM-PBM hybrid approach has successfully been used to predict particle size, liquid content, and porosity distributions in HSWG [6], [7].

Conclusion

Though HSWG has been used in a variety of applications, its understanding remains limited, and often relies on experience to achieve desired product, rather than quantitative prediction. The methods presented in this summary outline a potential route to developing a computationally tractable model of HSWG. The insights derived from simulating solid particle flow behavior and product characteristics could help draw links and patterns between the two to unlock a deeper understanding of the HSWG process.

Acknowledgements

This project was made possible by a grant from the Novo Nordisk Foundation.

References

1. P. Vonk, C.P.F. Guillaume, J.S. Ramaker, H. Vormans, N.W.F. Kossen, *Int. J. Pharm.* 157 (1) (1997) 93-102.
2. J. Seville, C.Y. Wu., *Particle Technology and Engineering*, Butterworth-Heinemann, Oxford, UK, 2016, Ch. 9.
3. S.B. Yeom, E.S. Ha, M.S. Kim, S.H. Jeong, S.J. Hwang, D.H. Choi, *Pharmaceutics* 11 (8) (2019) 414.
4. Sanchez-Gonzalez, J. Godwin, T. Pfaff, R. Ying, J. Leskovec, P.W. Battaglia, *arxiv* (2020)
5. S. Li, M. Sakai, *Chem. Eng. J.* 500 (2024).
6. Chaudhury, M.E. Armenante, R. Ramchandran, *Chem. Eng. Res. Des.* 95 (2015) 211-218.
7. K.F. Lee, M. Dosta, A.D. McGuire, S. Mosbach, W. Wagner, S. Heinrich, M. Kraft, *Comp. Chem. Eng.* 99 (2017) 171-184.

Sustainable biomethanation of pyrolysis gas from residual biomass

(November 2024 – November 2027)

7 AFFORDABLE AND CLEAN ENERGY



Contribution to the UN Sustainable Development Goals

The global transition from linear to circular economy has encouraged scientists to explore the sustainable use of waste products. The resulting innovations must be combined in such a way that waste is completely processed into products with a carbon-negative footprint. Pyrolysis combined with biomethanation of pyrolysis gas is a sustainable route to close the cycle of residual biomass conversion. Currently, pyrolysis gas is mainly used to generate heat and power. Biomethanation, on the other hand, results in high-quality methane gas for grid applications. Integration of this technology reduces the EU's reliance on fossil fuel-derived natural gas.



Anatolii Mishchuk

anami@kt.dtu.dk

Supervisors: Jesper Ahrenfeldt, Lasse R. Clausen, Hariklia N. Gavala, Ioannis V. Skiadas

Abstract

Nowadays, bioenergy research focuses on residual biomass. Pyrolysis of biomass is a sustainable solution. Biochar, bio-oil, and pyrolysis gas are the products of this technology. The exploitation of pyrolysis gas in a way that is cheap and climate-positive has not been achieved due to the presence of gas impurities. The biomethanation of pyrolysis gas in a trickle bed reactor (TBR) involving mixed microbial consortia (MMC) is considered an economically feasible route to producing carbon-negative fuels. Understanding the kinetics of impurity inhibition on microbial growth is crucial for the scale-up of TBRs. The present study focuses on the inhibitory effect of acetylene (C_2H_2) and ethylene (C_2H_4), which are found as impurities in pyrolysis gas and are known to hinder methanogenesis.

Introduction

Residual biomass is a readily available and renewable source of energy. Global unsustainable usage of such biomass is harmful to our ecosystem. Environmentally friendly ways of utilization must be established, preferably with a climate-positive effect [1]. Thermal decomposition of residual biomass is a possible approach. Pyrolysis is a widely recognized efficient method for producing biochar, bio-oil, and pyrolysis gas in an oxygen-free environment [2]. While the first two abovementioned products have a green use, pyrolysis gas lacks a suitable green application.

At present, pyrolysis gas is primarily utilized for power and heat generation due to its high impurity content [3]. This conversion is inefficient because of variations in power and heat demand on a daily, monthly, and seasonal basis [4]. It is possible to catalytically upgrade (e.g., Fischer-Tropsch synthesis) pyrolysis gas. However, a high-purity gas must be used as a feedstock, and this demands major capital and operational expenses [5]. Another strategy is the biomethanation of pyrolysis gas in a TBR hosting MMC.

Recently, Asimakopoulos, et al. [6, 7] experimentally demonstrated biomethanation of syngas supplemented with H_2 in lab and pilot-scale TBRs. High rates of CH_4 production and syngas conversion were achieved while retaining high product selectivity. Such production of CH_4 may facilitate: i) closing the sustainable route for the usage of residual biomass, and ii) eliminating the problem of gas storage, as CH_4 is a superior green energy carrier with a large storage capacity (i.e., natural gas infrastructure).

MMC are expected to have great resilience to a broad number of impurities [8]. However, research on the resistance of methanogenic MMC to gas impurities (such as light hydrocarbons) is scarce. Although microorganisms are relatively tolerant to such impurities, an inhibitory effect is expected. The current study addresses the inhibitory effect of light hydrocarbons, with the ultimate goal of developing inhibition models for C_2H_2 and C_2H_4 .

Specific Objectives

Furthermore, the plan is to connect a pilot-scale TBR to the off-gas line of the residual biomass pyrolysis process at the Stiesdal SkyClean A/S

plant in Skive. The off-gas (i.e., pyrolysis gas) will be converted to CH_4 in the presence of impurities. Potential reduction of gas cleaning operations can result in enhanced scaling and end-product cost.

The project's primary objective is to investigate the inhibitory effects of pyrolysis gas, emphasizing light hydrocarbons (C_2H_2 and C_2H_4).

Results and Discussion

Methanogenic activity in mixed microbial consortia was assessed in 300 mL anaerobic serum vials. Each vial was pressurized to 1.6 bar at ambient temperature with a gas mixture consisting of 45% H_2 , 25% CO_2 , 20% CO , and 10% N_2 . C_2H_2 and C_2H_4 were added in different quantities, and N_2 was used to adjust the final total pressure to 1.8 bar at ambient temperature. The vials were incubated at 60 °C and tested in triplicate. Treatment with C_2H_2 and C_2H_4 showed substantially different levels of inhibition (Table 1).

Table 3: Mean of relative CH_4 production rates under different concentrations of C_2H_2 and C_2H_4 . Means that do not share a letter are significantly different ($p < 0.05$, Tukey's HSD).

	Mean	Groups			
Control	100	A			
1.11% C_2H_4	101	A			
2.36% C_2H_4	64		B		
0.06% C_2H_2	57		B	C	
3.75% C_2H_4	57		B	C	
5.00% C_2H_4	49			C	
7.50% C_2H_4	33				D
0.22% C_2H_2	30				D
10.00% C_2H_4	17				E
1.11% C_2H_2	12				E F
5.00% C_2H_2	3				F

A moderately high C_2H_4 level of 3.75% resulted in a 43% reduction in CH_4 production rate, whereas a very low C_2H_2 content of only 0.06% had a relatively similar inhibitory impact. Such reactivity of C_2H_2 is defined by its molecular structure containing two π -bonds. Unlike C_2H_4 , which has a single π -bond. In general, increasing the gas-phase concentrations of C_2H_2 and C_2H_4 led to a higher inhibitory effect (Figure 2).

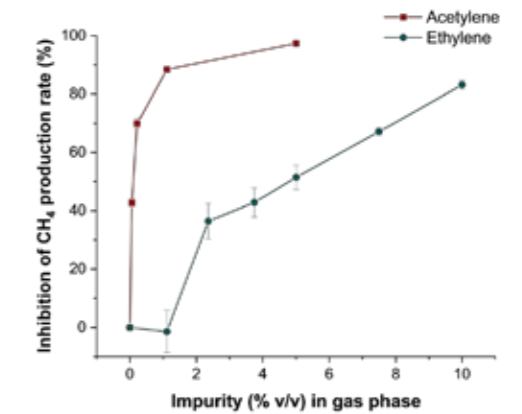


Figure 2: Effect of C_2H_2 and C_2H_4 on CH_4 production rate inhibition (%) in a methanogenic mixed microbial community

These findings, combined with additional experiments to determine inhibition kinetics for C_2H_2 and C_2H_4 , will allow the development of inhibition models for tested hydrocarbons.

Conclusions

A study of the effect of C_2H_2 and C_2H_4 on the growth rate of suspended methanogenic MMC showed various levels of inhibition. C_2H_2 demonstrated strong inhibition due to its chemical structure. The main discovery is that the normal concentrations of these light hydrocarbons in pyrolysis gas, 0.00 to 0.05% C_2H_2 and 1 to 5.00% C_2H_4 , do not completely inhibit methanogenesis.

Acknowledgements

This work is funded by the DTU Strategic PhD Initiative 2024.

References

1. N. Tripathi, et al. *Clim. Atmos. Sci.* 2, 35 (2019).
2. S. Shapiro-Bengtson, et al. *Energy Environ. Sci.* 15, 1950–1966 (2022).
3. J. Moško, et al. *Energies.* 13, 4087 (2020).
4. S.A. Tassou, et al. *Energy Convers. Manage.* 48, 2988–2995 (2007).
5. R.G. Santos, et al. *Int. J. Hydrogen Energy.* 45, 18114–18132 (2020).
6. K. Asimakopoulos, et al. *Waste Biomass. Valor.* 12, 6005–6019 (2021).
7. K. Asimakopoulos, et al. *Appl. Energy.* 290, 116771 (2021).
8. Grimalt-Alemany, et al. *Biofuels Bioprod. Bioref.* 12, 139–158 (2018).

Terahertz Spectroscopy for Sustainable Maritime Coatings

(November 2024 – November 2027)

9 INDUSTRY, INNOVATION AND INFRASTRUCTURE



Contribution to the UN Sustainable Development Goals

This research contributes to **Goal 9: Industry, Innovation, and Infrastructure**. By improving non-destructive testing of maritime coatings, the project supports sustainable industrial practices and enhances infrastructure resilience. Improved diagnostics reduce maintenance costs and environmental impact by preventing premature failures. The integration of terahertz technology with coating science fosters innovation and supports the development of greener, longer-lasting protective coatings for marine applications.



Behnam Mohammadi

behmo@kt.dtu.dk

Supervisors:
Simon Jappe Lange,
Kim Dam-Johansen,
Jochen Dreyer

Abstract

The project explores the use of Terahertz Cross Correlation Spectroscopy (CCS) and imaging for non-destructive analysis of maritime coatings. These coatings protect marine structures from corrosion, fouling and environmental damage but degrade over time. The research aims to develop methods for accurate thickness measurement, extract optical parameters like refractive index and absorption coefficient, and monitor curing processes. Terahertz imaging will be used to detect defects and corrosion beneath the surface. The goal is to enhance maintenance practices and extend the lifespan of marine infrastructure through advanced, non-invasive diagnostics.

Introduction

Steel structures operating in marine environments face continuous exposure to saltwater, high humidity, and biological activity, all of which accelerate corrosion and surface deterioration. Biofouling caused by marine organisms further increases drag and fuel consumption, leading to higher operational costs and environmental impact. To mitigate these issues, protective polymer coatings—particularly epoxy-based systems—are widely used for their strong adhesion, durability, and resistance to corrosion [1].

Ensuring the integrity of these coatings, especially maintaining their thickness, is essential for long-term performance and compliance with international standards. However, conventional inspection techniques often fall short: many are invasive, struggle with complex geometries, and lack reliability on aged or corroded surfaces. These limitations underscore the need for a non-destructive, accurate, and field-deployable solution for routine coating evaluation [2].

Terahertz spectroscopy has emerged as a promising alternative, offering high-resolution, contact-free analysis of coating thickness and subsurface features. Among these, terahertz

cross-correlation spectroscopy (THz-CCS) stands out for its compact design and cost-efficiency, making it suitable for maritime applications [3].

Specific Objectives:

This project aims to develop a robust terahertz cross-correlation spectroscopy (THz-CCS) framework for inspecting maritime coatings. The specific objectives are:

- 1) Measure and distinguish coating layer thickness using THz-CCS.
- 2) Extract refractive index and absorption from THz data.
- 3) Study curing effects on optical properties.
- 4) Detect defects and corrosion with THz imaging.

Material and Method

Different polymer coating systems were formulated for this study. Steel panels with two surface finishes, smooth and sand-blasted, were used as substrates. Coatings were applied manually or using an automatic film applicator to ensure uniformity, producing films of constant thickness. The coated panels were then dried under ambient laboratory conditions.



Figure 43: Terahertz cross-correlation spectroscopy and imaging system used in this study in reflection mode for coating characterization.

Coating characterization was carried out using a terahertz cross-correlation spectroscopy (THz-CCS) system developed at the Department of Electrical and Photonics Engineering at DTU (see Figure 1). The setup utilized a broadband optical source, fiber-based beam splitting, and photoconductive antennas for both emission and detection. Terahertz radiation was directed onto the coated samples, and the reflected signals were collected and analyzed to assess coating properties. All experiments were performed under standard laboratory conditions.

Result and discussion

A baseline pulse was first recorded with the polymer sample removed from the terahertz (THz) beam path to eliminate material influence. Subsequently, each polymer specimen was measured under identical conditions. Figure 2a shows the reference and sample THz waveforms, where the sample pulse exhibits a delay due to the optical path difference from its finite thickness.

For the determination of optical parameters, data obtained in the time domain from the reference and sample measurements were numerically converted into frequency-domain spectra through the application of a discrete Fourier transform (DFT) in Python, as demonstrated in Figure 2b. Analysis of these complex spectral outputs enabled the estimation of polymer film thickness and refractive index.

The obtained results showed excellent agreement with expectations—the calculated thickness closely matched the actual value and the derived refractive indices were highly consistent, confirming the experiment's accuracy and reliability.

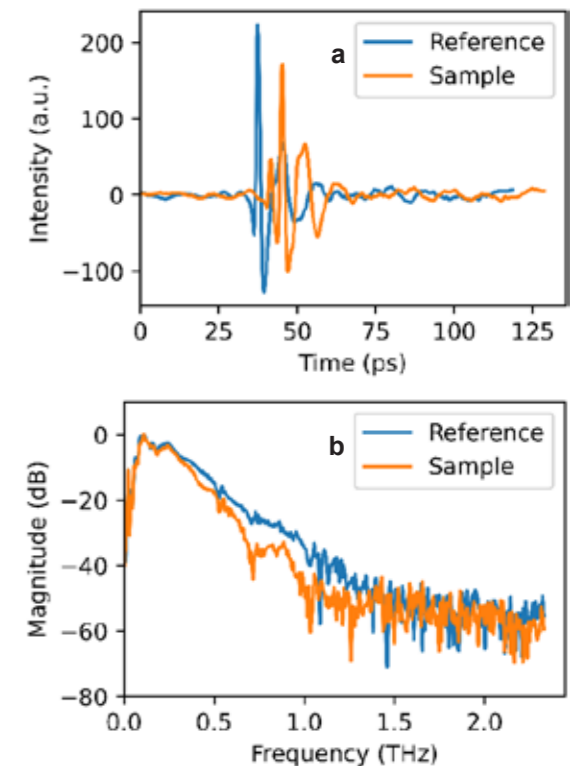


Figure 2: (a) Time-domain waveform of the recorded THz pulse. (b) Corresponding Fourier-transformed spectra derived from these pulses.

Acknowledgment

We are grateful to Hempel Foundation for its financial support to CoaST (The Hempel Foundation Coating Science and Technology Center).

References

1. X. Wu, C. Yang, L. Wu, C. Zhang, G. Cui, Y. Xin, Self-repairing and anti-fouling performance of anticorrosive coating in marine environment, *Polym Test* 124 (2023). <https://doi.org/10.1016/j.polymertesting.2023.108090>.
2. G. Vukelic, G. Vizentin, J. Brnic, M. Brcic, F. Sedmak, Long-term marine environment exposure effect on butt-welded shipbuilding steel, *J Mar Sci Eng* 9 (2021). <https://doi.org/10.3390/jmse9050491>.
3. M. Picot, H. Ballacey, J.P. Guillet, Q. Cassar, P. Mounaix, *Terahertz Paint Thickness Measurements: from Lab to Automotive and Aeronautics Industry*, 2017. <http://www.ndt.net/?id=22188>.

Next generation of deNO_x technology for WtE plants

(May 2023 – April 2026)



Contribution to the UN Sustainable Development Goals

By 2050, the world is expected to generate 3.40 billion tons of waste annually, increasing drastically from today's 2.01 billion tons. Waste-to-energy (WtE) plants are an effective option for recovering energy from waste, helping the world's population to access renewable energy. However, when solid waste is combusted, nitrogen oxide is emitted, becoming an environmental concern. Currently, most deNO_x processes in WtE plants suffer from environmental variability. The aim of this project is to develop a deNO_x technology that is more resilient to these changes.



Claudia

Pastor Morell

clamor@kt.dtu.dk

Supervisors: Peter Glarborg, Hamid Hashemi, Hao Wu.

Abstract

Due to the increasingly stringent emission limits, the control of nitrogen oxide emissions in waste incineration plants has become a significant technical challenge. Selective non-catalytic reduction has proven to be an effective strategy to mitigate NO_x emissions during combustion. However, the effectiveness of this strategy is affected by fluctuations in temperature and gas composition. In light of this, the aim of this project is to develop a more robust NO_x control technology.

Introduction

Selective non-catalytic reduction (SNCR) is an effective strategy to mitigate NO_x emissions during combustion. Its benefits include its simplicity, the absence of a catalyst (and therefore other associated challenges) and the ease of installation in existing plants [1]. The process involves injecting into the flue gas a reducing agent, which reacts with NO_x to form mainly N₂ and H₂O. The reaction occurs within a temperature window roughly between 1123 and 1423 K, depending on the choice of reducing agent, the composition of the flue gas, and the mixing in the furnace. The most common reagents are ammonia, urea, and cyanuric acid.

The flue gas composition is directly influenced by the waste composition and operational conditions of the grate. Jepsen [2] reported CO levels in the first pass of a full scale WtE furnace between 1000–3000 ppm, with peaks up to 7000 ppm. Several studies have shown that CO influences SNCR by shifting the optimum temperature for NO reduction to lower temperatures and narrowing it [3],[4]. Temperature shifts of about 100–350 K have been reported, depending on the CO levels, with consistent trends observed for both ammonia and urea-based processes [3],[4],[5].

Efforts to improve SNCR efficiency have focused on extending the operational window through additives co-injected with ammonia or urea. Studies have shown that substances such as

hydrogen, hydrogen peroxide, hydrocarbons, alcohols, carbon monoxide and other additives can shift the active temperature towards lower temperatures. However, these additives can lead to potential side effects such as increased CO emissions, formation of by-products and, in some cases, reduced optimal NO_x control efficiency [6].

Although many additives have been investigated to extend the SNCR window, little attention has been paid to its combined effect with CO.

Specific Objectives

The main objective of the project is to develop deNO_x technology, which is more robust towards the fluctuating environment in a WtE plant. This objective will be achieved using alternative reducing agents, agent mixtures, or additives that can shift the process temperature window as needed. A key focus will be on evaluating the SNCR process with different operational conditions under fluctuating temperature and CO conditions, using chemical kinetic modelling combined with a Monte Carlo approach.

Modelling and Sampling method

The chemical kinetic model used in this work, including rate coefficients and thermodynamic data, is based on the nitrogen chemistry review by Glarborg et al. [7], with updates from more recent studies, e.g. [8][9]. Simulations were performed

using Cantera software at temperatures between 973–1473 K and a residence time of 100/T [K] s. Temperature and CO fluctuations, were obtained from measured data in the first pass of the furnace reported by Jepsen [2] at the AffaldPlus WtE plant in Næstved, Denmark. Temperature ranged from 1245 to 1392 K, with fluctuations up to 70 K. CO levels fluctuated considerably over time, remaining between 1000 and 3000 ppm for most of the period, and reaching peak values of up to 7000 ppm.

The temperature and CO fluctuations were modelled using a Monte Carlo sampling approach. The data was sampled with Latin Hypercube Sampling (LHS) to ensure full coverage, including the tails. A Monte Carlo based uncertainty analysis was conducted to ensure result convergence.

Progress and Future Work

The effect of temperature and CO fluctuations on SNCR was evaluated for ammonia, urea, and cyanuric acid. (CA). Under the temperature fluctuations, ammonia achieved the highest expected NO_x reduction (53%), followed by urea (49%) and cyanuric acid (14%). For varying CO at constant temperature, the impact depended strongly on temperature. When the temperature was maintained at the mean of the measured temperature fluctuations (1321 K), negative overall conversions were obtained, meaning that NO_x was formed rather than removed. In contrast, lowering the mean temperature by 200–300 K improved NO_x conversion across most CO concentrations, although conversion remained limited at low CO levels.

Figure 1 shows the expected NO_x reduction under both temperature and CO fluctuations. Cyanuric acid provided the highest NO_x removal and was the least affected by the fluctuations, achieving 63 % of NO_x removal at 1171 K, followed by urea and ammonia. Both cyanuric acid and urea also generated notable amounts of N₂O, which, although not currently regulated in the EU, is critical given its impact as a greenhouse gas.

Future work will assess the effectiveness of various additives used in combination with urea and ammonia, focusing on their resistance to temperature fluctuations and CO levels.

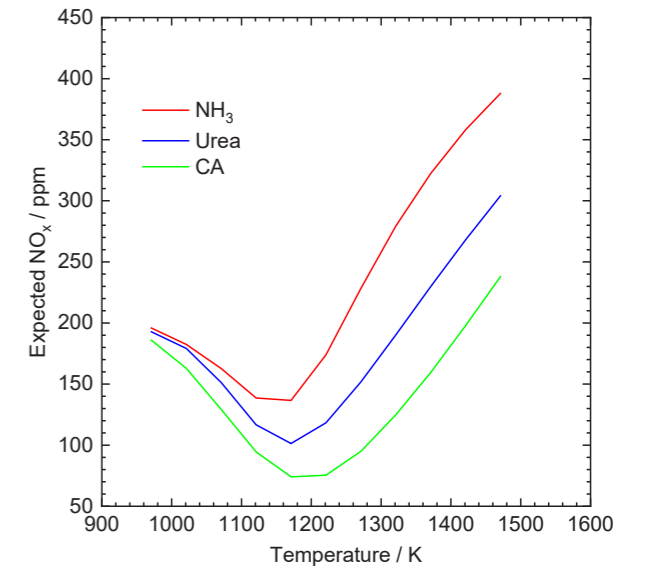


Figure 1. Expected NO_x reduction under fluctuating temperature and CO. Inlet concentrations: NO= 200 ppm, NH₃ = 400 ppm, Urea 200 ppm, CA 133 ppm, H₂O= 25 %, O₂ = 6.67 %. Residence time = 100/T(K), P = 1.05 atm.

Acknowledgements

The project has received financial support from the Sino-Danish Center for Education and Research.

References

1. M. Tayyeb Javed, N. Irfan, B. M. Gibbs, J. Environ. Manage. 83 (3) (2007) 251-289.
2. M. S. Jepsen, PhD Thesis, Technical University of Denmark (2018).
3. R. K. Lyon, J. E. Hardy, Ind. Eng. Chem. Fundam. 25 (1986) 19-24.
4. W. Duo, PhD Thesis, Technical University of Denmark (1990)
5. M.U. Alzueta, R. Bilbao, A. Millera, A.M. Olivia, J.C. Ibáñez, Energy Fuels 12 (1998) 1001-1007.
6. J. Cai, W. Zheng, Q. Wang, Sci. Total Environ. 772 (2021).
7. P. Glarborg, J.A. Miller, B. Ruscic, S.J. Klippenstein, Prog. Energy Combust. Sci. 67 (2018) 31-68.
8. J. Jian, H. Hashemi, H. Wu, P. Glarborg, A.W. Jasper, S.J. Klippenstein, Combust. Flame 261 (2024) 113325.
9. C. P. Morell, C. K. Juhl, A. Chanpirak, H. Hashemi, H. Wu, P. Glarborg, Fuel 385 (2025) 134090.

Molecular-level understanding of the adhesion mechanisms of waterborne epoxy coatings on steel

(January 2024 – January 2027)

9 INDUSTRY, INNOVATION AND INFRASTRUCTURE



Contribution to the UN sustainable Development Goals

This research advances several UN SDGs by upgrading the performance and durability of low-VOC waterborne epoxy coatings. Stronger, longer-lasting films reduce recoating cycles, material consumption, and waste—supporting SDG 9 (Industry, Innovation & Infrastructure) and SDG 12 (responsible consumption & production). Lower solvent emissions and cleaner application improve worker and community safety, contributing to SDG 3 (good health & well-being). By extending asset lifetimes in sectors like construction and automotive and trimming life-cycle emissions, the work also reinforces SDG 13 (climate action) and promotes more sustainable industrial practice.



Ali Moshkriz

mosal@kt.dtu.dk

Supervisors: Søren Kiil, Stefan Urth Nielsen

Abstract

The research investigates the adhesion mechanisms of waterborne epoxy coatings on steel substrates, focusing on understanding and characterizing the covalent and physical bonds at the interface. The study aims to enhance adhesion while preserving the environmental advantages of waterborne coatings. It addresses challenges such as surface preparation and the impact of contaminants like oil and rust on interfacial chemical bonds. Initial findings indicate that optimizing surface interactions and chemical bonds during the curing process can improve adhesion strength, thereby enhancing the longevity and effectiveness of waterborne coatings in industrial applications. Key objectives include characterizing covalent and physical bonds using techniques such as X-ray Photoelectron Spectroscopy (XPS) and Attenuated Total Reflection Infrared Spectroscopy (ATR-IR). The study also explores how contamination impacts these bonds and seeks to elucidate the mechanisms behind insufficient surface tolerance in waterborne epoxy coatings. Additionally, integrating wettability characterization with mechanical testing will provide a comprehensive understanding of the adhesion mechanism.

Introduction

Waterborne epoxies deliver clear environmental and health gains by cutting VOCs, yet they often underperform in adhesion to steel—especially on industrial surfaces carrying oil, rust, or dust [1]. Compared with solvent-borne systems, waterborne formulations are more sensitive to interfacial water, surfactants, and higher surface tension, which can hinder wetting and delay access to reactive sites. Because corrosion protection hinges on a resilient coating/steel interface, closing this adhesion gap is critical. This project targets the molecular origin of adhesion in waterborne epoxy. The formation of hydrogen bonding and covalent Fe–O–C linkages is examined as epoxide groups are reacted with hydroxylated iron-oxide/oxyhydroxide films; –OH groups, generated via dissociative water adsorption, are presented as acid/base sites that drive nucleophilic epoxide ring-opening (Fig.1) [2]. Methodologically, XPS depth profiling (low-energy Ar⁺/GCIB to minimize damage), ATR-FTIR, and wetting measurements are coupled with performance tests (pull-off adhesion and controlled humidity/salt/thermal exposures).

In parallel, the effects of contaminants (oil films, corrosion products, dust) and pretreatments (degreasing, blasting, conversion layers) on interfacial bond populations are quantified. The outcome is a set of structure–performance guidelines that enable waterborne epoxies to match—or even surpass—the adhesion reliability of solvent-borne benchmarks.

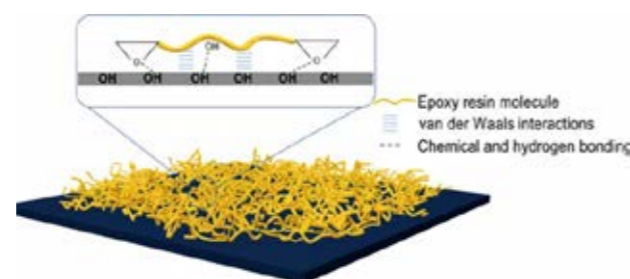


Fig.1. Epoxy resin adheres to steel via van der Waals interactions as well as hydrogen and chemical bonds with surface hydroxyl groups, thereby strengthening adhesion [1].

As shown in Fig.2, covalent bonds are several times stronger than van der Waals forces and

even hydrogen bonds. Therefore, examining the presence or absence of such covalent bonds at the interface is essential for understanding the adhesion mechanism and durability of the coatings.

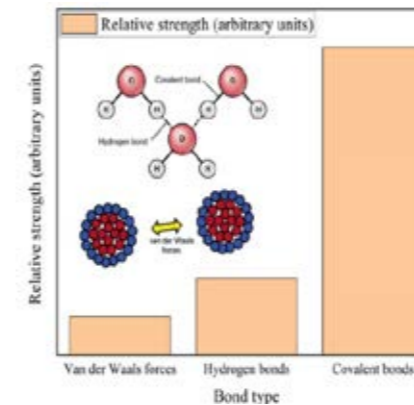


Fig. 2. Relative strength of different interactions. Covalent bonds are several times stronger than van der Waals and hydrogen bonds, highlighting the importance of investigating their presence at the coating–steel interface.

Objectives

This study seeks to uncover how waterborne epoxy coatings adhere to steel and what governs their durability under different aspects:

Early-stage wetting and contact: Characterize how the epoxy spreads and anchors on steel (native oxide/hydroxyl surface), capturing the initial interfacial contact that precedes bonding.

Adhesion build-up and mechanisms: Track how adhesion develops during cure, distinguishing chemical contributions (e.g., interfacial bond formation) from physical ones (mechanical interlocking, secondary interactions).

Durability under exposure: Determine how environmental stressors (moisture, temperature, salts) degrade the interfacial bond over time and quantify the resulting loss in adhesion.

Sensitivity to surface contaminants: Evaluate how oils, corrosion products, and other residues on steel affect adhesion performance and identify conditions or pretreatments that mitigate their impact.

Analytical Techniques

XPS with low-energy Ar⁺ sputter depth profiling maps elemental and chemical-state changes across the buried epoxy–steel interface, pinpointing adhesion-relevant bonds (e.g., Fe–O–C, Fe–O, C–O/C=O). Using gentle etching (or GCIB) and calibrated sputter rates minimizes reduction, mixing, and preferential sputtering. Polishing with sandpaper combined with XPS

depth profiling reveals and allows analysis of the buried epoxy–steel interface (Fig. 3).

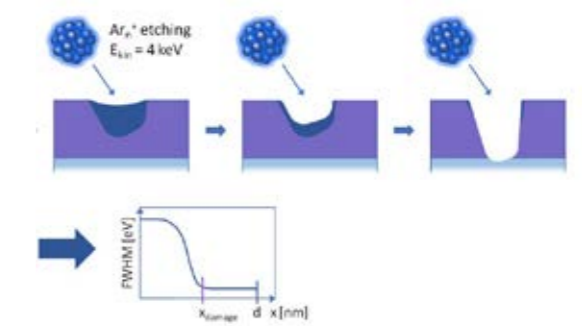


Fig. 3. Segment of an XPS depth profile [4].

Progress and future work

Fourier Transform Infrared Spectroscopy (FTIR)—preferably ATR-FTIR on a polished cross-section or surface-proximal region—can probe the functional groups near the buried epoxy–steel interface and track cure/conversion (e.g., epoxide ring band $\approx 915\text{ cm}^{-1}$, aromatic reference $\approx 1508\text{ cm}^{-1}$, β -OH stretch $\approx 3200\text{--}3600\text{ cm}^{-1}$). By resolving these interfacial signatures, FTIR clarifies the molecular interactions that govern adhesion. Crucially, understanding the adhesion mechanism in this way also guides improvements—informing resin/curing-agent ratios, additives, and steel pretreatments to enhance interfacial bonding and overall adhesion performance.

Acknowledgment

Financial support from the Hempel Foundation to CoaST (The Hempel Foundation Coating Science and Technology Center).

References

1. Kotb, Yosra, et al. "What makes epoxy-phenolic coatings on metals ubiquitous: Surface energetics and molecular adhesion characteristics." *Journal of Colloid and Interface Science* 608 (2022): 634-643.
2. Posner, R., M. Santa, and G. Grundmeier. "Wet-and corrosive de-adhesion processes of water-borne epoxy film coated steel: I. Interface potentials and characteristics of ion transport processes." *Journal of the Electrochemical Society* 158.3 (2010): C29.
3. Z. Xu, Y. Zhang, Y. Wu, X. Lu, Spectroscopically Detecting Molecular-Level Bonding Formation between an Epoxy Formula and Steel, *Langmuir* 38 (2022) 13261–13271.
4. Quantifying XPS Depth Profiling Damage in Organic Conjugated Polymers – Y. J. Hofstetter, Y. Vaynzof, Univ. Heidelberg.

Cyclic poly(dimethylsiloxane) networks with reactive double bonds enabling post-curing functionalization

(January 2023 – January 2026)

3 GOOD HEALTH AND WELL-BEING



Contribution to the UN Sustainable Development Goals

In recent years, silicone elastomers have received considerable interest for their use in stretchable electronics, medical devices, and soft robotics. Silicone elastomers consisting of a network of cyclic polymers are expected to exhibit improved mechanical properties compared to their linear counterparts. Moreover, the enhanced dielectric permittivity of the presented networks can improve actuation efficiency, enabling the development of softer and more responsive materials for devices such as artificial muscles. Additionally, integrating these silicone elastomers into textiles can revolutionize the production of soft wearables and lightweight exoskeletons, helping users with reduced mobility regain independence and improve their overall quality of life.



Cristina

Nedelcu

crined@kt.dtu.dk

Supervisors: Anne Ladegaard Skov; Frederikke Bahrt Madsen

Abstract

Silicone elastomers have received vast attention due to their potential use in stretchable electronics, implants, and medical devices. There has been growing interest in developing elastomers with softness and elasticity resembling those of human soft tissue, particularly for use in soft robotics. In this context, the present study introduces polydimethylsiloxane (PDMS) elastomers with a network of cyclic polymers with preserved alkene moieties. This unique network architecture of elastomers gives them properties distinct from those of linear polymers. While they allow post-cure modifications, their mechanical flexibility and durability are what make them especially suitable for mechanical devices and soft robotics applications.

Introduction

Silicone elastomers are increasingly employed in emerging technologies such as stretchable electronics, where their flexibility and durability enable the development of adaptable electronic components that can conform to complex surfaces and dynamic movements. Recently, extremely soft PDMS-based elastomers with exceptional elongation and strain recovery have been reported.^[1,2] These networks are characterized by a unique architecture made of interconnected cyclic polymers. In addition, silicone elastomer properties can be further enhanced through post-curing functionalization, enabling direct integration of functional groups into the final material. This is particularly advantageous for applications requiring surface-specific modification, including sensing, adhesion, and biomolecular conjugation.^[3,4]

In this study, we investigate the feasibility of functionalizing a network of cyclic polymers to improve their dielectric properties for advanced applications. First, telechelic dihydride-PDMS was converted to alkene-terminated PDMS via hydrosilylation. Secondly, the prepolymer was cured with a commercial dihydride-terminated

PDMS in the presence of a platinum catalyst, without the addition of a cross-linker. Subsequently, the alkene moieties were reacted with thiols bearing polar moieties, such as chlorine atoms and amino groups, via a thiol-ene UV-initiated reaction.

Specific Objectives

- To develop a network of interconnected cyclic polymers containing alkene moieties.
- To functionalize the networks after the network curing.
- To study the influence on the dielectric permittivity.



Figure 1: Illustration of an interconnected cyclic polymer network.

Experimental

The pre-polymer (DMS-DT) was synthesized via hydrosilylation between telechelic hydride-terminated PDMS (DMS-H11, $M_n=1100 \text{ g mol}^{-1}$) and 1,5,9-decatriene at room temperature. After the reaction, the platinum catalyst was removed, and the product was dried using a rotavapor. For elastomer synthesis, DMS-DT was cured with DMS-H11 ($M_n=1100 \text{ g mol}^{-1}$) and DMS-H21 ($M_n=5500 \text{ g/mol}$) in the presence of a platinum catalyst. Post-curing functionalization involved a thiol-ene reaction with 3-chloro-1-propanethiol, 2-chlorothiophenol, and 2-aminoethanethiol. Elastomers were swollen in tetrahydrofuran (THF) with 2,2-dimethoxy-2-phenylacetophenone (DMPA) and thiols, then exposed to UV-Vis light.

Results and discussion

The elastomers were formed by hydrosilylation of the DMS-DT prepolymer with commercial DMS-H11 in the presence of a platinum catalyst. The possible reaction pathway involves the intramolecular reaction of linear polymers, resulting in interconnected cyclic structures within the network.

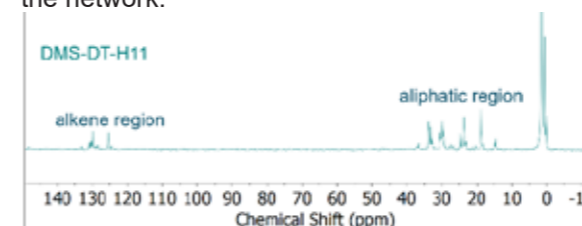


Figure 2: Solid state ^{13}C -NMR spectra of the resulting elastomer DMS-DT-H11.

Solid-state ^{13}C -NMR spectroscopy confirmed the presence of resonances associated with the internal carbon-carbon double bonds (Fig. 2). The available internal carbon-carbon double bonds were further functionalized with 3-chloro-1-propanethiol, 2-chlorothiophenol, and 2-aminoethanethiol to increase the dielectric permittivity of the prepared elastomers. The permittivity results are shown in Fig. 3. The functionalization with 3-chloro-1-propanethiol, 2-chlorothiophenol, and 2-aminoethanethiol increased the relative permittivity from $\epsilon_r = 2.8$

(reference DMS-DT-H11) to $\epsilon_r = 8.7$, $\epsilon_r = 6.2$, and $\epsilon_r = 4$, respectively.

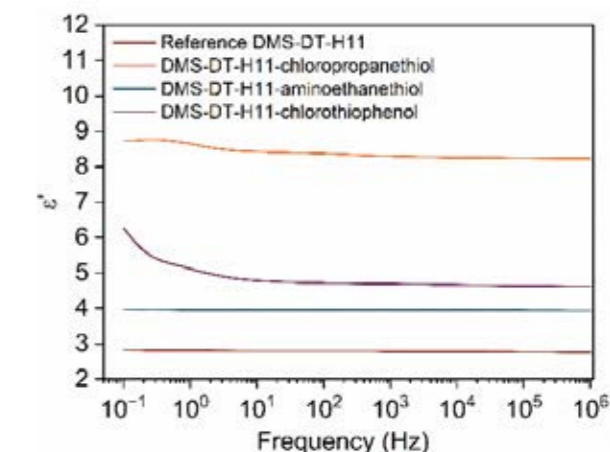


Figure 3: Relative dielectric permittivity of the functionalized elastomers.

Conclusions

In this work, a network of interconnected cyclic polymers with preserved alkene moieties was prepared from modified commercial PDMS. The internal carbon-carbon double bonds enabled the postcure functionalization of the cyclic networks via thiol-ene addition, thereby improving the dielectric permittivity.

Acknowledgments

The project is supported by the European Union's Horizon 2021 SOFTWAREAR project under the Marie Skłodowska-Curie grant agreement.

References

1. J. Goff, S. Sulaiman, B. Arkles, J. P. Lewicki, J. Goff, S. Sulaiman, B. Arkles, J. P. Lewicki, *Advanced Materials* **2016**, *28*, 2393.
2. P. Hu, J. Madsen, Q. Huang, A. L. Skov, *ACS Macro Lett* **2020**, *9*, 1458.
3. Y. Xiao, Y. Song, X. Cao, Z. Chen, X. Lu, J. Mao, Q. Q. Rao, S. Fu, T. Li, Y. Luo, *Chemical Engineering Journal* **2022**, *449*, 137734.
4. H. Hu, S. Li, C. Ying, R. Zhang, Y. Li, W. Qian, L. Zheng, X. Fu, Q. Liu, S. Hu, C. P. Wong, *Appl Surf Sci* **2020**, *503*, 144126.

Physiological bioprocess control

(September 2023 – September 2026)



Contribution to the UN Sustainable Development Goals

Applying advanced control strategies to the cultivation of microbial cells enables a more efficient and sustainable production of a wide range of products. A focus on the physiology of the cells promises more or higher quality products with less raw material input. Gaining more control over the process can furthermore reduce the risk of failed batches and the resulting loss of material and energy input. Therefore, the methods and results of this work contribute towards the responsible production of cultivation products.



Philipp

Pably

phpa@kt.dtu.dk

Supervisors:

Julian Kager,
Jakob K. Huusom

Abstract

Monitoring and control of microbial bioprocesses is essential for its industrial applications. Often simple algorithms and open-loop strategies are applied, which can result in suboptimal cultivation conditions. Using process models with a focus on physiological descriptors of the cell conditions promises a better understanding of the current state and opens the door for advanced predictive feedback control. The project investigates the development of such controllers and compares them to traditional process design and control strategies. The commonly used bacteria *Escherichia coli*, modified to produce Green Fluorescent Protein (GFP), is used as a model organism to show potential improvements for two case studies. First a model predictive controller is set up for the dissolved oxygen level of a bioreactor. Secondly, the productivity for a process using separate substrate and inducer feeds shall be improved using physiological bioprocess models.

Introduction

Optimal bioprocess control is a key to enabling competitive production of many biological products from cell cultivation. The physiological conditions inside the bioreactor greatly influence the performance of these processes, since they affect the health of the microorganisms directly [1].

Process modelling can help to improve the understanding, planning and control of such bioprocesses. By including physiologically focused descriptors such as the specific substrate uptake rate or cell viability, the highly complex and non-linear influences on microbial performance can be captured better. The resulting models present a potent basis for advanced control algorithms, which then not only monitor the cell broths' condition over time, but are also able to predict its future development and stir it towards a defined optimum [2,3].

This work tries to showcase the possible improvements for process performance and controllability through physiological bioprocess models for a bacterial cultivation. Two case studies are presented, applying model-based control for the dissolved oxygen (DO) level of a

bioreactor and for the productivity of a recombinant protein.

Methods

The model organisms used are *Escherichia coli* strains which have green fluorescent protein encoded into their expression system. The production can be triggered by adding lactose or a structural analog chemical to the broth. The strain used for the 2-feed process additionally is capable of fully digesting lactose, making the induction mechanism reversible. The reactor setup used for parameterization, verification and testing is shown in Fig. 1.



Fig. 44: Experimental setup for 1–5L cultivations

A combination of online and offline signals is used to analyze the broth of the bioreactor, combining dry cell weight, optical density, HPLC, enzymatic assay, fluorescence and online mass spectrometer measurements.

The data is then processed and used for modelling and control using code generated in python. The algorithms are tested *in-silico* through simulation studies and experimentally using a Rest-API connection to the local SCADA system of the bioreactor.

Results and discussion

The capabilities of physiological bioprocess models for process monitoring and control are discussed for two implementations.

Model predictive control (MPC) for DO level

A model predictive controller for the DO level was developed and tested against a more traditional sliding-mode PID control setup. The parameterized controllers are compared in a simulation study in Pably et. al [4], showing the advantages of the MPCs predictive nature. The benefits throughout a designed process are showcased in Figure 2. Less time underneath the set threshold due to proactive control action is achieved with overall similar inputs. Future publication of the authors discusses the verification experiments and implications for physical bioreactor systems (manuscript under preparation).

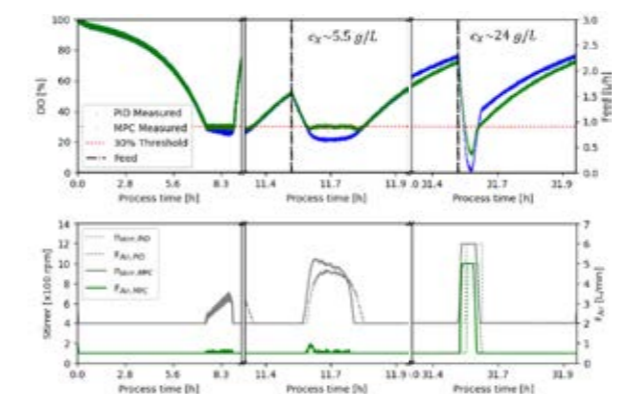


Fig. 45: *In-silico* comparison of MPC vs PID control for the DO level of a bioreactor [4]

Productivity model for 2-feed system

A productivity model is identified and parameterized using data from a miniature scale high-throughput facility with working volume of ~10mL and compared to an analogue procedure using a 2L reactor setup. The difference in the data obtained led to two alternative model structures and parameter values, suggesting different optimal process strategies (data not shown). In the next steps these 2 optimal process strategies will be carried out in a 2L reactor setup

and used to discuss scale-transfer effects for bioprocess modelling. A refined model will then be used for advanced control strategies to optimize the productivity of the used process.

Conclusion

Model predictive control shows promising results for improved process control over conventional reactive controllers, shown by a simulation study for the DO level of a bioreactor. The experimental implementation shows challenges that need consideration, also for implementations of other model-based control algorithms for bioprocesses.

The second case study showed that modelling, as a first step towards improved process control, creates better process understanding but is influenced by the data used for creating. The reactor scale and process strategy used needs to be considered when transferring results to different equipment.

Future work will further investigate the application of physiological bioprocess models for advanced bioreactor control and improved performance.

Acknowledgements

The authors acknowledge financial support through the Novo Nordisk Foundation Start Package grant for Bioprocess Control and Digitalization (NNF220C0081250).

References

1. P. Wechselberger, P. Sagmeister, H. Engelking, T. Schmidt, J. Wenger, C. Herwig, *Bioprocess Biosyst Eng* 35 (2012), 1637–1649.
2. J. Kager, A. Tuveri, S. Ulonska, P. Kroll, C. Herwig, *Process Biochemistry* 90 (2020), 1–11.
3. R. Babuška, M.R. Damen, C. Hellinga, H. Maarleveld, *Journal of Intelligent Manufacturing* 14 (2003), 255–265.
4. P. Pably, J.K. Huusom., J. Kager, *Systems and Control Transactions* 4 (2025), 2486–2491.

Deciphering the anaerobic microbiome for construction of robust microbial consortia for mixed culture fermentations

(May 2024 – April 2027)



Contribution to the UN Sustainable Development Goals

Advancing the development of biofuels and bioproducts through anaerobic fermentation, this project focuses on creating comprehensive metabolic models of mixed-microbial communities to optimize the production of medium-chain fatty acids. These fatty acids can find many applications substituting fossil-based fuels and products, alternative to fossil fuels and reducing greenhouse gas emissions. The use of microbial consortia enhances the efficiency and scalability of the fermentation processes. This approach supports the transition to renewable energy sources, reducing carbon footprints and fostering a sustainable energy future.



**Konstantinos
Papasakellariou**

konpa@kt.dtu.dk

Supervisor: Irini
Angelidaki

Abstract

This project aims to develop a comprehensive mathematical model of the metabolic reactions occurring within mixed-species cultures of anaerobic microorganisms, specifically focusing on taxa involved in chain elongation. This research will involve the development of a laboratory protocol for the chain elongation of volatile fatty acids, investigation of microbial consortia interactions, and the generation of community genome-scale metabolic models. The objective is to establish synthetic mixed microbial cultures capable of efficiently producing medium-chain fatty acids. In parallel, the project aims to identify novel microbial species capable of producing medium-chain fatty acids through microbial chain elongation. This will be achieved by employing advanced bioinformatics approaches to compare genes associated with metabolic pathways relevant to chain elongation. This work will advance the field of microbial community dynamics and contribute to the development of sustainable biofuel production processes.

Introduction

Anaerobic fermentation represents a pivotal sector in biotechnology, contributing significantly to the green transition. The deployment of anaerobic microorganisms is particularly advantageous due to their capacity to produce secondary metabolites in substantial quantities, which are extensively utilized in industrial applications. Prominent examples include the biosynthesis of lactic acid [1] and volatile fatty acids [2].

The application of single-species anaerobic cultures for the bioremediation of heterogeneous and toxic compounds is impractical, as such conditions inhibit microbial proliferation. An effective alternative is the utilization of mixed-species cultures, comprising microbial species that engage in synergistic interactions. These mixed cultures exhibit superior adaptability to environments characterized by extreme thermodynamic conditions, such as fluctuations in

pH and temperature, compared to single-species cultures [3].

The selection of appropriate microbial species capable of establishing a robust microbial community in environments with heterogeneous and toxic organic wastes is crucial. This can be assisted by developing models that describe the metabolic reactions occurring within microbial communities of different species. An efficient approach to modelling microbial metabolism is the creation of genome-scale metabolic models (GSMMs). GSMMs are *in silico* representations of the metabolic reactions within a cell, including the enzymes that catalyze these reactions [4]. The design of GSMMs relies on information from published metabolic maps found in databases. With the increasing number of publications related to high-throughput sequencing, GSMMs now integrate data from various -omics sources, enhancing their predictive accuracy [5].

GSMMs are often combined with Flux Balance Analysis, a mathematical method that calculates

the flux of metabolites within a metabolic network [6]. This combination allows for the estimation of microbial growth rates and the production rates of specific metabolites.

In conclusion, the knowledge generated during the project will create the know-how to build faster and more efficient synergistic mix species microbial communities, capable of successfully transforming different raw materials into high-value chemicals.

Specific Objectives

The aim of this project is to develop a comprehensive mathematical model of the metabolic reactions occurring in mixed-species cultures for improving capacity and specificity of chain elongation process. The species to be modeled will be selected based on their collaborative mutualistic properties in chain elongation conversion processes. Metabolic models will be constructed to provide a complete understanding of the microbial community. These single-species models will be used to establish mixed-species microbial communities in the laboratory. The appropriate culture conditions will be explored to ensure the successful growth of the resulting microbial community.

The specific objectives of the project are:

1. Development of a laboratory protocol to perform chain elongation of volatile fatty acids using microbial consortia
2. Investigate the interactions of the microbial consortia
3. Generate community Genome Scale Metabolic Models
4. Establish synthetic mixed microbial cultures

Materials and Methods

Lab-scale batch experiments will be conducted under anaerobic conditions. Enrichment cultures will be established with various carbon sources to perform chain elongation. The production metabolites will be monitored regularly. Upon observing a significant increase in the production

of medium-chain fatty acids, comprehensive taxonomical and functional analyses will be performed. These analyses will aim to elucidate the structural composition and metabolic activities of the microbial communities, utilizing high-throughput sequencing. To facilitate the discovery of novel microbial species involved in chain elongation, metagenomic datasets will be analyzed using state-of-the-art bioinformatics tools. Comparative genomic analyses will be conducted to identify genes implicated in chain elongation pathways, enabling the characterization of previously uncharacterized microbial species. By integrating this data, *in silico* genome-scale metabolic models will be developed to describe the microbial community responsible for the chain elongation of short-chain fatty acids to medium-chain fatty acids. The species constituting these communities will be isolated using molecular tools, cultured separately, and subsequently utilized to create synthetic mixed microbial cultures that will produce the desired products.

Acknowledgement

This work was financially supported by European Research Council Advanced Grant Project "The ANAEROBic treasure trunk" (Grant agreement No. 101098064)

References

1. J.L. Rombouts, E.M.M. Kranendonk, A. Regueira, D.G. Weissbrodt, R. Kleerebezem, M.C.M. van Loosdrecht. *Biotechnology and Bioengineering* 117 (2020) 1281 – 1293.
2. M. Zhou, B. Yan, J.W.C. Wong, Y. Zhang. *Bioresource Technology* 248 (2018) 68-78
3. R.D. Hoelzle, B. Viridis, D.J. Batstone. *Biotechnology and Bioengineering* 111 (2014) 2139-2154
4. Thiele, B.Ø. Palsson. *Nature Protocol* 5 (2010) 93-121
5. Passi, J.D. Tibochoa-Bonilla, M. Kumar, D. Tec-Campos, K. Zengler, C. Zuniga. *Metabolites* 12 (2022) 14
6. J.D. Orth, I. Thiele, B. Ø. Palsson. *Nature Biotechnology* 28 (2011) 245-248

Modelling and simulation of electrochemical CO₂ and H₂O reduction

(April 2025 – April 2028)



Contribution to the UN Sustainable Development Goals

CO₂ electrolysis utilized in tandem with renewable energy reduces anthropogenic CO₂ emissions, by recycling CO₂ into various precursors for the chemical industry [1]. These include CO, ethylene and ethanol, which find use in fuel and plastic production [1]. Implementing CO₂ electrolysis in these processes on a large scale will disrupt conventional fossil-based production and lower emissions [1]. Thus, the technology contributes towards the 9th sustainable development goal, by providing solutions for retrofitting the chemical industry with clean technologies.



Magnus Nørager Pedersen

manope@kt.dtu.dk

Supervisors:

Prof. Anker Degn Jensen
Prof. Brian Seger
Assoc. Prof. Jakob Munkholt Christensen

Abstract

CO₂ electrolysis provides the means for utilizing renewable energy in recycling CO₂ into a variety of industrially relevant products, disrupting conventional fossil-based industries [1]. The proposed CO₂ electrolyzer designs currently face several challenges limiting their operational stability [2]. This PhD project studies these reactors through multiphysics modelling to elucidate how species transport, cathode material and electrolyzer design influence system performance. In addition to system understanding, the models allow for optimization aimed at accelerating technology implementation.

Introduction

Anthropogenic carbon dioxide emissions are the largest driver for climate change [3], and thus industrial and academical focus has increasingly been on reducing these emissions from various high emission sectors [1]. To achieve this, much focus has been put on carbon capture and utilization technologies, as they provide a means of recycling CO₂ into various carbon-based chemicals [1]. One such method of carbon utilization is CO₂ electrolysis (CO₂E), capable of converting CO₂ and renewable energy into a variety of industrially relevant compounds [1]. The products depend on the material utilized for the cathode electrode in the electrochemical cell [4]. Silver is commonly known to primarily reduce CO₂ to CO, while copper produces a variety of multi-carbon products including ethylene and ethanol [4]. These products are applicable in various chemical industries, including the fuel and plastic sectors, thus allowing for emission reduction by disrupting conventional fossil-based industries [1].

The potential of CO₂ electrolysis to produce industrially relevant compounds in conjunction with emission reductions motivates the development of industrially mature CO₂E systems.

The low solubility of CO₂ in water defines the design of the electrolyzer, as porous gas diffusion

electrodes (GDE) are employed for CO₂ to be transported to the electrode in gas-phase [5]. This increases reactant transport and CO₂ reduction partial current densities [5]. GDEs are often utilized in membrane electrode assembly (MEA) structures, where the electrochemical cell consist of the cathode and anode contacting each side of an anion exchange membrane, stacked between two flow plates providing the reactants and electrolyte [6,7]. These configurations allow for the system to reach industrially relevant current densities, and are therefore preferred in current literature [6,7].

Despite the positives of the MEA design, issues such as CO₂ crossover, salt formation, flooding and the competing hydrogen evolution limit the stability and scale-up potential of the system [2,6]. The aim of this PhD project is to assist the development of these CO₂E MEA systems through the use of multiphysics models, to elucidate how species transport, cathode material and electrolyzer design impact the system. The models will then increase system understanding,

guide optimization and assist in scale-up efforts for accelerating technology implementation.

Modelling methodology

Developing a multiphysics model of a CO₂E MEA system follows a similar methodology to any other reactor model. Specifically, conservation- and transport equations are stated for charge, mass, momentum and heat, which then are coupled to some source terms describing reaction rates [8]. The boundary conditions are then stated, and the model is solved with a numerical solver.

Unique to the electrochemical reactor models are the need for charge conservation- and transport (Ohm's law) equations [8]. Additionally, charged aqueous species experience migration induced by the potential gradient across the cell [9]. The Nernst-Planck equation then describes the total transport [8,9]:

$$\mathbf{J}_j = -D_j \nabla C_j - \frac{z_j F}{RT} D_j C_j \nabla \phi + C_j \mathbf{v}$$

Different from ordinary chemical reactions, rates of electrochemical reactions are described by a partial current density, determined by the Tafel equation [8]:

$$i_k = -i_{o,k} \left(\frac{c_j}{c_j^{ref}} \right)^{\gamma_k} \exp \left(-\frac{\alpha_{c,k} F}{RT} \eta_k \right)$$

Electrochemical reactions are charge transfer reactions, and thus the partial current density of a reaction relates to the rate of reaction, by the amount of charge transferred per reaction [8].

Project objectives

The project presented here is still in its early phases, and therefore, no results have been produced yet. However, the first models are being set up, following the previously stated methodology. With this, the project aims to cover a variety of different topics, in particular the ones listed in the following:

- Perform a comprehensive literature study, outlining the current state of the field and highlighting gaps in literature that can be studied throughout this project.
- Model how various spatial and geometric changes to the reactor system effects species transport, and study how this effects flooding, salt formation and CO₂ crossover.
- State models for different cathode materials, such as silver and copper, to study the differences in the systems.
- Work in collaboration with experimental groups to perform model validation and

use the models to guide the design of new experiments.

These projects are loosely stated, as the field moves fast, and new ideas and discoveries can change the focus of each of the objectives.

Acknowledgements

This project is funded under the Pioneer Center for Accelerating P2X Materials Discovery (CAPeX), DNRf grant number P3.

References

1. B. Belsa, L. Xia, F.P. García De Arquer, ACS Energy Lett. 9 (2024) 4293–4305.
2. S. Subramanian, K. Yang, M. Li, M. Sassenburg, M. Abdinejad, E. Irtem, J. Middelkoop, T. Burdyny, ACS Energy Lett. 8 (2023) 222–229.
3. World Meteorological Organization (WMO), State of the Global Climate 2024, World Meteorological Organization, Geneva, Switzerland, 2025.
4. S. Nitopi, E. Bertheussen, S.B. Scott, X. Liu, A.K. Engstfeld, S. Horch, B. Seger, I.E.L. Stephens, K. Chan, C. Hahn, J.K. Nørskov, T.F. Jaramillo, I. Chorkendorff, Chem. Rev. 119 (2019) 7610–7672.
5. D. Higgins, C. Hahn, C. Xiang, T.F. Jaramillo, A.Z. Weber, ACS Energy Lett. 4 (2019) 317–324.
6. M. Sassenburg, M. Kelly, S. Subramanian, W.A. Smith, T. Burdyny, ACS Energy Lett. 8 (2023) 321–331.
7. D.U. Lee, B. Joensen, J. Jenny, V.M. Ehlinger, S.-W. Lee, K. Abiose, Y. Xu, A. Sarkar, T.Y. Lin, C. Hahn, T.F. Jaramillo, ACS Sustainable Chem. Eng. 11 (2023) 16661–16668.
8. L.-C. Weng, A.T. Bell, A.Z. Weber, Energy Environ. Sci. 12 (2019) 1950–1968.
9. A.J. Bard, L.R. Faulkner, H.S. White, Electrochemical Methods: Fundamentals and Applications, Third edition, Wiley, Hoboken, NJ, USA Chichester, West Sussex, UK, 2022.

In-situ online corrosion and solvent degradation monitoring at Pilot Scale

(December 2024 – November 2027)



Contribution to the UN Sustainable Development Goals

Climate change is the biggest threat to development, with widespread impacts that hit the poorest and most vulnerable hardest. CO₂ is the main greenhouse gas driving climate change. The best way to cut emissions is to avoid producing CO₂, but this is not always possible. That is why CO₂ capture is an important complementary solution to reduce emissions into our atmosphere. This project works toward making CO₂ capture cheaper, more sustainable, and more efficient, with the goal of turning it into a mature technology to mitigate climate change.



Ward Peeters

warpe@dtu.dk

Supervisors: Philip Loldrup Fosbøl, Alexander Shapiro, Randi Neerup

Abstract

Rising CO₂ levels demand efficient and sustainable capture technologies. The CESAR1 solvent blend offers lower energy use and improved stability compared to MEA, but solvent degradation remains a challenge. This work develops a FTIR based calibration method for online monitoring of CESAR1, enabling real-time solvent health tracking during pilot campaigns. Continuous monitoring will provide key insights into degradation, efficiency, and process sustainability within the European MISSION-CCS project.

Introduction

The concentration of CO₂ in the atmosphere continues to rise, currently at 422 ppm, with projections suggesting the concentration could exceed 500 ppm by 2050 if no significant changes are made to current practices or policies [1]. Amine-based carbon capture remains one of the most developed and widely researched approaches in carbon capture.

At the end of the 20th century, Statoil implemented one of the first full-scale post-combustion CO₂ capture systems, using monoethanolamine (MEA) as the solvent of choice. As amine-based CO₂ capture technology evolved throughout the 21st century, it faced increasing criticism due to the high regeneration energy requirements and overall degradation rates of MEA. Therefore, different solvent possibilities were investigated to improve energy consumption and reduce degradation rates.

The CESAR project was initiated with the aim of developing a low-cost post-combustion CO₂ capture technology. Its primary objectives included reducing energy requirements, capital expenditures, and overall energy efficiency losses, as well as exploring novel integration concepts. The CESAR1 solvent is a blend of 3 M 2-amino-2-methyl-1-propanol (AMP) and 1.5 M

piperazine (PZ). The CESAR1 solvent has been used by many research campaigns so far and its interest has risen over the past years. CESAR1, demonstrated the best performance when used with Lean Vapor Compression (LVC) and intercooling (IC) configuration, achieving an energy consumption of 2.6 GJ/ton CO₂ [2]. Compared to the widely known 4 MJ/kg CO₂ energy requirement for MEA, CESAR1 appears to outperform this benchmark. Besides reducing energy consumption, CESAR1 also proved to be more stable than MEA, lowering solvent degradation rates [3].

Solvent degradation has gained increasingly more attention in recent years due to its importance in the operation of a carbon capture plant. Solvent degradation occurs when solvent degrades to a point where it cannot be effectively regenerated in the stripper column.

Solvent degradation diminishes overall capture capacity, increases energy consumption, can damage equipment, induces corrosion, and is responsible for a big amount of solvent loss making it highly undesirable in any scenario.

Objectives

The objective is to develop a method for online and continuous monitoring of the CESAR1 solvent by using FTIR.

Results & Discussion

Calibration sets were first prepared in the laboratory. These will include:

- Lean and loaded solvent samples without degradation products
- Lean and loaded solvent samples from previous campaigns containing degradation products.

The mid-infrared spectra of all available and prepared samples will be collected using an FTIR spectrometer with an ATR attachment. Since the concentrations of the components in these samples are known, the measured spectra can be linked to the solvent composition using advanced data analysis methods. This analysis will be carried out in collaboration with the SLB Cambridge Research Centre. The resulting calibration method will then be used to validate both laboratory and pilot-scale data.

In figure 3 an ATR probe can be seen. In collaboration with ART Photonics, an ATR probe will be used for inline measurements at a CO₂ capture plant (Aalborg Portland, Denmark). By applying the laboratory-developed calibration model, solvent composition can be continuously monitored during plant operation.



Figure 1: ATR Probe ART Photonics

The ultimate goal is to enable continuous measurement of CESAR1 solvent composition over the course of a CO₂ capture campaign. This will provide valuable insights into solvent health and its evolution during long-term operation.

Conclusion

A laboratory calibration strategy has been established using FTIR spectroscopy and advanced data analysis, ensuring that solvent components can be reliably quantified. Integration with an ATR probe will enable translation of this methodology to pilot plant conditions, where real-time monitoring of solvent composition will be possible.

The ability to continuously track solvent health over extended campaigns will provide valuable information about solvent degradation, operational efficiency, and overall process sustainability. This work therefore represents a key milestone towards finalising inline monitoring devices and contributes directly to the MISSION-CCS objective of mitigating solvent degradation across the CCS chain.

Acknowledgments

The author would like to acknowledge funding provided via the European Commission's Horizon Europe research and innovation program under the Marie Skłodowska-Curie Grant Agreement ID: 101118369, Material Science Innovation for Accelerated, Sustainable and Safe Implementation of Carbon Capture and Storage (MISSION-CCS) and the support from the Technical University of Denmark (DTU).

References

1. "Unmitigated monthly global atmospheric CO₂ rise until 2050." Accessed: Nov. 27, 2024. [Online]. Available: https://www.researchgate.net/publication/356264803_Unmitigated_monthly_global_atmospheric_CO2_rise_until_2050
2. "Final Report Summary - CESAR (CO₂ Enhanced Separation and Recovery) | FP7," CORDIS | European Commission. Accessed: Dec. 18, 2024. [Online]. Available: <https://cordis.europa.eu/project/id/213569/reporting>
3. D. Morlando *et al.*, "Available data and knowledge gaps of the CESAR1 solvent system," *Carbon Capture Sci. Technol.*, vol. 13, p. 100290, Dec. 2024, doi: 10.1016/j.ccst.2024.100290.

Integrated model for up- and downstream bioprocess intensification

(September 2024 – August 2027)

12 RESPONSIBLE CONSUMPTION AND PRODUCTION



Contribution to the UN Sustainable Development Goals

Biobased production is increasingly recognized as a more sustainable alternative to traditional chemical manufacturing. While several preliminary studies have demonstrated the potential of bioprocesses, the path from proof of concept to a fully intensified and economically competitive process remains long and often complex. By developing integrated models that link upstream and downstream processing in fermentation-based manufacturing, the overall process can be designed and optimized more efficiently. This reduces waste, improves yields, and minimizes the use of raw materials and energy.



Deborah

Pfaff

debpf@dtu.dk

Supervisors: Julian Kager and John Woodley

Abstract

This project investigates the interlinking between upstream and downstream processing in fermentation-based manufacturing, with the aim of enhancing overall process efficiency and product quality. To approach this task, mechanistic and statistical models are developed for individual unit operations, capturing the physical principles and kinetic behavior of each step. These models are then connected to an integrated process model, which enables a holistic optimization strategy. Accounting for the complex and nonlinear dependencies between unit operations, the integrated model supports informed decision-making throughout the production process, from microbial production to product purification.

Introduction

As a case study, the microbial production of L-tyrosine is investigated. L-tyrosine is an aromatic amino acid and widely used in pharmaceutical, food, and chemical industries. This study focuses on a L-tyrosine producing *Escherichia coli* strain, which already went through strain engineering (pts-knockout and overexpression of key genes *aroG*, *tyrA*, and *aroB*) to increase the product titer to several g/L [1]. Fed-batch experiments were conducted in a 2 L stirred tank reactor at pH 6.5 and 37 °C. During the microbial production, L-tyrosine begins to form crystals due to its low solubility in the fermentation solution conditions. As the fermentation progresses, the solute concentration of L-tyrosine increases until the solubility limit is reached. Beyond this point, the solute concentration remains approximately constant while excess L-tyrosine precipitates [2]. This in situ crystallization offers benefits such as partial product purification but also presents challenges. The needle-shaped morphology of L-tyrosine impairs filtration due to poor flow properties, and its density, which is close to that of cells, complicates the separation by centrifugation [3]. Although the fermentation process has been described in the literature [4-5], the dynamics of

tyrosine crystallization during fermentation have not yet been studied.

Crystallization kinetics of L-tyrosine

Crystallization is a separation and purification process that is particularly beneficial for processes involving solid products. In the pharmaceutical industry, crystallization is used as an intermediate concentration or final polishing step in the manufacturing process of antibiotics, amino acids, and vitamins, among other products [6]. To ensure product quality, the purity, morphology, and size distribution of the crystals are determined. These properties depend heavily on the mode of crystallization, vessel geometry, and process parameters.

Therefore, this study aims to investigate the crystallization kinetics of L-tyrosine by considering both crystallization process parameters (e.g., cooling rate, supersaturation level, and agitation) and fermentation-related factors (e.g., medium composition and the presence of by-products such as L-phenylalanine). A mechanistic model is based on population balance equations and captures the nucleation, growth, agglomeration,

and breakage phenomena as well as the resulting crystal size distribution. The model would then be able to simulate the crystallization at varying operating conditions during the fermentation, as well as the crystallization as a purification step in the downstream process. The operating conditions can then be optimized to achieve the required quality attributes of L-tyrosine.

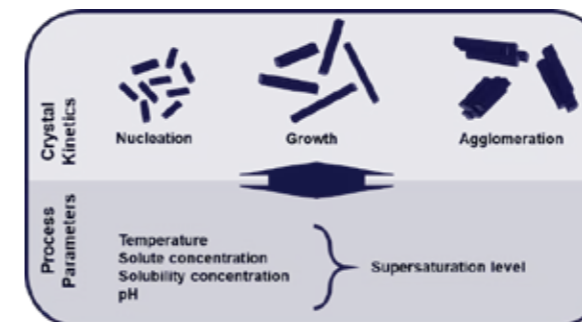


Figure 1: Illustration of the crystal dynamics and the process parameters which captured by the model.

Experimental setup

Batch cooling experiments were performed in a 3 L glass reactor from Biostream. First, experimental studies were conducted using deionized water as a solvent to generate a baseline. Then, the complexity of the solvent was increased by incorporating compounds from the fermentation medium. The process involved the application of controlled cooling profiles, saturation levels, and agitation, along with the in-situ measurement of solute concentration using the ATR-FTIR probe ReactIR from Mettler Toledo and the offline measurement of crystal size distribution using the ParticleTech Solution from Particle Tech Aps. Additionally, the solubility data for L-tyrosine were determined across varying pH values, temperatures and solvents using the Crystal 16 from Technobis Crystallization Systems.

Conclusion

The model establishes a link between process conditions and crystal properties, enabling a more efficient design and optimization of the overall production process of L-tyrosine. Comparing the crystallization behavior in deionized water versus the fermentation broth provides insights into the influence of salts, by-products, and operating conditions of the fermentation process. These findings contribute to a deeper understanding of in situ crystallization during microbial production and support the development of integrated strategies for improved downstream processing.

Acknowledgement

The authors acknowledge the financial support through the Novo Nordisk Foundation within the framework of Fermentation-Based Biomanufacturing Initiative (Grant no.: NNF17SA0031362).

References

1. T. P. Pieters, et al., Fed-Batch Fermentation of Genomically Engineered *E. coli* for the Production of L-Tyrosine, (Manuscript in preparation)
2. G. Li, Z. Chen, N. Chen, Q. Xu, Enhancing the efficiency of L-tyrosine by repeated batch fermentation, *Bioengineered* (11) (2020) 852-861.
3. R. Patnaik, R. R. Zolandz, D. A. Green, and D. F. Kraynie, L-tyrosine production by recombinant *Escherichia coli*: fermentation optimization and recovery, *Biotechnology and Bioengineering* (99) (2008) 741-752.
4. J. Ping, L. Wang, Z. Qin, Z. Zhou, and J. Zhou, Synergetic engineering of *Escherichia coli* for efficient production of L-tyrosine, *Synthetic and Systems Biotechnology* (8)(2023) 724-731.
5. Z. Chen et al., Systems metabolic engineering and process optimization for efficient L-tyrosine production from high-purity glucose syrup in *Escherichia coli*, *Bioresource Technology* (425) (2025).
6. S. Bhoi, M. Lenka, and D. Sarkar, Principles of crystallization process, in *Mass Transfer Operations in the Food Industry*, Elsevier, (2025) 15-43.

Oxygen-enzyme in biocatalytic oxidation

(January 2023 – March 2026)



Contribution to the UN Sustainable Development Goals

Most chemical products are produced in industry in multi-step pathways from petrochemical-based feedstocks. One potential alternative and sustainable route is biocatalysis whereby enzymes are used as chemical catalysts. Biocatalysis not only uses milder reaction conditions, but also renewable substrates such as sugars and provides a higher substrate selectivity. This project aims to tackle industry-related problems in biocatalysis, associated to oxygen-related enzymes to achieve economically feasible biocatalytic processes scalable to industry.



Ariadna Pié Porta

arip@kt.dtu.dk

Supervisors: Elif Erdem, Helena Junicke, John M. Woodley

Abstract

One of the most important and yet also challenging reactions in industrial chemistry is oxidation. Biochemically based reactions use molecular oxygen as a substrate and while this has many advantages for the process, the kinetics and stability of the enzymes are often limited by the low solubility of oxygen in water. The research of enzymes with a higher affinity for oxygen and a standard method to characterize them, is crucial for unleashing the potential of industrial oxygen-related biocatalysis.

Introduction

Many products we use in our daily life contain modified organic chemicals (from pharmaceuticals to the plastic used for packaging). These compounds must be manufactured by a serial of (often catalytic) steps and it is common that at least one of these steps is oxidation [1].

Metal-based catalysts are traditionally used to oxidize chemicals to produce valuable products. This process involves the mining and processing (curation) of the metals by using organic solvents before they can be used as catalysts. During the catalysis, high temperatures (up to 500°C) and pressures are applied, requiring a big expense of energy. Large amounts of catalysts are used in the reaction and end up becoming hazardous waste difficult to discard [2].

Biocatalytic oxidation provides a sustainable, safe, and highly selective alternative to chemical catalysis. This is, enzymes are produced by bacteria which grow on renewable materials and produce only organic waste (which can be upcycled or easily disposed). Enzymes are extracted and used as catalysts in biocatalytic reactions. Molecular oxygen is supplied to be the final electron acceptor (oxidizing agent) instead of metals [3].

In industrial setups, oxygen is typically provided to the reaction mixture by bubbling air since it is cheap, widely available and non-toxic.

Complexity derived from working with gases make K_{MO} to be overlooked in many cases. Moreover, there is a lack of off-the-shelf instruments (and methods) that allow to supply oxygen into an enzymatic system in a controlled manner. Hence, it is in very few cases that K_{MO} has been accurately measured.

Oxygen transfer limits reaction rate

Oxygen is unfortunately, a quite insoluble gas: the maximum concentration of oxygen in water in equilibrium with air is 250 μM (at 30 °C and ambient pressure). The gaseous nature of oxygen implies that it must be constantly bubbled to keep up with the oxygen demand of enzymes, and its low solubility implies that oxidative processes are often oxygen-limited.

In oxidative reactions, two substrates are involved: the main substrate which will be oxidised (e.g. NADH for NADH oxidase, NOX) and oxygen as the final electron acceptor (Figure 1). In industry, reaction rates must be as high as possible to achieve economically-feasible processes. Maximum reaction rates are only achieved when the enzyme is saturated with both the substrates. In general, it is feasible to saturate with the main substrate, but the low solubility of oxygen prevents to achieve the saturation of many enzymes and becomes the main bottleneck of industrial oxidation processes.

These saturation conditions must be achieved also when studying the pure kinetics of an enzyme. This is, the maximum rate of reaction (r_{max}) must be reached to then calculate the absolute Michaelis-Menten constants for both main substrate and oxygen (K_{MS} and K_{MO}) (Figure 2). These constants are crucial to characterize enzymes and understand how to unlock their full potential.

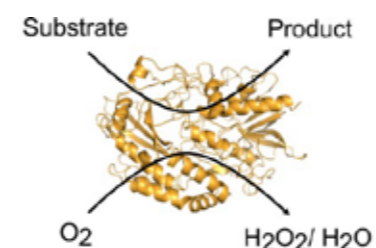


Figure 1. Typical reaction performed by an oxidase, where a substrate gets oxidised into a product by oxygen releasing H_2O_2 or H_2O as by-product.

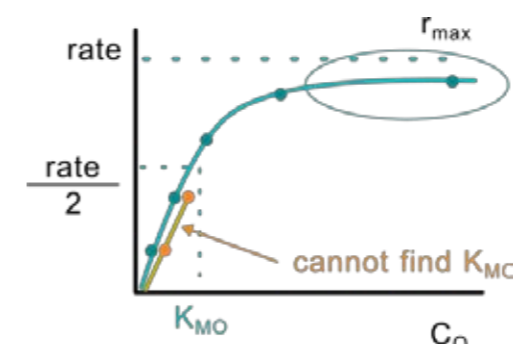


Figure 2. Typical Michaelis-Menten plot. Provided saturation with the main substrate, increasing concentrations of oxygen are supplied (x axis). For the yellow line, only low concentrations can be supplied, so K_{MO} cannot be calculated. For the blue line, higher concentrations of oxygen can be supplied, the r_{max} plateau can be reached meaning that the enzyme is saturated with oxygen and K_{MO} can be found.

Tube-in-Flask reactor system

There is a need for systems that allow to provide controlled amounts of oxygen and thereby measure the reaction rates to ultimately calculate K_{MO} .

This work presents for the first time the Tube-in-Flask (TIF) Reactor system, a novel tool that allows to study oxygen transfer in a controlled manner to extract oxygen-related reaction rates and the possibility to then, calculate K_{MO} .

The TIF is composed of a silicone tube coiled inside a 250 mL flask with a wide lid with multiple orifices that allow to insert temperature, pH and dissolved oxygen (DO) probes, the sampling tube and the silicone tube itself. The reaction happens in the buffer that the flask holds, and the gas is being supplied by flowing it through the silicone tube at a slight overpressure. The porous nature of the silicone allows the gas to permeate through the tube wall and get dissolved into the liquid without creating major bubbles.

The TIF allows concentrations of oxygen in water up to 1,2 mM through tuning the oxygen partial pressure (which can go from 5-100%) by mixing varying concentrations of pure oxygen and nitrogen through mass flow controllers. The system collects samples automatically by means of a piston pump, which recirculates a constant flow of the reaction mixture through a flow cell integrated into a UV detector. The detector is set to take a sample every 12 seconds. This ensures a large amount of data collected which allows to follow the whole curve of the substrate decay (or product formation).

The data can be analyzed by using a derivative method, and extract multiple rates of reaction (for different substrate concentrations) from one single experiment. These data can then be used to calculate K_{MO} of virtually any enzyme.

1. Liu J, Wu S, Li Z. *Curr Opin Chem Biol* 2018; 43:77–86
2. Yu H, Ru S, Dai G, Zhai Y, Lin H, Han S, et al. *Angew Chemie - Int Ed* 2017; 56:3867–71
3. Woodley JM. *Top Catal* 2019; 62:1202–7

Functionalization of PDMS via click chemistry for dielectric elastomers with protein integration

(January 2023 – January 2026)

7 AFFORDABLE AND CLEAN ENERGY



Contribution to the UN Sustainable Development Goals

Silicone elastomers are attractive materials for developing wearable electronics. While most current applications focus on their benefits as soft wearables for life improvement and health benefits, silicone elastomers can also be applied as a material for triboelectric generators, converting mechanical energy into electric energy from sources like wind and tidal energy. This versatility makes silicone elastomers promising candidates for innovative energy-harvesting applications in addition to their established wearable roles.



Pavle

Ramah

pavra@dtu.dk

Supervisors: Anne Ladegaard Skov, Anders Egede Daugaard

Abstract

A facile synthetic route of converting a commercial polydimethylsiloxane (PDMS) to a prepolymer capable of non-metal-catalyzed cross-linking *via* Thiol-Michael addition is presented. Two prepolymers and their respective cross-linked networks are thus compared: Maleimide (MI)-terminated PDMS, and maleamic acid amide (MA)-terminated PDMS. We demonstrate the potential of maleamic acid amide functionalities in particular as both a good platform for construction of dielectric elastomer actuators and protein integration, making PDMS not only biocompatible, but also containing biological materials which have synergistic effects in improving permittivity.

Introduction

Polydimethylsiloxane (PDMS) is a flexible polymer with a low glass transition temperature. It is widely used as a silicone elastomer in applications like soft robotics and dielectrics. When forming a network, PDMS is normally cured in the presence of a metal catalyst (e.g., Pt).

Metal-free silicone elastomers are cured under mild conditions, enhancing their application and recyclability and reducing metal-related conductivity issues, where the presence of a metal catalyst can lead to unwanted conductivity of the dielectric [1]. Michael addition, a type of click chemistry, involves coupling a nucleophile (thiol) with an unsaturated bond (vinyl), known for rapid, selective reactions with minimal use of catalysts.

Proteins have been shown to possess interesting dielectric properties [2]. However, their integration in silicone-based DEAs is challenging due to their disparate behaviour in water.

In this study, aminopropyl-terminated PDMS (APDMS) is converted to maleamic acid amide-terminated PDMS (MA) and then to maleimide-terminated PDMS (MI) through a two-step process (Scheme 1). These prepolymers are cross-linked via Thiol-Michael addition using triethyl amine as

a catalyst, making the process metal-free and oxygen-insensitive. During this cross-linking, an aqueous solution containing both isinglass (IG), a model large molecular weight protein, and keratin hydrolysate (KH), a peptide, are added and successfully integrated into the silicone matrix. The dispersion is stable in MA-based systems, due to the amide backbone polarity and emerging amphiphilicity.

Specific Objectives

The primary objective of this project is to:

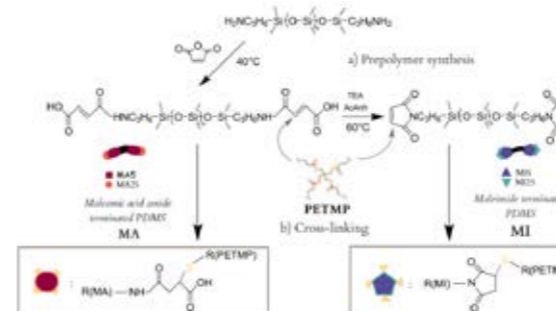
- Develop a facile and robust methodology for synthesizing PDMS networks using metal-free cross-linking.
- Adapt the network by using novel additives (e.g. proteins) for improved dielectric properties.
- Produce dielectric elastomer actuators or triboelectric nanogenerators.

Current progress has met the first two points, while work on the last one is ongoing.

Results and Discussion

The MI and MA networks were formed from their respective prepolymers (as shown in Scheme 1, in

two molecular weights, named based on the chain length of their prepolymer) in a simple robust process without use of metallic catalysts. While they possess higher permittivity in the entire spectra compared to a commercial reference (Sylgard™ 184, $\epsilon_r = 2.73$), MA system is shown as superior to the MI network.



Scheme 1. The reaction scheme of the synthesis and cross-linking of the MA and MI prepolymers.

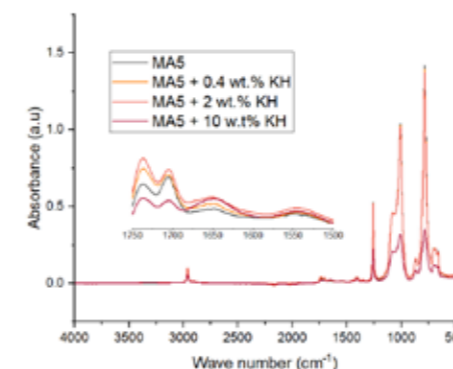


Figure 1: FTIR spectra of KH peptide containing MA5 PDMS, with inset of the amide region.

A concentrated aqueous solution (28 wt./wt.% containing isinglass and keratin hydrolysate) was prepared and added directly during the cross-linking process to the 5 kDa MAPDMS due to the increased relative polar group content. Protein presence was confirmed by FTIR, with notable amide I+II band stretching at 1450-1650 cm^{-1} (Figure 1) [3]. Protein effects on the permittivity showed significant differences based on the protein used (Figure 2). Notably, the peptide KH ($\approx 2\text{kDa}$) showed a decrease in permittivity compared to base MA5 with increasing content, while the protein IG ($\approx 100\text{kDa}$) showed an increase with increasing content. This could be explained in terms of their aggregation – KH is a smaller additive and can agglomerate more easily, reducing the ability to align with the electric field. Isinglass meanwhile shows an increase in permittivity with an increase in protein content. Especially notable is their low frequency performance, characteristic of polarizable molecules.

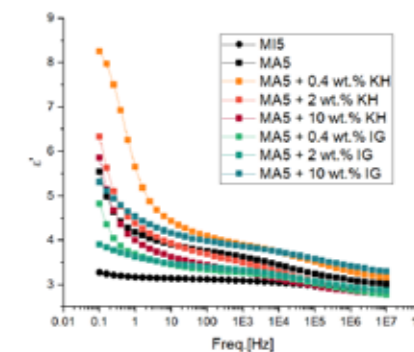


Figure 2. a) Optical microscopy of MA5 containing 4 wt.% IG (400x magnification) b) dielectric permittivity as a function of frequency for protein dispersions in MA5 PDMS.

Conclusions

Two different cross-linked networks based on Michael-addition were prepared from modified commercial PDMS. MA networks can be integrated with physical dispersions of both proteins and peptides which leads to increased permittivity at certain loadings. Further work is necessary to optimize the dispersity and formulations.

Acknowledgments

The authors would like to thank the Novo Nordisk Foundation for funding this project.

References

1. H. Silau, N. B. Stabell, F. R. Petersen, M. Pham, L. Yu, A. L. Skov, *Advanced Engineering Materials* **2018**, *20*, 1800241.
2. L. Li, C. Li, Z. Zhang, E. Alexov, *J. Chem. Theory Comput.* **2013**, *9*, 2126–2136.
3. J. H. Muyonga, C. G. B. Cole, K. G. Duodu, *Food Chemistry* **2004**, *86*, 325–332.

List of Publications

P. Ramah, L. Yu, A. E. Daugaard, A. L. Skov, *RSC Appl. Polym.* 2024, *2*, 891–904.

Toward oxyfuel cement calcination for efficient CO₂ capture: CFD modeling of a cold-pilot scale calciner

(April 2023 – April 2026)



Contribution to the UN Sustainable Development Goals

Cement production is one of the largest industrial sources of CO₂ emissions, accounting for about 7% globally. This PhD project develops CFD models of cement calciners under both cold and hot conditions to investigate flow behavior, heat transfer, and chemical reactions when a calciner is operated at oxyfuel conditions. The findings support the transition toward low-carbon cement manufacturing through the application of oxyfuel combustion technology. By enabling efficient CO₂ capture and improved process performance, the research contributes to the UN's Goal 13: Climate Action, advancing cleaner and more sustainable industrial processes.



Mohammad Reza Abdollahi Senoukesh

mohasen@dtu.dk

Supervisors: Peter Arendt Jensen, Peter Glarborg, Mohamadali Mirzaei, Lars Skaarup Jensen, Satyanarayana B

Abstract

Reducing CO₂ emissions from cement production through oxyfuel combustion requires a detailed understanding of the calcination process under alternative combustion conditions. This PhD project develops a Computational Fluid Dynamics (CFD) model to analyze flow behavior, gas–solid interactions, and chemical reactions in a cement calciner as a step toward industrial oxyfuel implementation. This report focuses on cold-flow pilot-scale modeling, with the CFD model validated against experimental velocity, temperature, and pressure drop data. The study further examines the effects of increased solid-to-gas ratios caused by reduced gas flow rates and their influence on stable operation and raw meal particle fall-off. The validated model provides a solid basis for large-scale reactive oxyfuel simulations.

Introduction

The production of one ton of cement releases on average 0.5–0.6 tons of CO₂, with approximately two-thirds originating from the calcination of limestone [1]. Over time, the cement industry has adopted several strategies to reduce CO₂ emissions, including substituting fossil fuels, improving process energy efficiency, and utilizing alternative clinker materials. While these measures have achieved notable reductions, the potential for further improvement through conventional approaches is now limited. Therefore, the integration of Carbon Capture, Utilization, and Storage (CCUS) technologies has become essential for achieving further CO₂ emission reductions. Among these, oxyfuel combustion is considered a highly important pathway toward reaching net zero targets in the cement industry [2,3].

In oxyfuel combustion, oxygen is used as the fuel oxidant instead of air, producing a flue gas composed mainly of CO₂. In current oxyfuel systems, part of the flue gas is recirculated to control temperature and maintain gas velocity

within the calciner [4]. However, reheating this recycled flow is energetically inefficient, and the calcination reaction, being equilibrium-limited, may be hindered by the high CO₂ concentration. For these reasons, minimizing or ideally eliminating flue gas recirculation and thereby increasing the solid-to-gas ratio is therefore investigated in this work, as it could lead to a more fuel efficient calcination process.

Experimental measurements

Measurements were carried out on a cold (gas heated to 70°C) pilot-scale riser-calciner setup with a total height of 7 meters and a calciner diameter of 0.7 meters. In addition to recording the overall pressure drop, the temperature distribution along various heights of the setup was measured using multiple temperature sensors. To obtain velocity profiles, a Laser Doppler Anemometer (LDA) was employed at the same axial positions where the temperature was recorded. The experiments were conducted at high solid-to-gas ratios that provided stable and repeatable operating conditions. The collected data provide

insight into local flow characteristics and potential particle fall-off to the bottom of the riser, which can be used for CFD model validation.

CFD Modeling

A CFD model was developed using ANSYS Fluent to simulate the multiphase gas–solid flow in the calciner. The Discrete Phase Model (DPM), based on an Eulerian–Lagrangian approach, was employed to track particle motion and capture gas–solid interactions. Turbulence was modeled using the $k-\omega$ Shear Stress Transport (SST) model, which is widely applied in the literature for gas–solid systems due to its numerical stability and computational efficiency. Heat exchange between the particle and gas phases was represented using the Ranz–Marshall correlation, and heat loss through the calciner walls was also accounted for in the simulations. In addition, an agglomeration sub-model was implemented to predict particle agglomeration within the system.

Results and Discussion

The comparison between the CFD-predicted velocities and the LDA measurements in Figure 1 was performed at three different heights of the calciner, along two perpendicular measurement lines intersecting at the center of the cross-section.

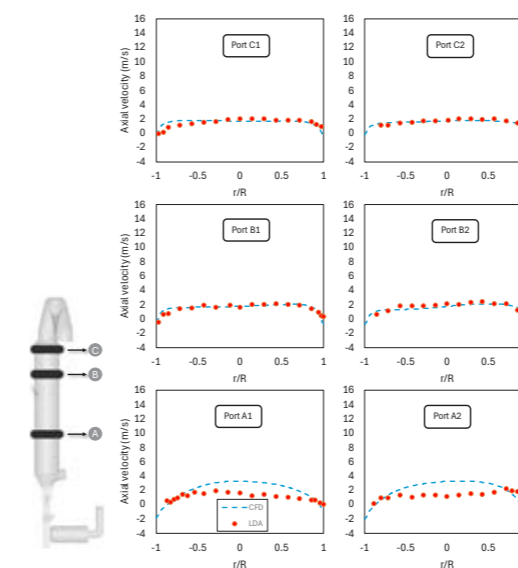


Figure 46: Comparison of time-averaged axial velocity profiles obtained from CFD simulations and LDA measurements.

The results indicate that the CFD model accurately reproduces the velocity profiles along the calciner height. At the lower section, referred to as cross-section A, minor deviations are observed, while as the flow develops at higher positions, the predicted and measured velocities are in close agreement. For the temperature field,

the CFD model successfully captures the overall distribution, with deviations of approximately 5 °C in absolute values. The predicted pressure drop across the calciner also shows good agreement with the experimental data, confirming the reliability of the model in representing the gas–solid hydrodynamics under cold flow conditions.

Conclusions

A validated CFD model of a cold pilot-scale cement calciner was successfully developed and compared with experimental measurements of velocity, temperature, and pressure drop. The model showed strong agreement with the LDA data and accurately captured the thermal and hydrodynamic behavior of the gas–solid flow. This validated framework provides a robust basis for extending the analysis to reactive oxyfuel conditions relevant to CO₂ capture in cement production.

Acknowledgments

The project was carried out as part of the INNO-CCUS program funded by Innovation Fund Denmark, which is gratefully acknowledged. Collaboration with FLSmidth Cement, Faxe Kalk, DTU Compute, and DTI is also appreciated.

References

1. Energy Technology Perspectives 2020 – Analysis – IEA.
2. 20 Years of Carbon Capture and Storage | OECD.
3. Clark G, Davis M, Kumar A. The development of a framework to compare carbon capture and storage technologies as a means of decarbonizing cement production. *Renewable and Sustainable Energy Reviews* 2025;214:115556. <https://doi.org/10.1016/J.RSER.2025.115556>.
4. Carrasco F, Grathwohl S, Maier J, Ruppert J, Scheffknecht G. Experimental investigations of oxyfuel burner for cement production application. *Fuel* 2019;236:608–14. <https://doi.org/10.1016/j.fuel.2018.08.135>.

Optimising Cell Potential and Current for Enhanced CO₂-to-Methane Conversion in Continuous Microbial Electrosynthesis Reactors

(October 2024 – October 2027)



Contribution to the UN Sustainable Development Goals

This research supports SDG 7 (Affordable and Clean Energy) and SDG 13 (Climate Action) by exploring how electroactive microbial communities can efficiently convert CO₂ into methane — a renewable energy source. By optimising cell potential to improve reactor performance, the project promotes cleaner and more sustainable energy production. This approach not only helps reduce greenhouse gas emissions but also transforms waste CO₂ into a valuable fuel, contributing to the development of innovative, low-carbon energy technologies that support a more sustainable future.



Rudini Tua
Silitonga

rtusi@kt.dtu.dk

Supervisors:
Hariklia N. Gavala,
Alexander Shapiro,
Ioannis V. Skiadas

Abstract

This study explores how cell potential and current affect performance and microbial stress during continuous microbial electrosynthesis (MES) for CO₂-to-methane conversion. Two MES reactors were operated at voltages from 3.5 to 5.0 V (28–79 mA) to enrich electroactive microbial consortia and assess methane productivity and efficiency. Maximum methane productivity and coulombic efficiency were achieved at moderate voltages (3.5–4.4 V). Higher potential caused efficiency losses linked to stress-induced secretion of extracellular polymeric substances (EPS), which redirected electrons away from methane formation. The findings show that balancing potential and current is essential for stable, efficient electromethanogenesis and provide design insights for scalable, low-stress CO₂-to-methane bioelectrochemical systems.

Introduction

The biological conversion of CO₂ into methane offers a promising path toward carbon recycling and sustainable fuel generation [1]. Electromethanogenesis enables this transformation by coupling microbial metabolism with electrical energy, allowing the direct synthesis of methane from CO₂ and electrons [2]. However, process productivity remains a bottleneck for industrial implementation [3].

This study focuses on the systematic enrichment of electroactive microbial communities and the evaluation of key electrochemical parameters that dictate performance in continuous MES operation. By controlling and monitoring the applied potential and resulting current, the work aims to identify the optimal conditions for efficient electron utilization and high biomethane production.

Materials and methods

Two 700 mL MES reactors were inoculated with mixed microbial cultures derived from a syngas biomethanation effluent. After initial biofilm

formation under batch conditions (60 °C, pH 7, 3.5 V), both systems were transitioned to continuous flow (HRT = 5 days) to enrich the inoculum under different operational conditions. The applied voltage was sequentially varied between 3.5 V and 5.0 V for the two reactors. Reactor performance was evaluated based on methane productivity, coulombic efficiency (CE), and EPS secretion. The experimental setup is illustrated in Figure 1.

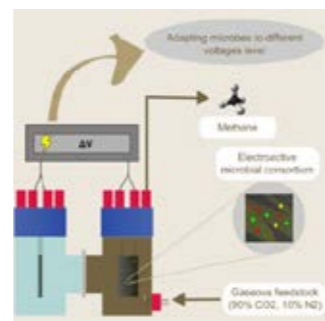


Figure 47. Schematic summary of electroactive microbial consortia enrichment for continuous

CO₂-to-methane conversion in a Microbial Electrosynthesis (MES) Cell

Results and discussion

Increasing the voltage from 3.5 V to 4 V resulted in 1.6–1.8-fold increase of the current and 1.5–1.7-fold enhancement of productivity. However, voltages above 4.4 V did not yield any notable improvement, suggesting a plateau in system performance (Figures 2 and 3). Electron balance calculations showed that coulombic efficiency (CE) remained high at 3.5–4 V (93–100%) but declined sharply at 5 V (70–75%). When the voltage was reduced, CE recovered, indicating that higher potentials compromise efficiency reversibly, at least up to the value tested in this study. This effect is likely due to increased electrical stress, which elevates cellular maintenance requirements and stimulates EPS secretion to protect and stabilise the biofilm. Supporting this, EPS measurements showed a 2.5-fold increase in polysaccharide content at 5 V compared to 4 V. Consequently, under high-potential conditions, cells redirect electrons toward stress mitigation and EPS production rather than methane synthesis, resulting in reduced overall yield and coulombic efficiency.

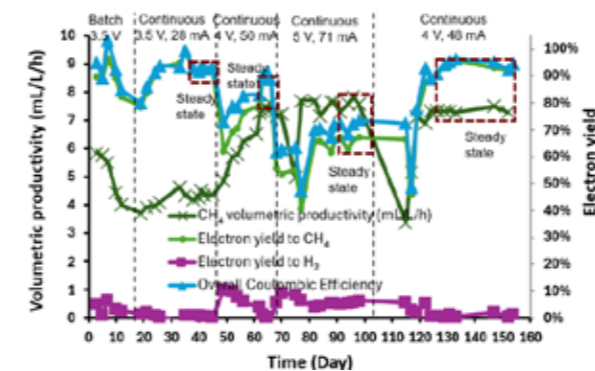


Figure 48. Volumetric productivity and electron conversion over time in MES 1

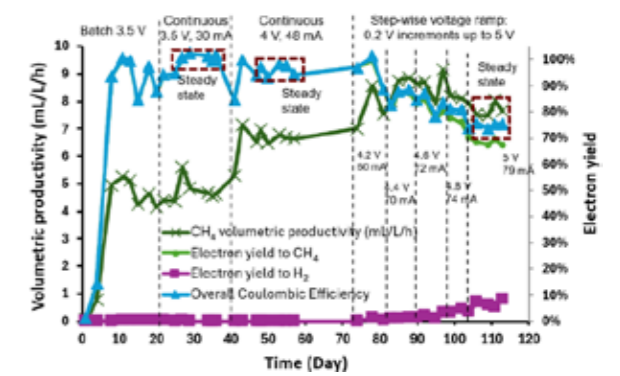


Figure 49. Volumetric productivity and electron conversion over time in MES 2

Conclusions

Cell potential and the resulting electrical current are critical factors in controlling electromethanogenesis. Moderate voltages (3.5–4.4 V) promoted both methane productivity and coulombic efficiency, whereas higher potentials induced cellular stress that reduced overall performance. The enriched MMC demonstrated robustness, recovering performance once optimal conditions were reinstated. These results provide foundational insights for the development of next-generation MES reactors aimed at minimizing microbial stress, improving electron utilization, maximizing methane output, and advancing the CO₂-to-methane bioelectrosynthesis process toward practical, commercial applications.

References

1. G. Cwicklinski, R. Miras, J. Pérard, C. Rinaldi, E. Darrouzet, C. Cavazza, *Sustain. Energy Fuels* 8 (2024) 1068–1076.
2. R. Blasco-Gómez, P. Battlle-Vilanova, M. Villano, M.D. Balaguer, J. Colprim, S. Puig, *Int. J. Mol. Sci.* 18 (2017) 874.
3. P. Dessi, L. Rovira-Alsina, C. Sánchez, G.K. Dinesh, W. Tong, P. Chatterjee, et al., *Biotechnol. Adv.* 46 (2021) 107675.

Acknowledgement

The work was financially supported by DTU and the Novo Nordisk Foundation (NNF).

Mechanism investigation of corrosion protection and coating degradation

(April 2023 – March 2026)



Contribution to the UN Sustainable Development Goals

Corrosion costs 3 trillion US dollars annually, about 3% of global GDP. In addition to this, it also imparts the material and environmental cost as well. Understanding degradation and protection mechanisms of organic coating would help mitigating these effects. This will help guide the coating formulation design with improved corrosion protection performance, thereby prolonging the lifetime of protected structures and products, directly lowering consumption of raw materials used in their manufacturing.



Mehmet Bengi Taysun

mbeta@kt.dtu.dk

Supervisors: Huichao Bi, Kim Dam-Johansen

Abstract

The results of corrosion and failure modes of coating protection are known and internalized by the academy and industry professionals. But the distinct mechanisms that led to those failure modes are not that clear. Anti-corrosive coating formulations, by their nature, take considerable time in development and especially testing. Knowing how the coating protects & fails and understanding the mechanism behind it would provide significant guidance for the new coating formulation development and facilitate the coating performance improvement. In light of this, the project is on the fundamental understanding of the protection and degradation mechanism of anti-corrosive coatings and the key factors affecting the coating performance, thereby providing guidance to the coating formulation improvement.

Introduction

Metallic corrosion is the degradation of the metals due to exposure, humidity, chemicals, and similar factors. Corrosion affects every aspect of modern life and has important consequences; it costs around 3.4% of the global gross economic product annually.

Organic coatings are widely applied on marine and offshore structures for corrosion prevention. The results of corrosion and failure modes of coating protection are well known, namely what happens when materials corrode. But distinct mechanisms that led to those failure modes still need further research. Investigations on the mechanism for corrosion protection and coating degradation have been ongoing for decades. However, until today, there is no such clear understanding of how coating provides corrosion protection and degrades.

If the coating completely restricts the oxygen, water and ionic species transfer, corrosion reaction could not take place. This situation is rarely the reality. Aggressive species find their

way into the substrate, through even visually intact coatings.

Failure mechanisms of coatings are influenced by an extensive array of factors, like the coating type, application methods, environmental exposure, formulation, and more [1]. There are two main ways coatings fail: coating defects or, in the absence of defects, insufficient protective characteristics. Among these, barrier properties against water are paramount. Crosslinked polymer networks, such as epoxy, are polar in nature, with an inherent affinity for water, and readily absorb water even when no defects are visible or present [2].

Specific Objectives

This project aims to relate molecular structure of crosslinked epoxy network to its barrier properties along with furthering understanding on pigment-resin interactions and their effect on corrosion protection.

Results and Discussion

Water is not the limiting factor for corrosion rate, but it is essential [3]. Numerous network

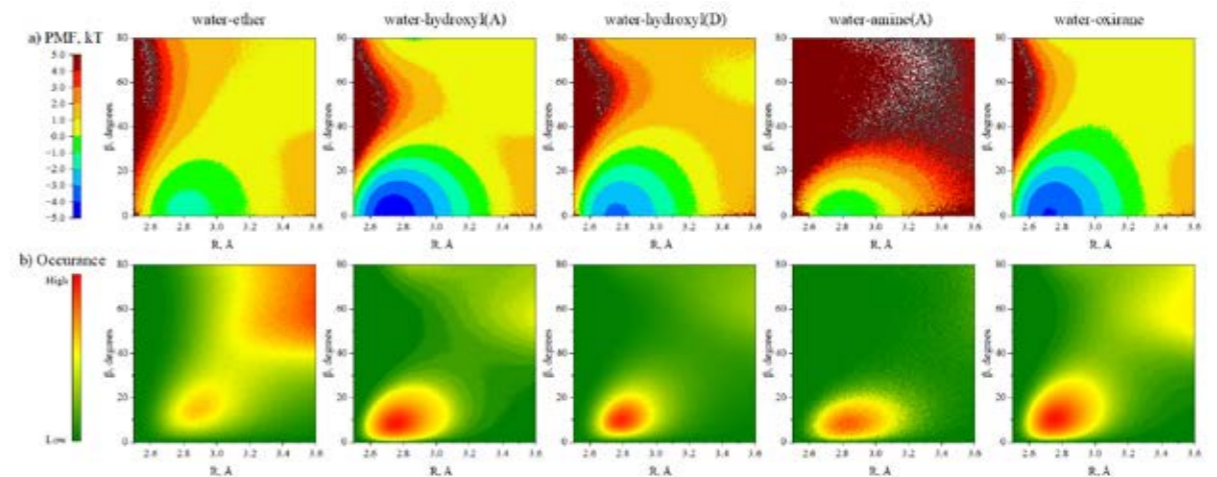


Figure 2 Hydrogen bond configurations (a) and probability density (b) for possible bonding sites and absorbed water in amine cured epoxy system

parameters can influence water uptake, but these can be narrowed into two fundamental network properties: polarity and free volume. Results showed that among the varied stoichiometric ratio samples, higher free volume does not lead to higher water absorption, but higher polarity does (Figure 1).

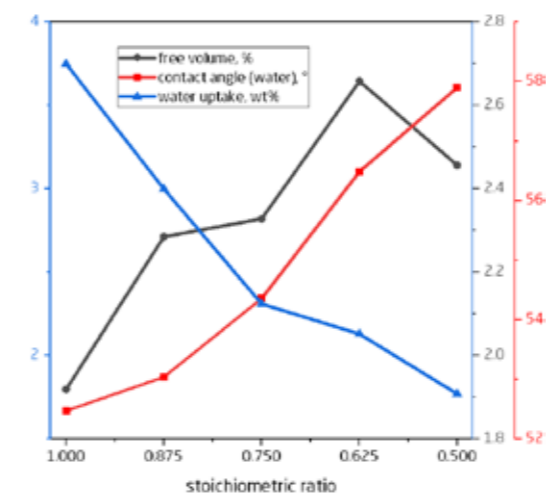


Figure 1 Variation of water uptake, contact angle and free volume through the stoichiometric ratio

Water can form hydrogen bonds with the epoxy network and unexpectedly, cause anti-plasticization. Therefore, characterization of absorbed water in terms of its hydrogen bonding state must be made [4]. Simulations show that among the polar groups present in the crosslinked epoxy-amine network, hydroxyl groups have the most significant impact on water absorption.

Figure 2 shows hydrogen bonding strength configuration of bonding sites in the amine cured epoxy network. Among the possible sites, hydroxyl is the only one can act as both hydrogen bond donor and acceptor. The most favorable hydrogen bond configuration is the linear

arrangement of the donor, hydrogen, and acceptor atoms. This arrangement features in particularly at hydroxyl (A) sites with a broad minimum in the range of 2.6–2.9 Å for R and 0–10° β , and to a lesser extent, at the oxirane sites. Both sites exhibit comparatively lower steric hindrance to water molecules—the hydroxyl group due to its branch-like structure and the oxirane group due to its terminal location.

Conclusions

Water absorption in epoxy-amine systems is governed primarily by polarity rather than the free volume of the network. Different groups in the network adds to the polarity differently. Among the polar groups present in the crosslinked epoxy-amine network, hydroxyl groups have the most significant impact on water absorption and hydrogen bonding behavior. This group not only facilitates higher water uptake but also serves as strong and persistent hydrogen bonding sites for the absorbed water. At residual water uptake, this interaction enhances the network's structural integrity by acting as secondary crosslinks, resulting in an anti-plasticization effect that is more pronounced in hydroxyl-rich, high stoichiometric ratio, networks.

References

1. S. B. Lyon, R. Bingham, and D. J. Mills, Progress in Organic Coatings 102 (2017) 2-7.
2. S. Morsch, S. Lyon, and S. R. Gibbon, Progress in Organic Coatings 102 (2017) 37-43.
3. J. E. O. Mayne, in Corrosion (1976) 15-24.
4. J. Zhou and J. P. Lucas, Polymer 40 (1999) 5505-5512.

List of Publications

M. B. Taysun, K. Dam-Johansen, and H. Bi, Progress in Organic Coatings 209 (2025) 109602.

Chemical and Catalytic Conversion of Lignin to Organic Coatings

(September 2023 – August 2026)



Contribution to the UN Sustainable Development Goals

By executing the high-value extraction of **lignin**, a renewable byproduct of the paper industry, from **black liquor**, we are converting a substantial industrial waste stream into a versatile chemical resource. The core innovation is the application of this bio-based material into **coatings** and, specifically, to replace **Bisphenol A (BPA)**, offering a sustainable alternative to a petroleum-based and potentially harmful chemicals. This approach not only promotes the efficient use of industrial waste (Target 12.5) but also encourages the adoption of environmentally safer, renewable resources, reducing reliance on non-renewable materials and fostering more sustainable production and consumption patterns (Target 12.4).



Alberto Goicoechea Torres

algoto@dtu.dk

Supervisors:

Martin Høj,
Narayanan Rajagopalan,
Hao Wu,
Kim Dam-Johansen

Abstract

This research focuses on developing a streamlined methodology for lignin extraction and property tailoring from black liquor (BL) for advanced applications. Current lignin isolation involves a cumbersome two-step process: bulk precipitation followed by solvent-based fractionation. Our objective is to integrate this into a single, efficient process that selectively isolates lignin fractions with characteristics suitable for high-value industrial uses. Specifically, the recovered lignin will be utilized either as a functional additive in coating systems or as a bio-based precursor for resin synthesis, offering a sustainable alternative with the potential to replace Bisphenol A (BPA) in polymer formulations. This approach enhances resource efficiency and promotes the circular economy by valorizing a major industrial waste stream.

Introduction

The pulp and paper industry generates vast quantities of black liquor (BL), a high-volume byproduct of the Kraft pulping process that contains approximately 40-45% of the original wood's lignin [1]. While traditionally incinerated to recover inorganic pulping chemicals and energy, this approach underutilizes lignin's potential as the most abundant natural aromatic biopolymer [2]. The valorization of lignin into high-value products is a cornerstone of the modern bio-refinery concept, offering a pathway to replace fossil-based materials and drive industrial sustainability [3].

Current methodologies for lignin isolation from BL are often multi-step and inefficient. The standard approach involves an initial bulk precipitation via acidification, followed by complex solvent-based fractionation techniques to obtain specific lignin fractions [4]. This two-step process is often resource-intensive, limiting the economic and environmental viability of large-scale lignin

valorization. Consequently, there is a critical need for streamlined, cost-effective methodologies that can produce tailored lignin with specific properties in a single, integrated process.

The objective of this research is to develop a streamlined methodology for extracting lignin from black liquor and tailoring its properties for use in advanced coating systems and polymer formulations. Our approach aims to integrate the precipitation and fractionation steps into a single, efficient process. This will enable the selective isolation of lignin fractions suitable either as functional coating additives or as bio-based precursors for resin synthesis, with the potential to replace hazardous petroleum-based chemicals such as bisphenol A (BPA). The successful implementation of this work will not only provide a more efficient route to a valuable bio-material but also directly contribute to the transition towards a circular, bio-based economy.

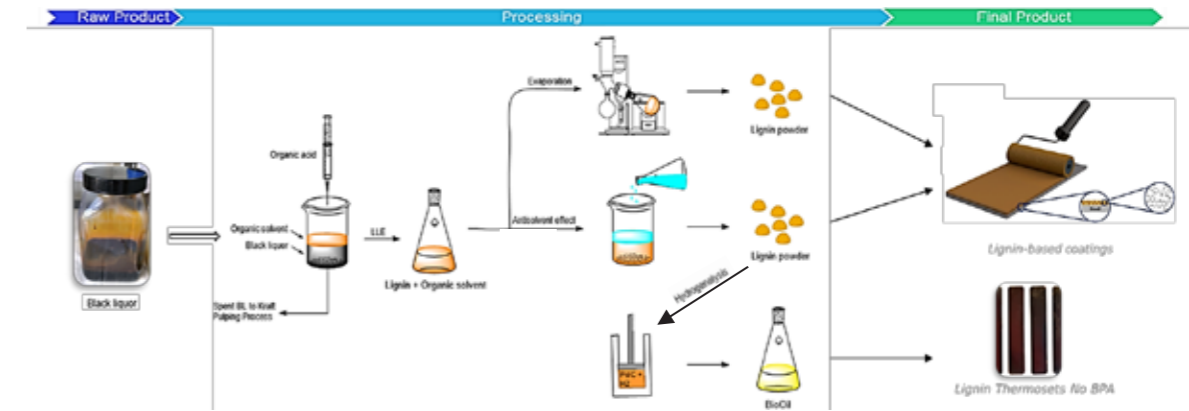


Figure 1: Process flow diagram.

Results

Using this novel, integrated methodology, a series of lignin fractions with distinct and predictable characteristics were successfully produced, as detailed in *Table 1*. The use of various solvent systems yielded fractions with significantly lower average molecular weights (Mw) and narrower polydispersity indices (PDI), indicating successful fractionation and a more uniform polymer structure compared to the benchmark. Specifically, the fraction obtained with Solvent 3 exhibited the lowest Mw of 722 g/mol.

Furthermore, the process maintained or enhanced the total hydroxyl (OH) group content, a key functional property for downstream chemical modification, with Solvent 3 yielding the highest value at 7.71 mmol/g. The fractions also showed a notable reduction in sulfur content (S wt%), indicating a high degree of purity. The versatility of the methodology is underscored by the ability to achieve widely varying levels of lignin-carbohydrate complexes (LCCs), with Solvent 2 producing an LCC-rich fraction and Solvent 3 yielding an exceptionally pure, LCC-minimal product. The structural integrity and composition of these fractions were further confirmed by advanced spectroscopic analysis. For example, the 2D ¹H-¹³C HSQC NMR diagram of the Solvent

2 sample provided detailed insight into the presence and proportion of key structural units and linkages, corroborating the findings.

Table 1: Analysis of Different Lignin Fractions.

Properties	Benchmark*	Solvent 1	Solvent 2	Solvent 3
Mw(g/mol)	3546	2474 to 1387	1263	722
Mn(g/mol)	1272	1395 to 768	917	491
PDI	2.79	1.7 to 1.59	1.376	1.47
Ph-OH (mmol/g)	4.08	4.76 to 4.3	4.01	5.28
Total_OH (mmol/g)	6.92	6.9 to 6.38	7.35	7.71
G units (mmol/g)	1.86	2.58 to 1.94	1.88	3.94
LCCs to 100 G ₂ Units		3.89	171.89	0.05
Carbs to 100 G ₂ Units		2.88	~0	0.7
S (wt.%)	~0.47%	~0.45 to 0 %	~0.28%	~0.23%
Water Soluble?	No	No	YES	No

*UPM BioPiva 395 Lignin

References

- Sixta H, editor. *Handbook of pulp*. 2 vol. set. Weinheim: John Wiley & Sons; 2006.
- Argyropoulos DD, Crestini C, Dahlstrand C, Furesjö E, Gioia C, Jedvert K, Henriksson G, Hultberg C, Lawoko M, Pierrou C, Samec JS. Kraft lignin: a valuable, sustainable resource, opportunities and challenges. *ChemSusChem*. 2023 Dec 7;16(23):e202300492.
- Tanis MH, Wallberg O, Galbe M, Al-Rudainy B. Lignin extraction by using two-step fractionation: A review. *Molecules*. 2023 Dec 22;29(1):98.
- Abolore RS, Jaiswal S, Jaiswal AK. A comprehensive review on sustainable lignin extraction techniques, modifications, and emerging applications. *Industrial Crops and Products*. 2025 Nov 1;235:121696.

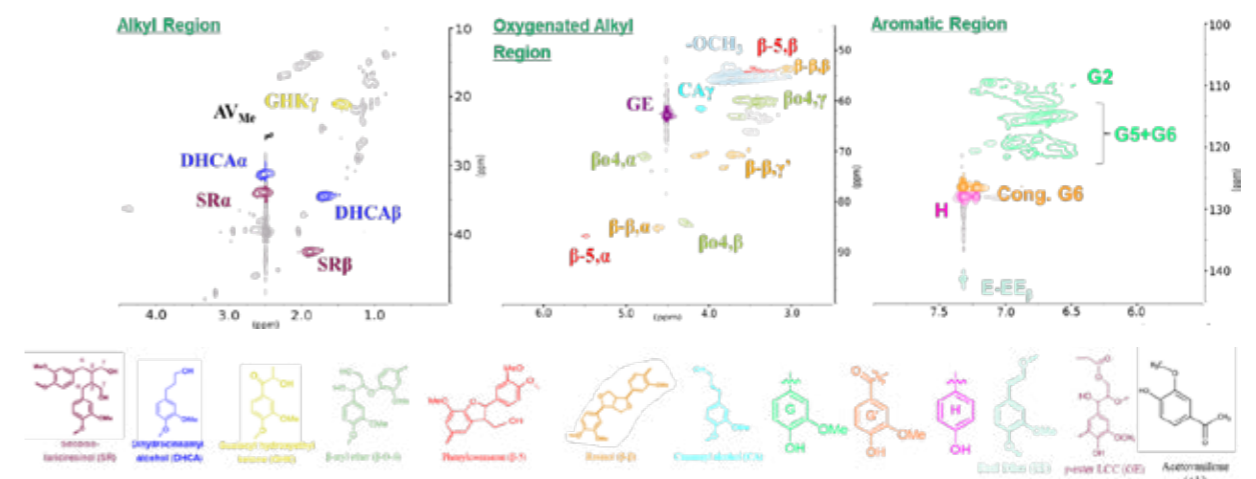


Figure 2: Lignin product from solvent 2 – 2D ¹H-¹³C HSQC NMR.

Fermentation of carbon monoxide to chemical precursors

(November 2023 – October 2026)

13 CLIMATE ACTION



Contribution to the UN Sustainable Development Goals

Increasing global population and reliance on fossil-based resources emphasize the urgent need for sustainable technologies for chemical production. The valorization of renewable feedstocks, including residual biomass and industrial C1 waste gases (mainly CO, CO₂), offers a promising route toward a low-carbon future. Gas fermentation represents this approach by integrating waste management with chemical synthesis, thereby reducing greenhouse gas (GHG) emissions and promoting climate change-resilient industrial development.



Berivan Tunca

bertu@kt.dtu.dk

Supervisors:
Hariklia N. Gavala
Ioannis V. Skiadas
Manuel Pinelo

Abstract

Carbon monoxide (CO), a highly toxic industrial waste gas generated from processes such as steel production and gasification/pyrolysis, can serve as a valuable feedstock for sustainable chemical production. However, CO bioconversion remains challenging due to microbial sensitivity and limited gas-liquid mass transfer, which constrain production rates. In this study, strategies to enhance acetic acid productivity and selectivity from CO were investigated using CO-adapted mixed microbial consortia in continuous trickle bed reactors (TBR) under mesophilic (37 °C) conditions and ambient pressure. In particular, the effect of hydraulic retention time (HRT) and media composition with a focus on tungsten elimination were explored.

Introduction

To mitigate climate change, transitioning from fossil-based chemicals to renewable processes that recycle carbon and reduce greenhouse gas emissions is essential. Biomass gasification coupled with biological conversion of the resulting syngas, primarily CO, CO₂, and H₂, has gained attention as an alternative sustainable route to production of fuels and chemicals. Gas fermentation enables the conversion of CO/CO-rich streams into valuable chemicals such as acetic acid, providing a renewable alternative to fossil-based production [1]. Efficient CO bioconversion remains challenging due to CO biotoxicity and limited gas-liquid mass transfer, which constrain microbial growth and acetic acid productivity.

Bioreactor design plays a critical role in overcoming mass transfer limitations. Trickle bed reactors (TBRs) offer enhanced gas-liquid contact with low energy requirements, making them particularly suitable for gas fermentation [2]. While extensively studied for biomethanation, their application in liquid product formation is limited. TBRs thus present a highly promising reactor type

for the microbial conversion of CO into value-added chemicals.

In addition to reactor configuration, operational parameters and medium composition, including trace elements such as tungsten and hydraulic retention time (HRT), may significantly affect acetic acid productivity and selectivity. Tungsten serves as a cofactor for enzymes involved in ethanol and butyric acid formation, potentially diverting carbon from acetic acid; modulating or omitting tungsten can therefore favor acetic acid production [3]. HRT influences the acetic acid titer in which may limit formation of reduced by-products, such as butyric acid, and therefore enhance acetic acid productivity and selectivity. Optimizing both TBR operation and medium composition is thus crucial for maximizing acetic acid production and process efficiency.

This study aims to enhance acetic acid production from CO by investigating the effects of HRT and tungsten on productivity and product selectivity.

Specific Objectives

- Assessing the role of tungsten in acetic acid selectivity

- Achieving high CO conversion rate and acetic acid production rate
- Exploring the effect of HRT on acetic acid production rate

Results and Discussion

The reactors were operated under identical conditions (pH 7.5, 37 °C, Q_{gas} 3.8 ml/min) through five phases: **Phase I** at HRT 3 days with tungsten; **Phase II** at HRT 1.5 days *without tungsten*; **Phases III–V** at HRTs 3, 4.5, and 6 days *without tungsten*.

The data indicated that shortening HRT and removing tungsten enhanced the %CO consumption in both TBRs (94% for TBR1 and 91.7% for TBR2), whereas extending HRT beyond 4.5 days caused a decline in %CO consumption resulting in 84.5% CO consumption for TBR1 and 82.3% CO consumption in TBR2 (Fig. 1).

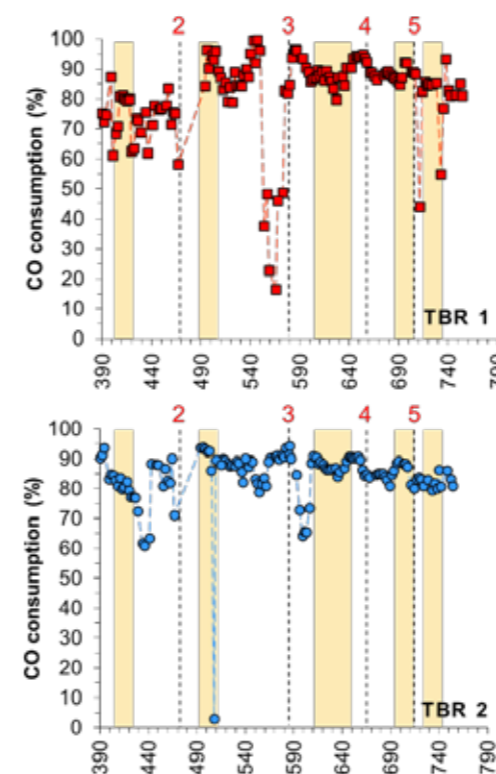


Fig 1. CO consumption (%) in (A) TBR1 and (B) TBR2.

Reducing HRT substantially increased acetic acid productivity (4.1 ± 0.2 g/l_{bed}/d) and reduced butyric acid formation (0.56 ± 0.04 g/l_{bed}/d) (Fig. 2); this is most likely reflecting both greater CO uptake and enhanced acetic acid selectivity after tungsten removal. Although acetic acid productivity decreased at longer HRTs, as anticipated the acetic acid titer rose notably, reaching 19.0 ± 2.4 g/l in TBR1 and 20.8 ± 1.1 g/l in TBR2.

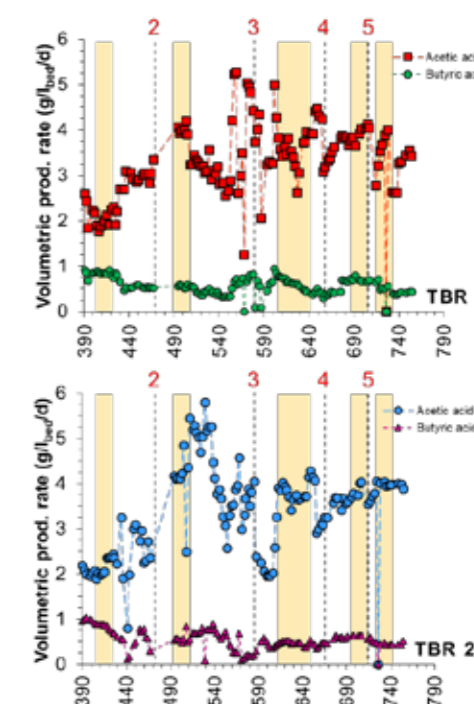


Fig 2. Volumetric production rate (g/l_{bed}/d) of acetic and butyric acids at steady state conditions (A) TBR1 and (B) TBR2

Conclusion

The results showed that removing tungsten and operating at lower HRTs improved acetic acid selectivity relative to butyric acid, while higher HRTs led to increased acetic acid titers. Future studies will focus on developing in-situ separation strategies to further enhance acetic acid selectivity while enabling simultaneous product recovery.

Acknowledgement

This work was supported by DTU and the European Innovation Council (Grant Agreement Project 101115403; acronym: ECOMO).

References

- Gavala, H.N., Grimalt-Alemany, A., Asimakopoulos, K., Skiadas, I. V.: Gas Biological Conversions: The Potential of Syngas and Carbon Dioxide as Production Platforms. *Waste Biomass Valorization*. 12, 5303–5328 (2021). <https://doi.org/10.1007/s12649-020-01332-7>
- Asimakopoulos, K., Gavala, H.N., Skiadas, I. V.: Reactor systems for syngas fermentation processes: A review. (2018)
- He, Y., Kennes, C., Lens, P.N.L.: Enhanced solventogenesis in syngas bioconversion: Role of process parameters and thermodynamics. *Chemosphere*. 299, (2022). <https://doi.org/10.1016/j.chemosphere.2022.134425>

Hydrodynamics effect on gas bubble size distribution in stirred bioreactors

(May 2023 – April 2026)



Contribution to the UN Sustainable Development Goals

Many chemical processes impact the climate in various ways. They are fully optimised, so more sustainable and green technologies need to be adopted. One way to address some of these issues is through the use of biocatalysts. Biocatalytic oxidation offers a sustainable and safe alternative, operating with high selectivity. Additionally, using a biocatalyst is a much faster process compared to fermentation, meaning production times are significantly reduced. To minimise environmental impact, these processes must be fully optimised, particularly in relation to oxygen supply.



Emilie Overgaard Willer

eoje@kt.dtu.dk

Supervisors:
Juliet J. Victoria,
Ulrich Krühne,
John M. Woodley,

Abstract

Biocatalysis has started to overtake chemical processes to enhance the sustainable aspects of production. However, many biocatalytic processes are oxygen dependent, which comes with challenges, such as low oxygen solubility in water. Therefore, new bioreactor configurations must be tested to enhance the oxygen mass transfer. This project aims to test new impeller and sparger configurations to optimise bioprocesses concerning bubble size distribution and mass transfer.

Introduction

The growing population, climate change, geopolitical instabilities, and supply chain issues all require us to adopt more green and sustainable technology in production. [1] However, many processes are already well-optimised, meaning an entirely new synthesis is required, which is a demanding development process. A potential route would be the use of biocatalysis, which means enzymes are used as chemical catalysts in an isolated format. [2]

Numerous biocatalytic reactions have already been adopted in industry, particularly enzymes like lipases and dehydrogenases. These biocatalytic reactions offer significant advantages, such as excellent selectivity under mild conditions and very high reaction rates compared to fermentation. [3]

Oxidation is one of the most important targets in potential next generation biocatalysis. It is vital for industrial organic chemistry but presents several challenges. One of the biggest issues is that enzyme reactions often use molecular oxygen, which is limited by its low water solubility, around 250 μM under ambient conditions. [4]

Specific objectives

The project's primary objective is to evaluate alternative bioreactor configurations to overcome the challenges of the kinetics of biocatalytic gas-dependent reactions. A particular focus will be placed on oxidation using molecular oxygen. To try and overcome the solubility challenges that affect mass transfer and enzyme stability, gas bubble size distribution will be a primary factor.

Experimental work will investigate the bubble size distribution using the most conventional bioreactor type used for industrial organic chemistry, the stirred tank reactor (STR). Different impeller setups will be tested and evaluated compared against the standard Rushton turbines. Moreover, viscosity yields an essential factor in solubility and mass transfer in general. Therefore, varying viscosities will be investigated.

Experimental setup

A new reactor has been built in collaboration with the KT workshop to explore the options for different reactor configurations. The reactor is shown in Figure 1. The reactor is equipped with a ring sparger, four equal baffles, four Rushton turbines, and four oxygen probes attached to one of the baffles to ensure a homogenous oxygen distribution.



Figure 50: Pilot scale reactor, with a working volume of 180 L. Equipped with standard ring sparger, Rushton turbines, and baffles.

The six blue inlets on the side of the reactor were spaced 25 cm apart at different heights to facilitate measurements of the local gas bubbles using an inline ParticleSight endoscope. This enables detection of the gas bubble size distribution at various heights, tracking how the bubble sizes change throughout the reactor.

Focusing on oxygen mass transfer, some essential parameters to be tested include the volumetric mass transfer coefficient, $K_L a$, local and overall gas holdup, bubble size distribution, and local interfacial area.

Bubble size distribution

An inline ParticleSight (Dantec Dynamics, Denmark) is employed to capture images of the gas bubbles in the solutions (Figure 2).



Figure 2: Use of ParticleSight in the reactor and an example of an analysed bubble image.

To capture the images, a high-speed camera connected to the inline endoscope allows capturing up to 1600 frames per second. A segmentation model has been trained to analyse the raw images, meaning the gas bubbles are analysed based on pixels. From this, it is possible to determine bubble size, volume, area, and

bubble count for each image. Therefore, it is possible to gain an understanding of local values such as size distribution, gas holdup, and interfacial area.

Combining all the knowledge gained from the endoscope, it will be possible to determine the specific process in which impeller setup and reactor configuration would be most optimal for oxygen mass transfer.

Conclusion

Based on the experimental work and implemented models, the project aims to identify the most suitable bioreactor configuration for oxygen-dependent biocatalytic reactions.

Acknowledgements

This project has received funding from the European Research Council (ERC) under the European Union's Horizon 2020 research and innovation programme. (Grant agreement No. 101021024) and DTU. Thanks to the KT workshop for building the reactor and making the use of inline ParticleSight at pilot scale possible.

References

1. R. A. Sheldon & J. M. Woodley. Chemical Reviews 118 (2) (2018) 801-838.
2. C. Wittmann & J. C. Liao, Industrial Biotechnology: Products and Processes, Wiley-VCH, Weinheim, Germany, 2017.
3. G. Torello, U. Hanefeld, & F. Hollmann. Catalysis Letters 145 (1) (2015) 309-345.
4. D. J. Leak, R. A. Sheldon, & J. M. Woodley. Biocatalysis and Biotransformation 27 (1) (2009) 1-26.

Phosphorus Release and Transformation during Biomass Pyrolysis and Char Conversion

(Jan 2023 – Jan 2026)



Contribution to the UN Sustainable Development Goals

Biomass, as a renewable resource, could be converted to bio-oil and char through pyrolysis. Adding phosphorus additives in biomass is an effective approach to promote the selective production of high-value organics, increasing the content of furan and anhydrosugars in bio-oil. However, phosphorus undergoes release and transformation during pyrolysis and char conversion, and subsequently influence these processes. The aim of this work is to investigate the release and transformation of phosphorus species during pyrolysis and char conversion of biomass with phosphorus additives.



Wenkai Zhang

wenzh@kt.dtu.dk

Supervisors: Hao Wu; Peter Glarborg

Abstract

Phosphorus additives have been employed in biomass pyrolysis to enhance bio-oil quality, generating phosphorus-rich char as a co-product that is often combusted for providing the energy needed in the pyrolysis process. However, high-temperature char conversion induces phosphorus release and transformation, potentially causing operational issues such as ash fusion and challenges for phosphorus recovery. In this work, we investigated the release and transformation of three commonly used phosphorus additives, $\text{NH}_4\text{H}_2\text{PO}_4$, $\text{Ca}(\text{H}_2\text{PO}_4)_2$, and NaH_2PO_4 , during the pyrolysis of pine wood and wheat straw at 550 °C, and the subsequent char conversion processes at 550-1100 °C.

Introduction

Biomass, as a renewable resource, can be pyrolyzed at around 550 °C to produce bio-oil containing high-value organics such as furans and anhydrosugars [1]. However, their typically low concentrations limit efficient refining and separation [2]. The addition of phosphorus additives, such as $\text{NH}_4\text{H}_2\text{PO}_4$, into biomass during pyrolysis has proven effective in enhancing the content of valuable organics in bio-oil, while also generating phosphorus-rich char as a co-product [1]. In industrial applications, the char is often combusted in a combustor above 800 °C to provide energy needed for the pyrolysis process [3]. However, such high-temperature conversion of char leads to phosphorus release and transformation, potentially posing challenges for phosphorus recovery and causing operational issues such as ash fusion, corrosion, and slagging [4]. Previous studies have shown that phosphorus species can react with inorganic ash components in biomass during pyrolysis [5], and that carbothermic reactions above 800 °C promote the release of phosphorus into the gas phase as elemental phosphorus [3]. Despite increasing research interest, the mechanisms governing phosphorus release and

transformation during these processes for biomass doped with phosphorus additives remain poorly understood.

Specific Objectives

The overall objective of this PhD project is to develop a thorough understanding of the release and transformation of phosphorus during pyrolysis and char conversion of biomass doped with phosphorus additives. Specifically, the project aims to:

- Understand experimentally the transformation of phosphorus additives during biomass pyrolysis.
- Establish knowledge on the interactions of phosphorus additives and potassium species.
- Understand experimentally the release and transformation of phosphorus during char conversion.

Materials and Methods

Two typical woody and herbaceous biomasses, pine wood and wheat straw, were used in this study.

Three anhydrous phosphorus additives, $\text{NH}_4\text{H}_2\text{PO}_4$ ($\geq 99.99\%$, product no. 467782), $\text{Ca}(\text{H}_2\text{PO}_4)_2$ ($\geq 95\%$, C8017), and NaH_2PO_4 ($\geq 99.0\%$, S0751), were purchased from Merck. The phosphorus additives were mixed with biomass in a mortar mechanically for 10 mins, with biomass at a PO_4^{3-} /biomass mass ratio of 1/20 to prepare pine wood-phosphorus additive and wheat straw-phosphorus additive mixtures.

Pyrolysis of three types of feedstocks, including phosphorus additives, biomasses, and their mixtures, were carried out with a fixed-bed reactor. The diagram of the equipment is shown in Figure 1. In each run of experiment: a corundum boat containing 2 g sample was placed into a water-cooling section; the carrier gas of N_2 with a flow rate of 3 NI/min was introduced to purge air; the horizontal reactor was then heated to 550 °C by 10 °C/min; after 30 minutes of oven temperature stabilization, the corundum boat was swiftly pushed into the reactor from cooling section, the heating rates of feedstocks were higher than 100 °C/min; after 40 minutes' reaction, the corundum boat was pulled out into water-cooling section for fast cooling with the presence of N_2 . The residues in the corundum boat were weighed and collected for further analysis.

The pine wood- $\text{NH}_4\text{H}_2\text{PO}_4$ char and wheat straw- $\text{NH}_4\text{H}_2\text{PO}_4$ char were further subjected to conversion under different conditions: secondary pyrolysis at 800-1100 °C in N_2 for 1 h, high-temperature combustion at 800-1100 °C in 5% O_2 for 1 h, or low-temperature combustion at 550 °C in 5% O_2 for 2.5 h. The resulting secondary-pyrolyzed chars and ashes were weighed and collected for further analysis.

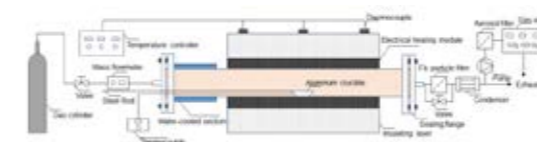


Figure 1: The diagram of fixed-bed reactor.

Preliminary results

During 550 °C pyrolysis, ash-forming elements (P, K, Ca, and Na) were retained in the char. Phosphorus from $\text{NH}_4\text{H}_2\text{PO}_4$ dehydrated into H_3PO_4 and $\text{H}_4\text{P}_2\text{O}_7$ in both pine wood and wheat straw chars. In addition, it reacted with potassium species to form KPO_3 in wheat straw char. Both $\text{Ca}(\text{H}_2\text{PO}_4)_2$ and NaH_2PO_4 dehydrated and reacted with potassium in pine wood and wheat straw chars to form KPO_3 , while $\text{Ca}(\text{H}_2\text{PO}_4)_2$ also transformed into $\text{Ca}_3(\text{PO}_4)_2$ and $\text{Ca}_2\text{P}_2\text{O}_7$.

The release of the three major ash-forming elements, P, K, and Ca, from the pine wood- $\text{NH}_4\text{H}_2\text{PO}_4$ char and wheat straw- $\text{NH}_4\text{H}_2\text{PO}_4$ char during secondary pyrolysis and combustion are shown in Figure 2. The release

of P was much more significant than that of K, whereas Ca was barely released. During secondary pyrolysis (800-1100 °C), 0.30-0.97 mol/kg char (16.4-53.3%) of P was released from pine wood- $\text{NH}_4\text{H}_2\text{PO}_4$ char and 0.08-0.74 mol/kg char (4.6-41.4%) from wheat straw- $\text{NH}_4\text{H}_2\text{PO}_4$ char. Combustion at 800-1100 °C released 1.16-1.44 mol/kg char (63.6-78.7%) from pine wood- $\text{NH}_4\text{H}_2\text{PO}_4$ char and 0.53-0.82 mol/kg char (29.7-45.9%) from wheat straw- $\text{NH}_4\text{H}_2\text{PO}_4$ char. At 550 °C combustion, P release reached 0.64 mol/kg char (34.9%) for pine wood- $\text{NH}_4\text{H}_2\text{PO}_4$ char and 0.26 mol/kg char (14.3%) for wheat straw- $\text{NH}_4\text{H}_2\text{PO}_4$ char. P remained amorphous in secondary-pyrolyzed pine wood- $\text{NH}_4\text{H}_2\text{PO}_4$ chars but crystallized as KPO_3 in secondary-pyrolyzed wheat straw- $\text{NH}_4\text{H}_2\text{PO}_4$ chars. Wheat straw- $\text{NH}_4\text{H}_2\text{PO}_4$ char ashes (800-1100 °C) contained more Ca-P and K-Ca-P compounds ($\text{Ca}_3(\text{PO}_4)_2$, $\text{Ca}(\text{PO}_3)_2$, KCaPO_4) than the corresponding pine wood- $\text{NH}_4\text{H}_2\text{PO}_4$ char ashes.

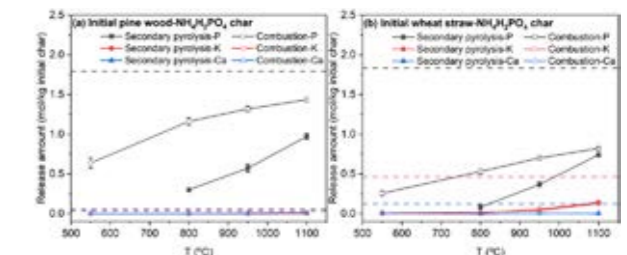


Figure 2: Release of P, K, and Ca from (a) pine wood- $\text{NH}_4\text{H}_2\text{PO}_4$ char and (b) wheat straw- $\text{NH}_4\text{H}_2\text{PO}_4$ char during secondary pyrolysis at 800-1100 °C and combustion at 550-1100 °C. The dashed colored horizontal lines represent the elemental contents in the corresponding chars, representing the maximum possible release.

Acknowledgments

This work is supported by Institute of Process Engineering, Chinese Academy of Sciences and Technical University of Denmark.

References

1. S. Li, S. Li, C. Wang, X. Zhu, Fuel Processing Technology 209 (2020) 106525.
2. G. Kabir, B.H. Hameed, Renewable and Sustainable Energy Reviews 70 (2017) 945-967.
3. E.O.L. Olsson, D. Schmid, O. Karlström, K. Enemark-Rasmussen, H. Leion, S. Li, P. Glarborg, K. Dam-Johansen, H. Wu, Fuel 341 (2023) 127706.
4. E.O.L. Olsson, P. Glarborg, K. Dam-Johansen, H. Wu, Energy & Fuels 37 (2023) 6907-6998.
5. Q. Wang, K. Han, J. Gao, J. Wang, C. Lu, Energy & Fuels 31 (2017) 2822-2830.

Molecular equations of state for Electrolyte Solutions

(September 2024 – September 2027)

7 AFFORDABLE AND CLEAN ENERGY



Contribution to the UN Sustainable Development Goals

By developing more accurate thermodynamic models for electrolyte solutions, we can improve the design of industrial processes in areas such as energy, water treatment, and chemical production. Reliable models help reduce waste, optimize the use of raw materials, and lower energy consumption. In the longer term, this supports cleaner technologies and more sustainable production methods, providing benefits for both industry and society.



Ziyi Zhou

ziyzh@dtu.dk

Supervisors:

Xiaodong Liang;
Georgios M.
Kontogeorgis;
Nefeli Efftosyni Novak

Abstract

Electrolyte solutions play a crucial role in many industrial and environmental processes, yet their thermodynamic description remains a significant challenge. In my PhD project, I focus on advancing the electrolyte SAFT-VR Mie equation of state, with special attention to the role of ion-ion and ion-solvent interactions. A key part of my work compares different approaches for representing ion size in the electrostatic contributions, assessing how these choices affect predictions of density and mean ionic activity coefficients (MIAC). The results show that the model can capture experimental trends across a wide range of salts, while also highlighting limitations for specific systems. The research contributes to more reliable process design, with potential applications in areas such as sustainable energy, water treatment, and green chemistry.

Introduction

Electrolyte solutions play a vital role in numerous processes across energy, environmental, and industrial applications, including carbon capture and storage, corrosion prevention, water purification, and chemical production. However, accurately describing their behavior remains one of the most challenging tasks in thermodynamics. This complexity arises from the coexistence of short-range molecular interactions, such as dispersion and hydrogen bonding, and long-range electrostatic forces between charged species.

Over the years, various modeling strategies have been developed to capture these effects. Empirical activity-coefficient models, such as NRTL, UNIQUAC, and Pitzer, offer practical correlations for industrial use, while molecular-based equations of state (EOS) like CPA and SAFT provide a more fundamental understanding by linking macroscopic properties to intermolecular potentials. Despite these advances, achieving a consistent balance between physical accuracy, transferability, and computational simplicity remains an open challenge. In particular, the proper treatment of electrostatic interactions within a physically meaningful yet efficient molecular framework

continues to drive research in the development of modern electrolyte equations of state.

Specific Objectives

The main objective of this project is to enhance the electrolyte SAFT-VR Mie equation of state by improving the description of electrostatic interactions in solutions. In particular, the work compares alternative definitions of ion size in the Debye-Hückel and Born contributions, evaluating their impact on thermodynamic properties such as density and mean ionic activity coefficients. Further goals include testing the model across a range of aqueous electrolyte systems, identifying its limitations for specific salts, and exploring extensions that ensure physical consistency while maintaining practical applicability.

In this model, we use two distances to describe ion size: σ and d . σ is the fixed, geometric diameter of the ion, like its actual size in a crystal. The effective diameter d changes with temperature and represents how big the ion behaves in real conditions, because higher temperature makes particles move faster and interact differently. In short, σ is the ion's ideal size, while d is its real, temperature-dependent size in solution.

Results and Discussion

It is important to understand why the distance and temperature matter in electrolyte modeling. The distance determines how close ions can approach each other and how strongly they interact, which directly affects the predicted activity and structure of the solution. Temperature, on the other hand, changes the movement and energy of the ions, higher temperatures make them move faster and interact less. Together, these two factors control how accurately the model can describe real experimental behavior.

Figure 1 compares how well our model predicts the experimental data when using the two distances, σ and d , for different salts. Each bar shows the difference between the model and real measurements. The figure helps us see that some salts, especially those with ions carrying more charges like magnesium or calcium, are more sensitive to which distance we choose. In other words, the choice between σ and d can slightly change how accurately the model describes certain salts.

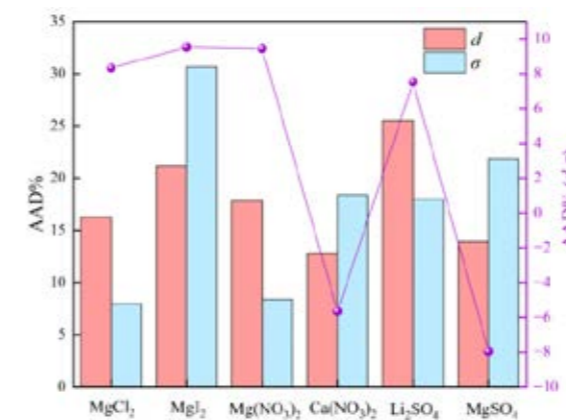


Figure 51: Comparison of the absolute average deviation (AAD%) between experimental and model predictions for selected salts, using either the d or σ .

Figure 2 shows how the mean ionic activity coefficient of sodium chloride (NaCl) changes with concentration and temperature. The squares are experimental data, while the solid and dashed lines represent model predictions using the two distance definitions, d and σ , respectively. As the temperature increases, the ions move faster and interact less strongly, so the activity coefficient becomes smaller. Both definitions follow this general trend, but at higher concentrations, the results start to differ, the model using σ tends to predict slightly stronger interactions. This figure helps us see how temperature and the choice of distance affect the accuracy of the model.

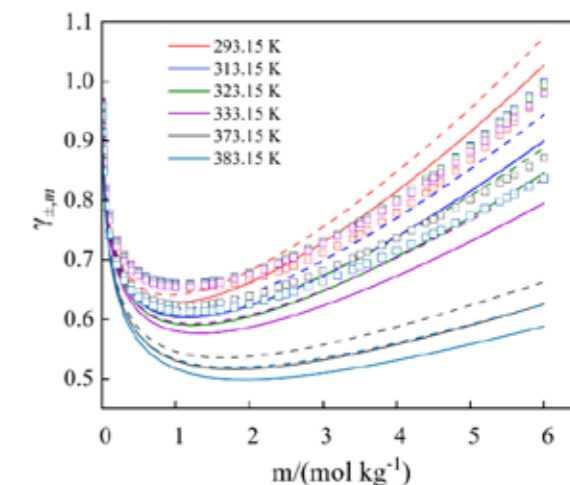


Figure 2: Comparison of model and experimental data for NaCl. Solid lines use distance d , dashed lines use σ , and squares show experiments. The figure illustrates how temperature affects ion interactions in solution.

Conclusions

In conclusion, both the distance definition (σ or d) and the temperature play key roles in predicting how ions behave in electrolyte solutions. While σ represents the fixed size of an ion and d adjusts with temperature, both give similar results for simple salts but can differ for complex or multivalent ones. Temperature also changes the strength of ion interactions, showing that no single setting works best for all cases. Understanding these effects helps us build more accurate and reliable thermodynamic models for electrolyte systems.

Acknowledgements

This work is part of a project that has received funding from the Independent Research Fund Denmark (Case number: 3105-00024B) and is also co-funded by the European Union (ERC, REMOTE, 101171135). Views and opinions expressed are however those of the author(s) only and do not necessarily reflect those of the European Union or the European Research Council Executive Agency. Neither the European Union nor the granting authority can be held responsible for them. The authors would also like to thank Ioannis and Marcelo for providing the database.

References

1. M.A. Selam, I.G. Economou, M. Castier, *Fluid Phase Equilibria* 464 (2018) 47-63.
2. G.M. Kontogeorgis, G.K. Folas, *Thermodynamic Models for Industrial Applications: From Classical and Advanced Mixing Rules to Association Theories*, John Wiley & Sons, 2009.

Department of Chemical and Biochemical Engineering

Technical University of Denmark

Building 228A

Søltofts Plads 228A

DK-2800 Kgs. Lyngby

Denmark

Phone: +45 4525 2822

E-mail: kt@kt.dtu.dk

Web: www.kt.dtu.dk

Jan 2025 ISBN: 978-87-93054-98-1

Editor in Chief

Professor Kim Dam-Johansen,

Head of Department

Editors

Peter Szabo,

Associate Professor

Gcinisizwe Msimisi Dlamini,

PhD student

Print

Step Print Power

Coverdesign

Daniella Pilegaard Jensen,

Graphic designer

